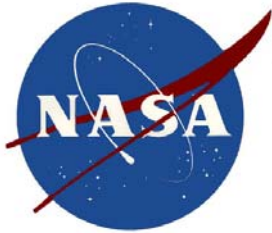NASA/ CR-2004-213551

Measurements of Man-Made Spectrum Noise Floor

Per Enge, Dennis Akos, Juyong Do
Stanford University, Palo Alto, California

Joel B. Simoneau, L. Wilson Pearson, Venkatesh Seetharam
Clemson University, Clemson, South Carolina

November 2004

The NASA STI Program Office ... in Profile

Since its founding, NASA has been dedicated to the advancement of aeronautics and space science. The NASA Scientific and Technical Information (STI) Program Office plays a key part in helping NASA maintain this important role.

The NASA STI Program Office is operated by Langley Research Center, the lead center for NASA's scientific and technical information. The NASA STI Program Office provides access to the NASA STI Database, the largest collection of aeronautical and space science STI in the world. The Program Office is also NASA's institutional mechanism for disseminating the results of its research and development activities. These results are published by NASA in the NASA STI Report Series, which includes the following report types:

- TECHNICAL PUBLICATION. Reports of completed research or a major significant phase of research that present the results of NASA programs and include extensive data or theoretical analysis. Includes compilations of significant scientific and technical data and information deemed to be of continuing reference value. NASA counterpart of peer-reviewed formal professional papers, but having less stringent limitations on manuscript length and extent of graphic presentations.

- TECHNICAL MEMORANDUM. Scientific and technical findings that are preliminary or of specialized interest, e.g., quick release reports, working papers, and bibliographies that contain minimal annotation. Does not contain extensive analysis.

- CONTRACTOR REPORT. Scientific and technical findings by NASA-sponsored contractors and grantees.

- CONFERENCE PUBLICATION. Collected papers from scientific and technical conferences, symposia, seminars, or other meetings sponsored or co-sponsored by NASA.

- SPECIAL PUBLICATION. Scientific, technical, or historical information from NASA programs, projects, and missions, often concerned with subjects having substantial public interest.

- TECHNICAL TRANSLATION. English-language translations of foreign scientific and technical material pertinent to NASA's mission.

Specialized services that complement the STI Program Office's diverse offerings include creating custom thesauri, building customized databases, organizing and publishing research results ... even providing videos.

For more information about the NASA STI Program Office, see the following:

- Access the NASA STI Program Home Page at *http://www.sti.nasa.gov*

- E-mail your question via the Internet to help@sti.nasa.gov

- Fax your question to the NASA STI Help Desk at (301) 621-0134

- Phone the NASA STI Help Desk at (301) 621-0390

- Write to:
  NASA STI Help Desk
  NASA Center for AeroSpace Information
  7121 Standard Drive
  Hanover, MD 21076-1320

NASA/CR-2004-213551

Measurements of Man-Made Spectrum Noise Floor

Per Enge, Dennis Akos, Juyong Do
Stanford University, Palo Alto, California

Joel B. Simoneau, L. Wilson Pearson, Venkatesh Seetharam
Clemson University, Clemson, South Carolina

November 2004

Acknowledgements

Available from:

NASA Center for AeroSpace Information (CASI) (NTIS)	National Technical Information Service
7121 Standard Drive	5285 Port Royal Road
Hanover, MD 21076-1320	Springfield, VA 22161-2171
(301) 621-0390	(703) 605-6000

Table of Contents

Appendices

Executive Summary

Telecommunications deregulation, globalization, mobile wireless connectivity, and disruptive innovation are only some of the forces driving demand for access to radio frequency spectrum. While demand is elastic, the useful capacity of the radio frequency spectrum continues to be interference limited as governed by Shannon's Law. Examining the noise floor is the starting point for understanding channel capacity and determining spectrum utility as defined by diverse demands for communications quality and reliability.

In many instances, new wireless technologies support applications in unlicensed bands or "underlay" existing services on an unlicensed basis. The use of unlicensed spectrum has fostered many innovative applications in recent years. Without technical, economic or regulatory incentives for self-governance, however, the growth of unlicensed uses may not be sustainable due to degradation of the noise floor environment. Such degradation can harm both current and prospective uses of spectrum as it can undercut the utility of wireless applications for governmental and commercial purposes that require high service quality and reliability [Refs. 1 & 2]. As a step toward a better understanding of how the noise floor is being affected today and how it may be affected tomorrow, the National Aeronautics and Space Administration (NASA) and US Department of Transportation (DOT) have sponsored research to study the noise floor in selected bands. This study examines whether observed noise floor results are consistent with the applicable regulations governing those bands. As might be expected, NASA is particularly concerned with the noise floor in bands used for crucial safety and scientific purposes.

This document consolidates research carried out at Clemson University and Stanford University where a series of measurements were undertaken to identify the man-made radiation present in four bands used by rather different services, namely, L1 Band (1563.42 – 1587.42 MHz) used by GPS, the Unified S-Band (2025 – 2110 MHz), the 2.4 GHz Industrial, Scientific, and Medical (ISM) Band (2400 – 2482.50 MHz), and the 23.6 - 24.0 GHz Passive Sensing Band. The GPS Laboratory at Stanford University measured the radio environment in L1, Unified S-Band, and 2.4 GHz ISM Band [Ref.3]. The Center for Research in Wireless Communications at Clemson University conducted measurements in the 23.6 - 24.0 GHz Passive Sensing Band [Ref.4].

The GPS signal is broadcast from a constellation of satellites over 20,000 km above Earth's surface and its received power density is only approximately 10^{-13} W/m^2. The GPS L1 Band is in a strictly controlled and protected band supporting safety-of-life and national security applications. Hence the maintenance of a low, stable noise floor is an important objective for the operational utility of these applications and for continuing innovation. At the consumer level, GPS is being integrated into cell phones in order to provide position information to emergency services when those cell phone users call 911 from either outdoor or indoor locations. At a broader level, GPS is helping improve the productivity of the nation's infrastructure through various augmentations. The Nationwide Differential GPS (NDGPS) is an expansion of the U.S. Coast Guard Maritime DGPS (MDGPS) and provides a single seamless ground-based augmentation to GPS for surface-transportation in critical applications such as Intelligent Transportation Systems (ITS), positive train control, and harbor and harbor entrance navigation. Similarly, the Wide Area Augmentation System (WAAS) is a satellite-based GPS augmentation and is primarily used in aviation applications such as en-route flight and Lateral Precision with Vertical Guidance (LPV) runway approaches where a high degree of signal integrity is required.

NASA and other international space agencies use the Unified S-Band for communication with satellites, and rural sites are used for the associated ground terminals. Electronic newsgathering services also use the Unified S-Band for terrestrial communications. Specifically, TV field operations use this band to transmit their broadcasts back to the station and these TV news vans can certainly be found in urban areas as well as airports and harbors. This band is an example of controlled shared use by different licensed services.

The ISM 2.4 GHz Band is a frequency band allocated for unlicensed applications and is finding increased use for a broad range of technologies such as wireless computer networks and cordless telephones. It also contains radio energy from microwave ovens and other common sources. The open nature of this band means that diverse applications and users are likely to be found anywhere and anytime.

The 23.6-24.0 GHz Passive Sensing Band is critical to weather prediction by the National Oceanic and Atmospheric Administration (NOAA). The frequency range of this band is uniquely located on the radiometric peak for water vapor emissions. The NOAA weather satellite fleet carries radiometers that measure the presence of water vapor through passive sensing of emissions in this band. These radiometers constitute a substantial investment and the loss or degradation of the information gained by these radiometers would substantially impair current weather prediction capabilities.

Measurements in the L1, Unified-S, and ISM 2.4 GHz bands show distinctive differences in the measurement data for each frequency band, which should be expected based on the function and regulation associated with each. The GPS L1 Band contained little to no man-made emission sources, but the ISM 2.4 GHz Band had a large number of man-made sources regardless of the site and the time. Table 1 depicts the average power spectral density measured with color coding displaying the relative power level against the noise power provided by nature which is approximately -112 dBm/MHz. 'Green' indicates closeness to the natural noise power level and 'Yellow' and 'Orange' mean higher level of noise power in that order. The Unified S-Band showed mixed results depending on the sites.

Measurements in the 23.6-24.0 GHz Passive Sensing Band do not contain appreciable levels of man-made radiation. Nineteen spectral peaks were, however, deduced to be man-made signals. Eleven of these signals were observed at the airport sites—three observations at a single frequency at Hartsfield-Jackson Airport and ten others at the Oconee County airport. The Hartsfield-Jackson signal was observed in measurements in the direction of the airport's main radar, suggesting spurious emission from the radar as a source. The ten spectral peaks at Oconee County occurred at multiple frequencies and showed arrivals from different directions. Figure 1 shows a composite plot of these signals.

Based on the measurement data, the spectral environment was shown to be consistent with what was expected based on the applicable regulations.

- The 1.5 GHz GPS Band is relatively pristine and quiet
- The 2.0 GHz Band has emissions due to non-Government services
- The 2.4 GHz ISM Band is discernibly noisier than these regulated bands.
- Urban areas are noisier than rural environments
- Airports and harbors are generally similar to urban areas

In the protected bands where strict regulations are applied, the spectrum was nearly free of

interference and it was mostly only the natural thermal noise floor that was observed. In open bands where less strict regulations are applied, the spectrum was full of man-made signals and the natural thermal noise floor was hardly observed.

- In open bands, the power spectrum is far above the thermal noise floor
- In protected bands, the power spectrum is close to the thermal noise floor.

In other words, the reality of the radio spectrum reflects the regulation applied within it and the existing regulations appear to support and protect the individual spectrum use as allocated. In the protected band, the spectrum is kept clean and this assures secure and stable service. In the open bands, the spectrum is frequently noisy and this limits the effective range and increases susceptibility to communication failure but the emerging applications in those bands can accept such environment.   (This study did not examine the difference among unlicensed bands and the migration of technologies to achieve improved performance from dense use open bands supporting diverse technologies to less dense open bands.)

The measurement results show that *current rules are effective in determining the radio environment and regulations must be sensitive to the function of the band*. Each band supports different types of applications. Some of them are critical systems that cannot tolerate any sort of operational failure and need to be protected from any interference. Some of them can tolerate a certain level of failure and work even under severe interference while requiring more bandwidth. Spectrum policy has been sensitive to the varying objectives and requirements of specific radio frequency applications and corresponding functions of individual frequency bands. The spectrum environment has been successfully managed to ensure stable operations and the best utilization of frequency bands by properly allocating bands to each category of application, locating them with sufficient spectral separation, and adopting application sensitive regulations. To sustain the radio frequency environment for current and future users, the same level of sensitivity should be applied to the introduction of any new spectrum policy or new applications.

Measurement Site	GPS L1 Band	Unified S Band	ISM 2.4 GHz Band
Urban I	-111.0	-109.2	-83.1
Urban II	-111.5	-111.4	-92.2
Rural I	-112.1	-111.8	-85.1
Rural II	-112.1	-111.7	-97.1
Airport I	-112.5	-77.4	-82.2
Airport II	-112.3	-112.0	-92.5
Harbor I	-112.9	-106.9	-87.6
Harbor II	-111.9	-110.9	-88.8

*Note: The power measurements by a horizontally polarized horn antenna in dBm/MHz.
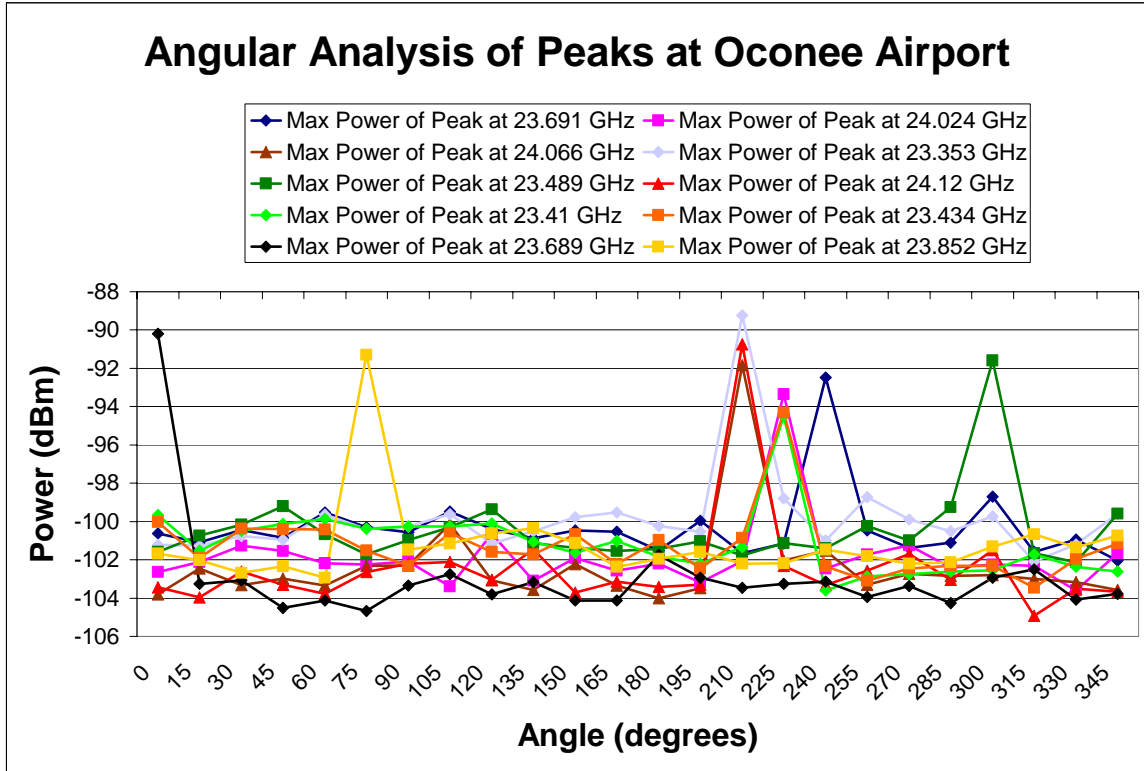
Table 1. Average Received Power

Figure 1. Composite of Peak Spectrum Data Showing Apparent Man-Made Signals at the Oconee County Airport.

Acronyms and Symbols

APD	Amplitude Probability Distribution
ANT	Antenna
ANSI	American National Standard Institute
CRWC	Center for Research in Wireless Communications (Clemson University)
dB	Decibel
dBi	Decibel isotropic radiator
DGPS	Differential GPS
FCC	Federal Communications Commission
FE	Front End
GHz	Gigahertz
GPS	Global Positioning System
GPS L1	GPS L1 frequency band centered at 1575.42 MHz
HOR	Horizontally polarized horn antenna
ISM	Industrial, Scientific and Medical frequency bands
ISM 2.4	Industrial, Scientific and Medical frequency band at 2.4 GHz
ITS	Intelligent Transportation Systems
LNA	Low Noise Amplifier
LPV	Lateral Precision with Vertical Guidance
LSSM	L Band and S Band Spectrum Measurement system
MDGPS	Maritime Differential GPS
MEO	Medium Earth Orbit
MHz	Megahertz
MMIC	Monolithic Microwave Integrated Circuit
NA	Network Analyzer
NASA	National Aeronautics and Space Administration
NDGPS	Nationwide Differential GPS
NF	Noise Figure
NOAA	National Oceanic and Atmospheric Administration
NTIA	National Telecommunications and Information Administration
RF	Radio Frequency
SA	Spectrum Analyzer
SNR	Signal to Noise Ratio
TAC	Technical Advisory Committee (to the FCC)
TDRS	Tracking and Data Relay Satellite
TV	Television
UNI-S	Unified S Band centered at 2067.5 MHz
UWB	Ultra Wide Band
VER	Vertically polarized horn antenna
WAAS	Wide Area Augmentation System
WiFi	Wireless Fidelity, IEEE 802.11b wireless networking

(This page was left intentionally blank)

Abstract

This report consolidates research carried out at Clemson University and Stanford University where a series of measurements were undertaken to identify the man-made radiation present in four bands used by rather different services, namely, L1 Band (1563.42 – 1587.42 MHz), the Unified S-Band (2025 – 2110 MHz), the 2.4 GHz Industrial, Scientific and Medical (ISM) Band (2400 – 2482.50 MHz), and the 23.6-24.0 GHz Passive Sensing Band. Results show that there were distinctive differences in the measurement data in the frequency bands, which should be expected based on the function/regulation associated with each. The GPS L1 Band had little to none terrestrial man-made sources, but the ISM 2.4 GHz Band had a large number of man-made sources regardless of the site and the time. The Unified S Band showed mixed results depending on the sites. The Passive Sensing Band does not contain appreciable man-made radiation.

1. Introduction

Telecommunications deregulation, globalization, mobile wireless connectivity, and disruptive innovation are only some of the forces driving demand for access to radio frequency spectrum. While demand is elastic, the useful capacity of the radio frequency spectrum continues to be interference limited as governed by Shannon's Law. Examining the noise floor is the starting point for understanding channel capacity and determining spectrum utility as defined by diverse demands for communications quality and reliability.

In many instances, new wireless technologies support applications in unlicensed bands or "underlay" existing services on an unlicensed basis. The use of unlicensed spectrum has fostered many innovative applications in recent years. Without technical, economic or regulatory incentives for self-governance, however, the growth of unlicensed uses may not be sustainable due to degradation of the noise floor environment. Such degradation can harm both current and prospective uses of spectrum as it can undercut the utility of wireless applications for governmental and commercial purposes that require high service quality and reliability.

"The [FCC] Technological Advisory Committee (TAC) has expressed concern that noise floor levels could be 'a very serious emerging problem caused by the explosive growth of both intentional and unintentional radio sources,' a development that could compromise the continued reliability of existing communications systems." [Ref. 1]

"The TAC forsees that we could potentially be entering a period of rapid degradation of the noise environment. Such degradation would reduce our ability to meet the communications needs of the country. The principal negative impacts are likely to be reductions in the performance or reliability of wireless systems or increases in their costs." [Ref. 2]

As a step toward a better understanding of how the noise floor is being affected today and how it may be affected tomorrow, the National Aeronautics and Space Administration (NASA) and US Department of Transportation (DOT) have sponsored research to study the noise floor in selected bands. This study examines whether observed noise floor results are consistent with the applicable regulations governing those bands. As might be expected, NASA is particularly concerned with the noise floor in bands used for crucial safety and scientific purposes.

This document consolidates research carried out at Clemson University [Ref. 3] and Stanford University [Ref. 4] where a series of measurements were undertaken to identify the man-made radiation present in four bands used by rather different services, namely, L1 Band (1563.42 – 1587.42 MHz), the Unified S-Band (2025 – 2110 MHz), the 2.4 GHz Industrial, Scientific, and Medical (ISM) Band (2400 – 2482.50 MHz), and the 23.6 - 24.0 GHz Passive Sensing Band. The GPS Laboratory at Stanford University measured the radio environment in L1, Unified S-Band, and 2.4 GHz ISM Band. The Center for Research in Wireless Communications at Clemson University conducted measurements in the 23.6 - 24.0 GHz Passive Sensing Band. Figure 2 depicts the bands of the FCC Spectrum Allocation Chart that were evaluated in these studies.
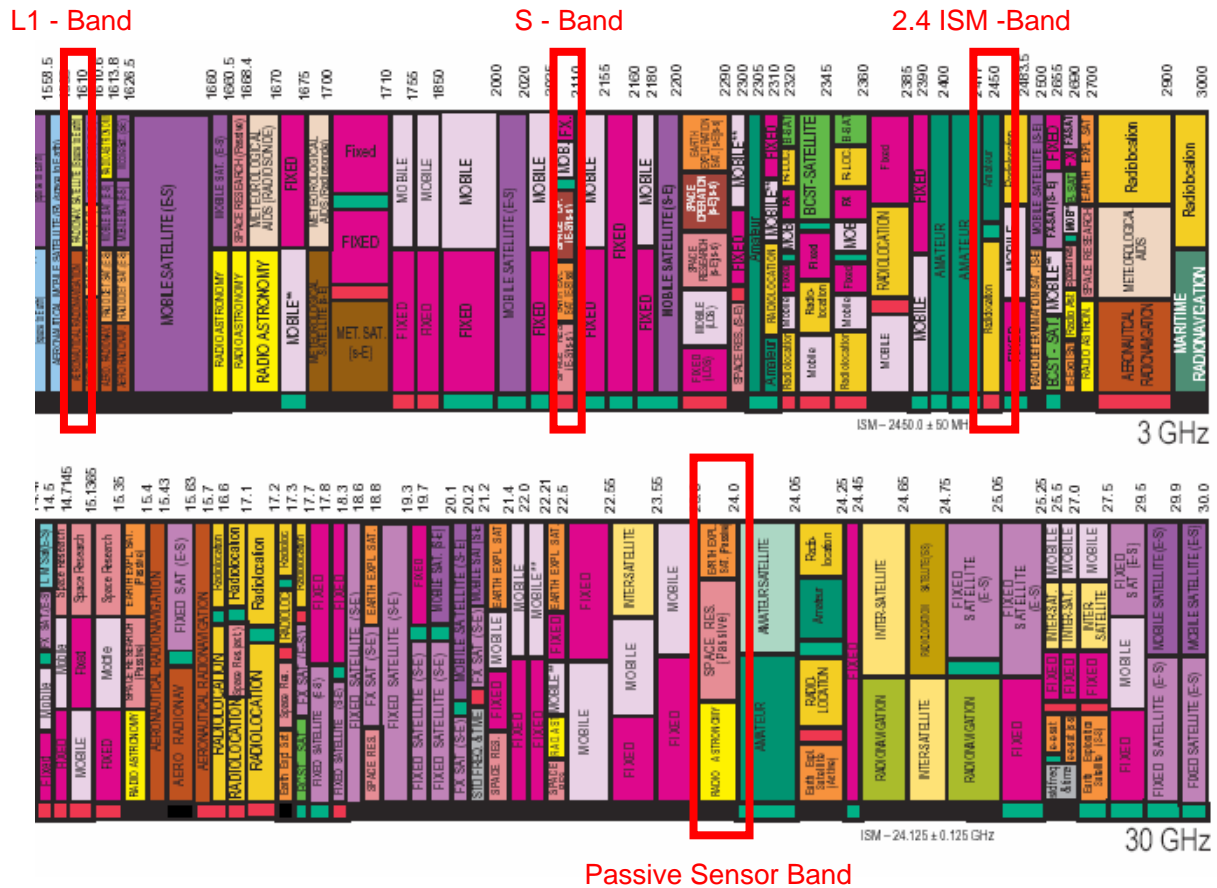
Figure 2: Bands of FCC Spectrum Allocation Chart Evaluated in These Studies

(Allocation Chart from www.ntia.doc.gov)

The Stanford University study measured the radio spectrum in the three bands at eight sites. Two of the sites are downtown in San Jose and Palo Alto. Two sites were remote from densely populated areas - Yosemite Park and the Jasper Ridge Preserve. Two sites are at airports (San Jose and Palo Alto). Two sites are at harbors or marinas (Port of Oakland and Coyote Point Marina).

All eight sites are operationally significant to GPS. Indeed, GPS helps coordinate police and fire efforts in urban areas like San Jose and Palo Alto. It is also an important part of the transportation system in cities. GPS is being integrated into an ever increasing number of cell phones and, in some parts of the country, provides position information that is automatically relayed when users call 911. The Nationwide Differential GPS (NDGPS) is an expansion of the U.S. Coast Guard Maritime DGPS (MDGPS) and provides a single seamless ground-based augmentation to GPS for surface-transportation in critical applications such as Intelligent Transportation Systems (ITS), positive train control, and harbor and harbor entrance navigation. The Wide Area Augmentation System (WAAS) is a satellite-based GPS augmentation and is primarily used in aviation applications such as en-route flight and Lateral Precision with Vertical Guidance (LPV) runway approaches. The GPS signal, however, is broadcast from a constellation of satellites over 20,000 km above Earth's surface and its received power density is only approximately 10^{-13} W/m^2, which makes it more vulnerable to interference compared to a broadcast from the surface.

The Unified S Band is used by the National Aeronautics and Space Administration (NASA) for communication with satellites, and rural sites are used for the ground terminals. Electronic news gathering also uses the Unified S Band. Specifically, TV field operations use this band to transmit their broadcasts back to the station and these TV news vans can certainly be found in urban areas as well as airports and harbors.

The ISM 2.4 GHz Band is a frequency band allocated for unlicensed spectrum use and is finding increased use for technologies such as wireless networks and cordless telephone operations. It also contains radio energy from microwave ovens. The open nature of this band means that applications will vary, but users will be found anywhere and anytime.

The Clemson University study measured the radio spectrum present in the 23.6-24.0 GHz Passive Sensing Band at six sites in South Carolina, North Carolina, and Georgia. The subject band is critical to weather prediction by the National Oceanic and Atmospheric Administration. The frequency range of this band is chosen specifically because of its position on the radiometric peak for water vapor emissions. NOAA weather satellite fleet carries radiometers measuring the presence of water vapor through emissions in this band. These radiometers constitute substantial investment that is in orbit. Loss of the information gained by these radiometers would substantially impair current weather prediction capability.

(This page was left intentionally blank)

2. L, S, and ISM Bands Survey

2.1. Overview

This survey supports a worldwide search for new usable radio spectrum. National spectrum managers are considering increasing allocations for unlicensed spectrum use and allowing increased unlicensed sharing with existing allocations. This test program supports efforts to understand and quantify the current operational environment of radio systems. The data should help to provide a scientific basis for future decisions on spectrum policy. It compares actual radio power measurements made in three rather different radio bands to the power due to natural noise alone. The power density due to natural noise is the product of the Boltzmann's constant and the so-called noise temperature in Kelvin (kT_O). The noise power in a given bandwidth (B) is the noise power density times the bandwidth (kT_OB). In bands used by satellite services, the total measured power should be close to the natural noise floor. After all, the satellites are far away and so the satellite signal power is low. In bands used by terrestrial services, the total measured power may be quite high relative to the natural noise floor. Three rather different radio frequency bands are included in this study. These bands are described in Table 2, which gives the corresponding frequency range, bandwidth, allocation, and regulatory part.

Band	Center Frequency [MHz]	Bandwidth [MHz]	Allocation	Regulatory Part
GPS L1 Band	1575.42	24	Aero-RadioNav Radionav-Sat	Aviation Part 87
Unified S Band	2067.5	85	Space Science Aux Broadcast	Part 74F, Part 78, and Part 101J
ISM 2.4 GHz Band	2441.75	83.5	Fixed & Mobile Radiolocation Amateur	Part 18 and Part 97

Table 2. Frequency Bands Under Study

First, we study the L1 Band used by the Global Positioning System. GPS provides a safety critical service from space. The GPS signal is broadcast from a constellation of some 29 satellites (in January of 2004) that are in medium Earth orbit (MEO). The satellites have an altitude of 20,200 km, which provides global coverage. However, the received signal has low power, because of the path loss. On the Earth's surface, the GPS signal power is below that of the natural noise floor.

Second, we study the Unified S-Band used by the National Aeronautics and Space Administration (NASA) to communicate with satellites. NASA used this band to re-circularize the orbit of TDRS1 (Tracking and Data Relay Satellites) when that spacecraft was in danger. Electronic news gathering also uses the Unified S Band. Specifically, TV field operations use this band to transmit their broadcasts back to the station. As such, the Unified S-Band is shared between terrestrial and space use.

Third, we study the 2.4 GHz band that is allocated for unlicensed use by industrial, scientific, and medical (ISM) use. This band is finding increased use for unlicensed wireless

technologies such as wireless networks and cordless telephone operations. It also contains radio energy from microwave ovens. The open nature of the ISM Band means that applications will vary, but terrestrial users are likely to be anywhere and everywhere.

The three bands find diverse use. The GPS L1 Band is for signals from space to thirty million (or so) users all over the globe, many of whom are involved in activities critical to safety of life. The Unified S Band serves a finite number of fixed sites with satellite signals and then a limited number of terrestrial users. The ISM Band serves an enormous number of terrestrial users that may be found anywhere.

Our study measures radio power in these three bands at a variety of sites. Two of the sites are downtown in San Jose and Palo Alto. Two sites were remote from thickly settled areas - Yosemite Park and the Jasper Ridge Preserve. Two sites are at airports (San Jose and Palo Alto). Two sites are at harbors or marinas (Port of Oakland and Coyote Point Marina). In summary, this report contains a matrix of measurements. We measure the radio spectrum in the three bands that serve very different purposes at eight diverse sites.

This study had the following objectives:

1. At sites of operational significance to GPS, measure the radio environment in the GPS L1 frequency band. For all sites, contrast the measured power to the theoretical value for natural thermal noise (kT_O). Identify site-to-site trends.

2. At sites of operational significance to the users of the Unified S Band, measure the radio environment. For all sites, compare the measured values to the theoretical value for natural thermal noise (kT_O). Identify site-to-site trends.

3. At sites of operational significance to the users of the ISM Band at 2.4 GHz, measure the radio environment. For all sites, contrast the measured power to the theoretical value for natural thermal noise (kT_O). Identify site-to-site trends.

As mentioned earlier, two of our measurement sites are downtown in San Jose and Palo Alto. Two sites were remote from thickly settled areas - Yosemite Park and the Jasper Ridge Preserve. Two sites are at airports (San Jose and Palo Alto). Two sites are at harbors or marinas (Port of Oakland and Coyote Point Marina). All sites are listed and numbered in Table 3, and then mapped in Figure 3. We will use the numbers to identify the sites in the figures to come.

All of these sites are operationally significant to GPS. Indeed, GPS helps coordinate police and fire efforts in urban areas like San Jose and Palo Alto. It is also an important part of the transportation system in cities. GPS is being integrated into an increasing fraction of cell phones. In some parts of the country, GPS provides the position information that is automatically relayed when cell phone users call 911. GPS is also critical in rural areas. It is finding increased application in precision farming and mining. Of course it is an important navigation aid for hikers. Clearly, GPS is important to aviation and therefore critical in the airport environment. Indeed, GPS is included on every new Boeing jet and finds widespread use in regional carriers and general aviation. With the July 10, 2003 commissioning of the Wide Area Augmentation System, GPS is used during the approach procedure as well as enroute flight. Finally, GPS is the primary position-fixing tool used by ships during harbor and harbor entrance navigation. The U.S. Coast Guard maintains a network of DGPS radiobeacons to augment these critical operations.

All of our sites are of operational significance to the users of the Unified S Band. Rural sites are used for the ground terminals of NASA satellite communication. TV news vans use this band to transmit their broadcasts back to the station and can certainly be found in urban areas as well as airports and harbors.

The ISM 2.4 GHz Band is allocated for unlicensed use, and the open nature of this band means that applications will vary, but users will be found anywhere and anytime.

Finally, local site selection is also influenced by logistics. We sought ground level so that our measurement equipment could be delivered easily, because it is heavy. We felt that ground level also best represented the operating environment for most users of the GPS, Unified S and ISM bands. Availability of a stable power supply is also important since batteries could not power a 24-hour measurement campaign. Security was also factored into site selection to avoid measurement interruptions and to ensure the safety of our people.

Category	Index	Site
Urban	1	San Jose Downtown
	2	Palo Alto Downtown
Rural	3	Yosemite Park
	4	Jasper Ridge Preserve
Airport	5	San Jose Airport
	6	Palo Alto Airport
Harbor	7	Port of Oakland
	8	Coyote Point Marina

Table 3. List of Measurement Sites

Figure 3. Measurement Sites (from www.mapquest.com)

2.2 Measurement System

The measurement equipment, the calibration procedure, and the results of those calibration processes are discussed in this section. Previous spectrum surveys [Refs. 5, 6, 7, 8, 9, 10] and standards [Ref. 11] were used to develop the test procedures.

2.2.1 System Design

The multi-band instrument built for the radio power measurement campaign is described in this section. This instrument is used for: the GPS L1 Band (24 MHz centered at 1575.42 MHz), the Unified S-Band (85 MHz centered at 2067.5 MHz), and the 2.4 GHz ISM Band (83.5 MHz centered at 2441.75 MHz). The instrument is called the L and S bands Spectrum Measurement system (LSSM). It has a customized multi-band front end design combined with a spectrum analyzer. The data collection process is automated using a notebook PC and Labview instrument control software to minimize the possibility of human error and provide repeatability in the data collections. Figure 4 shows the LSSM block diagram and Figure 5 a photo.
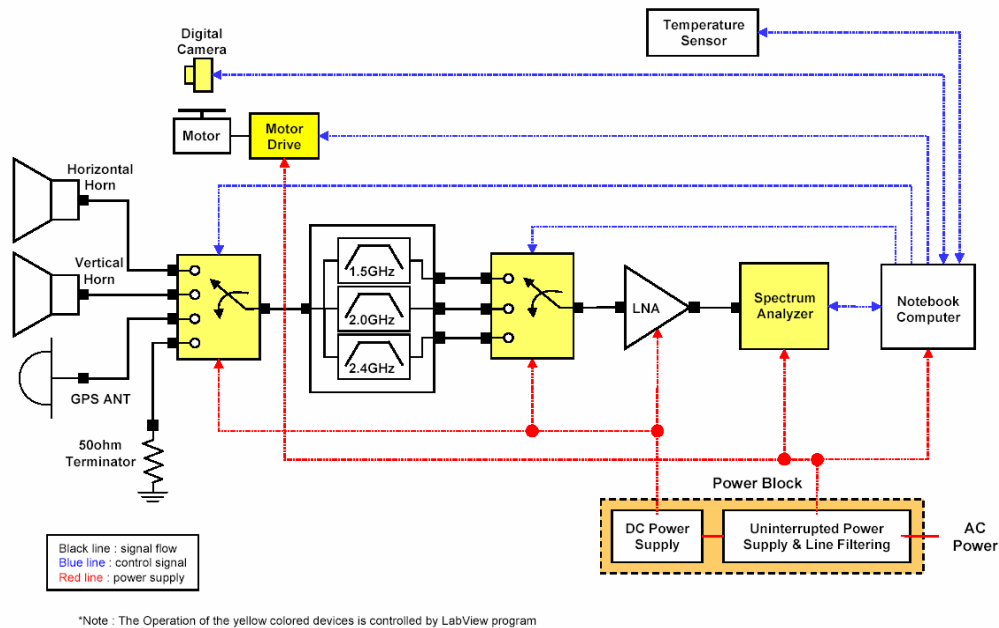
Figure 4. L and S Band Spectrum Measurement System (LSSM)

Two horn antennas, a GPS antenna, and a 50 ohm terminator are used as signal inputs to the system. The three antennas are used to measure radio power (natural noise plus man-made signals). The two horn antennas are used to azimuthally localize any man-made signals. The first horn antenna is horizontally oriented to capture the horizontally polarized signal and the second horn antenna is vertically oriented to capture the vertically polarized signal. The GPS antenna has a nearly hemispherical pattern directed skyward like an operational GPS antenna. The 50 ohm terminator is used for a reference measurement approximately equal to the natural noise floor. It is used to validate the health of the antenna measurements.

The directional horn antennas amplify the man-made signals from sources near the horizon when they come under the main lobe of the antenna gain pattern. However, the natural noise will not be amplified if the noise background has a uniform noise temperature, and thus the measurement results by a directional antenna and ones by an omni-directional antenna are same

9

in this case. Therefore, the measurement data will be presented without compensation for antenna gain to avoid a bias on measurements of the natural noise floor which can be introduced by the gain compensation process. Readers should be notified that the spectrum survey results are dependent on the type of a measurement antenna when man-made signals exist in the measured spectrum. The horn antenna gain is 12.3 dBi at 1.5 GHz, 14.5 dBi at 2.0 GHz, and 15.9 dBi at 2.4 GHz at its main lobe of the gain pattern. The GPS antenna is nearly hemispherical antenna but still has directivity, 5 dBi at the GPS L1 Band at its main lobe of the gain pattern.

The LSSM front end includes: three custom cavity bandpass filters, a low noise amplifier (LNA) and two RF switches used to route the signal inputs. The RF switches are used to implement a fully automatic measurement system, which operates without any human intervention during the measurement campaign. The design is a mechanical relay type switch with fairly low loss (< 0.2 dB) and low impact on the noise figure. The filter bank is located prior to the LNA in order to remove out-of-band-emissions (OOBE) from the measurements and prevent LNA signal overloads. The cavity filters have low insertion loss (< 1.0 dB). The overall loss caused by the two RF switches and the filter bank is less than 1.4 dB.

A spectrum analyzer measures the power spectrum of an incoming signal. A notebook computer controls all components, and data is recorded on a hard disk in the computer. A stepping motor is used for azimuth scanning providing repeatability with high accuracy. A temperature sensor records the ambient temperature and the temperature of the LNA. A site photo is taken by a built-in digital camera right after each measurement to monitor the activities in the surrounding area and provide information to investigate possible man-made signal sources.
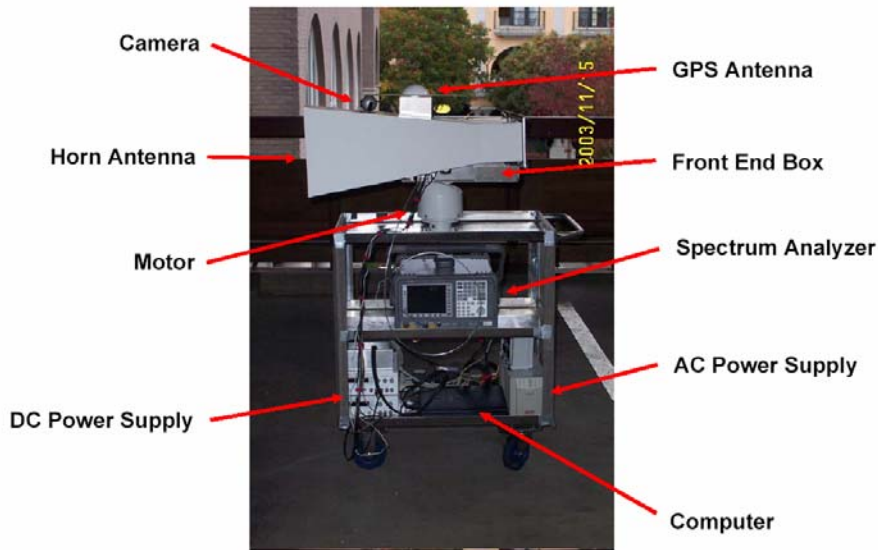
Figure 5. Photo of LSSM

The component list of the LSSM is given in Table 4 with the model number and related specifications.

Equipment	Model	Relevant Specification
Horn Antenna	Q-par Angus, QH7N	Frequency = 1.2 ~ 2.5 GHz Gain = 10.2 ~ 16.3 dBi
GPS Antenna	AIL, DM C146	Frequency = 1.56 ~ 1.59 GHz Gain = 5 dBi
Filter Bank	Delta Microwave, 3 Band Cavity Filter Bank	Center Frequencies = 1575.42, 2067.5, 2441.75 GHz Loss = 1.0 dB (Max)
RF Switch 1	Narda, SEM143D	4 to 1 switch Frequency = DC ~ 18 GHz Loss = 0.2 dB (Max) (DC-3GHz) Isolation = 80 dB (Min)
RF Switch 2	Narda, SEM133DT	3 to 1 switch Frequency = DC ~ 18 GHz Loss = 0.2 dB (Max) (DC ~ 3 GHz) Isolation = 80 dB (Min)
LNA	MITEQ, AFS3-01500250-10-10P-4	Frequency = 1.5 ~ 2.5 GHz Gain = 40 dB (Min) Noise figure = 1.0 dB (Max)
Spectrum Analyzer	Agilent, E4404B	Frequency = DC ~ 6.7GHz
Notebook Computer	Sony, VAIO FXA63	
Digital Camera	Logitech, QuickCam Pro 4000	
Temperature Sensor	Supco, LOGiT LT2	Temperature Range = 0 ~ 60 °C Accuracy = +/- 0.5 °C
Motorized Mount	Pelco PS20	Stepper motor Operating Voltage = 24 VAC
Motor Drive	Ultrak DTMRX	Operating Voltage = 24 VAC
Transformer	Ultrak CC-TX2440	Supply Voltage = 24 VAC
LabView Software	National Instrument LV6.1	
PCMCIA(GPIB) card	National Instrument NI-488.2M	Connection between computer and Spectrum Analyzer
PCMCIA(DAQ) card	National Instrument DAQCard-DIO-24	Connection between computer and RF switch
DC Power Supply 1	Agilent E3611A	Supply Voltage = 0 ~ 35 V (0.85 A max),
DC Power Supply 2	Agilent E3630A	Supply Voltage = -20 ~ +20 V (0.5 A max),
Uninterrupted Power Supply & Line Filtering	APC Smart-UPS 700	Full time multi-pole noise filtering, Surge voltage let-through 0.7% Capacity = 700VA/450W,

Table 4. LSSM Component List

(This page was left intentionally blank)

2.2.2 Calibration

The following subsections describe: the system power gain calibration, the noise figure calibration, the dynamic range calibration, and the temperature sweep calibration.

Gain Calibration

The gain calibration measures the front end power gain of the LSSM for all input paths and the frequency bands under study. As shown in Figure 6, the LSSM is divided into three parts for the purpose of the calibration: the antenna, the LSSM front end (filter bank, switch, LNA and cable), and the spectrum analyzer. The spectrum analyzer, Agilent E4404B, was calibrated by Agilent Technologies Inc. on June 26, 2003, and the antenna gain is provided by the manufacturer. A network analyzer, the Agilent 8714ES, is used to measure the gain of the LSSM front end, and all calibrations are based on an average of 64 measurements. These gain calibrations are conducted before and after a spectrum survey at a measurement site. This care is required, because the LSSM front end and antenna rotates continuously during the spectrum survey, and the cable from the LSSM front end to the spectrum analyzer is flexed as these subsystems rotate. Hence, the calibration is used to detect any failures due to this flexure.

There are ten signal paths based on the allowable combinations of the four input ports and the three frequency bands. Each path is separately calibrated. Figure 4 shows schematically the RF components of the LSSM. Calibration points are shown with blue dashed lines and blue labels.
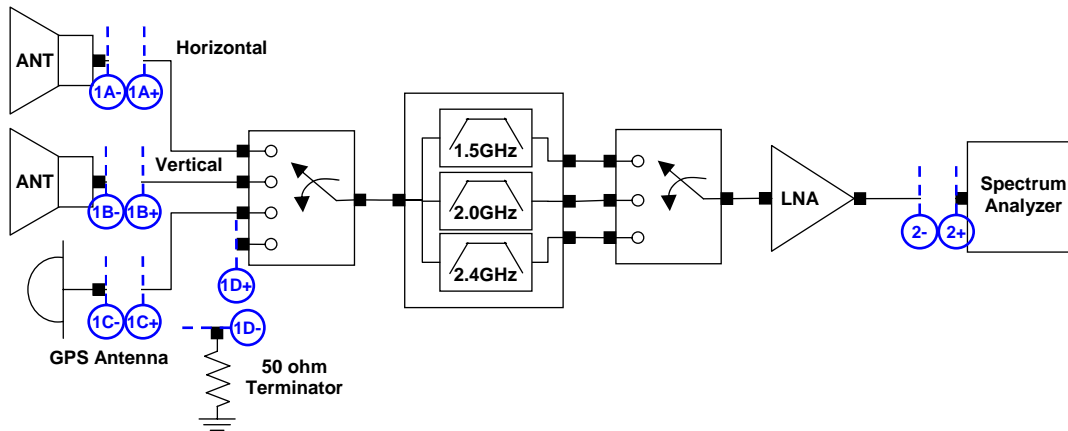
Figure 6. LSSM Gain Calibration Test Setup

The received signal is amplified by the LSSM and then measured by the spectrum analyzer. Therefore, the original received signal power can be obtained by subtracting the overall gain of the LSSM from the measured signal power. The overall gain is the sum of the gain and the loss of the LSSM.

$$P_{ANT} = P_{SA} - (G_{ANT} + G_{FE} - L_{FE})$$

where G_{ANT} = Antenna gain provided by the manufacturer
  G_{FE} = Front end gain measured by the network analyzer from cal. point 1+ to point 2–
  L_{FE} = Front end loss due to impedance mismatch
  P_{SA} = Signal power measured by the spectrum analyzer
  P_{ANT} = Signal power received by the antennas

13

As mentioned in Section 2.2.1 the antennas do not amplify the natural noise if the noise background has a uniform noise temperature. Therefore, the antenna gain, G_{ANT}, is considered as 0 dB in this study.

L_{FE} is the loss due to impedance mismatch. When the input impedance and the output impedance are not matched, a certain portion of the incoming signal is reflected back to the source and the received power becomes less than the delivered power. To measure this loss, the network analyzer was used to measure the impedance at each denoted junctions, 1A–, 1A+, 1B–, 1B+, 1C–, 1C+, 1D–, 1D+, 2–, 2+. The power loss due to the mismatch is calculated and factored into the overall gain. Frequency sweeping measurements are made for the full width of each band, because the measured quantities are functions of frequency.

The measured impedance at each junction is used to determine a power reflection coefficient accounting for the impedance mismatch and the corresponding loss.

$$\Gamma = \frac{Z_+ - Z_-}{Z_+ + Z_-}$$

where Γ = Reflection coefficient
   Z_- = Source impedance
   Z_+ = Load impedance

The loss can be obtained from the reflection coefficients at each junction.

$$L_{FE} = (1 - |\Gamma_1|^2) \cdot (1 - |\Gamma_2|^2)$$

where Γ_1 = Reflection coefficient between the antennas and the LSSM front end
   Γ_2 = Reflection coefficient between the LSSM front end and the spectrum analyzer
   L_{FE} = front end loss due to mismatch

Table 5 summarizes our front end gain calibration. As shown, the gain is slightly different for ten channels and varies between 36.8 and 38.8 dB. The loss also varies slightly between 0.2 and 0.6 dB. The overall gain is between 36.6 and 38.2 dB. For the purpose of presentation, the average value as a function of frequency is calculated and provided. Hence, the readers might note minor discrepancies in the table if an attempt is made to compute the overall gain from the gain and the loss given in the table. The overall gain is calculated based on the gain and loss versus frequency rather than the average values below.

Average Gain & Loss [dB]	GPS L1				UNI-S			ISM 2.4		
	HOR	VER	GPS	50ohm	HOR	VER	50ohm	HOR	VER	50ohm
Gain (avg)	37.1	37.2	36.8	37.4	37.7	37.8	38.0	38.5	38.5	38.8
Loss (avg)	0.2	0.2	0.3	0.2	0.4	0.3	0.3	0.6	0.6	0.6
Overall Gain	36.9	36.9	36.6	37.1	37.4	37.4	37.7	37.9	38.0	38.2

Table 5. LSSM Gain and Loss Calibration Data

Noise Figure Calibration

This section discusses the calibration of noise figure including the test procedure and results. There are several methods to measure noise figure, and the gain method described here is usually used for high gain systems. Noise figure is defined as follows.

> "Noise figure (NF): Of an active device, over the bandwidth of interest, the contribution by the device itself to thermal noise at its output. The noise figure is usually expressed in decibels (dB), and is with respect to thermal noise power at the system impedance, at a standard noise temperature (usually 20°C, 293 K) over the bandwidth of interest. It is determined by (a) measuring (determining) the ratio, usually expressed in dB, of the thermal noise power at the output, to that at the input, and (b) subtracting from that result, the gain, in dB, of the system." [Ref. 12]

In this report, the reference temperature is set at 23°C instead of 20°C to keep consistency with the LNA calibration data provided by the manufacturer calibrated at 23°C. Both 23°C and 20°C are commonly used as the standard noise temperature and the difference between them is minimal, 0.04dB. "Thermal noise power at the system impedance, at a standard noise temperature" can be obtained when the LSSM input is connected to the reference load at the system impedance, 50 ohm at 23°C and the system gain can be obtained by the gain calibration explained in the previous section. Therefore, noise figure can be measured as follows.

$$NF \quad = \text{Output Power} - \text{Front End Gain} - \text{Thermal Noise Power}$$

$$= P_{SA} - (G_{FE} - L_{FE}) - kT_0B$$

where NF $= $ LSSM noise figure
       P_{SA} $=$ Measured signal power by the spectrum analyzer
       G_{FE} $=$ front end gain
       L_{FE} $=$ front end loss
       k $=$ Boltzmann constant, 1.38×10^{-23} [J/°K]
       T_0 $=$ Room temperature, 23°C
       B $=$ Bandwidth of interest

Figure 7 displays the test setup and part numbers for the noise figure. The reference loads were drawn from the Agilent calibration kit.
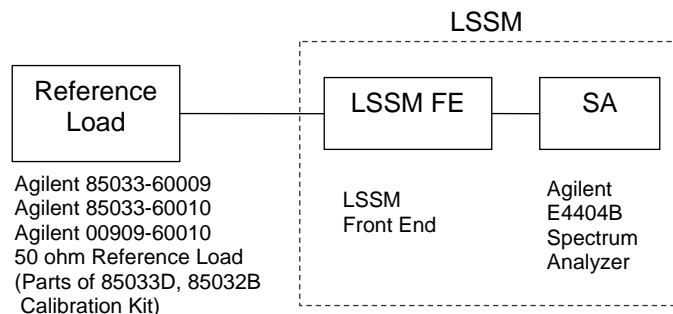
Figure 7. LSSM Noise Figure Calibration Test Setup

The output power is measured by averaging 4800 traces, and Table 6 gives the results. As shown, the noise figure is varies between 2.5 and 3.1 dB for our ten channels of interest. The high noise figure of GPS antenna is due to the longer cable to the LSSM front end.

	GPS L1				UNI-S			ISM 2.4		
	HOR	VER	GPS	50 ohm	HOR	VER	50 ohm	HOR	VER	50 ohm
Noise Figure [dB]	2.84	2.78	3.11	2.63	2.53	2.46	2.27	2.76	2.75	2.55
System Intrinsic Noise Floor [dBm/MHz]	-114.2	-114.4	-113.7	-114.7	-114.9	-115.1	-115.5	-114.4	-114.4	-114.9
System Intrinsic Noise Temperature [K]	273.6	264.8	310.1	245.9	233.8	225.4	203.1	262.9	261.5	236.9

* Note: System Intrinsic noise floor and noise temperature represent the noise generated by the LSSM itself excluding all external sources.

Table 6. LSSM Noise Figure Data

Dynamic Range Calibration

This section describes the dynamic range calibration including the test procedure and results. Figure 8 depicts the test setup. The dynamic range calibration measures the power gain of the LSSM front end over the range of expected input power, -114 ~ -60 dBm/MHz. This measurement determines the linearity of the power gain. A white noise generator with a fixed output power is used as a noise source and the noise power is adjusted by an attenuator. The resulting white noise with variable power is delivered to the LSSM through the port for the 50 ohm terminator, and the resulting noise power is measured by the spectrum analyzer by averaging 100 traces.
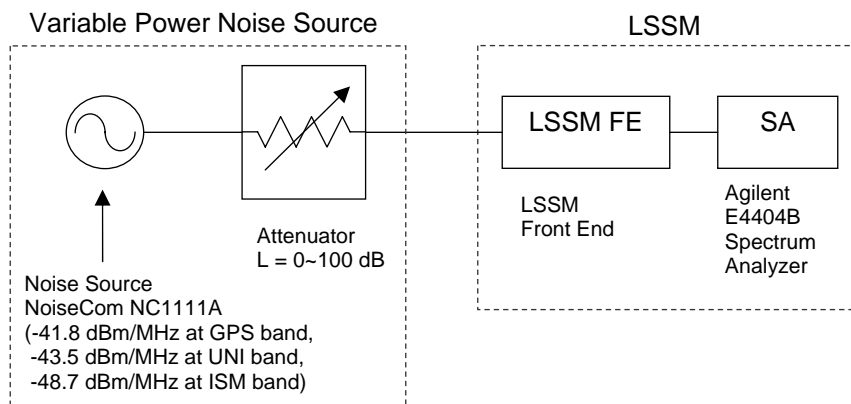
Figure 8. LSSM Dynamic Range Calibration Test Setup

The results of the dynamics range calibration are shown in Figure 9. As shown, the LSSM front end is linear over the expected range of inputs powers from -114 ~ -60 dBm/MHz. In fact, it continues to be linear to higher power levels between -60 and -50 dBm/MHz. Above -50 dBm/MHz, the LNA saturates and linearity is not preserved. Below -114 dBm/MHz, the self-noise of the LSSM front end becomes evident. At these low levels, the spectrum analyzer only can observe the system noise rather than the input noise.
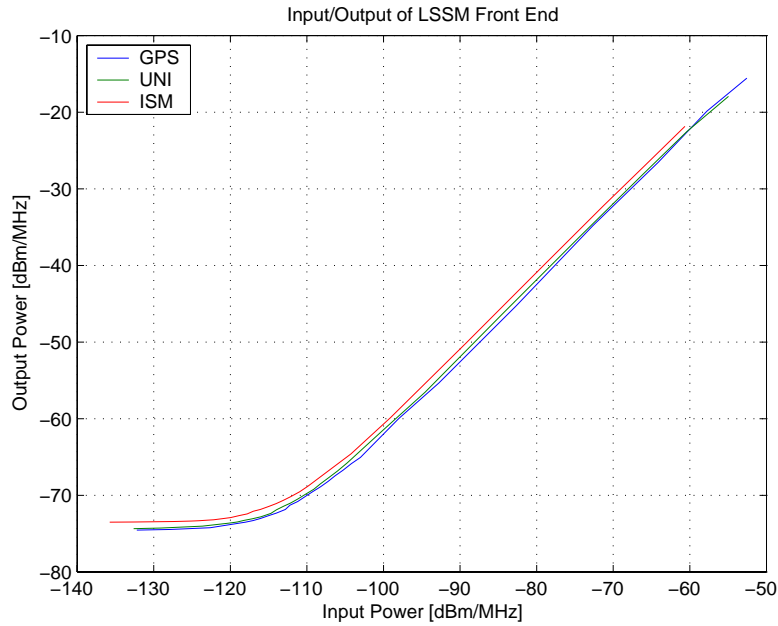
Figure 9. LSSM Dynamic Range Calibration Data

Temperature Sweep Calibration

This section describes our temperature sweep tests, including the test procedure and results. Figure 10 depicts the test setup. The temperature sweep calibration is aimed to measure the power gain of the LSSM front end over the range of the expected temperature, $0 \sim 40$ °C. The low noise amplifier (LNA) is known to be temperature sensitive and its gain sensitivity is approximately -0.01 dB/°C/stage. The LNA of the LSSM has three stages and hence the overall sensitivity is approximately -0.03 dB/°C. To compensate for this gain variation, the temperature is recorded every minute during the spectrum survey. The gain is recalculated based on the recorded temperature and the gain reduction rate of 0.03 dB/°C referenced to the room temperature 23 °C. The tests described in this section are to validate the gain sensitivity.
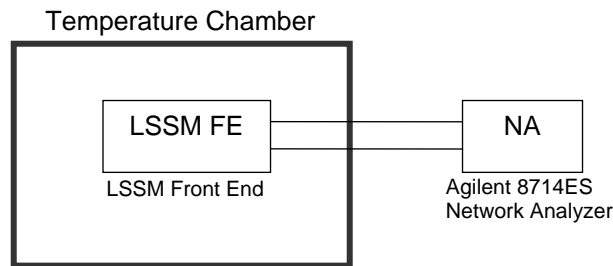
Figure 10. LSSM Temperature Calibration Test Setup

The LSSM front end is placed inside a temperature controlled chamber and its input and output are connected to the network analyzer. The gain is measured at nine discrete temperature points, 0, 10, 15, 20, 23, 26, 30, 35 and 40 °C. Each measurement allows sufficient time to stabilize the temperature. The spectrum analyzer averages 64 traces to measure the gain.

17

Figure 11 shows our measurements along with the expected gain based on -0.03 dB/°C. As shown, the expected gain sensitivity proves to be accurate over the expected temperature range of 0 to 40 °C. Consequently, this sensitivity is adopted for our temperature calibration.
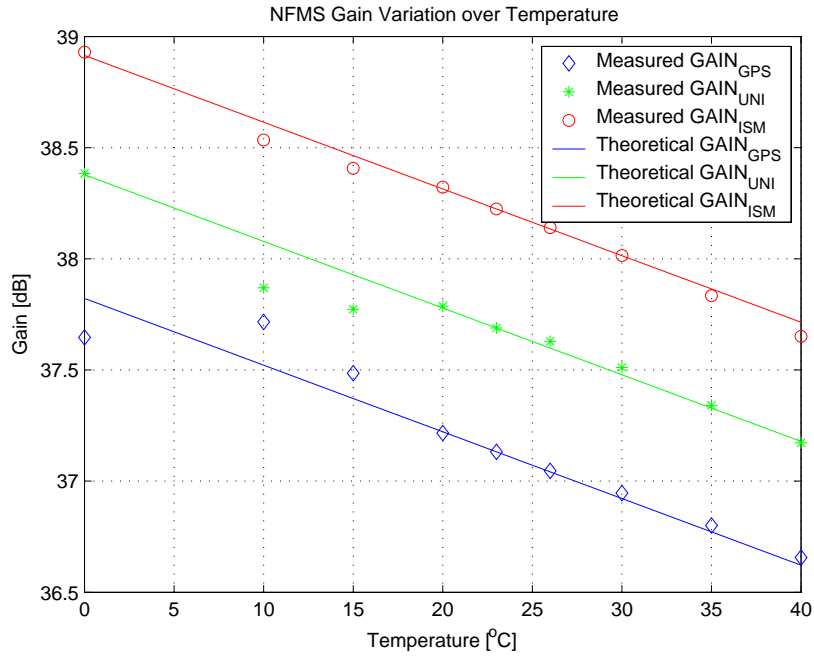
Figure 11. LSSM Gain Variation over Temperature

2.3 Measurement Procedure

Our procedure measures the radio environment over the course of a full day including early morning and late night (In a few cases, logistics prevented measurements after midnight.). The measurement cycle starts early in the morning and is repeated every hour. Each hour, the following ten measurement are made:

- GPS L1 Band – Horizontal horn, Vertical horn, GPS antenna, 50 ohm terminator
- Unified S Band – Horizontal horn, Vertical horn, 50 ohm terminator
- ISM 2.4 GHz Band – Horizontal horn, Vertical horn, 50 ohm terminator

The power spectrum traces are collected using the spectrum analyzer's (Agilent E4404B) sample detector and stored on the computer's hard disk without any data processing. No averaging or peak detection is used in data collection in order to maintain the characteristics of the random noise signals. At the post-processing analysis stage, the average and the distribution of the collected raw data are calculated. The following procedure is taken to measure the power spectrum at each measurement site.

Site survey: The site survey is conducted at the measurement site at least a day prior to the spectrum survey as follows:

1) Ensure the existence of a stable 110 AC power supply at the measurement site.
2) Ensure that the measurement site is at least 2 m away from pedestrian paths and at least 5m away from conspicuous radio sources.
3) Ensure the security of the measurement site.
4) Photograph the sites and record a detailed description.

Pre-measurement calibration: Calibrate the LSSM in accord with Section 2.2.1 and record the results.

Spectrum measurements: The actual measurements are executed as follows:

1) Set up the LSSM as shown in Figure 3 with one horn antenna oriented for horizontal polarization, and the second horn antenna oriented for vertical polarization and pointed to magnetic north. Set up the GPS antenna with its boresight directed vertically. All antennas should be 1.0 to 2.0 meters above the ground level to approximate the height of a handheld radio. Ensure that the LSSM components are not in direct sunlight so they will remain within their specified temperature range.
2) Level/plumb the antenna platform to ensure that it is horizontal.
3) Turn on the LSSM and wait for 20 minutes to ensure that the electronic systems have stabilized (constant temperature and the calibrated gain). Three minutes is a typical time constant for RF components. Thus five time constants with an additional 5 minute margin are used to ensure stabilization.
4) Execute a **Pre-measurement run** with the 50 ohm terminator at all frequency bands to ensure the proper operation of the LSSM.
5) Select the measurement start time and end time.
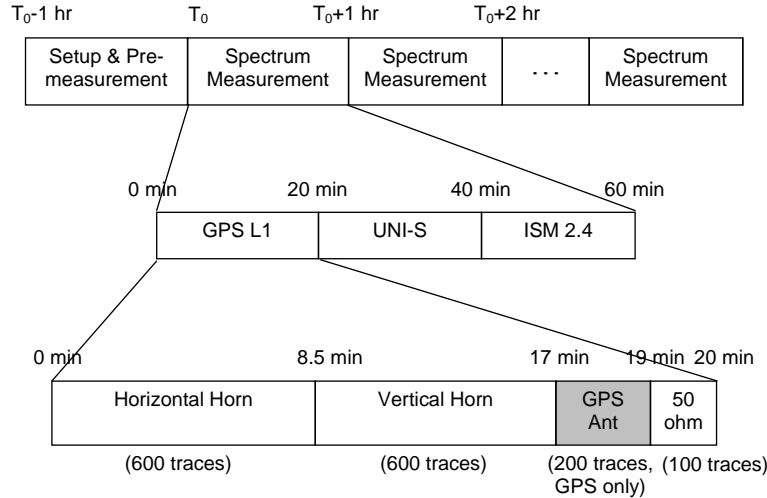
Figure 12. Measurement Cycle

Collected Traces per Hour	GPS L1				UNI-S			ISM 2.4		
	HOR	VER	GPS	50 ohm	HOR	VER	50 ohm	HOR	VER	50 ohm
	600	600	200	100	600	600	100	600	600	100

Table 7. Number of Collected Traces per Measurement Cycle

6) Follow the measurement schedule in Table 7 and Figure 12. For each measurement, the LSSM control software sets the center frequency, the frequency span, the resolution bandwidth, and the video bandwidth of the spectrum analyzer as shown in Table 8. The control software also switches to the desired frequency band and antenna type. The resolution bandwidth and the video bandwidth were chosen according to ANSI C63.4-2001 [Ref.11].

Band	Center Frequency [MHz]	Frequency Span [MHz]	Resolution Bandwidth [MHz]	Video Bandwidth [MHz]	Sweep Time [ms]	Detector Type	Measurement Bins
GPS L1	1575.42	24	1	1	4	Sample Detector	401
UNI-S	2067.5	85	1	1	4	Sample Detector	401
ISM 2.4	2441.75	83.5	1	1	4	Sample Detector	401

Table 8. Spectrum Analyzer Setting Parameters

7) The signal power spectrum in the frequency band is measured by the spectrum analyzer. Twenty-five (25) individual traces are recorded onto the computer hard disk with a picture of the site taken with the installed digital camera. The following measurement details are also recorded: the antenna type, the frequency band, the time, and the location. The temperatures of the ambient environment and the primary amplifier are recorded every minute by an independent thermometer.

8) The horn antenna is rotated clockwise in 15° increments. Fifteen degree increments adequately resolve the spectrum environment, because the antenna has a 3dB beamwidth between 22° and 38°.
9) Steps 7 and 8 are repeated until the antenna angle reaches 360°.
10) Steps 6 to 9 are repeated with the vertical horn antenna.
11) For GPS L1 Band measurements, Steps 6 and 7 are repeated with the GPS antenna until 200 individual traces are collected.
12) Steps 6 and 7 are repeated with the 50 ohm terminator until 100 individual traces are collected.
13) Steps 6 to 12 are repeated at the remaining frequency bands, the Unified S Band and the ISM 2.4 GHz Band.
14) Steps 6 to 13 are repeated every one hour according to the schedule specified in Step 6.

Post-Measurement Calibration: The post-measurement gain calibration is performed the day after the measurement campaign. The procedure follows the '*gain calibration*' subsection under 2.1.2.2 (Calibration), and the result is recorded. If the difference between the pre-measurement and post-measurement calibration is greater than +/-1.5 dB, then the measurement data is discarded and the measurement is repeated.

(This page was left intentionally blank)

2.4 Data Analysis Methods

This section describes our data analysis. As described earlier, we have radio power spectrum measurements from eight sites: two urban, two rural, two airports, and two harbors. At each site, the data is collected for a period of 15 ~ 24 hours, and this data is broken into measurement cycles that are repeated every hour. During each of these cycles, radio power in three frequency bands: GPS L1, UNI-S and ISM 2.4, are measured; and four signal inputs, the horizontal horn, the vertical horn, the GPS antenna, and the 50 ohm terminator, are used (see Figure 10). With the directive horn antennas, the LSSM rotates with a 15 degree step and measures the power spectrum at 24 angular points. We organize this data by site and then by frequency band, and so we have 24 data sets (8 sites times 3 bands).

Each of these 24 data sets is subject to four different analyses:
- Temporal analysis
- Spectral analysis
- Angular analysis
- Statistical analysis

These analyses give the power variation with time, frequency, angle, and probability.

The temporal analysis shows the signal variation over time and seeks any correlation between the received power and the ebb and flow of human activities through the day. It is also used to seek any connection to the operation of conspicuous electronic equipment in the immediate environment. The spectral analysis shows the power spectrum of the measured signals and reveals the power, bandwidth, and center frequency of any man-made signals that are in band. The angular analysis shows the direction of any man-made signals. If the received power is high at a specific angle, we can examine the photograph taken in that direction. Finally, the statistical analysis shows the power histogram of the measured signal. Any deviation from the distribution for thermal noise would suggest a man-made radio signal. The histogram estimates the probability of man-made signals at the measurement site.

Each of our four analyses results in a summary figure, and these figures are color coded as follows:
- Green : Natural thermal noise floor at 23 °C
- Blue : Horizontally polarized horn antenna
- Red : Vertically polarized horn antenna
- Cyan : GPS antenna
- Black: 50 ohm terminator

2.4.1 Temporal Analysis

The temporal analysis is straightforward, and the resulting plot gives power level in dBm/MHz versus local time. The plot gives one point per hour (per measurement cycle) and each point is the mean of the power spectrum in the hour. Thus, there are 24 points corresponding to 24 measurement cycles if the measurement lasted for the full 24 hours.

Figure 13 is an example outcome. The green line is the natural thermal noise floor assuming no man-made signal, and the blue line gives the measurement data by the horizontal horn antenna for 24 hours. Noise power was greatest at 8 PM (local time) and another peak occurred after midnight. At all times, the measured power was above the natural noise floor. This indicates that man-made RF activities occur for all day and night in the ISM Band near Stanford graduate student housing. This suggests that Stanford students work all night and use WiFi to deliver their homework assignments via email. Of course, the observed signals could also be due to microwave ovens filled with popcorn!
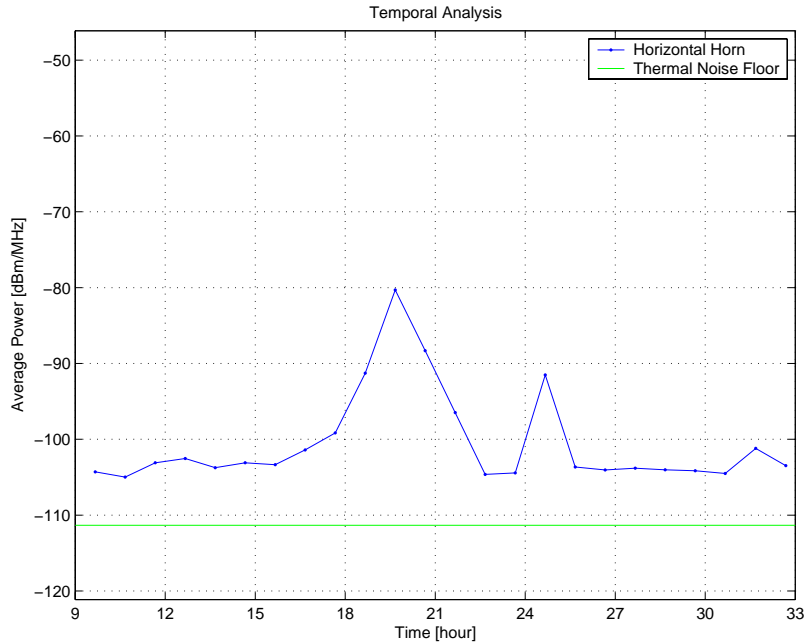
Figure 13. Example of Temporal Analysis

(Spectrum survey at Stanford graduate housing in ISM 2.4 GHz Band used as an example)

2.4.2 Spectral Analysis

The spectral analysis is also straight-forward and results in plots of power level (in dBm/MHz) versus frequency (in MHz). Each point is the mean power measured at the selected frequency. Figure 14 is an example outcome. The green line gives the natural thermal noise floor and assumes no man-made signal. The blue line is the mean power spectrum measured by the horizontal horn antenna for 24 hours. The highest power was received at 2455 MHz, and many narrow band signals are observed across the ISM Band. Once again, man-made activity is conspicuous at all frequencies.
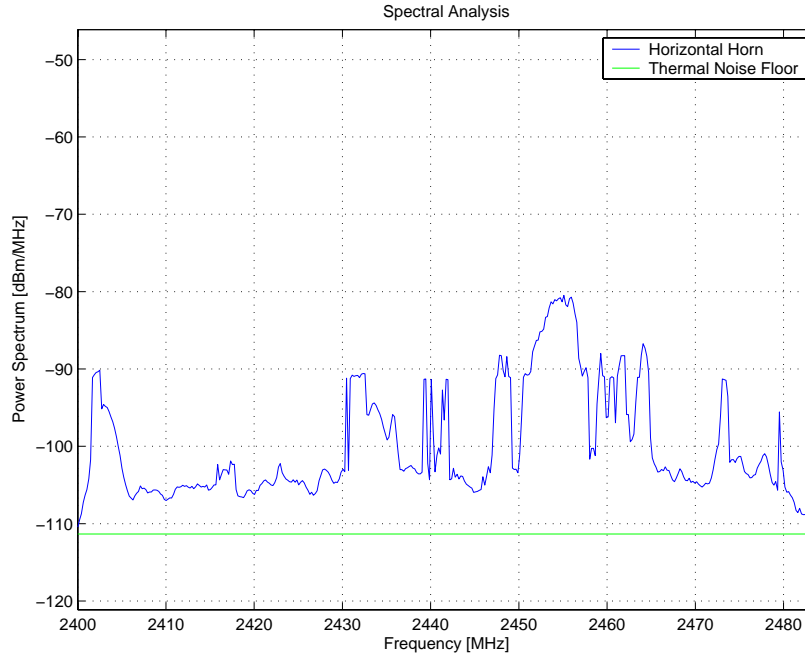
Figure 14. Example of Spectral Analysis

(Spectrum survey at Stanford graduate housing in ISM 2.4 GHz Band used as an example)

2.4.3 Angular Analysis

The angular analysis results in a plot of power level (in dBm/MHz) versus antenna direction (in degrees) with true North at 0 degree and all other angles are measured in a clockwise direction. Our measurements are made every 15 degrees, and so there are 24 angular points in a trace. The beamwidth of the horn antennas is wider than 20 degrees, and therefore the 15 degrees increment is narrow enough to capture the RF activity at all angles. Each point is the mean of the received power at the corresponding angle over the entire measurement time at a given site.

Figure 15 is a sample outcome. The green line gives the natural thermal noise floor assuming no man-made signal. The blue line gives the measurement data from the horizontal horn antenna for 24 hours. The highest power was received at an angle of 30 degrees corresponding to a graduate housing building, and the lowest power was observed at 180 degrees corresponding to an open space. At all angles, the receiver power was higher than the natural noise floor.
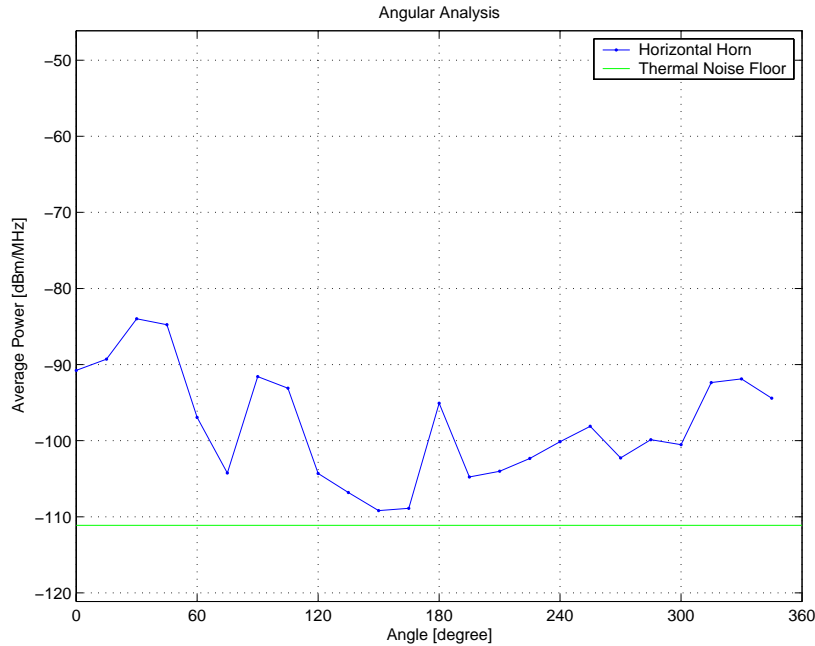
Figure 15. Example of Angular Analysis

(Spectrum survey at Stanford graduate housing in ISM 2.4 GHz used as an example)

26

2.4.4 Statistical Analysis

The statistical analysis seeks deviations from the mean behavior measured by the temporal, spectral, and angular analyses. It gives the rate at which power deviations were observed as a function of the size of the deviation. We use the amplitude probability distribution (APD), which gives the probability that the receiver power exceeds a certain value. For comparison, our APD plots also give the theoretical APD for thermal noise. The power for thermal noise is exponentially distributed, and so the corresponding APD plots as a straight line on a log scale.

$$p(n) = \frac{1}{\mu_N} e^{-\frac{n}{\mu_N}}$$

$$A(n) = \Pr(N > n) = \int_{n}^{\infty} p(x)dx = e^{-\frac{n}{\mu_N}}$$

where N   = Noise power
     μ_N = Average of noise power
     p(n)   = Probability density function of noise power
     Pr(N>n) = Probability that N exceeds n
     A(n)   = APD of noise power

If the measurements contain man-made signals, then the mean power will increase and the APD will follow a non-exponential distribution.

Figure 13 is an example outcome from our statistical analysis. It plots the power level (in dBm/MHz above kT_0B+NF) versus the percentage of measurements exceeding the specified power level. The green line is the APD for the natural thermal noise floor assuming no man-made signal. The blue line is the APD for the measured data from the horizontal horn antenna for 24 hours. The entire measurement set is used as the sample population in this analysis.

The impact of man-made signal is conspicuous in Figure 16. In the upper left part of the figure, the blue line deviates significantly from the green line indicating the existence of the man-made signals. The deviation occurs at low percentage levels, because the man-made signals do not occur all of the time. The measurement APD does not deviate at high percentage levels, because man-made signals do not affect the majority of the measurements.

APD could be used to measure the percentage of man-made signal among the power spectrum measurement data containing both the natural thermal noise and man-made signals. One way to do such task is to read the point where the distribution of the measured data and the theoretical distribution deviate from each other, but it is often too ambiguous to obtain accurate value. Another way is to set a threshold value which is not observable in the natural noise and to find a percentage of the measured data surpassing the limit. If there is no man-made signal, the percentage of data which is higher than 10 dB above the mean of the thermal noise floor, $\mu + 10$ dB, is 0.00454 %. Because we only consider APD as low as 0.01 % in this study, the value higher than such limit should not be seen. In the following example, we can find this percentage by drawing a straight line from Y axis at 10 dB parallel to X axis until it meets with distribution curves and reading the percentage of joint points. Without man-made signals, this percentage is less than 0.01 %. With the actual measurements, this percentage rises to approximately 4 %. In other words, there were 4 % of man-made signals contained in the measurement data.
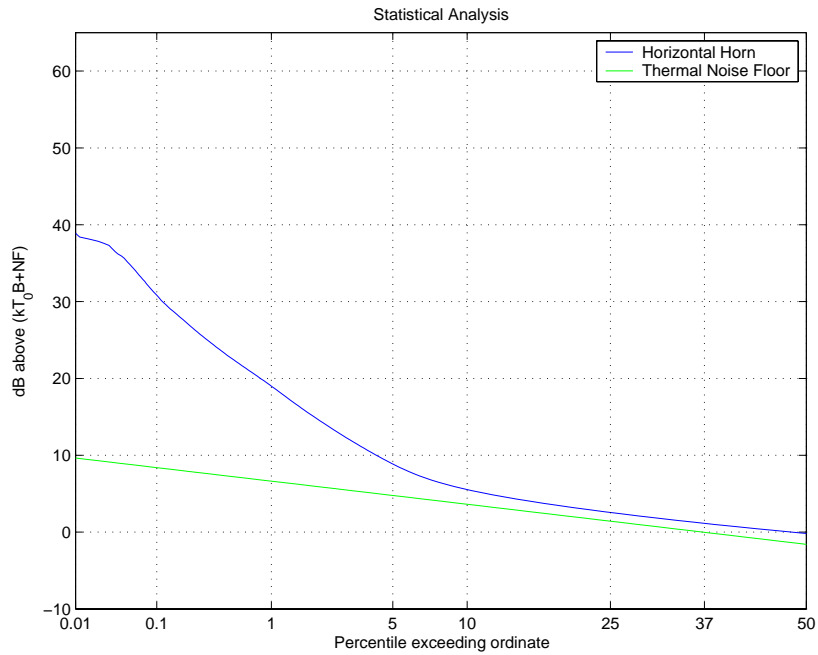
Figure 16. Example of Statistical Analysis

(Spectrum survey at Stanford graduate housing in ISM 2.4 GHz Band is used as an example)

2.5 Results

The eight measurement sites for the investigation were selected from the San Francisco Bay Area. The measurement campaign was initiated on August 28th and continued until November 15th for all autumn season in the moderate weather conditions typical of the San Francisco Bay Area. The measurement data is presented with the corresponding analysis plots, and we also provide notes that describe the site conditions and any obvious RF activities. The results are presented in the order shown in Table 9. Refer to Appendix A for the detailed measurement data.

Category	Site	Measurement Date	Measurement Time
Urban	San Jose Downtown	Oct 21 ~ 22	24 hours
	Palo Alto Downtown	Nov 5 ~ 6	24 hours
Rural	Yosemite Park	Nov 14 ~15	24 hours
	Jasper Ridge Preserve	Oct 9 ~ 10	24 hours
Airport	San Jose Airport	Oct 7 ~ 8	24 hours
	Palo Alto Airport	Sep 4	16 hours
Harbor	Port of Oakland	Oct 30	15 hours
	Coyote Point Marina	Aug 28	16 hours

Table 9. Measurement Sites and Schedule

The result of the spectrum survey is summarized on comparison between the frequency bands and the measurement sites. Distinctive differences were found in the measured power spectrum in the three frequency bands under study and also at the rural sites against the rest of the sites.

2.5.1 Band by Band Observation

There were distinctive differences in the measurement data in the three frequency bands, which should be expected based on the function/regulation associated with each. The GPS L1 Band was mostly quiet, but the ISM (2.4 GHz) Band was mostly noisy regardless of the site and the time. The Unified S Band showed mixed results depending on the sites.

GPS L1 Band

In all measurement sites, the average received power was approximately equal or less than the thermal noise floor and with very rare appearances of man-made signals. Table 10 displays the average received power and the percentage of man-made signals found among the measurement data at each site. Green represents quiet places, yellow indicates the existence of man-made signals, and orange implies severe man-made signals. Except the urban sites, all sites were green.

At the rural sites, the Palo Alto Airport and the Coyote Point Marina, no man-made signal was detected. The average received power was always below the thermal noise floor and

maintained the constant level showing that the natural thermal noise floor is quite constant regardless of site and time. At the urban sites, the San Jose Airport and the Port of Oakland, man-made signals were detected. However, they were contained in less than 0.02% of the measurement data observed only once and occupied minor portion of the spectrum with the bandwidth less than 1 MHz and consequently did not contribute significantly to the average received power. It is presumed to have been originated from a single source at a nearby building at each site, but the sources were not identified.

The GPS signals were visible just above the thermal noise floor in most of the sites except the Palo Alto Downtown where the measurement was conducted inside of a parking structure (a building with the open sides but with the shielded roof blocking the line of site GPS signal). At the other sites, the GPS signal rose over the background noise floor with maximum 2 dB elevation as is expected. The GPS signal from the individual GPS satellites is approximately 15 dB lower than the thermal noise floor, but the collective signal powers combined with antenna gain provide sufficient spectral detection capabilities.

Category	Site	Average Received Power* [dBm/MHz]				Percentage of Man-Made Signals* [%]		
		HOR	VER	GPS	50 ohm	HOR	VER	GPS
Urban	San Jose Downtown	-111.0	-111.7	-112.0	-111.6	0.01	0.01	0.01
	Palo Alto Downtown	-111.5	-110.7	-111.2	-111.7	0.00	0.02	0.01
Rural	Yosemite Park	-112.1	-112.3	-112.5	-111.9	0.00	0.00	0.00
	Jasper Ridge Preserve	-112.1	-112.3	-112.2	-111.8	0.00	0.00	0.00
Airport	San Jose Airport	-112.5	-113.4	-112.8	-111.7	0.01	0.00	0.00
	Palo Alto Airport	-112.3	-112.7	-112.5	-111.7	0.00	0.00	0.00
Harbor	Port of Oakland	-112.9	-113.3	-112.9	-111.7	0.00	0.01	0.00
	Coyote Point Marina	-111.9	-112.2	-112.3	-111.4	0.00	0.00	0.00

* Note: In the columns of the average received power, green indicates that the measurement is lower than the 50 ohm measurement. Yellow indicates that the measurement is no more than 5 dB higher than the 50 ohm measurement. Orange indicates that the measurement is more than 5 dB higher than the 50 ohm measurement.

** Note: In the columns of the percentage of man-made signals, green indicates no man-made signal or existence of man-made signals in no more than 0.05 % of measurement data. Yellow indicates existence of man-made signals in more than 0.05 % and no more than 2 % of measurement data. Orange indicates existence of man-made signals in more than 2 % of measurement data. All readings are based on APD plots and instead of the percentage for each antenna, the worst of them is presented.

Table 10. Average Received Power and Existence of Man-Made Signals (GPS L1)

A spectrum survey of the GPS L1 Band was conducted in the Los Angeles area in 2002 and the measurement results are shown in Table 11 [Ref. 10]. The results are in accordance with our study which is based on the measurements at a wider range of sites and times and with the automated spectrum survey technique to new frequency bands with great sensitivity.

Site	Average Received Power [dBm/MHz]	
	GPS	50 ohm
El Segundo	-113.2	-113.8
Culver City	-113.1	-113.0
Malibu	-112.2	-112.4
Century City	-112.5	-112.2

Table 11. Power Spectrum Measurements in GPS L1 Band

Unified S Band

The Unified S Band is found to be quiet except for man-made signals which are presumed to have been transmitted from remote television sources. All detected signals were located at a specific set of frequencies and excluding these left no other distinguishable man-made signals observed. The average received power was highly dependent on the proximity to the downtown area where more television operations are expected to be in use. In Table 12 there is a mixture of colors displaying the high variance of the power spectrum depending on the locations.

Category	Site	Average Received Power* [dBm/MHz]			Percentage of Man-Made Signals* [%]	
		HOR	VER	50 ohm	HOR	VER
Urban	San Jose Downtown	-109.2	-107.9	-111.4	1.35	1.67
	Palo Alto Downtown	-111.4	-110.6	-111.5	0.01	0.06
Rural	Yosemite Park	-111.8	-111.9	-111.6	0.00	0.00
	Jasper Ridge Preserve	-111.7	-111.9	-111.5	0.00	0.00
Airport	San Jose Airport	-77.4	-75.9	-111.4	6.45	8.71
	Palo Alto Airport	-112.0	-112.4	-111.4	0.00	0.01
Harbor	Port of Oakland	-106.9	-101.7	-111.6	2.23	2.77
	Coyote Point Marina	-110.9	-111.4	-111.4	0.40	0.30

Table 12. Average Received Power and Existence of Man-Made Signals (UNI-S)

At the rural sites and the Palo Alto Airport no man-made signal was detected, and the average received power was below that of thermal noise floor. But at the rest of locations, the urban sites, the harbor sites, and the Port of Oakland, man-made signals were detected. The San Jose Airport, the Port of Oakland, and the San Jose Downtown locations showed significant levels of RF activities within this band. In contrast, the data from Palo Alto Downtown and Coyote Point Marina contained a small percentage, less than 0.40 %, of man-made signals observed once. The measured man-made signals were mainly found at the specific set of frequencies, 2034, 2050, 2068, 2085, and 2101 MHz, which are specified for television.

ISM 2.4 GHz Band

At all measurement sites, the average received power was well above the thermal noise floor. The ISM 2.4 GHz Band, in particular, exhibited significant levels of man-made signals regardless of time and location. As depicted in Table 13, all sites are displaying the severe man-made signal levels.

Category	Site	Average Received Power* [dBm/MHz]			Percentage of Man-Made Signals* [%]	
		HOR	VER	50 ohm	HOR	VER
Urban	San Jose Downtown	-83.1	-84.4	-111.1	6.08	4.50
	Palo Alto Downtown	-92.2	-89.8	-111.3	4.35	3.58
Rural	Yosemite Park	-85.1	-82.5	-111.4	0.62	0.78
	Jasper Ridge Preserve	-97.1	-100.8	-111.3	2.64	3.67
Airport	San Jose Airport	-82.2	-89.8	-111.2	17.12	26.73
	Palo Alto Airport	-92.5	-101.7	-111.1	13.68	10.22
Harbor	Port of Oakland	-87.6	-78.7	-111.4	34.37	43.30
	Coyote Point Marina	-88.8	-80.8	-111.1	7.10	22.31

Table 13. Average Received Power and Existence of Man-Made Signals (ISM 2.4)

However, even within this band there was still an observable difference between the rural locations and the rest of sites. The detected man-made signals sources at the rural sites were one or two nearby identifiable objects while those at the other sites resulted from significant numbers of unknown objects. At the Yosemite Park, the average received power was below the thermal noise floor in a majority of the time. The man-made signals were observed only in the morning and the evening and are expected to have been originated from microwave ovens considering the discontinuous appearance and the high power. At the Jasper Ridge Preserve, the man-made signal was detected only in a single direction and is presumed to have originated from a WiFi transmitter operating in the area. At the remainder of the sites man-made signals dominated the complete ISM spectrum and provided with few opportunities when the observations were at the expected thermal noise levels. The average received power was always above the thermal noise floor and the man-made signals were detected in more than 3.5 % of the measurement data. The band was occupied with a mixture of narrow band and wide band signals and consequently caused the average received power to be higher, a maximum 33 dB, than the thermal noise floor. They are expected to have originated from multiple unknown sources with various types of operation including WiFi transmitters, cordless telephones, microwave ovens, and various consumer products.

2.5.2 Site by Site Observation

There are similarities between the urban sites, the airport sites and the harbor sites in their RF environments, but the observations from the rural sites are generally distinct. The rural sites were relatively quiet when compared with the other sites.

Urban Sites

In the urban sites, man-made signals were detected in all bands (Table 14). But the measurements in the GPS L1 Band contained detected levels of man-made signals in very limited portions of the collected data, less than 0.02 %, and the average received power was still approximately equal to the thermal noise floor. Contrastingly, in the ISM 2.4 GHz Band there was a significant amount of RF activity and the average received power was maximum 29 dB higher than the thermal noise floor. In the Unified-S Band, there were man-made signals but less than the ISM 2.4 GHz Band. These results follow what is expected based on the regulatory specifications for each of the bands.

Site	GPS L1				UNI-S			ISM 2.4		
	HOR	VER	GPS	50 ohm	HOR	VER	50 ohm	HOR	VER	50 ohm
San Jose Downtown	-111.0	-111.7	-112.0	-111.6	-109.2	-107.9	-111.4	-83.1	-84.4	-111.1
Palo Alto Downtown	-111.5	-110.7	-111.2	-111.7	-111.4	-110.6	-111.5	-92.2	-89.8	-111.3

* Note: All numbers are in dBm/MHz

Table 14. Average Received Power (Urban)

Rural Sites

At the rural sites, no man-made signal was detected in the GPS L1 Band and the Unified S Band. In both of these bands the average received power was below that of the thermal noise floor. However, in the ISM 2.4 GHz Band, man-made signals were detected, and the resulting average received power was above that of the thermal noise floor (Table 15).

Site	GPS L1				UNI-S			ISM 2.4		
	HOR	VER	GPS	50 ohm	HOR	VER	50 ohm	HOR	VER	50 ohm
Yosemite Park	-112.1	-112.3	-112.5	-111.9	-111.8	-111.9	-111.6	-85.1	-82.5	-111.4
Jasper Ridge Preserve	-112.1	-112.3	-112.2	-111.8	-111.7	-111.9	-111.5	-97.1	-100.8	-111.3

* Note: All numbers are in dBm/MHz

Table 15. Average Received Power (Rural)

Airport Sites

At the airport sites, each band showed unique RF environment. The GPS L1 Band was generally quiet, but in the ISM 2.4 GHz Band there was a significant amount of RF activity. In the Unified-S Band, the San Jose Airport had significant activity while the Palo Airport was quiet (Table 16).

Site	GPS L1				UNI-S			ISM 2.4		
	HOR	VER	GPS	50 ohm	HOR	VER	50 ohm	HOR	VER	50 ohm
San Jose Airport	-112.5	-113.4	-112.8	-111.7	-77.4	-75.9	-111.4	-82.2	-89.8	-111.2
Palo Alto Airport	-112.3	-112.7	-112.5	-111.7	-112.0	-112.4	-111.4	-92.5	-101.7	-111.1

* Note: All numbers are in dBm/MHz

Table 16. Average Received Power (Airport)

Harbor Sites

In the harbor sites, RF environments were shown again to be distinctively different in each band. The GPS L1 Band was generally quiet but in the ISM 2.4 GHz Band there were significant levels of RF activities. In the Unified-S Band, the airport sites were noisy but less than in the ISM 2.4 GHz Band. (Table 17)

Site	GPS L1				UNI-S			ISM 2.4		
	HOR	VER	GPS	50 ohm	HOR	VER	50 ohm	HOR	VER	50 ohm
Port of Oakland	-112.9	-113.3	-112.9	-111.7	-106.9	-101.7	-111.6	-87.6	-78.7	-111.4
Coyote Point Marina	-111.9	-112.2	-112.3	-111.4	-110.9	-111.4	-111.4	-88.8	-80.8	-111.1

* Note: All numbers are in dBm/MHz

Table 17. Average Received Power (Harbor)

2.6 Summary

The results from each frequency Band tested were quite unique as should be expected based on the varying regulations for each of the bands. The GPS L1 Band is a strictly controlled and protected band. Measurement at the GPS L1 Band displayed no or very rare appearances of man-made signals at all sites. The Unified S Band showed the mixed result. It is used for space science but also exposed to commercial use such as the auxiliary channel for TV broadcasting. Approximately half of the sites were relatively quiet, but in the rest of the sites, those in proximity to urban areas, significant levels of man-made signals were measured. The ISM Band is the most open band and is believed to be the most heavily used frequency band of the three tested. At all measurement sites, the band was fully occupied by the strong man-made signals.

- The 1.5 GHz GPS Band is relatively pristine (quiet).
- The 2.0 GHz Band has emissions due to non-Government services.
- The 2.4 GHz ISM Band is discernibly noisier than the foregoing bands.

The results from the rural sites were mostly quiet with the exception of the ISM 2.4 GHz Band while the urban sites, the airport sites and the harbor sites shared the close similarity in their noisy spectral environment. Rural areas are less populated and therefore are supposed to contain lower level of man-made signals compared to urban areas. It was true in the GPS L1 Band and the Unified S Band and only the natural noise floor was observed. But the ISM 2.4 GHz Band was shown to be the exception as a result of the high penetration of microwave ovens, cordless phones, and WiFi transmitters even into rural areas. Those devices are virtually ubiquitous and truly leave no place free of the man-made signals. In urban areas, man-made signals were detected in all bands. The measurements from the ISM 2.4 GHz Band contained significant levels of detectable man-made signal at all time periods and in all directions thus reflecting the high number of man-made signal sources. The Unified S Band was also with the strong man-made signals, but only in limited directions. The results from the GPS L1 Band also contained the man-made signals, but only in limited times and in limited directions. The airport sites and the harbor sites did not show much difference from the urban sites which is believed to be related to their proximity to urban areas.

- Urban areas are noisier than rural environments.
- Airports and harbors are generally similar to urban areas.

Based on the measurement data, the spectral environment was shown to be just what we expected based on the regulations. In the protected bands where strict regulations are applied, the spectrum was nearly free of interference and mostly only the natural thermal noise floor was observed. In the open bands where less strict regulations are applied, the spectrum was full of man-made signals and the natural thermal noise floor was hardly observed.

- In open bands, the power spectrum is far above the thermal noise floor.
- In protected bands, the power spectrum is close to the thermal noise floor.

In other words, the reality of the radio spectrum faithfully reflects the applied regulation within it and therefore the existing regulations are able to successfully support and protect the individual spectrum use as allocated. In the protected band, the spectrum is kept clean and thus secure and stable service is guaranteed. In the open bands, the spectrum is frequently noisy and therefore limits the effective range and increases susceptibility to communication failure but the

applications in those bands can tolerate such environment and the spectrum shows the highest density in terms of usage per bandwidth.

- Regulation determines reality in radio frequency environments.
- Open spectrum allows more applications but brings limitation to performance.
- Protected spectrum allows less applications but guarantees stability of critical systems.

Taken together, the measurement data and the analysis in this study send a message – *regulation must be very sensitive to the function of the band, because the rules determine the radio environment.* Each band supports different types of applications. Some of them are critical systems not tolerating any sort of operation failures and need to be protected from interferences. Some of them can tolerate certain level of failure and work even under severe interferences while requiring more bandwidth. The spectrum policy has been sensitive to such various objectives and requirements of RF applications and the corresponding function of the individual frequency bands. The spectral environment has been successfully managed ensuring the stable operation of applications and the best utilization of the frequency bands by properly allocating the frequency bands to each category of applications and locating them with sufficient spectral distance and adopting application sensitive regulations. To continue such success and sustain the radio frequency environment for current and future users, the same level of sensitivity should be applied to the introduction of any new spectrum policy or any new RF applications with the consideration of the current spectral environments based on which the existing applications are designed and operating successfully.

3. Passive Sensor Band Survey

3.1 Overview

Increasing demand for spectrum posed by an ever-growing collection of wireless applications poses pressure on many existing spectral allocations. The recent Federal Communications Commission Report and Order on Ultra-Wideband (UWB) spectral assignment [Ref. 13] has triggered special alarm to those who hold stewardship over the Global Positioning System (GPS) and over the so called "science bands." While the current Report and Order does not directly threaten these bands, expansion and/or change in level of the UWB envelope is under discussion and such an expansion could affect GPS and Science Bands.

This document reports a series of measurements undertaken to identify the man-made radiation present in the 23.6-24.0 GHz Passive Sensing Band. The measurements establish a baseline against which to judge interference in future years should interference sources emerge. The subject band is critical to weather prediction by the National Oceanic and Atmospheric Administration. The frequency range of this band is chosen specifically because of its position on the radiometric peak for water vapor emissions—*i.e.*, it is dictated by a particular behavior existing in nature, thereby precluding any arbitrary relocation of the band. Figure 17 (a) shows a segment of FCC spectral allocation chart with the science band at the extreme left. Figure 17 (b) shows emission peak for water vapor with the band located thereon. Moreover, the NOAA weather satellite fleet carries radiometers measuring the presence of water vapor through emissions in this band. These radiometers constitute substantial investment that is in orbit. Loss of the information gained by these radiometers would substantially impair current weather prediction capability.
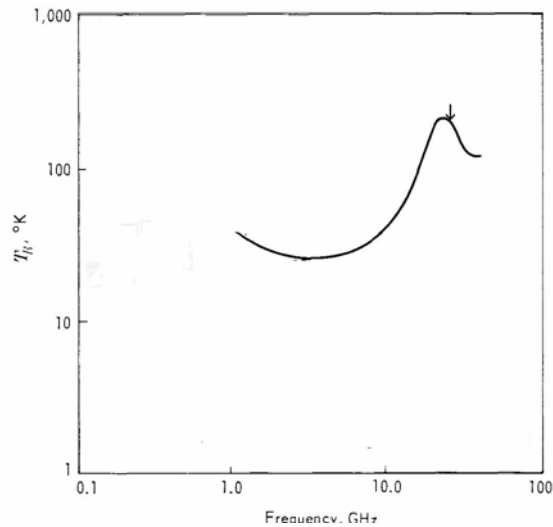
Figure 17. (a) Segment of FCC Spectrum Allocation Chart with Passive Sensing Band at Left; (b)H_2O Emission Spectrum With Location of Band Marked With Arrow

The Center for Research in Wireless Communication (CRWC) at Clemson University has made measurements in the passive sensor band and neighboring bands from 23.3 to 24.3 GHz. The measurements were undertaken with an instrument fabricated from state-of-the-art air cooled Monolithic Microwave Integrated Circuits (MMICs). The resulting instrument manifests a noise floor that is on the same order as the natural emission noise level from atmospheric water vapor. Indeed, data reported herein show that emissions are visible above instrument noise floor at some sites, while at other sites, the water vapor emission is hidden below the instrument noise floor. While it is possible to used cooled low-noise amplifiers to ensure that the instrument noise floor is always below emissions present, such an undertaking was beyond the scope of the present effort. The present survey is intended to identify the extent to which man-made signals might encroach currently into the passive sensor band, and the instrument sensitivity is adequate to indicate significant man-made incursions into the band.

This report describes the measurement system and results obtained from a diverse collection of sites in South Carolina, North Carolina, and Georgia. Measurements were made between 7:00 AM and 11:00 PM at each site. Specific sites are as follows:

- Oconee County Airport (South Carolina)

- Adjacent to Lake Hartwell near the Clemson University campus

- The high point of the Blue Ridge Parkway in Western North Carolina

- Atlanta Hartsfield-Jackson Airport

- Downtown Atlanta from a site atop the Electrical Engineering Building at Georgia Institute of Technology

- A rural site overlooking Interstate Highway 85 near Anderson, South Carolina

3.2 Measurement System

3.2.1 System Design

Clemson University has developed a radio frequency (RF) measurement system to assess the noise within the frequency range of 23.3 to 24.3 GHz. The system block diagram of the original design is shown in Figure 18. At these frequencies, the system is
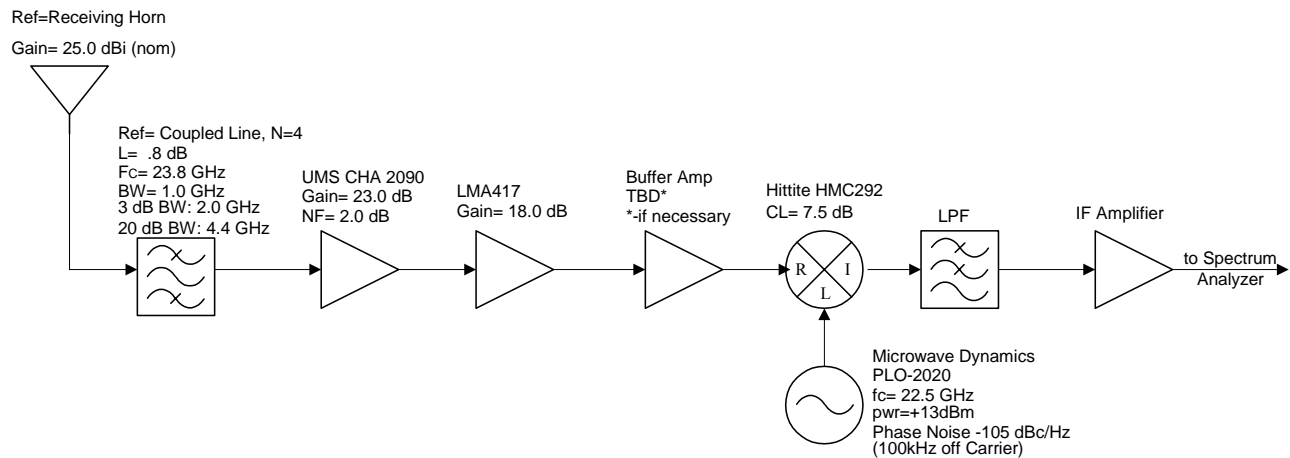
Figure 18. Block Diagram of 23.3 - 24.3 GHz Receiver Design

best realized in a hybrid fabrication using MMICs. These circuits are mounted on Rogers Duroid® microwave printed circuit board using silver-loaded epoxy. Connections to transmission lines on the circuit board are made with wirebond connections. The performance of this system is set by specifications of state-of-the-art off-the-shelf components. The key features being a 2.0 dB noise figure in the low-noise amplifier (United Monolithic Semiconductor CHA2090) and a microstrip preselection filter (A lower noise MMIC has become available since the design reported here was finalized. The Fujitsu FMM5701X LNA manifests a noise figure of 1.5 dB.). The in-band attenuation of this filter was designed to be less than 1 dB in the frequency band from 23.3 to 24.3 GHz.

The theoretical noise performance of this system is defined by its total noise figure which is a function of the gain and noise figure of each element in the chain above. The noise figures of the first few elements in the receiver chain present themselves most heavily in this calculation. The theoretical noise figure of the designed system is 3 dB.

After the input signal is amplified, it is down converted from the 23.3-24.3 GHz band to the range .7-1.7 GHz by mixing with a 22.6 GHz low-phase-noise local oscillator.

The reader is referred to Appendix B where the calibration procedure for the system is spelled out in detail (obtained from Ref. 14).

3.2.2 System Fabrication and Performance

The design in Figure 18 was changed to that in Figure 19 below because the second-stage amplifier (LMA 417 in Figure 18) proved to require a relatively complex biasing network in order to operate reliably.
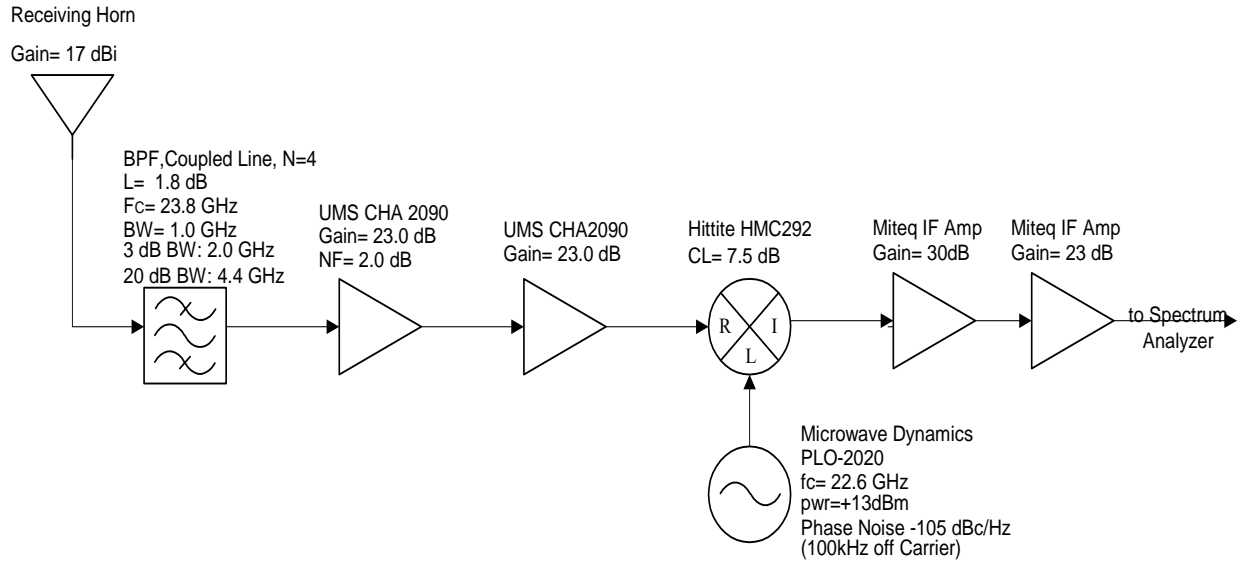
Figure 19. Block Diagram of 23.3-24.3 GHz Fabricated Receiver

Prior to assembly of the system, all amplifiers used were tested and found to be in compliance with the manufacturer's specifications. The testing of the microstrip preselection filter was performed, and it was found that the in-band attenuation of the filter was less than 1.8 dB for the range from 23.3 GHz to 24.3 GHz.

Measurements of the noise figure were performed using the Agilent 8973A Noise Figure Analyzer and HP 346C noise source according to the manufacturer's specifications for measuring the noise figure of a downconverting device with a fixed Local Oscillator [Ref. 15]. The results are given in Figure 20 (a). Attenuators have been inserted to verify the linearity of the noise figure of the receiver (linear within .4 dB over a 20 dB range).

The discrepancy in the theoretical and measured noise floor is due to a few factors. One factor is the fact that the noise figure of the LNA could range as high as 3 dB. Also, the input attenuation of the filter is 1.8 dB, rather than the .8 dB specified in the design section. If 1 dB is added in for connector losses, the result is a 6 dB noise figure, which matches up with the measured results.

The noise power associate with the noise figure is given by

$$P = 10\log(kB) + 10\log(T_{Source} + (F-1)T_0) + 30,$$

where k is Boltzman's constant ($1.38*10^{-23}$ Watts/(Kelvin*Hertz)); B is the Bandwidth in which the power is measured; T_0 is the temperature in of the system in degrees Kelvin; G is the gain of the receiver; and F is the noise figure of the system. (This expression is explained more fully in Appendix B, which is taken from Reference 14). The noise power is plotted in Figure 20 (b). In

40

the course of executing the measurements, two refinements to the system suggested themselves and were implemented. The first refinement came after measurement at the first field site (Oconee County airport). Oscillations in the system were observed at 23.36, 23.40, and 23.50 GHz. These oscillations reduced the gain and gain linearity in the system. (These two detrimental effects influenced the Oconee County Airport results negligibly. Measurements were conducted using only 15 dB of the dynamic range so that degraded linearity was minimal. The system noise floor observed with the spectrum analyzer was unchanged after the oscillations were eliminated.)

These oscillations were reduced by loading the shield casing for the circuit with microwave absorbing material. The gain increased by 24 dB after this modification, which was compensated by and adjustment of the input attenuation at the spectrum analyzer input. The second refinement was made after the first Hartsfield-Jackson measurements. In the configuration used there and in previous measurements, the first IF amplifier and the cable attached to it had proved mechanically problematic. A shift in the support structure led damage to the amplifier and cable in mid-afternoon at the Hartsfield-Jackson site. System gain was sufficiently high that this amplifier could be removed, compensating for the lost gain by reducing attenuation at the spectrum analyzer input. Therefore, the system gain following 9/24/03 was decreased by 30 to 40 dB. Table 18 shows this change between the two Hartsfield-Jackson measurements.

Measurement Site	System Gain (dB)	Compression at 30 dB range (dB)	SA input attenuation (dB)	1st IF amplifier present?
Oconee Airport	50	2	0	Yes
Lake Hartwell Dike	82.1	1.8	70	Yes
Blue Ridge Parkway	74.0	1.1	70	Yes
Atlanta Airport (9/24/03)	83.8	1.4	70	Yes
Atlanta Airport (10/22/03)	43.1	1.1	0	No
I-85 Anderson (4/16/04)	41.3	0.6	0	No
Georgia Tech (5/11/04)	45.3	1.9	0	No

Table 18. Comparison of System Parameters for All Measurement Sites.
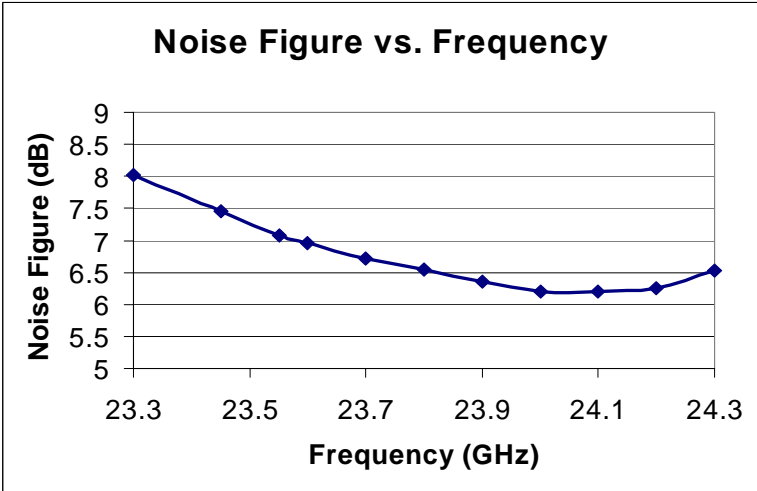
(a)
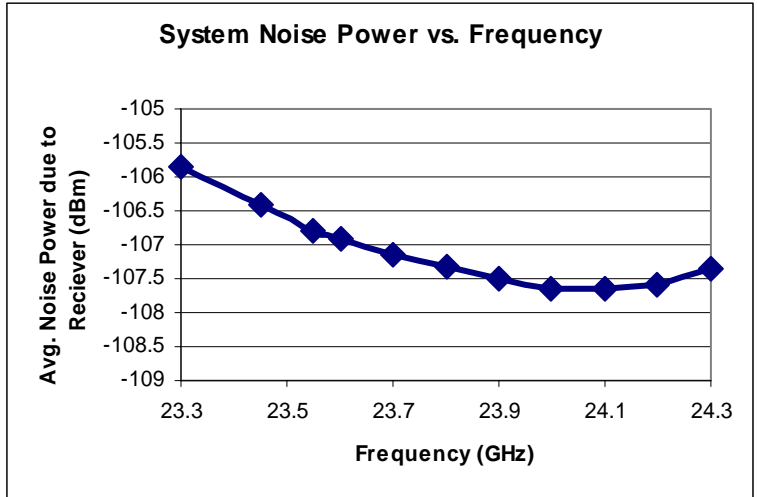
(b)

Figure 20. System Noise Performance vs. Frequency: (a) Noise Figure and (b) Noise Power

3.2.3 The Physical System

Figures 21, 22, 23, and 24 show the system and details of the key components.
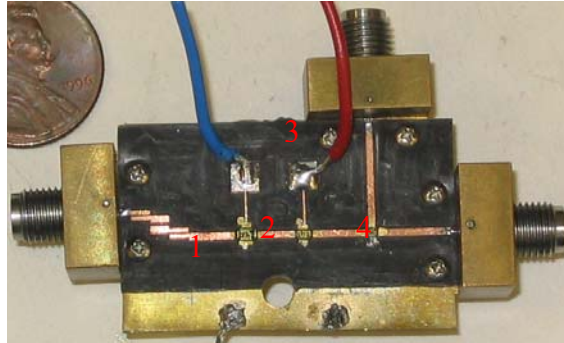
Figure 21. Prototype Fabricated Receiver Front End. (1) Microstrip filter, (2) MMIC amplifiers, (3) DC connections, and (4) MMIC mixer
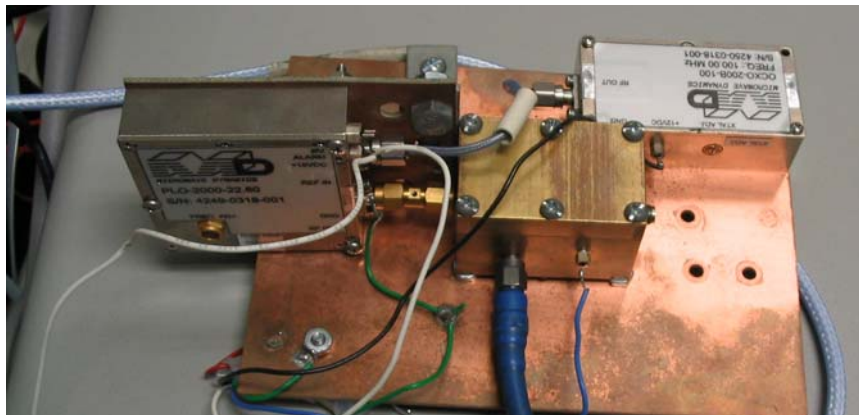
Figure 22. Final Receiver Fabrication, Mounted and Shielded
(The brass box in the center is the shielding for the receiver front end. Absorbing foam was added to the interior walls of this casing to reduce oscillations in the system after the first measurement site)

Figure 23. Entire Measurement System in Use at Hartsfield-Jackson Airport

Figure 24. Measurement System in Use at Hartsfield-Jackson Airport
(Red circle indicates point of mechanical damage and eventual failure in IF amplifier and
connecting cable. A failure in the thin cable, shown dangling, necessitated a field replacement
with the heavier cable, shown connected. The heavier cable created the damaging stress.)

3.3 Calibration, Calculations, and Interpretation of Results

3.3.1 Calibration Procedure

Figure 25 shows schematically the RF components of the K-band measurement system. Test ports have been introduced in this figure and are denoted with blue dashed lines and blue labels. Items characterized for calibration purposes are 1) the antenna and connecting cable, 2) the downconverter/amplifier 3) the interconnect cable, and 4) the spectrum analyzer. The rationale for the respective measurements is as follows:

Antenna and Cable Assembly Because of the frequency of the system, the interconnect cable between the antenna and the first amplifier contributes significantly to the overall noise figure. The cable is kept quite short and the downconverter is located immediately adjacent to the antenna. The antenna interface constitutes an uncorrected mismatch. The input impedances to the antenna and to the entire system with other measurement ports unbroken must be measured. The fraction of power lost to reflection due to mismatch between these impedances must be computed and used to compensate data for final display.

Processing System The effective gain between port 1+ and the output at port 3- is the system gain. The displayed data on the spectrum analyzer is increased by this gain, and precise knowledge of the gain is required.

Cable The cable between ports 2 and 3 is subject to continual flexure as the antenna is cycled during testing. It is prudent to measure the complete scattering parameters for the cable prior to and following each test cycle and to evaluate the results for change. This will bring to light any mechanical failure in the cable.

Spectrum Analyzer Input The spectrum analyzer is expected to exhibit a 50 ohm input impedance within its specified tolerance. While the system is apart, it is easy to do this measurement, so prudence dictates that it be verified.
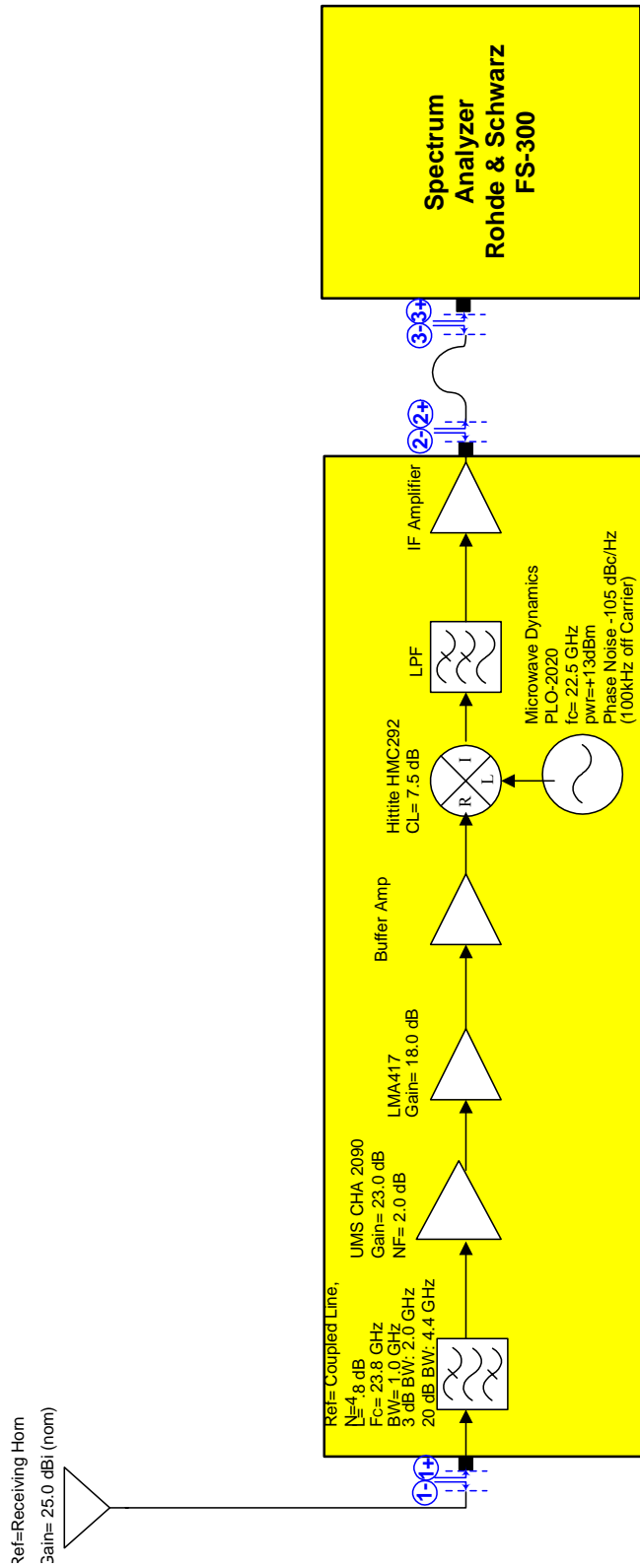
Figure 25. RF Sections of Passive Sensor Band
Noise Figure Test System

46

Procedures

Measurement Frequencies The K-band system shall be calibrated over its operational band: 23.3 - 24.3 GHz. Swept-frequency measurements of complex scattering parameters shall be made for the full span of the band for each specified quantity below

Antenna Input The port to antenna through its attachment cable (port 1-) shall be measured to obtain its complex reflection coefficient. The tabulation of values over the bands shall be preserved.

Downconverter/Amplifier Measurement The overall system shall be measured between ports 1+ and 3-. A complete tabulation of all four scattering parameters s_{11}, s_{21}, s_{12}, and s_{22} shall be preserved. The measurement requires a network analyzer operated in frequency offset mode. The presence of the active component in the system requires that attention be given to the input power level for which the measurements are made. The output level of the downconverter ranges nominally from –30 to +10 dBm; the former figure is dictated by the noise floor of the amplifier/mixer chain, while the latter is the dictated by the 1 dB compression point of the IF amplifier. Calibration data shall be taken with an output power 5 dB above the noise floor and with an output power 5 dB below the compression point for the IF amplifier.

Cable The cable shall be measured as a two-port device comprising ports 2+ and 3-. A complete tabulation of all four scattering parameters s_{11}, s_{21}, s_{12}, and s_{22} shall be preserved. Because this cable flexes, periodic recheck of the cable is advised throughout the course of the test program. *NB: This cable operates over the IF frequency range of 0.7 to 1.7 GHz.*

Data Adjustment The measurement at the ports 1- and 1+ are used to determine a power reflection coefficient accounting for antenna mismatch; namely,

$$|\Gamma|^2 = \left| \frac{Z_{1-} - Z_{1+}}{Z_{1-} + Z_{1+}} \right|^2 ,$$

where Z_{1-} and Z_{1+} are the respective measured impedances at the subject ports. This computation shall be made for all frequency samples collected at the antenna input port, as described above. Let $P_m(f)$ be the data collected on the spectrum analyzer for a given spatial observation. The actual power represented by this data is given by

$$P_a\left(f + 22.5 \right) = \frac{P_m\left(f \right)}{\left(1 - \left| \Gamma\left(f + 22.5 \right) \right|^2 \right) \left| s_{21}^{DA}\left(f \right) \right|^2} \times \begin{cases} 10^{NM/10} , & \text{for noise signals} \\ 1, & \text{for coherent signals} \end{cases},$$

where $s_{21}^{DA}\left(f \right)$ is the measured transfer function across the down converter / amplifier and NM is the noise marker value (approx. 2.5 dB) determined by the spectrum analyzer. The frequency variable f is referred to the spectrum analyzer. The mixer offset is added in the quantities that apply prior to mixing. In $s_{21}^{DA}\left(f \right)$, the frequency of the *output* signal is used to define the function.

Whole-System Power Level Calibration A frequency synthesizer is set to 23.8 GHz. The output of the synthesizer is delivered to a connecting cable, and the connecting cable is terminated with a pad attenuator whose value is at least 10 dB. This attenuator does not need to have a traceable calibration. The output of the pad attenuator is connected to a microwave power meter whose

calibration is also NIST traceable. The power meter is set to read accurately at the 23.8 GHz, in accord with correct operation of the meter.

The output power of the synthesizer is adjusted until the power meter reads –50 dBm. After this level is set, care is exercised to ensure that the synthesizer output power is not changed, and an attenuator with a nominal value of 10 dB and calibration traceable to NIST added to the pad attenuator. This ensures a fixed output power of nominally –60 dBm at the output of the attenuator. The exact value is known to be –50 –A_{10}, where A_{10} is the known value of the calibrated attenuator. The power meter is disconnected and the attenuator output is connected to the input of the NFMS. The spectrum analyzer is set to 1 MHz resolution bandwidth, tuned to display the output signal from the (down converting) NFMS. The value of the spectrum analyzer signal is noted. The ratio of this reading to –50–A_{10} dBm is noted as the top-of-range calibration factor.

A nominal attenuation of 40 dB is inserted between the pad attenuator and the spectrum analyzer. The exact value of this attenuation (or attenuation stack) is known through calibrations traceable to NIST. The spectrum analyzer reading of the resulting signal is noted. The ratio of this reading to –50 dBm – A_{10} –A_{40}, where A_{40} is the calibrated value of the attenuation stack, is noted as the bottom-of-range calibration factor.

The calibration factors are compared to ensure near-linearity of the system over the dynamic range –100 to –60 dBm.

Note: The calibration noise floor is set by the ambient temperature of the instrumentation, taken to be 293°K. This is approximately 5 dB higher than the noise level produced by a 100°K sky.

3.3.2 Noise Calculations and Interpreting Results

When interpreting the data from these noise-floor measurements, it is important to consider a few facts about the receiver system theory and performance. First of all, one must understand what the power level seen in these results represents. In general, the formula for the noise power (in decibels relative to 1 mW--dBm) at the output of a system is related to the input noise temperature (T_{Source}) by the following equation:

$$P_{out} = 10\log\left[kBG(T_{Source} + (F-1)T_0)\right] + 30$$

where k is Boltzman's constant (1.38*10^-23 Watts/(Kelvin*Hertz)); B is the Bandwidth in which the power is measured; T_0 is the temperature of the system in degrees Kelvin; G is the gain of the receiver; and F is the noise figure of the system. In the results here, we have calibrated out the gain of the receiver, and we may separate out the constant terms of this equation to get

$$P = 10\log(kB) + 10\log(T_{Source} + (F-1)T_0) + 30$$

Notice that the power depends on the sum of the source noise temperature and the system noise temperature. Component specifications and CAD modeling of our system predicts a noise figure of 3, which is clearly a lower bound. We have not yet measured the noise figure, however, and it is fruitless to quantify the source noise temperature until the measurement is made. Great care was taken to shield our system from direct sunlight so that T_0 would be approximately constant over the course of a day. In this way we can interpret changes in the output power as changes in the source noise temperature and make general inferences about the conditions which increase and decrease the source noise temperature.

In order to effectively measure the signal generated at 24 GHz, it was necessary to downconvert the signal by mixing with a 22.6 GHz oscillator. We designed the preselector for minimum loss with the result that its stopband is -20 dB below the passband. Thus images from the frequency range 20.9 to 21.9 GHz can show in the data attenuated by 20 dB. In other words, any man-made signal reported in this data in the range of 23.3 to 24.3 GHz may actually reside in the frequency band from 20.9 to 21.9 GHz at a level 20 dB above that reported. This does not however affect the noise floor appreciably, since the gain (G) in equation (1) is at least 15 dB below the gain for the noise power at 24 GHz.

(This page was left intentionally blank)

3.4 Measurement Procedure

The following procedure is used to measure noise floor at each location in the frequency range 23.3-24.3 GHz of K band.

1. Set up the noise floor measurement system (NFMS) as shown in Figure B.1 with the horn antenna 1.0 to 2.0 meter above the ground level (operationally significant height to the handheld communication devices). Ensure the equipment is not in direct sunlight to maintain all components within their specified operating temperature range.

2. Level/plumb the antenna platform to ensure that it is horizontal.

3. Supply power to the NFMS and wait for 20 minutes[1] to ensure that the electronic systems have stabilized (constant temperature and the calibrated gain).

4. Execute a Pre-Measurement Run with a matched termination to ensure the proper operation of the NFMS.

5. Start the software control panel of the NFMS and enter the coordinates, as determined by a handheld GPS receiver, of the site.

6. Select the "set zeros" function in the NFMS control panel.

7. Set the zero-degree azimuth position of the system to *magnetic* north for the given location.

8. Ensure that the elevation positioner for the antenna is level with the antenna platform.

9. Select "Horizontal" in the antenna type.

10. Orient the horn antenna in the horizontal polarization.

11. Ensure that 20 minutes[1] has elapsed since system power was applied to ensure full warm-up of electronics. Record time of day and local temperature. Push the start button.

12. The NFMS control system will select the appropriate frequency band, with the associated selection for the center frequency, the frequency span, the resolution bandwidth[2] and the video bandwidth of the spectrum analyzer as shown in Table 19. The sweep time will be automatically selected by the spectrum analyzer. The RF filter path will also be switched to the desired frequency band.

---

[1]Three minutes is a typical time constant for RF components. Thus five time constants with an additional five minute margin is used to ensure stabilization.
[2] The resolution bandwidth has been chosen according to ANSI C63.4-2001 (Revision of ANSI C63.4-1992) American National Standard for Methods of Measurement of Radio-Noise Emissions from Low-Voltage Electrical and Electronic Equipment in the Range of 9 kHz to 40 GHz.

Band	Center Frequency [GHz]	Frequency Span [GHz]	Resolution Bandwidth [MHz]	Video Bandwidth [MHz]
23.3-24.3	23.8	1	1	1

Table 19. Control System Settings

13. The noise power spectrum in band will be measured by the spectrum analyzer. Ten individual traces and the computed root means square (RMS) value will be recorded onto the computer hard disk with the following measurement details: the measurement antenna orientation, the target frequency band, the time, and the location. A picture of the site will be taken with a digital camera and recorded onto the computer hard disk with each group of ten traces.

14. The horn antenna will be rotated clockwise in 15° increments (The 3dB beamwidth of the antenna is 30.5° at mid-band so that 15° is a sufficient angular resolution to monitor the RF activities in the environment).

15. Steps 13 and 14 will be repeated under control software control until the measurement antenna angle reaches 360°.

16. Steps 9 to 14 will be repeated with the horn antenna oriented in the vertical polarization.

17. The horn antenna will be rotated to the initial angular position and the polarization returned to horizontal.

18. The elevation of the antenna will be incremented to 30° and steps 13 through 18 will be repeated. The elevation will be incremented to 60° and the sequence repeated a third time.

19. Steps 8 to 13 will be repeated beginning at every odd-numbered hour, beginning at 7:00 AM, with the last set beginning at 9:00 PM.

20. The antenna will be pointed vertically, and a reference sky noise measurement will be made.

21. Execute a Post-Measurement Run with a matched termination to ensure the proper operation of the NFMS.

Table 20 lists the hardware used in the Passive Sensor Band Noise Floor Measurement System.

EQUIPMENT	MANUFACTURER and MODEL	RELEVANT SPECIFICATIONS	CALIBRATION
Horn Antenna	Narda 638 Standard Gain Horn	18-26.5 GHz.	Calibrated by manufacturer
NFMS Hardware	As described in Sections II and III		Calibrated before and after each field measurement
Spectrum Analyzer	Rohde & Schwarz FS300	9 kHz – 3 GHz, USB Interface	Calibrated 3/21/03 and 2/27/04
Notebook Computer	Toshiba Satellite Pro 6100	PC card slot, USB, RS-232	Not necessary
Digital Camera	Logitech QuickCam Pro 4000	USB capable	Not necessary
Motorized Mount	Ultrak UL-MPTS	24VAC	Calibrated at each field measurement
Motor Drive	Ultrak DTMRX	RS-232 capable, 24VAC	Not necessary
Transformer	Ultrak CC-TX2440	AC transformer 110VAC to 24VAC	Not necessary
LabView Software	National Instrument LV6.1		Not necessary
Power Supply	HP E3631A	Multiple Output DC Supply	Not necessary
DC to AC converter	Radio Shack . AC Inverter 140 W	Converting DC 12V to AC 115V, Continuous power 140 W	Not necessary
Battery		Deep cycle 12V battery (2)	Not necessary
Calibrated Attenuators	Anritsu 43KB-10, 43KB-20	Used in system calibration	Expired 1/31/04
Noise Figure Measurement	Agilent N8973A, HP 346C	Noise Analyzer, 10MHz-3GHz; Noise source 10 MHz-26.5GHz	Calibrated 3/11/04

Table 20. Hardware of the Passive Sensor Band Noise Floor Measurement System

(This page was left intentionally blank)

3.5 Results

The measured data and observations of sites are presented in Appendix B. The measured data for each site is presented in four forms. In spectral form, the maximum, average, and minimum power level at each frequency is displayed. The angular plot form displays the power received as a function of azimuthal angle for each elevation measured (0°, 30°, and 60°). In temporal form, the average, maximum, and minimum power level are displayed as a function of time of day for each elevation measured. The statistical analysis compares the measured probability distribution to the theoretical probability distribution. This data presentation allows us to observe the extent to which the space-time ensemble adheres to Gaussian statistical distribution. The data is organized by measurement site and elevation angle.

3.6 Summary

A thorough review of the data in Appendix B reveals nineteen spectral peaks deduced to be man-made signals. The fact that only nineteen were detected implies that this entire band measured does not contain appreciable man-made radiation. Eleven of these signals were observed at the airport sites—three observations at a single frequency at Hartsfield-Jackson Airport and ten others at the Oconee County airport. The Hartsfield-Jackson signal was observed in measurements in the direction of the airport's main radar, suggesting spurious emission as a source. The ten at Oconee County occurred at multiple frequencies and showed arrivals from different directions. Figure 26 shows a composite plot of these signals. It should be noted that on this small airport grounds, the measurement site was in close proximity to airport communications and navigation aid facilities, as well as a hangar and the main (only) runway.

One spectral peak was observed on the campus of the Georgia Institute of Technology in downtown Atlanta, GA. The other seven spectral peaks were observed on Interstate 85 in Anderson, SC in the direction of traffic.

Viewed differently, of these nineteen spectral peaks, only five of these interference sources existed in the Passive Sensing Band from 23.6-24.0 GHz. Nine fell in the fixed-service/satellite-mobile band below, and five fell in the amateur radio/ISM Band above. Such a small sample precludes drawing any conclusion regarding how the Passive Sensing Band compares with neighboring bands.

It is encouraging that interference is minimal in the Passive Sensing Band at the present time. The relatively quiet *status quo* will allow future observers to discern clearly incursions into the Passive Sensing Band should they emerge.
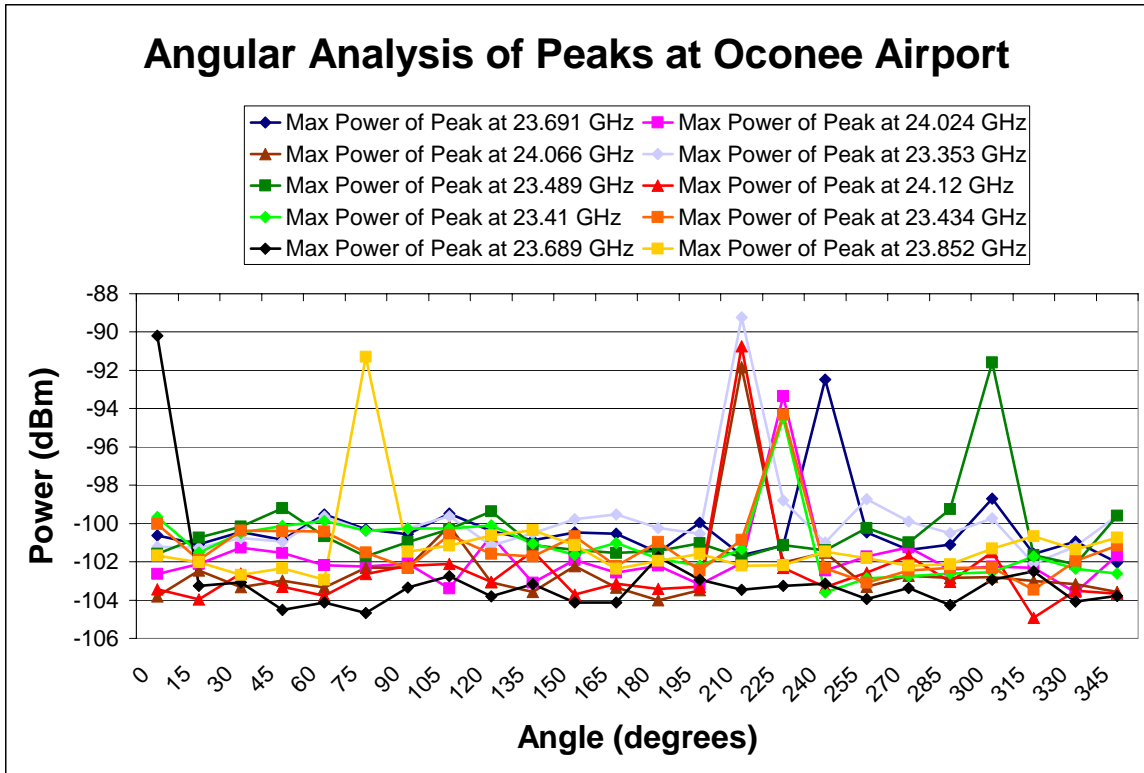
Figure 26. Composite of Peak Spectrum Data Showing Apparent Man-Made Signals at the Oconee County Airport

4. Conclusions

4.1 L, S, and ISM Bands Survey

Table 21 reports the average power density measured in the L, S, and ISM bands at the eight sites. The cells are colored green if the measured power is indistinguishable from the noise power provided by nature. The cells are colored yellow if the measured power is slightly above the natural noise power. The cells are colored orange if the measured power is significantly greater than the natural noise power.

Site Category	Measurement Site	GPS L1 Band			Unified S Band		ISM 2.4 GHz Band	
		HOR	VER	GPS	HOR	VER	HOR	VER
Urban	San Jose Downtown	-111.0	-111.7	-112.0	-109.2	-107.9	-83.1	-84.4
	Palo Alto Downtown	-111.5	-110.7	-111.2	-111.4	-110.6	-92.2	-89.8
Rural	Yosemite Park	-112.1	-112.3	-112.5	-111.8	-111.9	-85.1	-82.5
	Jasper Ridge Preserve	-112.1	-112.3	-112.2	-111.7	-111.9	-97.1	-100.8
Airport	San Jose Airport	-112.5	-113.4	-112.8	-77.4	-75.9	-82.2	-89.8
	Palo Alto Airport	-112.3	-112.7	-112.5	-112.0	-112.4	-92.5	-101.7
Harbor	Port of Oakland	-112.9	-113.3	-112.9	-106.9	-101.7	-87.6	-78.7
	Coyote Point Marina	-111.9	-112.2	-112.3	-110.9	-111.4	-88.8	-80.8

* Note: 'HOR', 'VER' and 'GPS' in the table each represent the power measurement by a horizontally polarized horn antenna, a vertically polarized horn antenna and a GPS antenna.
* Note: All numbers are in dBm/MHz.

Table 21. Average Received Power

Table 22 reports the estimated percentage of man-made signals in the measurement data for these same bands, which is based on the number of the measurement results exceeding the distribution of the natural noise power. The cells are colored green if this percentage is less than 0.05 %. The cells are colored yellow if this percentage is between 0.05 and 2 %. The cells are colored orange if man-made signals appear in more than 2 % of the measurements.

The total power in the GPS Band is never significantly greater than the power due to nature alone, and man-made signals appear in less than 0.02 % of the measurements. This finding makes sense. When received on Earth, the GPS signal is below the *noise floor* due to nature. After all, it travels 20,200 km from medium Earth orbit to Earth and the received power density is approximately 10^{-13} W/m^2. Moreover, regulatory efforts to protect this low power signal have been conspicuously successful. Few man-made signals are seen in any of the GPS measurements described in this report. The few signals observed were very weak.

The Unified-S Band also exhibits sensible results. At the two rural sites, this band is as quiet at the GPS Band, and no man-made signals appear above the natural noise floor. However, man-made signals are more apparent in populated areas.

The ISM 2.4 GHz band is a frequency band allocated for unlicensed spectrum use and is finding increased use for unlicensed wireless technologies such as wireless networks and cordless telephone operations. It also contains radio energy from microwave ovens. The open nature of this band means that applications will vary, but users will be found anywhere and anytime

Site Category	Measurement Site	GPS L1 Band			Unified S Band		ISM 2.4 GHz Band	
		HOR	VER	GPS	HOR	VER	HOR	VER
Urban	San Jose Downtown	0.01	0.01	0.01	1.35	1.67	6.08	4.50
	Palo Alto Downtown	0.00	0.02	0.01	0.01	0.06	4.35	3.58
Rural	Yosemite Park	0.00	0.00	0.00	0.00	0.00	0.62	0.78
	Jasper Ridge Preserve	0.00	0.00	0.00	0.00	0.00	2.64	3.67
Airport	San Jose Airport	0.01	0.00	0.00	6.45	8.71	17.12	26.73
	Palo Alto Airport	0.00	0.00	0.00	0.00	0.01	13.68	10.22
Harbor	Port of Oakland	0.00	0.01	0.00	2.23	2.77	34.37	43.30
	Coyote Point Marina	0.00	0.00	0.00	0.40	0.30	7.10	22.31

* Note: All numbers are in percentage (%) and represent the measurement data exceeding the distribution of the natural noise power.

Table 22. Percentage of Man-Made Signals in Measurement Data

The measurement results show that current rules are effective in determining the radio environment and regulations must be sensitive to the function of the band. Each band supports different types of applications. Some of them are critical systems that cannot tolerate any sort of operational failure and need to be protected from any interference. Some of them can tolerate a certain level of failure and work even under severe interference while requiring more bandwidth. Spectrum policy has been sensitive to the varying objectives and requirements of specific radio frequency applications and corresponding functions of individual frequency bands. The spectrum environment has been successfully managed to ensure stable operations and the best utilization of frequency bands by properly allocating bands to each category of application, locating them with sufficient spectral separation, and adopting application sensitive regulations. To sustain the radio frequency environment for current and future users, the same level of sensitivity should be applied to the introduction of any new spectrum policy or new applications.

4.2 Passive Sensor Band Survey

As already covered in Section 3.5, a thorough review of the data in Appendix B reveals nineteen spectral peaks deduced to be man-made signals. The fact that only nineteen were detected implies that this entire band measured does not contain appreciable man-made radiation. It is encouraging that interference is minimal in the Passive Sensing Band at the present time. The relatively quiet *status quo* will allow future observers to discern clearly incursions into the Passive Sensing Band should they emerge.

(This page was left intentionally blank)

Appendices

Appendix A: L, S, and ISM Bands Survey Measurement Data

Appendix A.1: San Jose Downtown

Site Description

The City of San Jose is the 11th largest city in the United States and the center of Silicon Valley with an area of 454 km^2 and a population of 925,000. Table A.1 and Figures A.1 through A.4 depict the measurement site location and conditions. The LSSM was located downtown. As shown in Figure A.1, nearby buildings included the Civic Auditorium (10 m away, north), the Crown Plaza Hotel (50 m away, southeast) and a parking garage (30 m away, south). Pedestrian traffic was high throughout daylight hours. Weather was mostly sunny. WiFi (IEEE 802.11b) activity (channel number = 11, SNR = 38) was detected during the site survey.

Time	Location	Weather	Distance to Building	Distance to Pathway	WiFi Channel	Address
Oct 21 0900 ~ Oct 22 0900	N37.33 W121.89	Sunny Clear	10 m	4 m	Channel 11 SNR = 38	120 Park Ave. San Jose CA 95113

Table A.1. Measurement Site Conditions (San Jose Downtown)
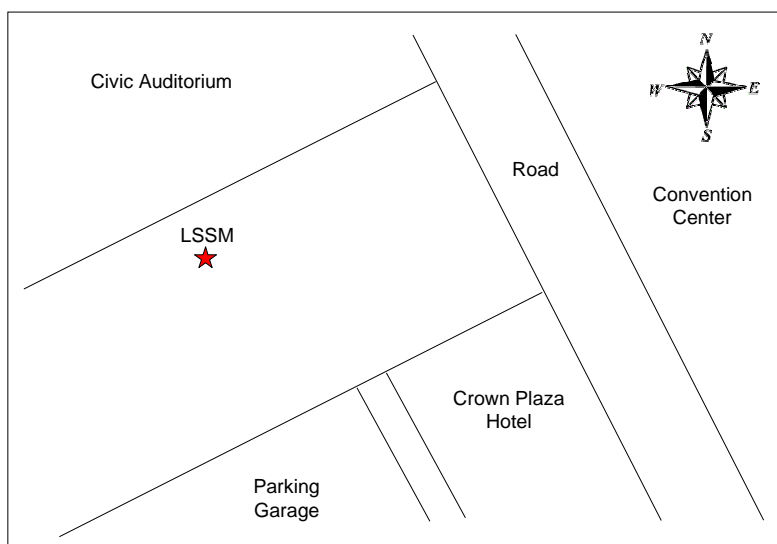
Figure A.1. Location of LSSM at San Jose Downtown

Figure A.2. Photo of Spectrum Survey at San Jose Downtown
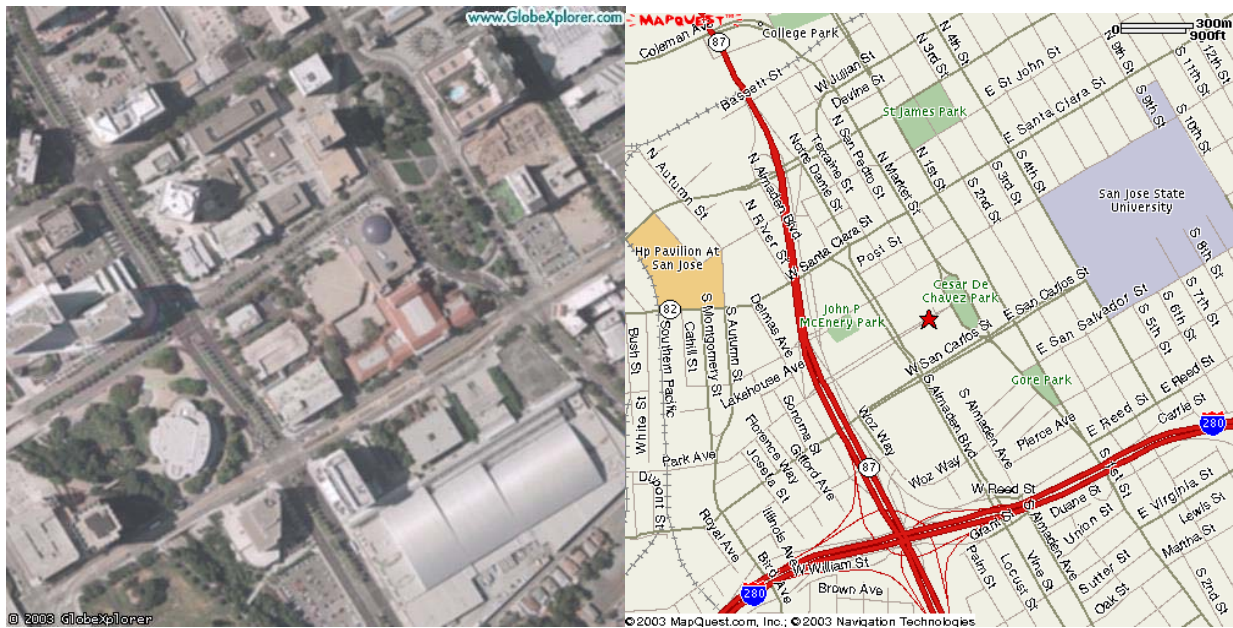
Figure A.3. Aerial Map and Street Map to San Jose Downtown

(via www.globexplorer.com & www.mapquest.com)
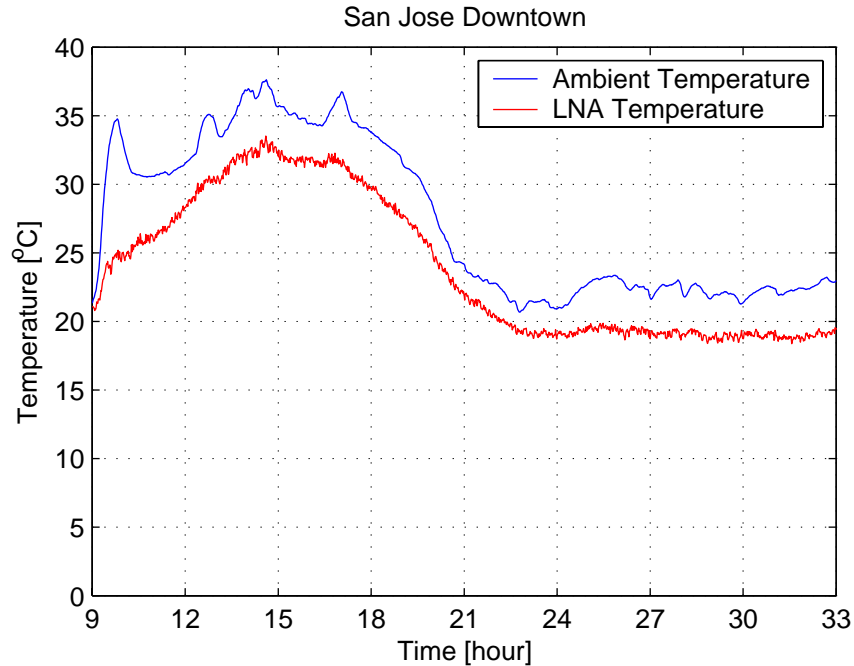
Figure A.4. Temperature Variation During Measurements at San Jose Downtown

Data Observation

Band		Comments
GPS L1 (Fig A.5)	Temporal analysis	The average received power was almost always between -112.2 and -111.4 dBm/MHz, below the thermal noise floor. At 24:00, it increased to -104.7 dBm/MHz. We suspect that this exceptional signal originated from a source in the Crown Plaza Hotel.
	Spectral analysis	The average received power was almost always between -112.6 and -110.6 dBm/MHz, below the thermal noise floor for all measurement frequencies. There were a few exceptional signals with bandwidths less than 1 MHz at 1575, 1576, 1577, 1582, 1583, and 1584 MHz. Amongst these, the highest power, -100.9 dBm/MHz, was measured at 1583.6MHz.
		GPS signals at 1575MHz also appeared slightly above the thermal noise floor. The GPS power received by the GPS antenna was approximately 1.5 dB higher than the signal received by the horn antennas, because it was directed skyward and the GPS antenna was able to aggregate the power from many GPS satellites while the horn antennas were directed at the horizon and were only able to receive the signals from the satellites near to the horizon. Similar observations were made at the rest of the measurement sites.
	Angular analysis	The average received power was almost always between -112.0 and -111.6 dBm/MHz, below the thermal noise floor for all measurement angles. The average received power increased to -106.4 dBm/MHz at an angle of 105 ~ 120 degrees, which is the direction to the Crown Plaza Hotel.
	Statistical analysis	Man-made signals were present in less than 0.01 % of the measurement data with a maximum power of -100.7 dBm/MHz.

UNI-S (Fig A.6)	Temporal analysis	The average received power was between -111.7 and -103.6 dBm/MHz, and was above the thermal noise floor for the most of the measurement period. The highest power, -103.6 dBm/MHz, was measured at 29:30. After 17:00, man-made signals were more or less continuous. Before 17:00, the band was mostly quiet. These man-made signals probably originated from multiple sources in the surrounding buildings.
	Spectral analysis	The average received power was variable and high, between -112.3 and -96.0 dBm/MHz, for all measurement frequencies. The highest power, -96.0 dBm/MHz, was received at 2050.5 MHz. Man-made signals were observed at 2050, 2068, and 2084 MHz, and the rest of the frequencies were quiet.
	Angular analysis	The average received power was between -110.8 and -105.0 dBm/MHz. It was above the thermal noise floor for all measurement angles. The highest power, -105.0 dBm/MHz, was measured at 225 degrees when the directional antennas pointed at the parking garage. Man-made signals were observed at all angles and no quiet angles were observed. The highest powers came from angles between 60 and 90 degrees corresponding to the Convention Center and angle between 180 and 255 degrees corresponding to the parking garage.
	Statistical analysis	Man-made signals were clearly indicated. They were present 1.67 % of the measurement data with a maximum power of -82.5 dBm/MHz.
ISM 2.4 (Fig A.7)	Temporal analysis	The average received power varied between -99.6 and -75.7 dBm/MHz, well above the thermal noise floor for all measurement time periods. The highest power, -75.7 dBm/MHz, was measured at 10:49. Man-made signals were continuous and no quiet moments were observed. These signals probably had multiple sources in the surrounding buildings.
	Spectral analysis	The average received power varied between -104.6 and -74.8 dBm/MHz, well above the thermal noise floor for all measurement frequencies. The highest power, -74.8 dBm/MHz, was monitored at 2472.9 MHz. Man-made signals were continuous in frequency, and no quiet frequencies were observed.
	Angular analysis	The average received power varied between -90.6 and -78.7 dBm/MHz, well above the thermal noise floor for all measurement angles. The highest power, -78.7 dBm/MHz, was monitored at 120 degrees, when the antenna pointed at the Crown Plaza Hotel.
	Statistical analysis	Man-made signals were prevalent. They appeared in 6.08 % of the measurement data with a maximum power of -49.4 dBm/MHz.
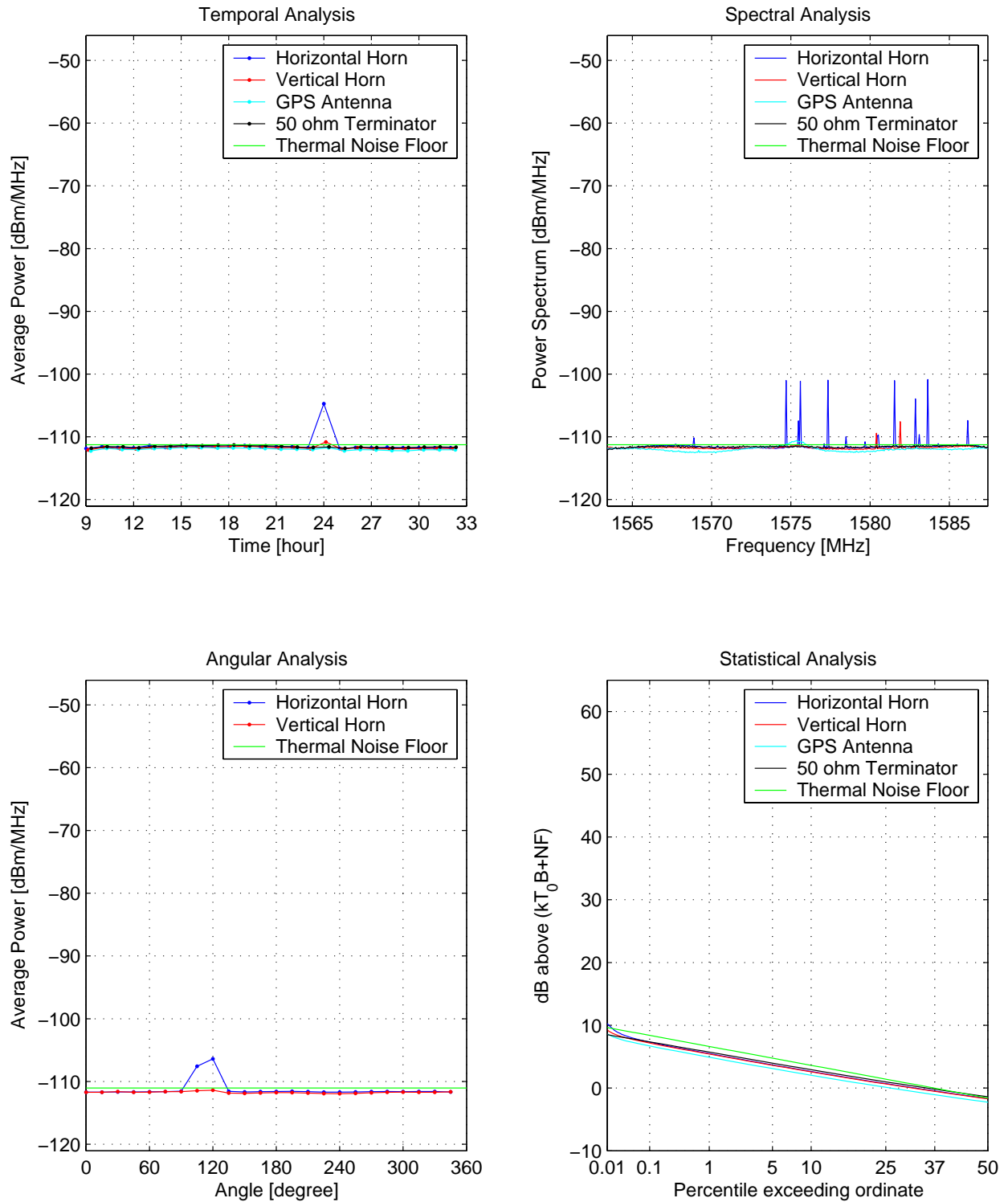
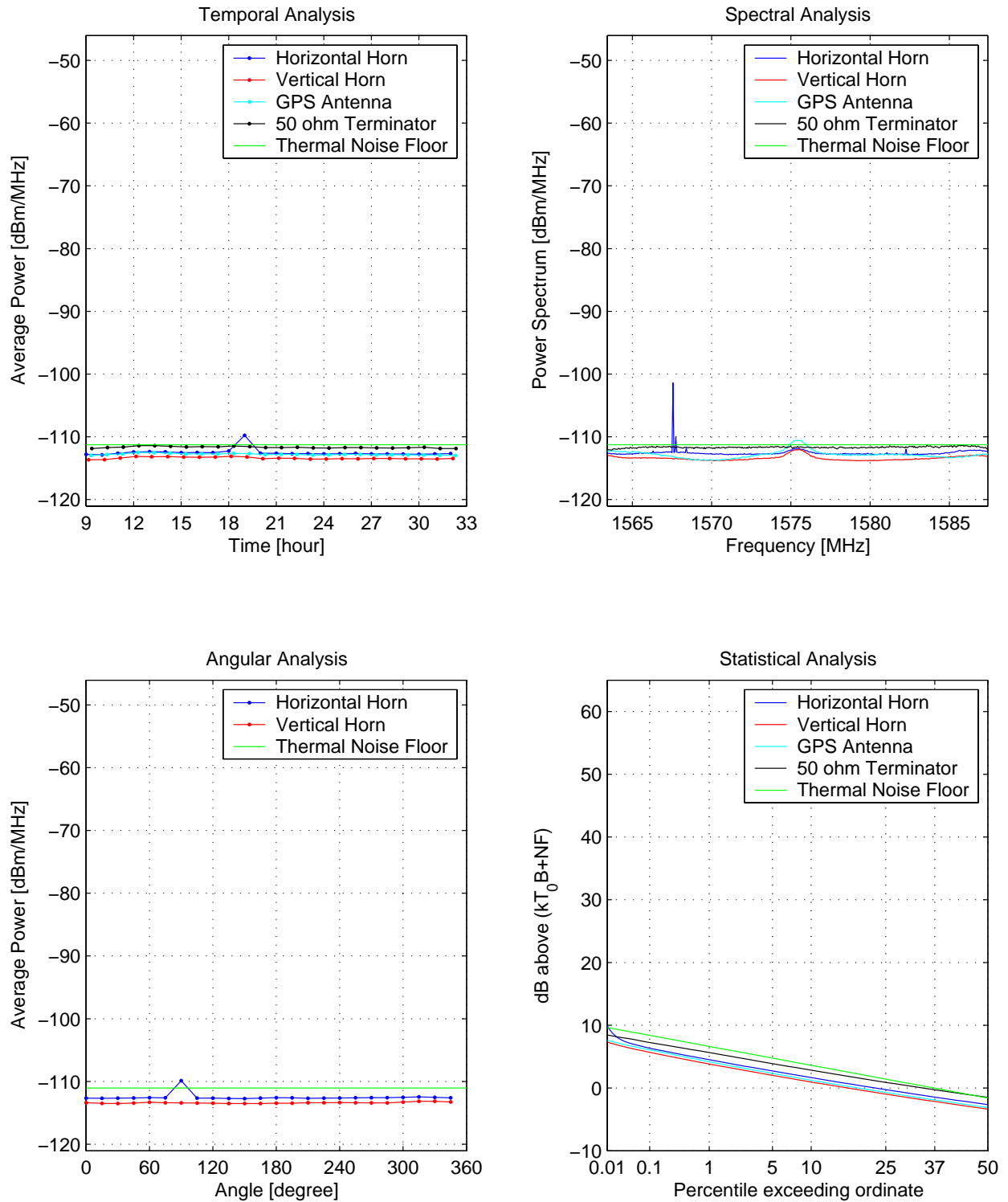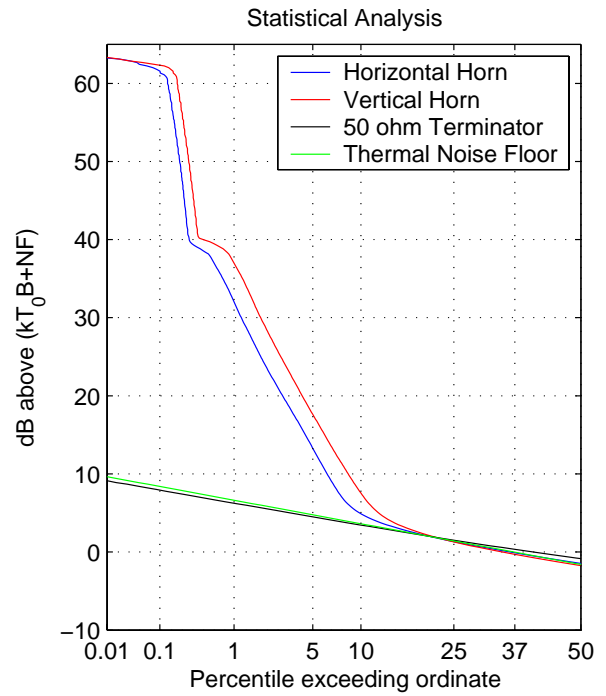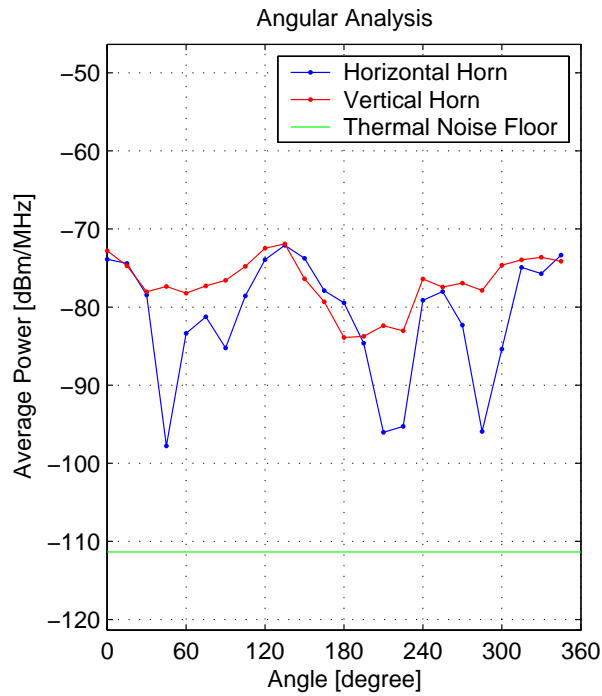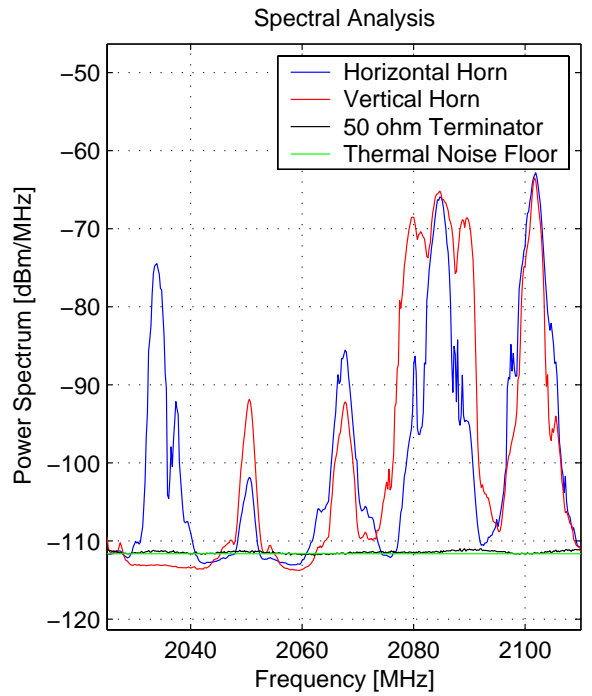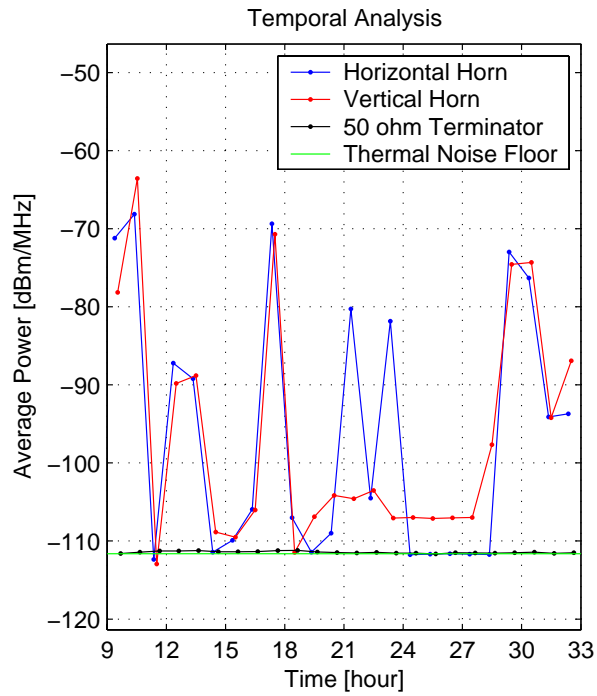Figure A.5. Spectrum Measurements at San Jose Downtown (GPS L1)
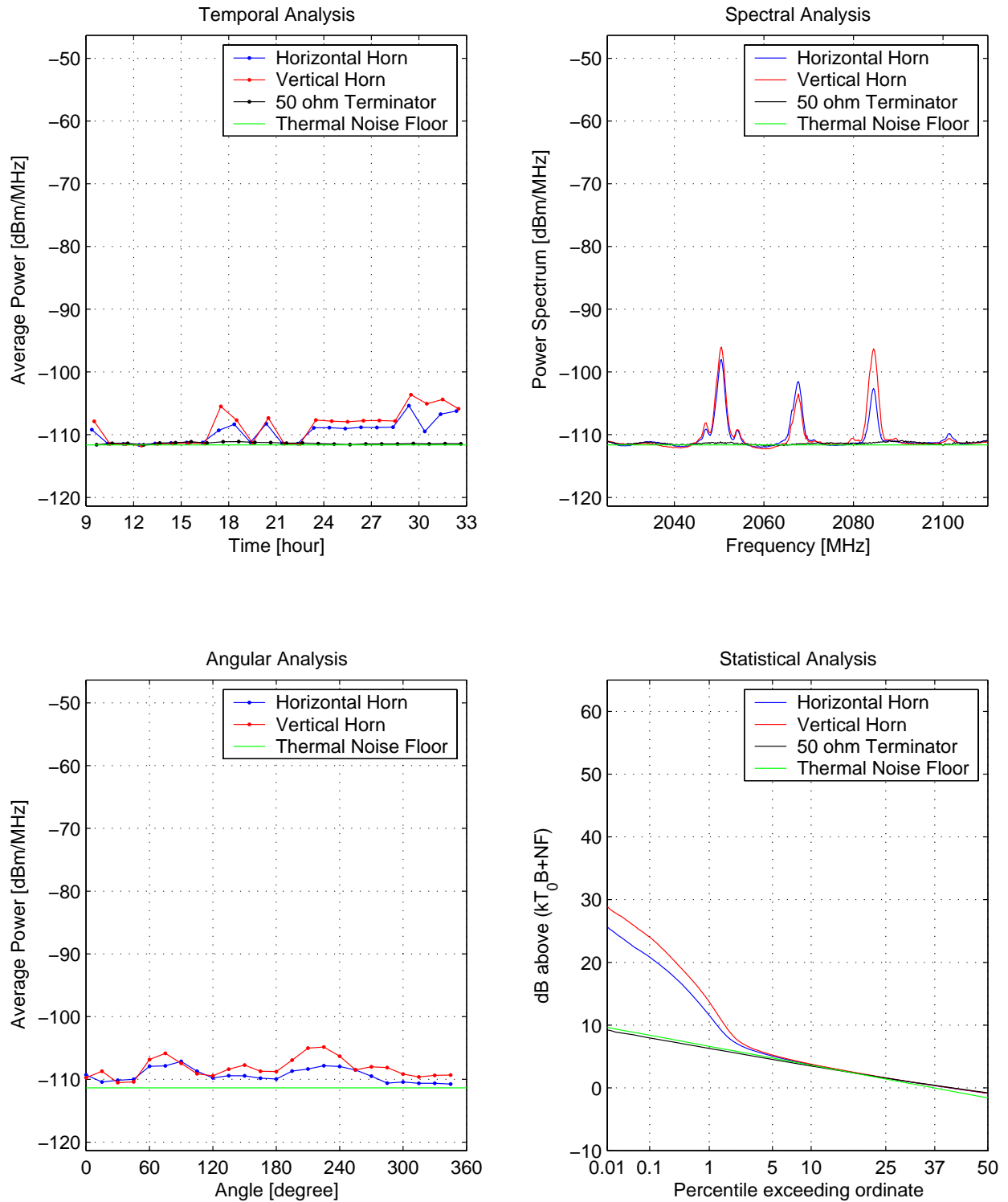
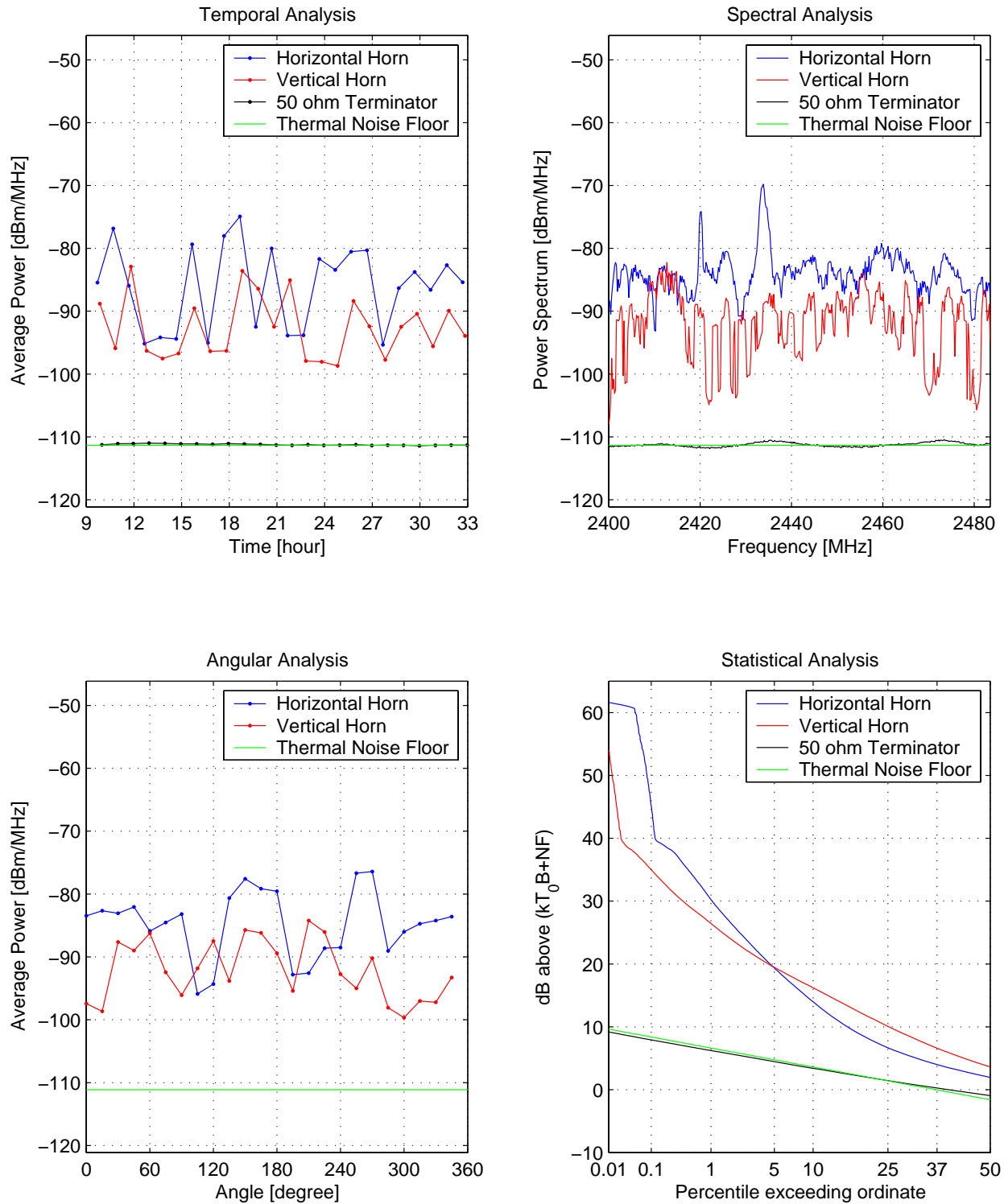Figure A.6. Spectrum Measurements at San Jose Downtown (UNI-S)
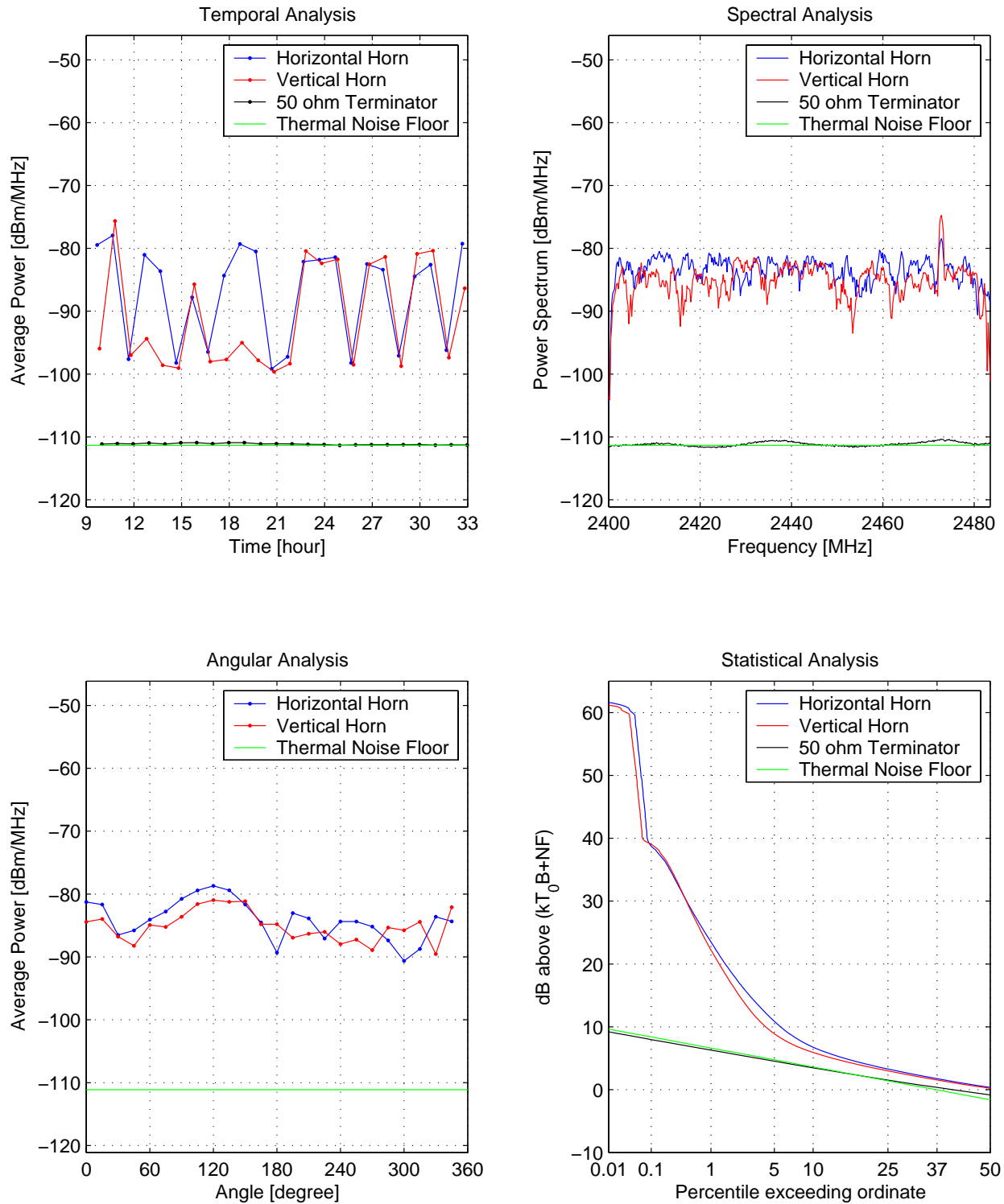
Figure A.7. Spectrum Measurements at San Jose Downtown (ISM 2.4)

(This page was left intentionally blank)

Appendix A.2: Palo Alto Downtown

Site Description

Palo Alto is a medium size city with an area of 67 km^2 and a population of 61,200 located 56 km south of San Francisco and 22 km north of San Jose. It is a part of the San Francisco Metropolitan Bay Area and Silicon Valley. Table A.2 and Figures A.8 through A.11 depict the measurement site location and conditions. The LSSM was located on the third floor of a five-floor parking garage in downtown Palo Alto surrounded by commercial buildings. The closest buildings were 10 m away to the northwest and 30 m away to the southeast. Pedestrian traffic was low for all measurements. The weather was mostly cloudy and rainy. WiFi activity (channel number = 6, SNR = 37) was detected during the site survey.

Time	Location	Weather	Distance to Building	Distance to Pathway	WiFi Channel	Address
Nov 5 0900 ~ Nov 6 0900	N37.44 W122.16	Cloudy Rainy	In Building	4 m	Channel 6 SNR = 37	550 Cowper St. Palo Alto CA 94301

Table A.2. Measurement Site Conditions (Palo Alto Downtown)
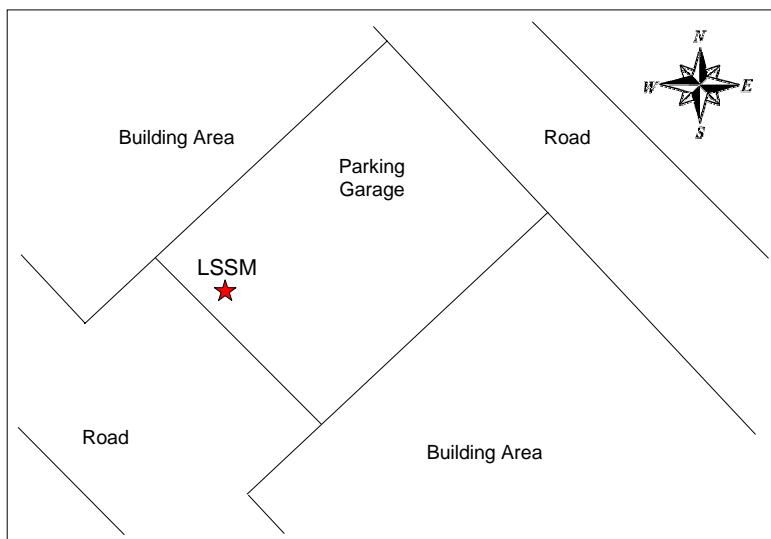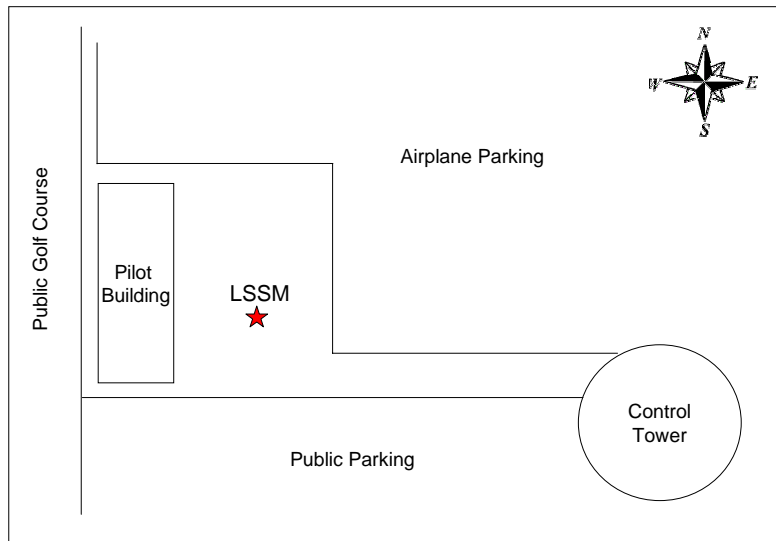

Figure A.8. Location of LSSM at Palo Alto Downtown

Figure A.9. Photo of Spectrum Survey at Palo Alto Downtown
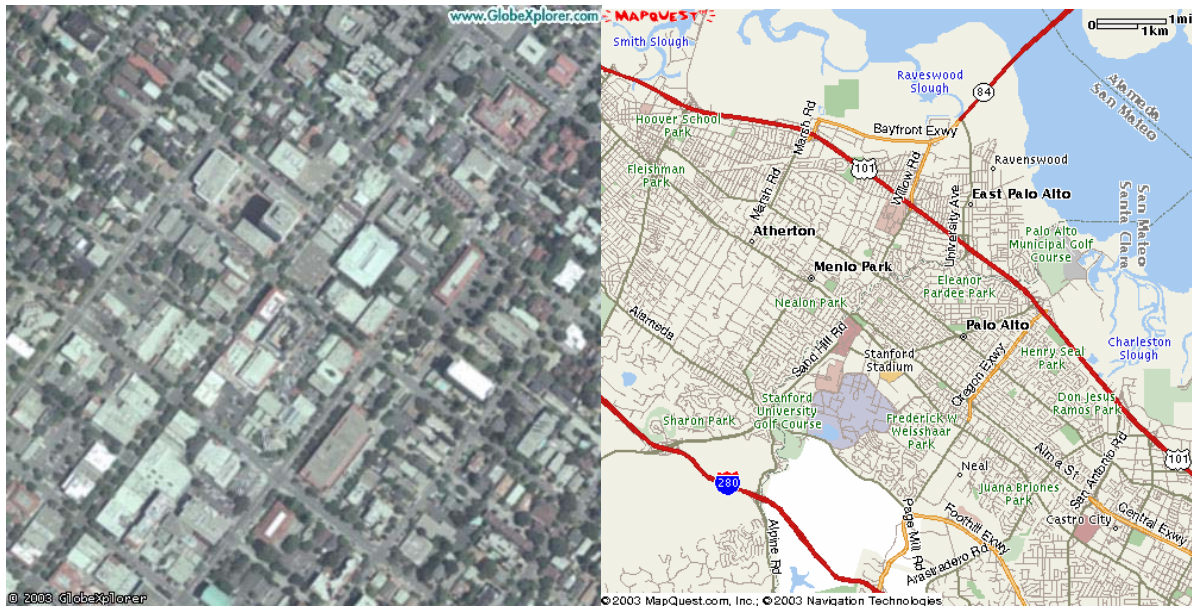
Figure A.10. Aerial Map and Street Map to Palo Alto Downtown

(via www.globexplorer.com & www.mapquest.com)
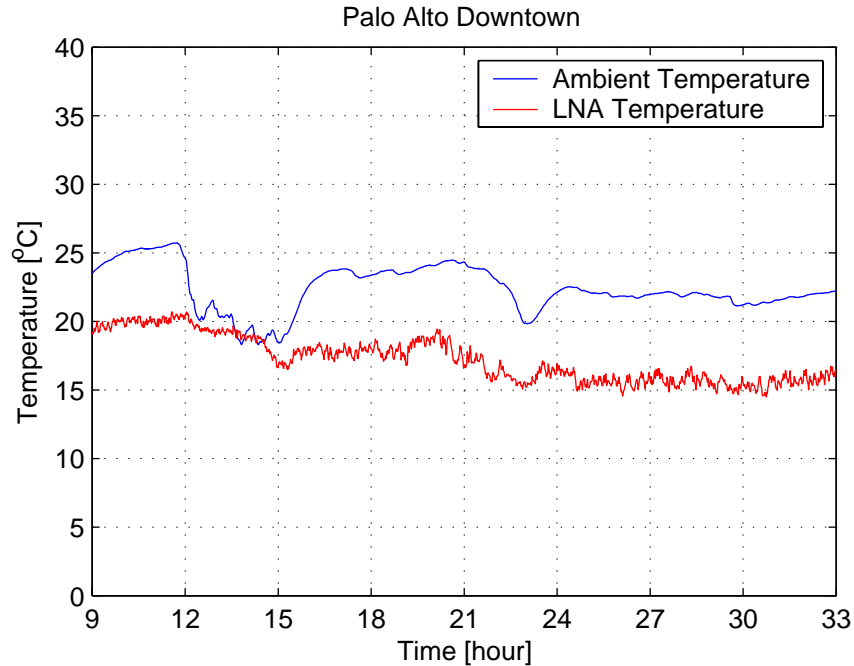
Figure A.11. Temperature Variation During Measurements at Palo Alto Downtown

Data Observation

Band		Comments
GPS L1 (Fig A.12)	Temporal analysis	The average received power was almost always constant between -111.7 and -110.8 dBm/MHz, at the thermal noise floor for all measurement time periods. At 21:12, the vertical horn antenna detected a power increase to -103.3 dBm/MHz. This exceptional signal probably originated from a single source in a surrounding building.
	Spectral analysis	The average received power was almost always between -111.8 and -110.2 dBm/MHz, at the thermal noise floor for all measurement frequencies. An exception was detected at 1570.5 MHz, where a signal with a bandwidth of less than 1 MHz appeared with a power of -101.2 dBm/MHz.
	Angular analysis	The average received power was almost always between -112.0 and -111.2 dBm/MHz, at the thermal noise floor for all measurement angles. The sole exception was detected at 15 degrees, where the power increased to -103.6 dBm/MHz.
	Statistical analysis	Man-made signals were measured only with the vertical horn, and these signals occurred in less than 0.02 % of the measurement data with a maximum power of -97.8 dBm/MHz.
UNI-S (Fig A.13)	Temporal analysis	The average received power was almost always constant between -111.7 and -111.2 dBm/MHz, at the thermal noise floor for all measurement time periods. At 18:30, an exception increased the power to -103.4 dBm/MHz through the vertical horn antenna. This exception probably originated from a single source in a surrounding building.

71

|		
	Spectral analysis	The average received power was almost always constant between -112.2 and -110.8 dBm/MHz and near the thermal noise floor for all measurement frequencies. A sole exception occurred at 2085.1 MHz where the signal had a bandwidth less than 5 MHz bandwidth and a power of -100.9 dBm/MHz.
	Angular analysis	The average received power was almost always constant between -111.9 and -110.5 dBm/MHz and near the thermal noise floor for all measurement angles. Exceptions occurred at measurement angles between 75 and 90 degrees and between 285 and 290 degrees. In these angular bins, the power level increased to -105.6 dBm/MHz.
	Statistical analysis	The only man-made signal that was indicated appeared in the vertical horn antenna measurement. This signal appeared in less than 0.06 % of the data with maximum density of -87.5 dBm/MHz.
ISM 2.4 (Fig A.14)	Temporal analysis	The power varied between -103.2 and -81.6 dBm/MHz, well above the thermal noise floor for all measurement time periods. The highest power was -81.6 dBm/MHz, and was measured at 21:53. Man-made signals were continuous in time and no quiet times were observed. These signals probably originated from multiple sources in the surrounding buildings.
	Spectral analysis	The power varied between -109.4 and -82.3 dBm/MHz, well above the thermal noise floor for all measurement frequencies. The highest power was -82.3 dBm/MHz and occurred at 2464.1 MHz. Man-made signals were continuous in frequency and no quiet frequencies were found.
	Angular analysis	The power varied between -105.5 and -83.5 dBm/MHz, well above the thermal noise floor for all measurement angles. The highest power was -83.5 dBm/MHz and occurred at 240 degrees. Man-made signals were observed at all angles, and no quiet angles were observed.
	Statistical analysis	Man-made signals were apparent in 4.35 % of the measurement data with a maximum power of -55.1 dBm/MHz.
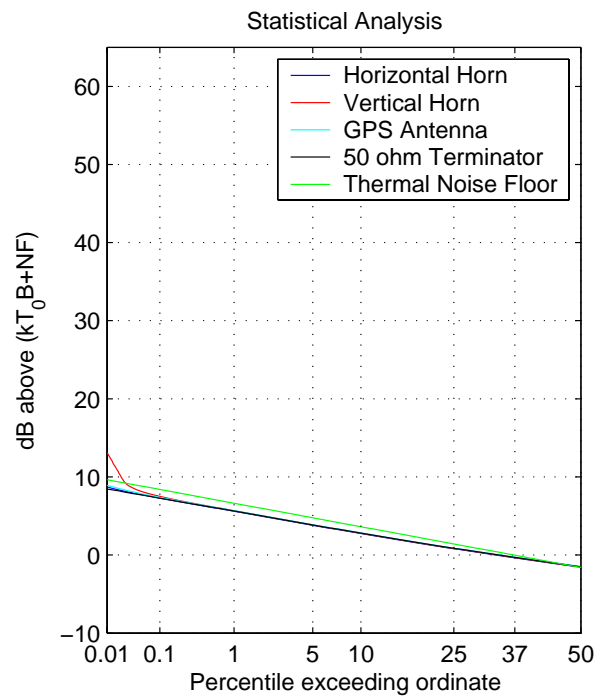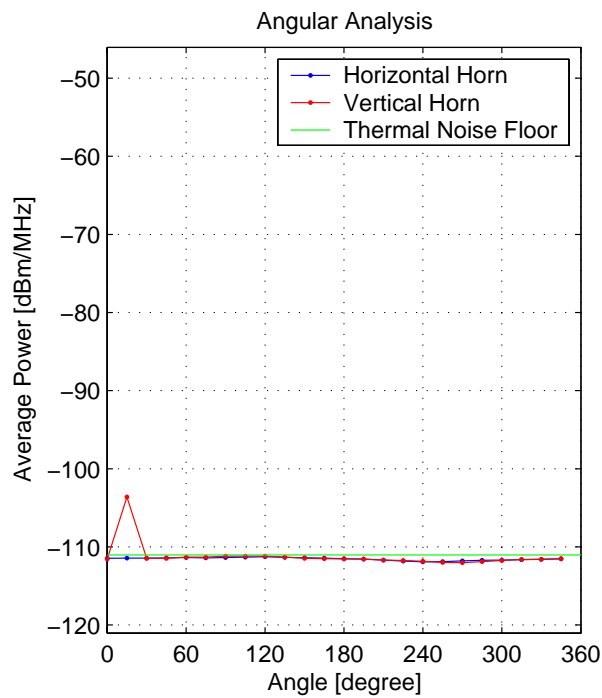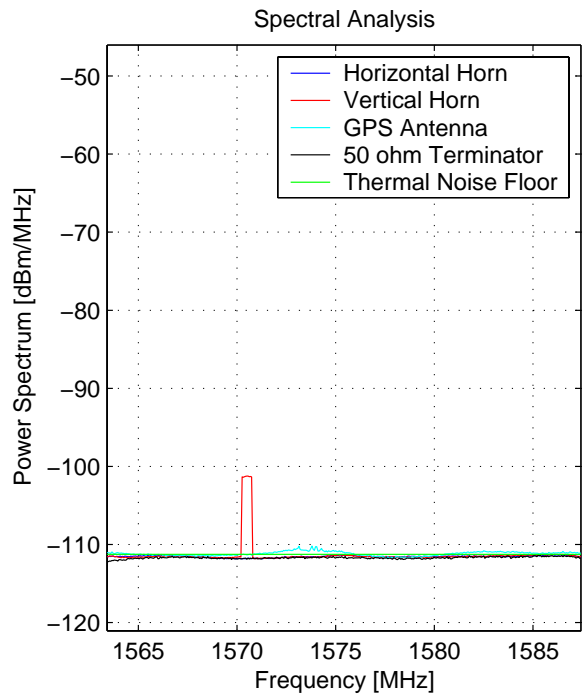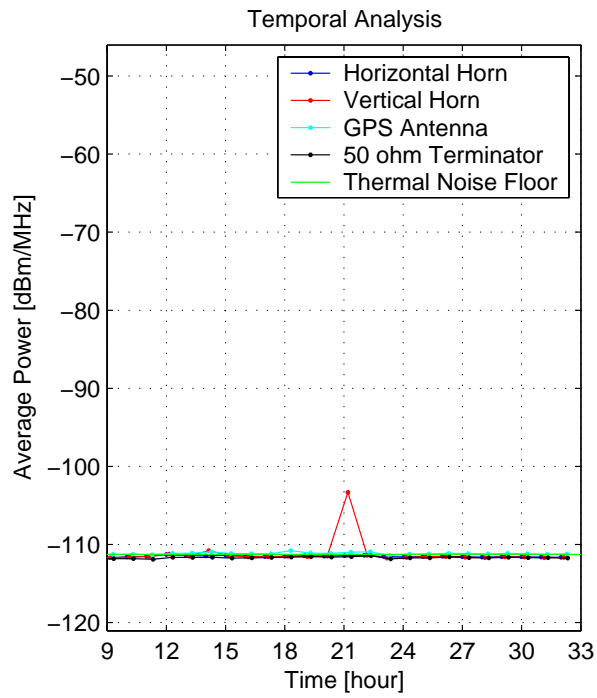
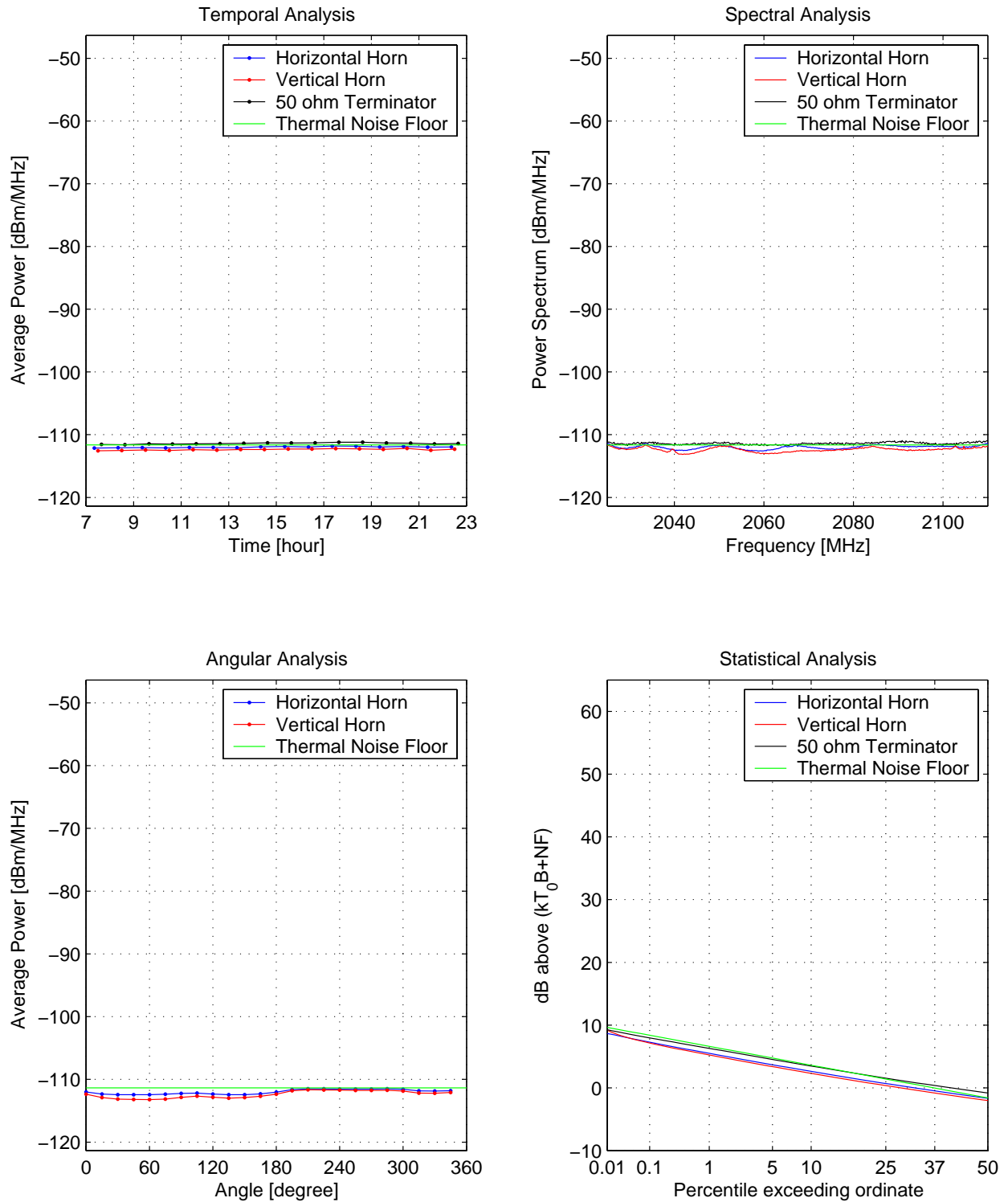Figure A.12. Spectrum Measurements at Palo Alto Downtown (GPS L1)
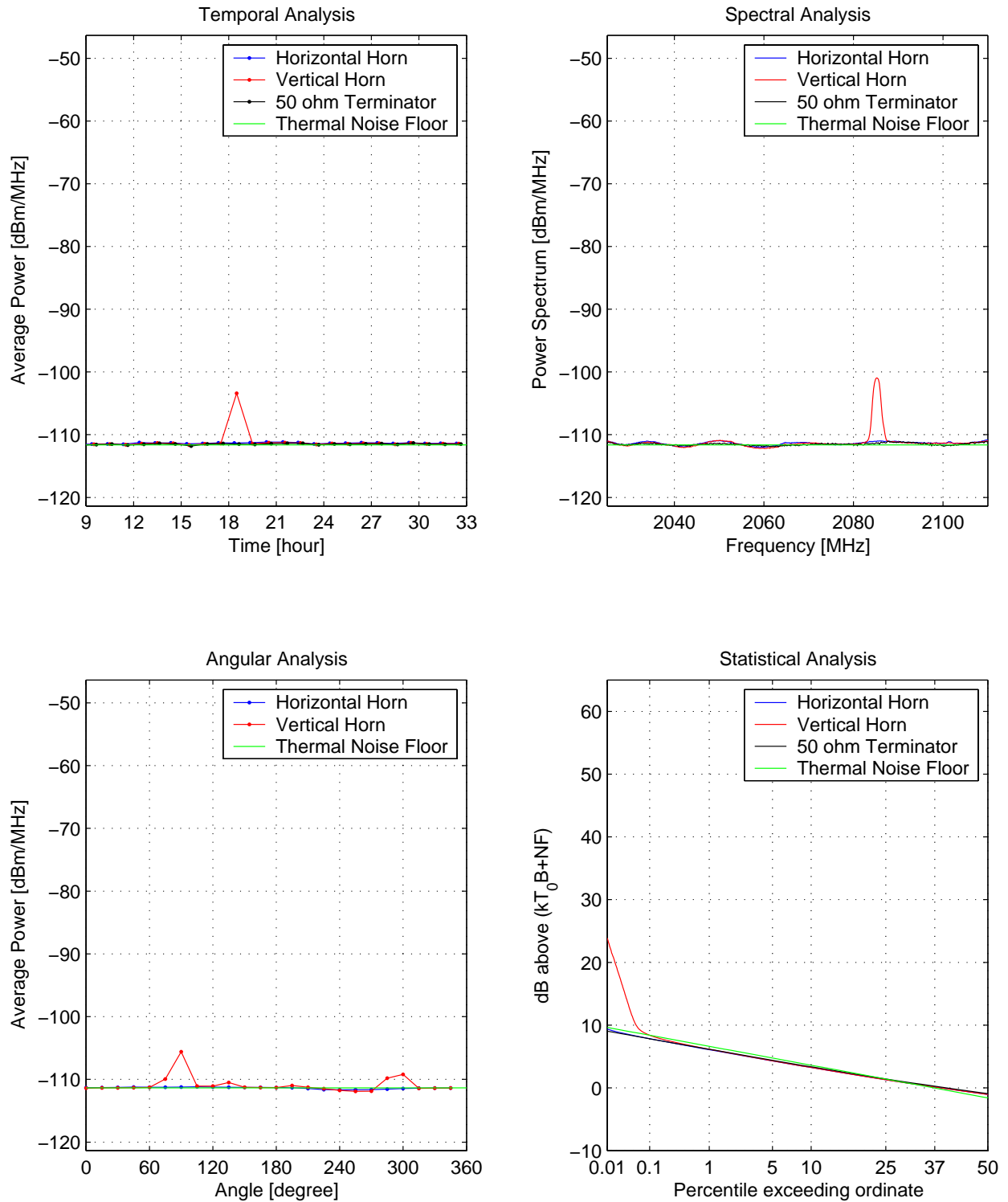
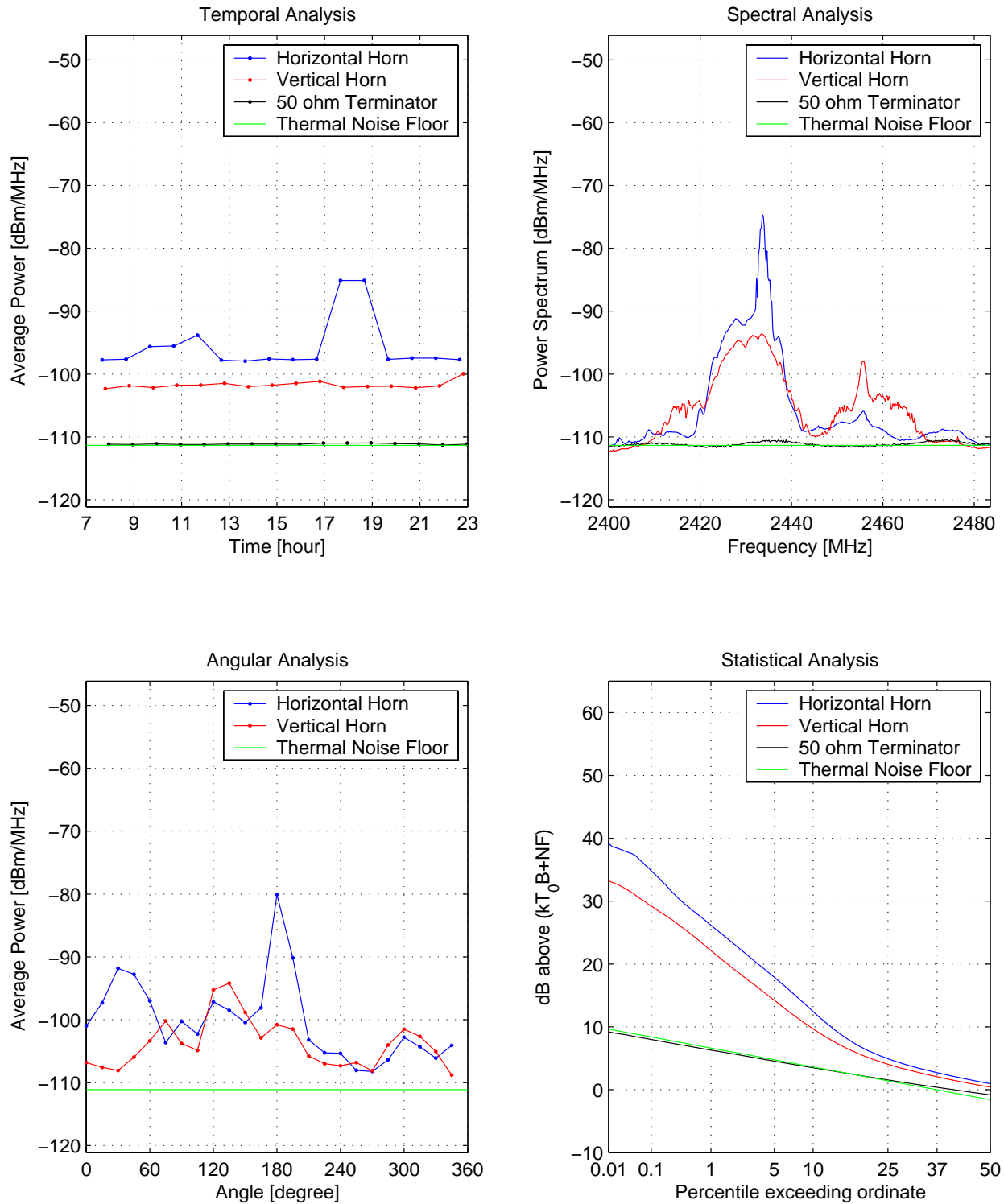Figure A.13. Spectrum Measurements at Palo Alto Downtown (UNI-S)
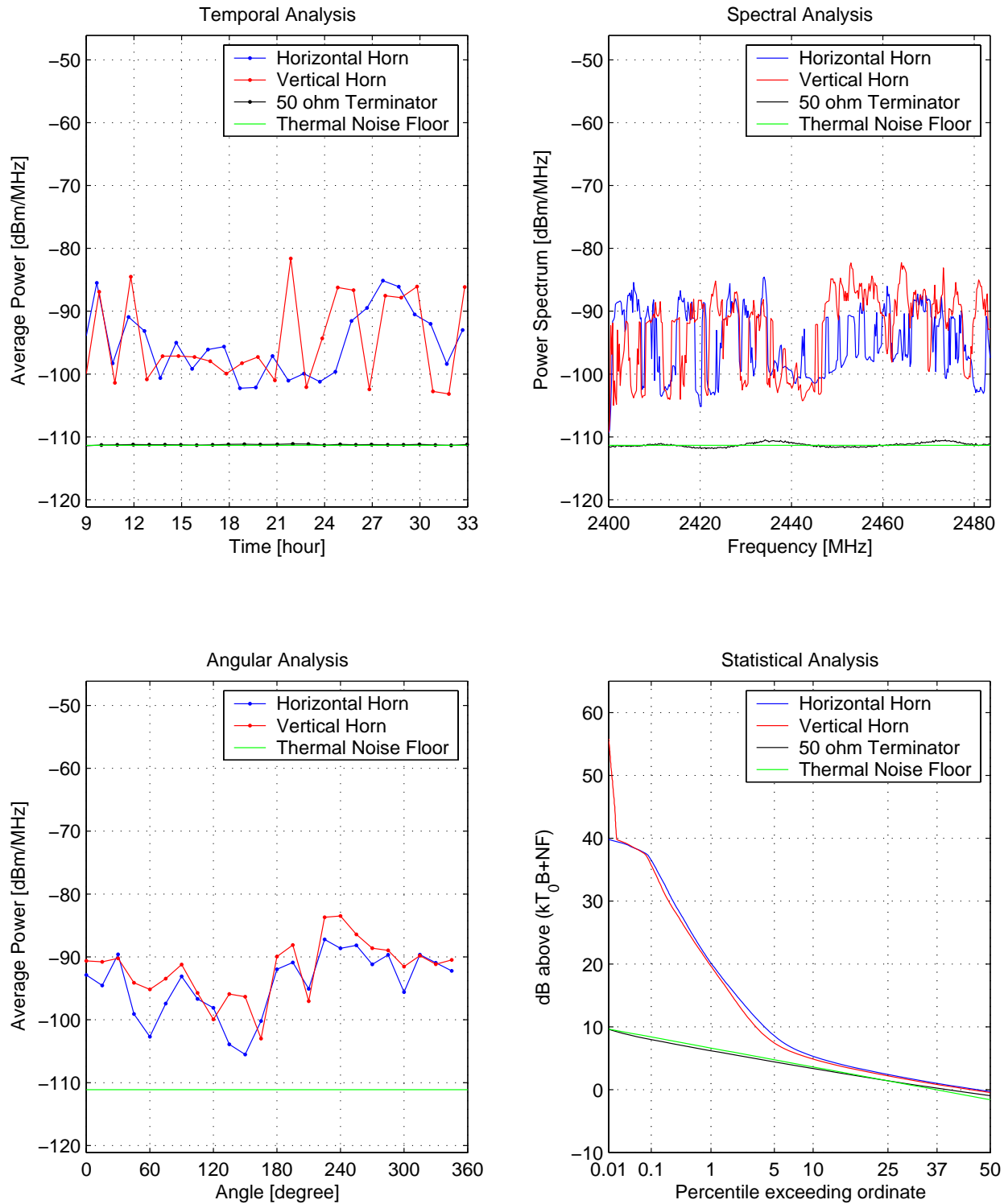
Figure A.14. Spectrum Measurements at Palo Alto Downtown (ISM 2.4)

(This page was left intentionally blank)

Appendix A.3: Yosemite National Park

Site Description

The Yosemite National Park is a national park region for the protection of the forest and the natural habitat within the area of 3045 km^2. Table A.3 and Figures A.15 through A.18 depict the measurement site location and conditions. The LSSM was located at a lodging house inside of the Yosemite National Park. Major objects in close proximity to the LSSM were the lodging houses (1 m away west and 50 m away east) and the surrounding hills (all sides). No pedestrians were observed. Weather was mostly sunny and clear. No WiFi activity was detected during the site survey.

Time	Location	Weather	Distance to Building	Distance to Pathway	WiFi Channel	Address
Nov 5 0900 ~ Nov 6 0900	N37.69 W119.76	Sunny Clear	1 m	N/A	N/A	1172 Danaway Foresta CA 95389

Table A.3. Measurement Site Conditions (Yosemite Park)
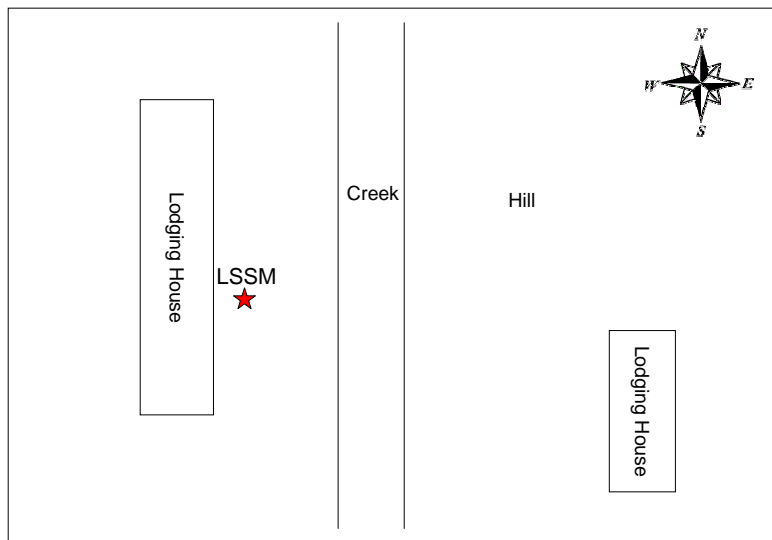
Figure A.15. Location of LSSM at Yosemite Park

Figure A.16. Photo of Spectrum Survey at Yosemite Park
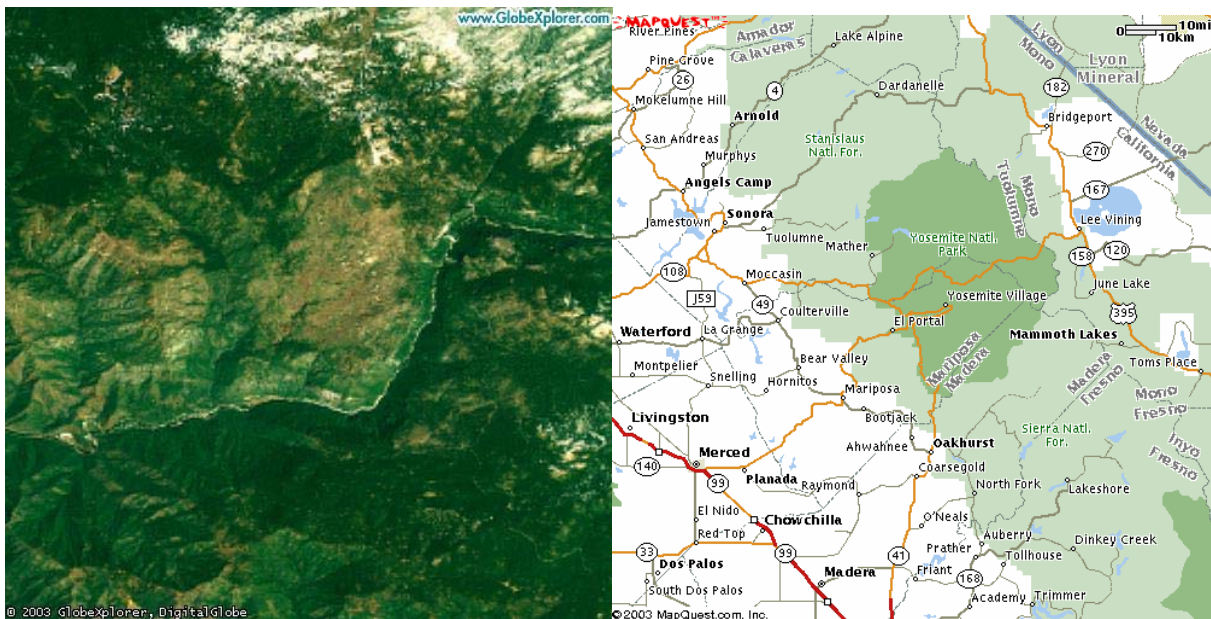
Figure A.17. Aerial Map and Street Map to Yosemite Park

(via www.globexplorer.com & www.mapquest.com)
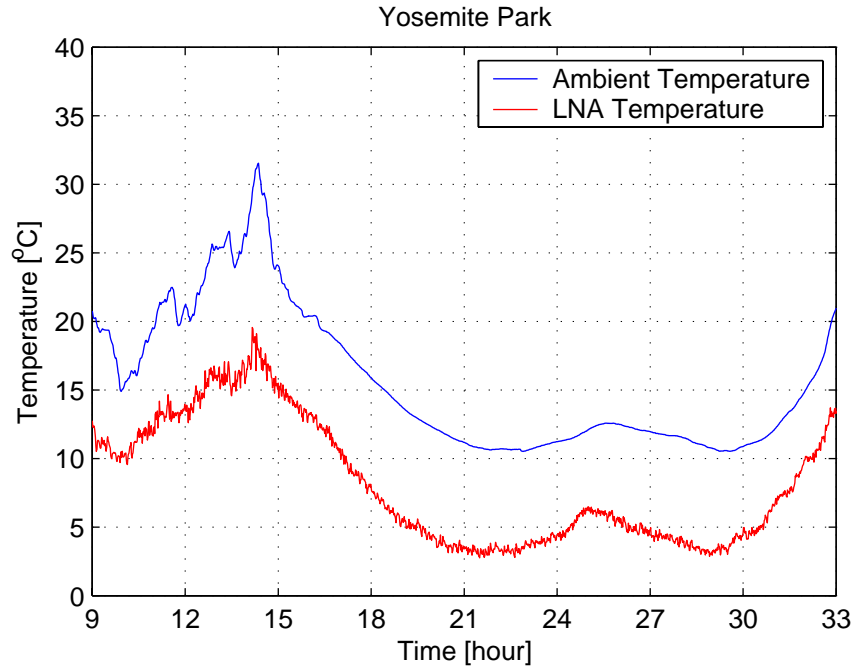
Figure A.18. Temperature Variation During Measurements at Yosemite Park

Data Observation

Band		Comments
GPS L1 (Fig A.19)	Temporal analysis	The average received power was between -112.8 ~ -111.9 dBm/MHz, below the thermal noise floor for all measurement time periods. The highest power, -111.9 dBm/MHz, was measured at 16:00.
	Spectral analysis	The average received power was between -113.3 ~ -110.9 dBm/MHz, below the thermal noise floor for most of the measurement frequencies. The highest power, -110.9 dBm/MHz, was measured at 1575.3 MHz, which is the GPS signal from the GPS satellites.
	Angular analysis	The average received power was between -112.8 ~ -111.7 dBm/MHz, below the thermal noise floor for the most of the measurement. The highest power, -111.7 dBm/MHz, was measured at 285 degrees, which is corresponding to the lodging house. It is because the antennas observed less of the sky and more of the building which is at the thermal equilibrium with the Earth.
	Statistical analysis	No man-made signal except the GPS signal was detected.
UNI-S (Fig A.20)	Temporal analysis	The average received power was between -112.1 ~ -111.6 dBm/MHz, at the thermal noise floor for all measurement time periods. The highest power, -111.6 dBm/MHz, was measured at 16:21.
	Spectral analysis	The average received power was between -112.7 ~ -111.1 dBm/MHz, at the thermal noise floor for all measurement frequencies. The highest power, -111.1 dBm/MHz, was measured at 2025.0 MHz.

|		
	Angular analysis	The average received power was between -112.3 ~ -111.5 dBm/MHz, at the thermal noise floor for all measurement angles. The highest power, -111.5 dBm/MHz, was measured at 225 degrees, which is corresponding to the lodging house. It is because the antennas observed less of the sky and more of the building which is at the thermal equilibrium with the Earth.
	Statistical analysis	No man-made signal was detected.
ISM 2.4 (Fig A.21)	Temporal analysis	The average received power was almost always between -111.9 ~ -111.4 dBm/MHz, below the thermal noise floor. At 10, 16 ~ 18 and 32 ~ 33 hours, there were exceptional increases. Among these, the highest power, -71.2 dBm/MHz, was measured at 32:49. Man-made signals were discontinuous and were not measured for the most of measurement time periods. These exceptional signals probably originated from the microwave ovens in the area considering the measured time periods and the high power level.
	Spectral analysis	The average received power was variable and high, -111.5 ~ -75.1 dBm/MHz, above the thermal noise floor for all measurement frequencies. The highest power, -75.1 dBm/MHz, was measured at 2462.4 MHz. Man-made signals were continuous in frequency and occupied most of frequency, but the upper end of the frequency band was relatively quiet. Two wide band man-made signals were observed in 2400 ~ 2475 MHz and 2430 ~ 2475 MHz.
	Angular analysis	The average received power was variable and high, -111.9 ~ -78.2 dBm/MHz, above the thermal noise floor for the most of the measurement angles. The highest power, - 78.2 dBm/MHz, was measured at 15 degrees. Man-made signals were continuous in the most angles but the angles between 90 and 120 degrees were relatively quiet.
	Statistical analysis	Man-made signals were clearly indicated. They were present 0.78 % of the measurement data with a maximum power of -50.2 dBm/MHz.
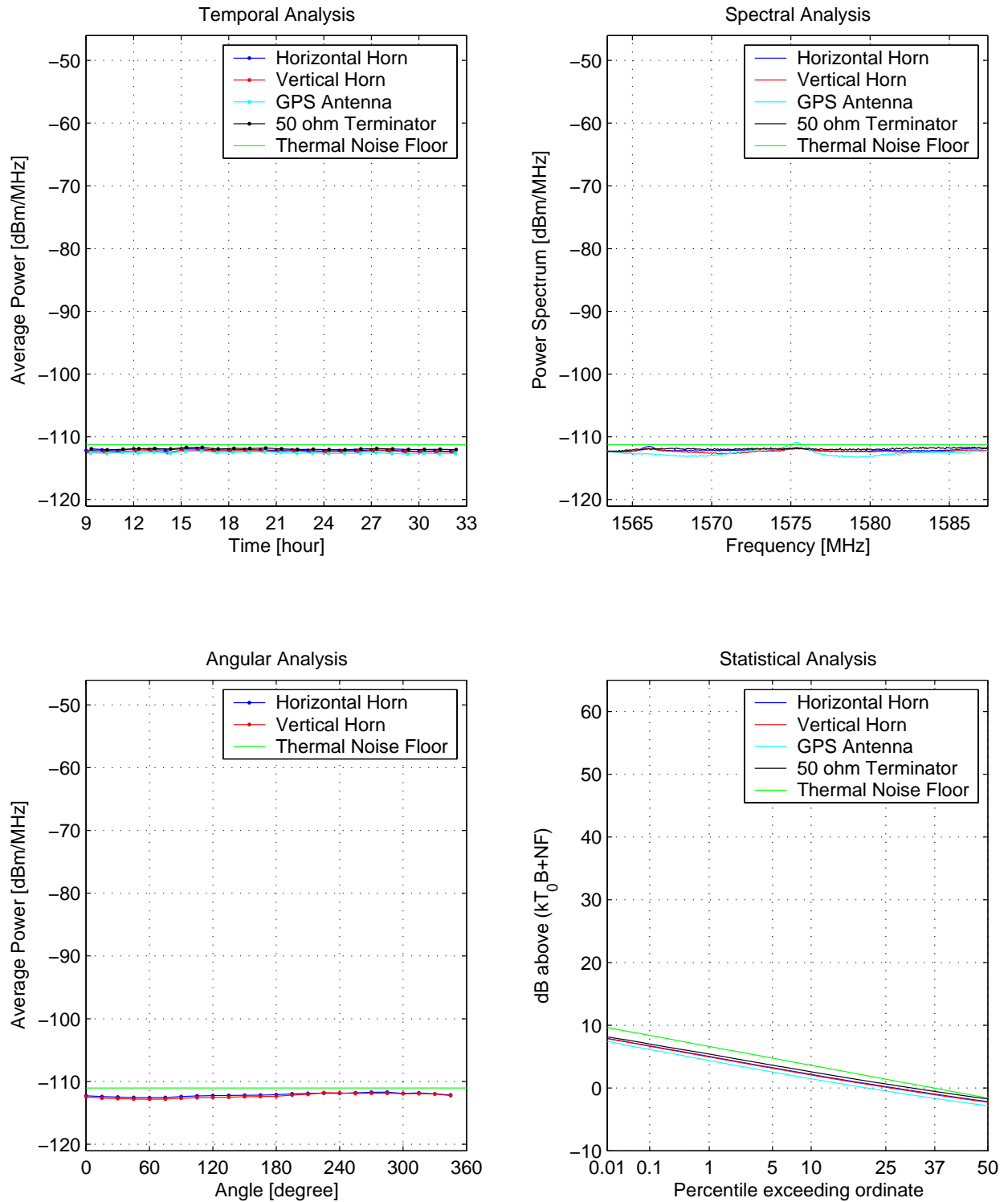
Figure A.19. Spectrum Measurements at Yosemite Park (GPS L1)
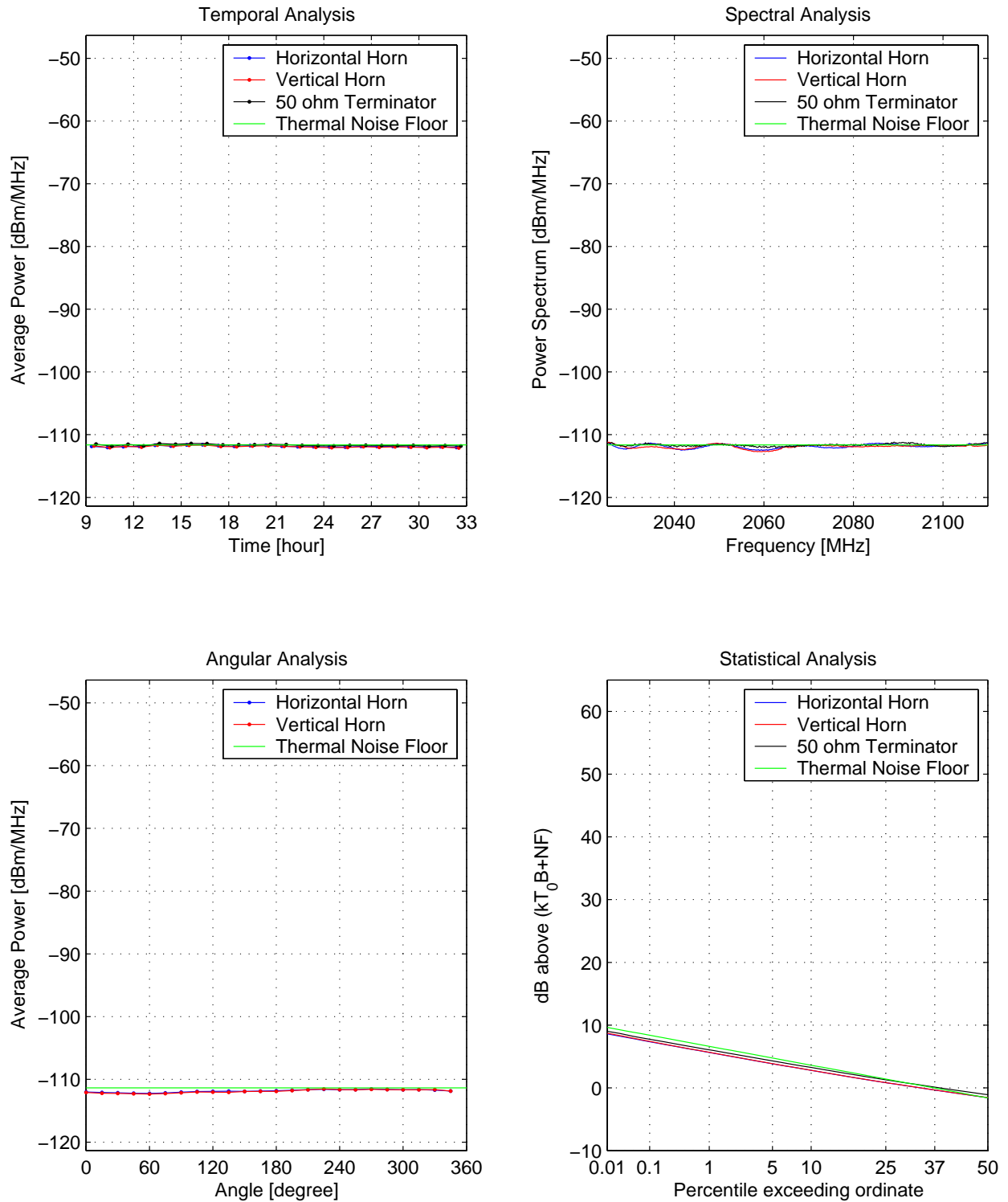
Figure A.20. Spectrum Measurements at Yosemite Park (UNI-S)
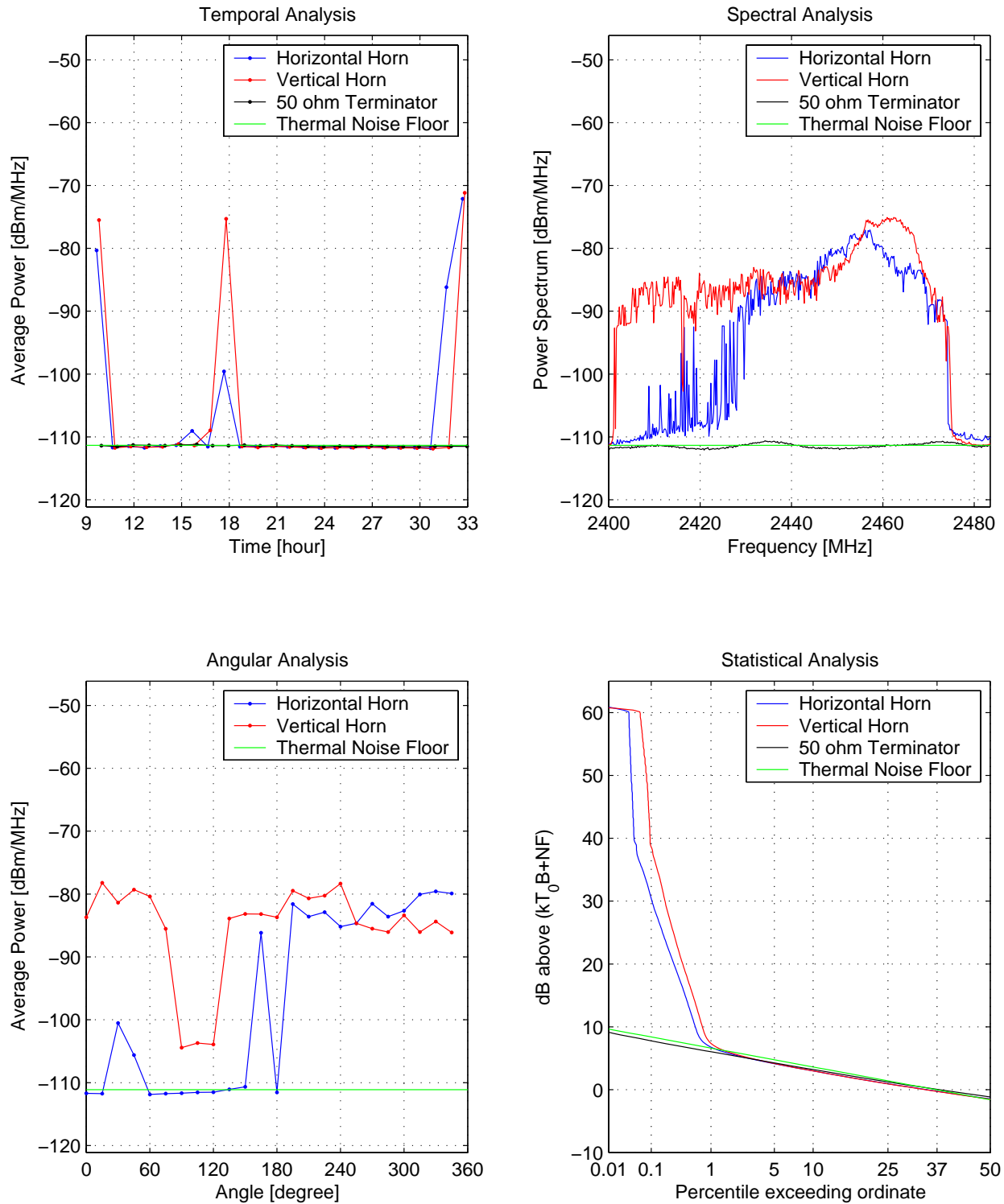
Figure A.21. Spectrum Measurements at Yosemite Park (ISM 2.4)

(This page was left intentionally blank)

Appendix A.4: Jasper Ridge Biological Preserve

Site Description

      The Jasper Ridge Biological Preserve is a serpentine grassland managed primarily for research and instruction within the area of 4.8 km^2 located near Stanford University in the eastern foothills of the Santa Cruz Mountains. Table A.4 and Figures A.22 through A.25 depict the measurement site location and conditions. The LSSM was located at the lakeside away from the major research facilities. Major objects in close proximity to the LSSM were an abandoned facility building (13 m away, northwest) and a WiFi transmitter used for research purposes (10 m away, southwest). No pedestrian was observed during the measurements. Weather was mostly sunny and clear. No WiFi activity was detected during the site survey.

Time	Location	Weather	Distance to Building	Distance to Pathway	WiFi Channel	Address
Oct 9 0900 ~ Oct 10 0900	N37.40 W122.24	Sunny	13 m	On pathway	N/A	4001 Sandhill Rd. Palo Alto CA 94305

Table A.4. Measurement Site Conditions (Jasper Ridge Preserve)
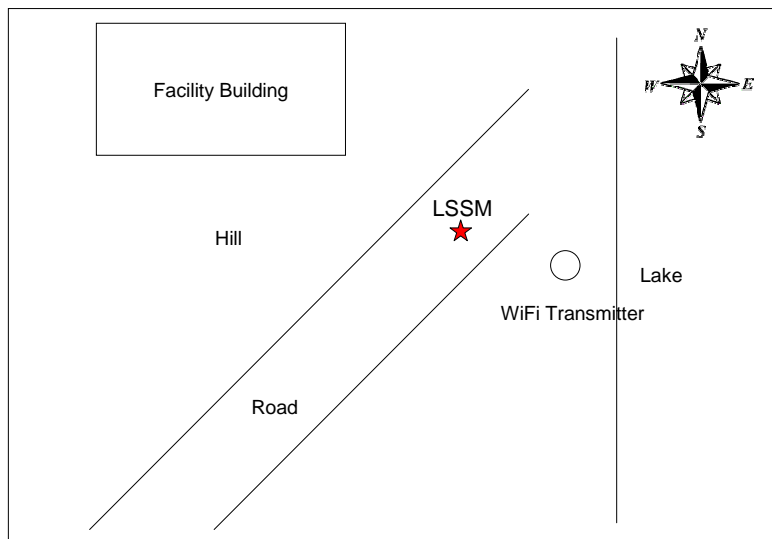
Figure A.22. Location of LSSM at Jasper Ridge Preserve

Figure A.23. Photo of Spectrum Survey at Jasper Ridge Preserve

Figure A.24. Aerial Map and Street Map to Jasper Ridge Preserve

(via www.globexplorer.com & www.mapquest.com)
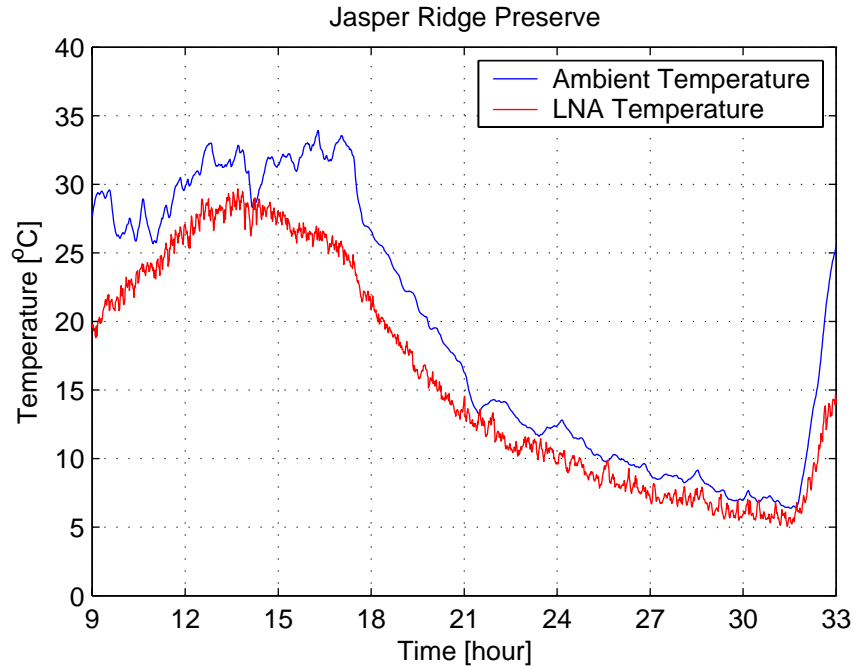
Figure A.25. Temperature Variation During Measurements at Jasper Ridge Preserve

Data Observation

Band		Comments
GPS L1 (Fig A.26)	Temporal analysis	The average received power was between -112.5 ~ -111.8 dBm/MHz, below the thermal noise floor for all measurement time periods. The highest power, -111.8 dBm/MHz, was measured at 14:00.
	Spectral analysis	The average received power was between -112.9 ~ -110.7 dBm/MHz, below the thermal noise floor for most of the measurement frequencies. The highest power, - 110.7 dBm/MHz, was measured at 1575.5 MHz which is the GPS signal from the GPS satellites.
	Angular analysis	The average received power was between -112.7 ~ -111.6 dBm/MHz, below the thermal noise floor for most of the measurement angles. The highest power, -111.6 dBm/MHz, was measured at 300 degrees, which is corresponding to the facility building. It is because the antennas observed less of the sky and more of the building which is at the thermal equilibrium with the Earth.
	Statistical analysis	No man-made signal except the GPS signal was detected.
UNI-S (Fig A.27)	Temporal analysis	The average received power was between -112.2 ~ -111.5 dBm/MHz, at the thermal noise floor for all measurement time periods. The highest power, -111.5 dBm/MHz, was measured at 17:21.
	Spectral analysis	The average received power was between -112.5 ~ -111.1 dBm/MHz, at the thermal noise floor for all measurement frequencies. The highest power, -111.1 dBm/MHz, was measured at 2110.0 MHz.

	Angular analysis	The average received power was between -112.3 ~ -111.4 dBm/MHz, at the thermal noise floor for all measurement angels. The highest power, -111.4 dBm/MHz, was measured at 330 degrees which is corresponding to the facility building. It is because the antennas observed less of the sky and more of the building which is at the thermal equilibrium with Earth.
	Statistical analysis	No man-made signal was detected.
ISM 2.4 (Fig A.28)	Temporal analysis	The average received power was almost always between -106.7 ~ -104.1 dBm/MHz, above the thermal noise floor for all measurement time periods. It exceptionally increased to -84.1 dBm/MHz at 10:40. Man-made signals were continuous and probably originated from the WiFi transmitter installed in the area for the purpose of the research data collection.
	Spectral analysis	The average received power was variable and high, -111.9 ~ -79.7 dBm/MHz, above the thermal noise floor for all measurement frequencies. The highest power, -79.7 dBm/MHz, was measured at 2433.4 MHz. Man-made signals were observed in the 3 frequency ranges and the upper end of the frequency band was relatively quiet. Three wide band man-made signals were observed in 2405 ~ 2415 MHz, 2425 ~ 2440 MHz and 2445 ~ 2465 MHz.
	Angular analysis	The average received power was almost always between -111.2 ~ -108.1 dBm/MHz, at the thermal noise floor for all measurement angles. At the angle between 105 ~ 225 degrees, there were exceptional increases due to the man-made signals. The highest power, -84.5 dBm/MHz, was measured at 120 degrees corresponding to the WiFi transmitter.
	Statistical analysis	Man-made signals were clearly indicated. They were present 3.67 % of the measurement data with a maximum power of -75.5 dBm/MHz.
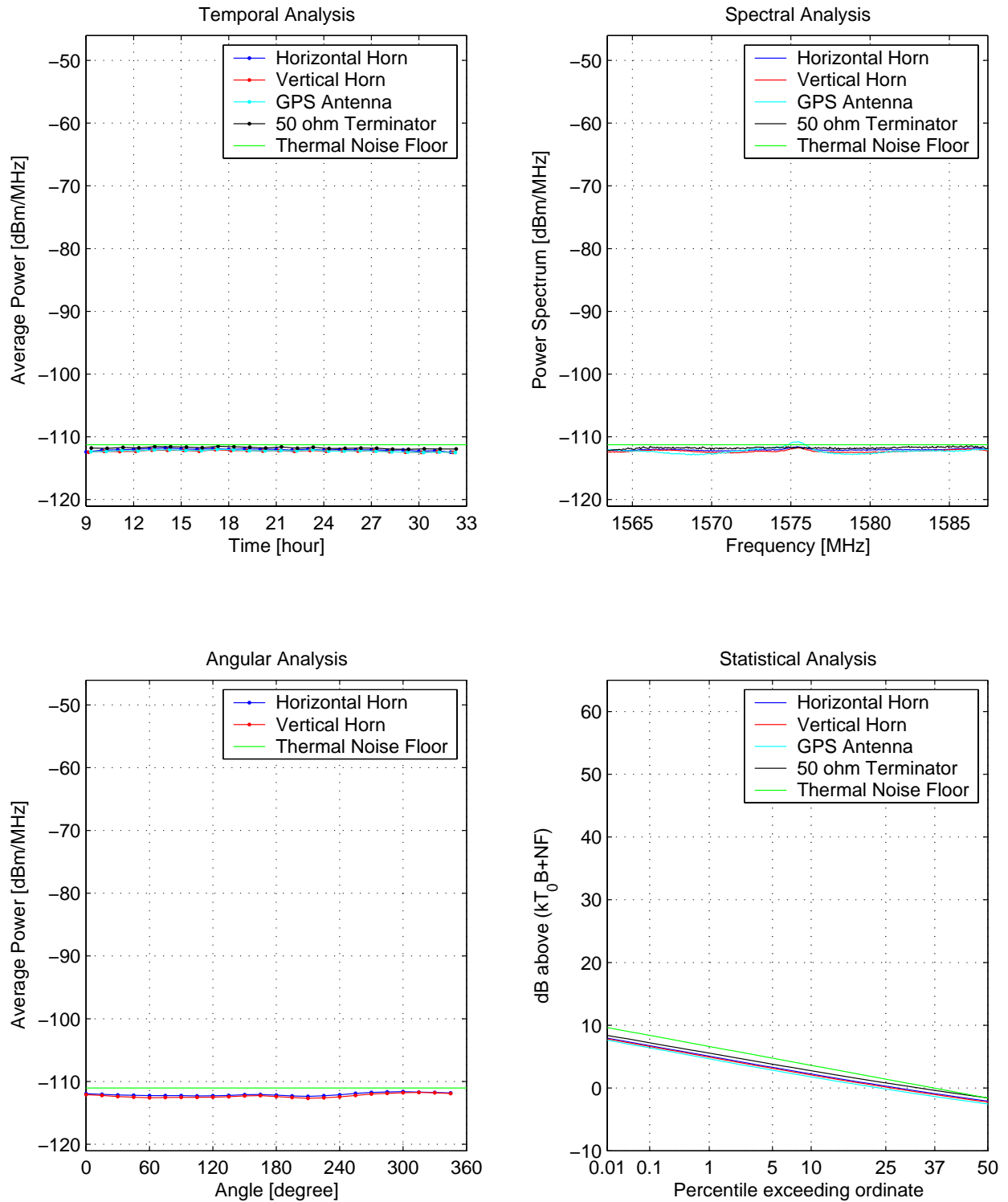
Figure A.26. Spectrum Measurements at Jasper Ridge Preserve (GPS L1)
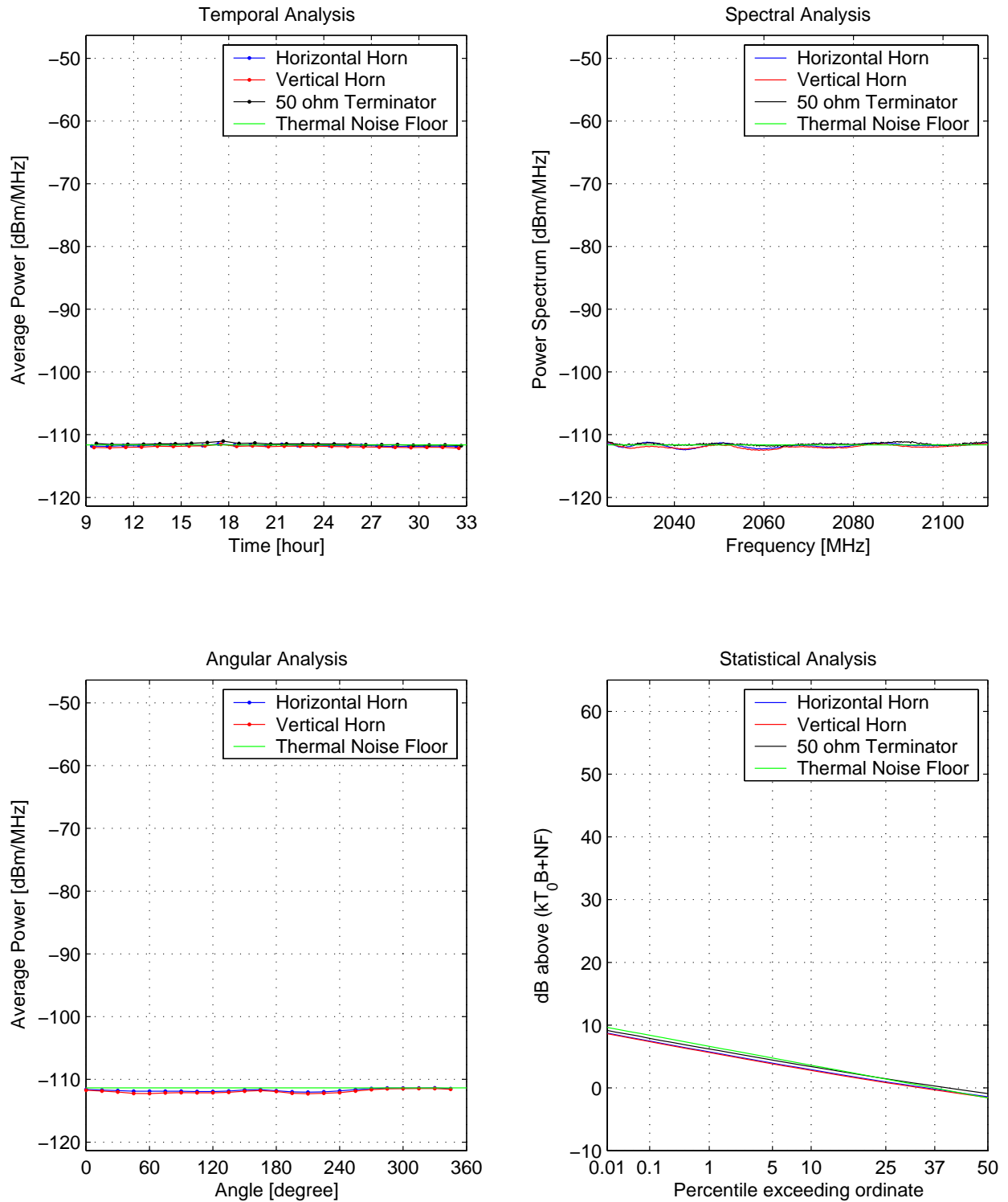
Figure A.27. Spectrum Measurements at Jasper Ridge Preserve (UNI-S)

90
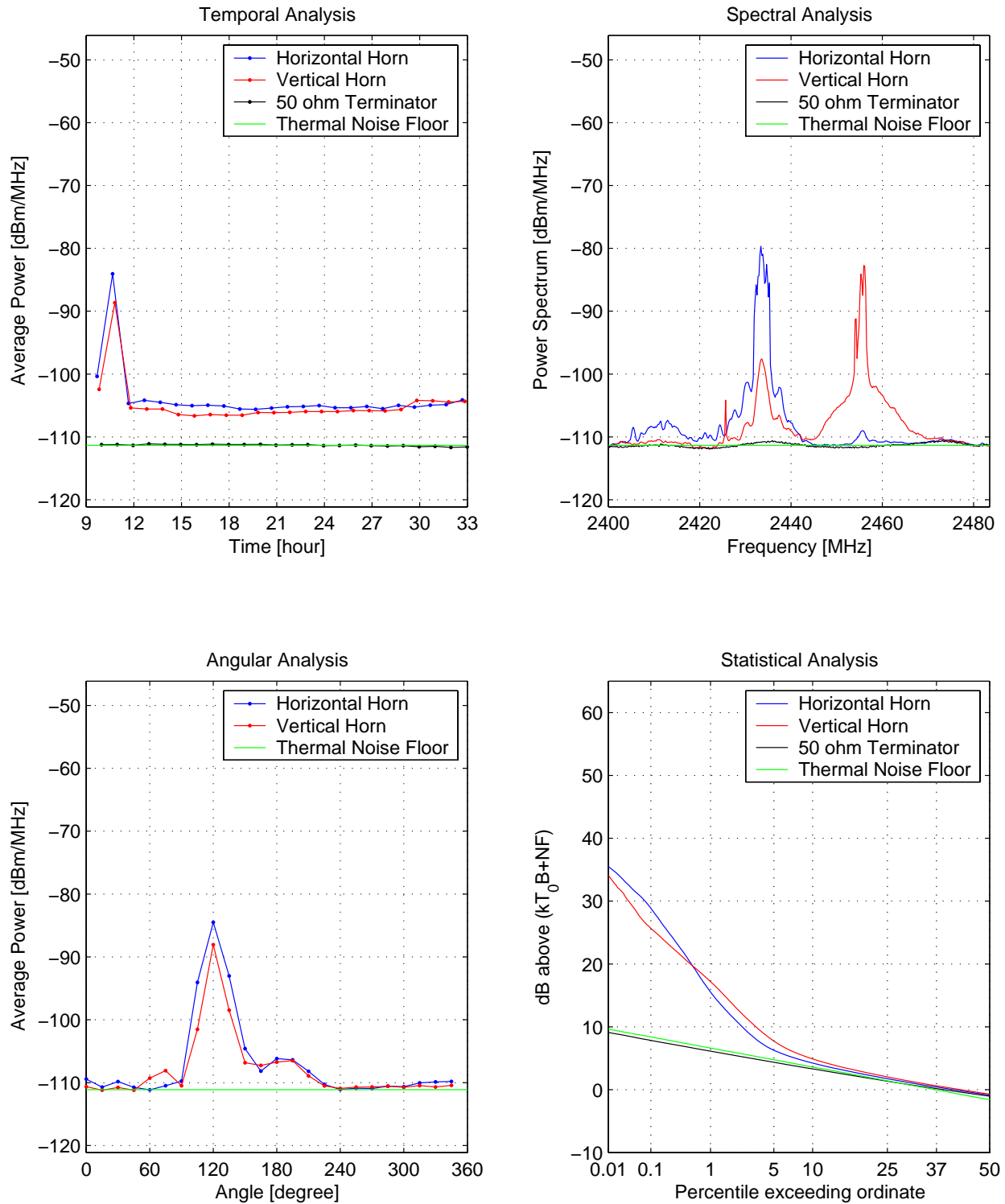
Figure A.28. Spectrum Measurements at Jasper Ridge Preserve (ISM 2.4)

(This page was left intentionally blank)

Appendix A.5: San Jose International Airport

Site Description

The San Jose International Airport is an international airport located 3 km away from the San Jose downtown. There are two terminals and three runways used by both passenger airplanes and cargo airplanes. Table A.5 and Figures A.29 through A.32 depict the measurement site location and conditions. The LSSM was located on the rooftop of the two-story terminal building overlooking the runways. Major objects in close proximity to the LSSM were the runways (southwest), the San Jose downtown (east), other terminal buildings (northwest), the communication antennas installed on the roof (three antennas with minimum 20 m separation from the LSSM) and the passenger airplanes around the terminal building. No pedestrian was allowed in the area. Weather was mostly sunny and clear. No WiFi activity was detected during the site survey.

Time	Location	Weather	Distance to Building	Distance to Pathway	WiFi Channel	Address
Oct 7 0900 ~ Oct 8 0900	N37.36 W121.93	Sunny Clear	On Rooftop of the building	N/A	N/A	1661 Airport Blvd. San Jose CA 95110

Table A.5. Measurement Site Conditions (San Jose Airport)
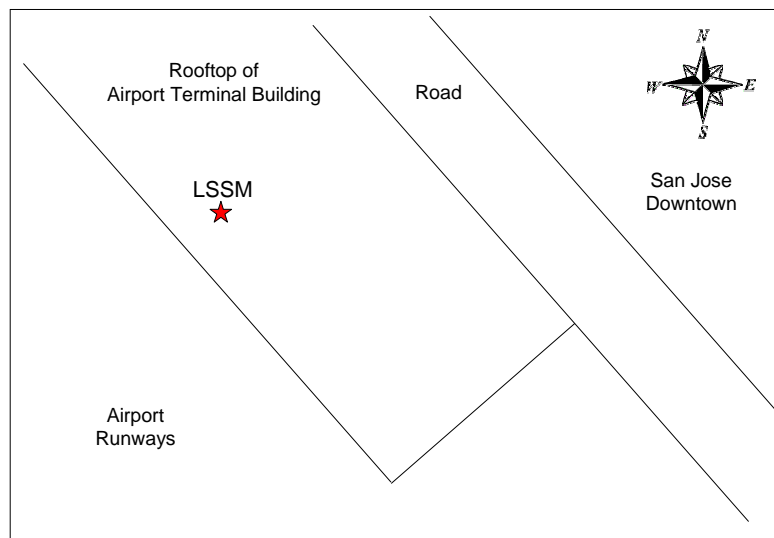
Figure A.29. Location of LSSM at San Jose Airport

Figure A.30. Photo of Spectrum Survey at San Jose Airport

Figure A.31. Aerial Map and Street Map to San Jose Airport

(via www.globexplorer.com & www.mapquest.com)
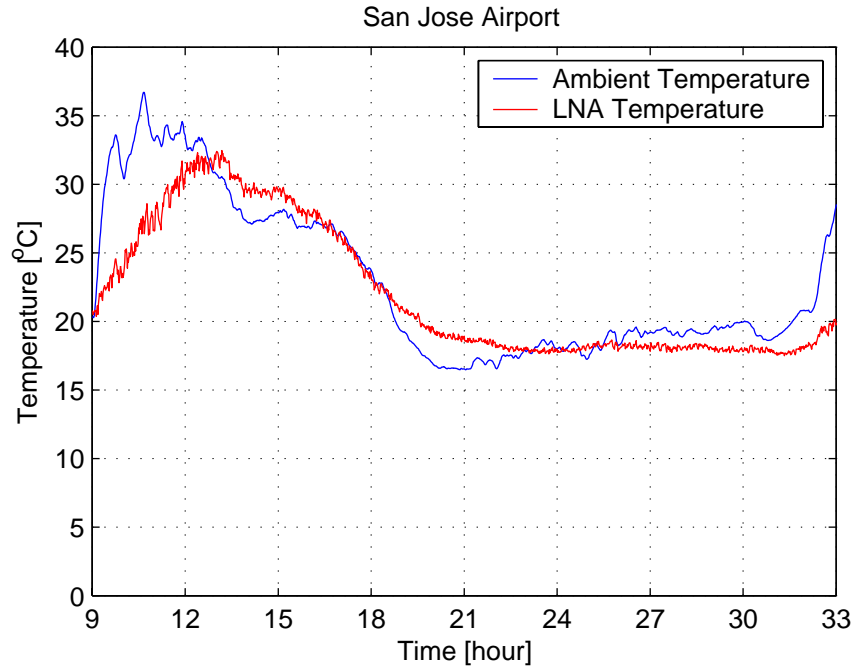
Figure A.32. Temperature Variation During Measurements at San Jose Airport

Data Observation

Band		Comments
GPS L1 (Fig A.33)	Temporal analysis	The average received power was almost always between -113.7 ~ -112.4 dBm/MHz, below the thermal noise floor for the most of the measurement time periods. At 19:00, when it increased to -109.8 dBm/MHz, it probably originated from a single source in the San Jose Downtown.
	Spectral analysis	The average received power was almost always between -113.8 ~ -110.6 dBm/MHz, below the thermal noise floor for the most of the measurement frequencies. At 1567.6 MHz, the narrow band man-made signals with less than 1 MHz bandwidth was measured with the power of -101.4 dBm/MHz.
	Angular analysis	The average received power was almost always between -113.5 ~ -112.5 dBm/MHz, below the thermal noise floor for the most of the measurement angles. At the angle of 90 degrees, it increased to -109.9 dBm/MHz. Ninety degrees corresponds to the San Jose Downtown area.
	Statistical analysis	Man-made signals were present in less than 0.01 % of the measurement data with a maximum power of -100.9 dBm/MHz.
UNI-S (Fig A.34)	Temporal analysis	The average received power was variable and high, -112.9 ~ -63.6 dBm/MHz, above the thermal noise floor for the most of the measurement time periods. The highest power, - 63.6 dBm/MHz, was measured at 10:30. Man-made signals were rather discontinuous, and a few quiet moments were observed between them. They probably originated from multiple sources including the communication antennas installed on the rooftop of the terminal building.

	Spectral analysis	The average received power was variable and high, -113.8 ~ -62.8 dBm/MHz, above the thermal noise floor for the most of the measurement frequencies. The highest power, - 62.8 dBm/MHz, was measured at 2101.9 MHz. Man-made signals were discontinuous in frequency, and a few quiet frequencies were observed. The relatively narrow band man-made signals with less than 10 MHz bandwidth were measured at 2034 MHz and 2050 MHz, and the wide band man-made signals with more than 10 MHz bandwidth were measured at 2068 MHz, 2085 MHz and 2102 MHz.
	Angular analysis	The average received power was variable and high, -97.8 ~ -71.9 dBm/MHz, above the thermal noise floor for all measurement angles. The highest power, -71.9 dBm/MHz, was measured at 135 degrees corresponding to the airport terminal building. It probably originated from the communication antennas installed on the rooftop of the terminal building. There were three communication antennas each at 0, 150, and 285 degrees. Man-made signals were continuous in angle.
	Statistical analysis	Man-made signals were prevalent. They were present 8.71 % of the measurement data with a maximum power of -48.0 dBm/MHz.
ISM 2.4 (Fig A.35)	Temporal analysis	The average received power was variable and high, -98.7 ~ -74.9 dBm/MHz, above the thermal noise floor for all measurement time periods. The highest power, -74.9 dBm/MHz, was measured at 18:40. Man-made signals were continuous in time and probably originated from multiple sources in the surrounding urban area.
	Spectral analysis	The average received power was variable and high, -108.0 ~ -69.8 dBm/MHz, above the thermal noise floor for all measurement frequencies. The highest power, -69.8 dBm/MHz, was measured at 2433.8 MHz. Man-made signals were continuous in frequency. The relatively high power narrow band man-made signals with less than 10 MHz bandwidth were measured at 2420 MHz and 2434 MHz.
	Angular analysis	The average received power was variable and high, -99.7 ~ -76.4 dBm/MHz, above the thermal noise floor for all measurement angles. The highest power, -76.4 dBm/MHz, was measured at 270 degrees corresponding to the edge of the airport terminal building. It probably originated from the communication antennas installed on the rooftop. Man-made signals were continuous in angle.
	Statistical analysis	Man-made signals were prevalent. They were present 26.73 % of the measurement data with a maximum power of -49.4 dBm/MHz.

Figure A.33. Spectrum Measurements at San Jose Airport (GPS L1)

Figure A.34. Spectrum Measurements at San Jose Airport (UNI-S)

98

Figure A.35. Spectrum Measurements at San Jose Airport (ISM 2.4)

(This page was left intentionally blank)

Appendix A.6: Palo Alto Airport

Site Description

      The Palo Alto Airport is a local municipal airport primarily used by general aviation aircraft. It is bordered by the San Francisco Bay and a public golf course. Table A.6 and Figures A.36 through A.39 depict the measurement site location and conditions. The LSSM was located at the corner of the parking area for the airplanes in close proximity to the runway. Major objects in close proximity to the LSSM were the pilot association building (8 m away, west, vacant during the measurement), the public golf course (10 m away, west), the arrays of airplanes (10 m away, east), and the air traffic control tower (30 m away, south east). Pedestrian traffic was very low all day. Weather was mostly sunny and windy. No WiFi activity was detected during the site survey.

Time	Location	Weather	Distance to Building	Distance to Pathway	WiFi Channel	Address
Sept 4 0700 ~ Sept 4 2300	N37.46 W122.11	Sunny Windy	8 m	2 m	N/A	1909 El Camino Rd. Palo Alto CA 94303

Table A.6. Measurement Site Conditions (Palo Alto Airport)

Figure A.36. Location of LSSM at Palo Alto Airport

Figure A.37. Photo of Spectrum Survey at Palo Alto Airport
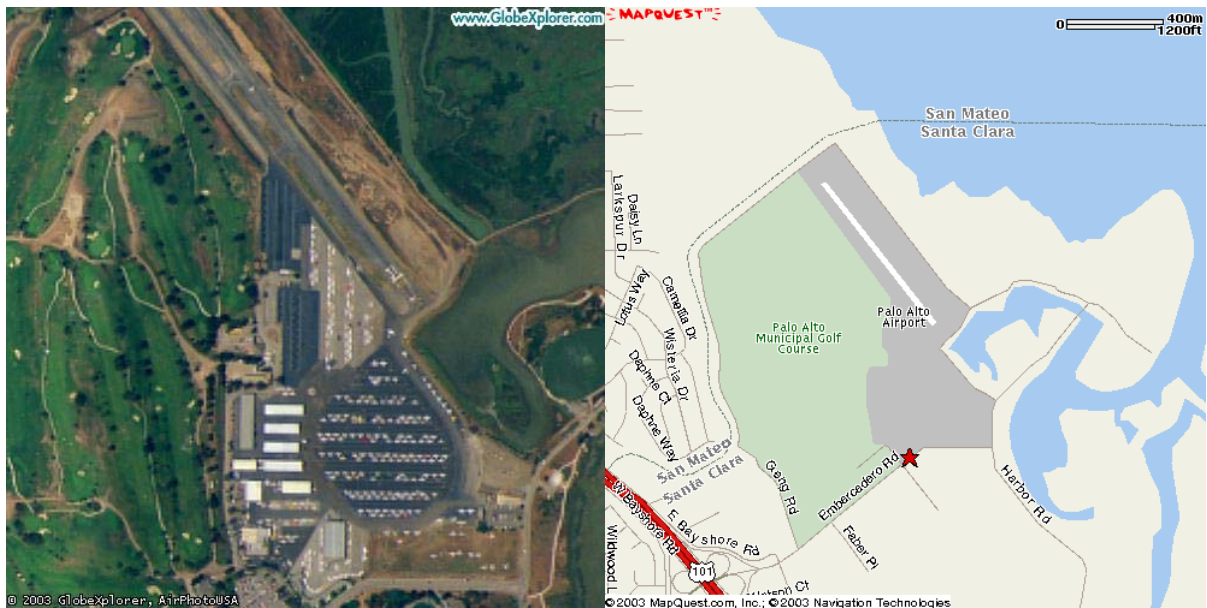
Figure A.38. Aerial Map and Street Map to Palo Alto Airport

(via www.globexplorer.com & www.mapquest.com)
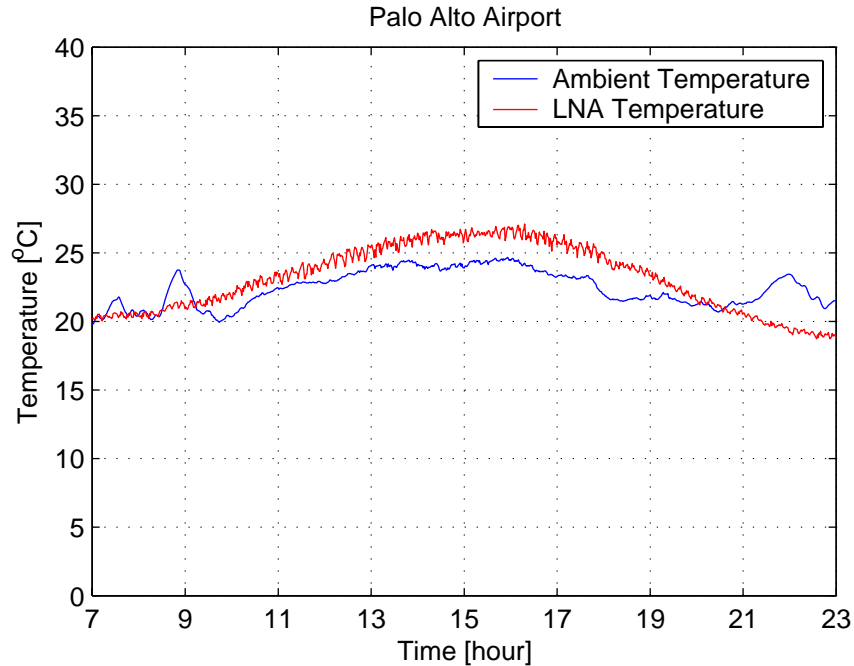
Figure C.39. Temperature Variation During Measurements at Palo Alto Airport

Data Observation

Band		Comments
GPS L1 (Fig A.40)	Temporal analysis	The average received power was between -112.9 ~ -112.1 dBm/MHz, below the thermal noise floor for all measurement time periods. The highest power, -112.1 dBm/MHz, was measured at 17:00.
	Spectral analysis	The average received power was between -113.2 ~ -110.6 dBm/MHz, below the thermal noise floor for the most of the measurement frequencies. The highest power, -110.6 dBm/MHz, was measured at 1575.5 MHz, which is the GPS signal from the GPS satellites.
	Angular analysis	The average received power was between -113.3 ~ -111.8 dBm/MHz, below the thermal noise floor for all measurement angles. The highest power, -111.8 dBm/MHz, was measured at 225 degrees, which is corresponding to the pilot association building. It is because the antennas observed less of the sky and more of the building which is at the thermal equilibrium with the Earth.
	Statistical analysis	No man-made signal except the GPS signal was detected.
UNI-S (Fig A.41)	Temporal analysis	The average received power was between -112.6 ~ -111.8 dBm/MHz, below the thermal noise floor for all measurement time periods. The highest power, -111.8 dBm/MHz, was measured at 17:21.
	Spectral analysis	The average received power was between -113.1 ~ -111.3 dBm/MHz, below the thermal noise floor for the most of the measurement frequencies. The highest power, -111.3 dBm/MHz, was measured at 2035MHz.

	Angular analysis	The average received power was between -113.2 ~ -111.5 dBm/MHz, below the thermal noise floor for all measurement angles. The highest power, -111.5 dBm/MHz, was measured at 210 degrees, which is corresponding to the pilot association building.
	Statistical analysis	Man-made signals were present in less than 0.01 % of the measurement data with a maximum power of -102.1 dBm/MHz.
ISM 2.4 (Fig A.42)	Temporal analysis	The average received power was variable and high, -102.3 ~ -85.1 dBm/MHz, above the thermal noise floor for all measurement time periods. The measurements by the horizontal horn antenna showed high variation, -98.0 ~ -85.1 dBm/MHz but those by the vertical horn antenna were mainly constant, -102.3 ~ -100.0 dBm/MHz. The highest power, -85.1 dBm/MHz, was measured at 17:40 and 18:40. Man-made signals were continuous in time and probably originated from multiple sources including WiFi transmitters in the surrounding urban area.
	Spectral analysis	The average received power was variable and high, -112.4 ~ -74.6 dBm/MHz, above the thermal noise floor for the most of the measurement frequencies. The highest power, -74.6 dBm/MHz, was measured at 2433.6 MHz. Man-made signals were observed in the two separate frequency ranges. The relatively high power narrow band man-made signals with less than 10 MHz bandwidth were measured at 2434 MHz and 2456 MHz, and the wide band man-made signals with more than 10 MHz bandwidth were measured at 2420 ~ 2440 MHz and 2450 ~ 2470 MHz. The wide band man-made signals probably originated from WiFi transmitters.
	Angular analysis	The average received power was variable and high, -108.8 ~ -80.1 dBm/MHz, above the thermal noise floor for all measurement angles. The highest power, -80.1 dBm/MHz, was measured at 180 degrees corresponding to the airport buildings over the public parking lot. Man-made signals probably originated from WiFi transmitters in the surrounding Palo Alto city area. Relatively low power was measured at 200 ~ 300 degrees because the pilot building blocked and attenuated the man-made signals. Man-made signals were rather continuous in angle.
	Statistical analysis	Man-made signals were prevalent. They were present 13.68 % of the measurement data with a maximum power of -71.9 dBm/MHz.
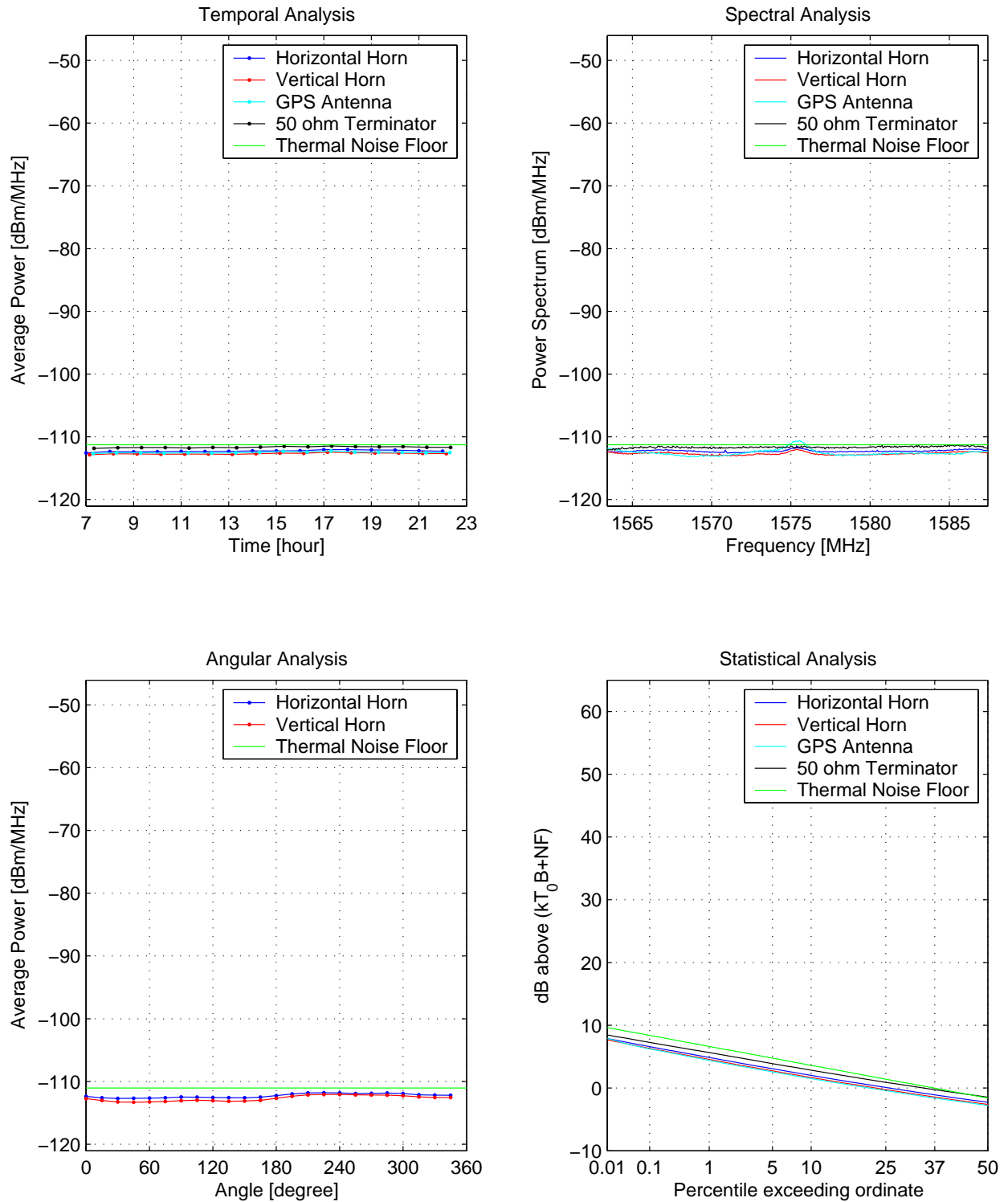
Figure A.40. Spectrum Measurements at Palo Alto Airport (GPS L1)

Figure A.41. Spectrum Measurements at Palo Alto Airport (UNI-S)

Figure A.42. Spectrum Measurements at Palo Alto Airport (ISM 2.4)

(This page was left intentionally blank)

Appendix A.7: Port of Oakland

Site Description

  The Port of Oakland is an international cargo transportation and distribution hub located on the mainland shore of San Francisco Bay and to the east of the Oakland downtown and to the west of the San Francisco downtown. There are 4.9 km^2 of marine terminals, intermodal rail facility, maritime support area, 20 deepwater berths, and 35 container cranes. Table A.1 and Figures A.43 through A.46 depict the measurement site location and conditions. The LSSM was located at the Middle Harbor Shoreline Park between the terminals. Major objects in close proximity to the LSSM were the terminal 30 (north), the terminal 55 (east) and a park facility building (20 m away, east). Pedestrian traffic was very low for all day. Weather was mostly cloudy and windy. No WiFi activity was detected during the site survey.

Time	Location	Weather	Distance to Building	Distance to Pathway	WiFi Channel	Address
Oct 30 0800 ~ Oct 30 2300	N37.80 W122.33	Cloudy Windy	20 m	2 m	N/A	2777 Middle Harbor Rd. Oakland CA 94607

Table A.7. Measurement Site Conditions (Port of Oakland)
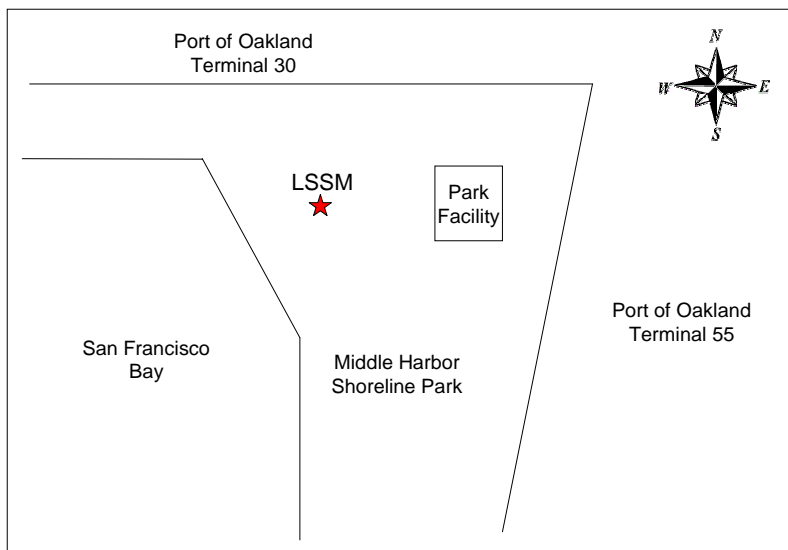
Figure A.43. Location of LSSM at Port of Oakland

Figure A.44. Photo of Spectrum Survey at Port of Oakland
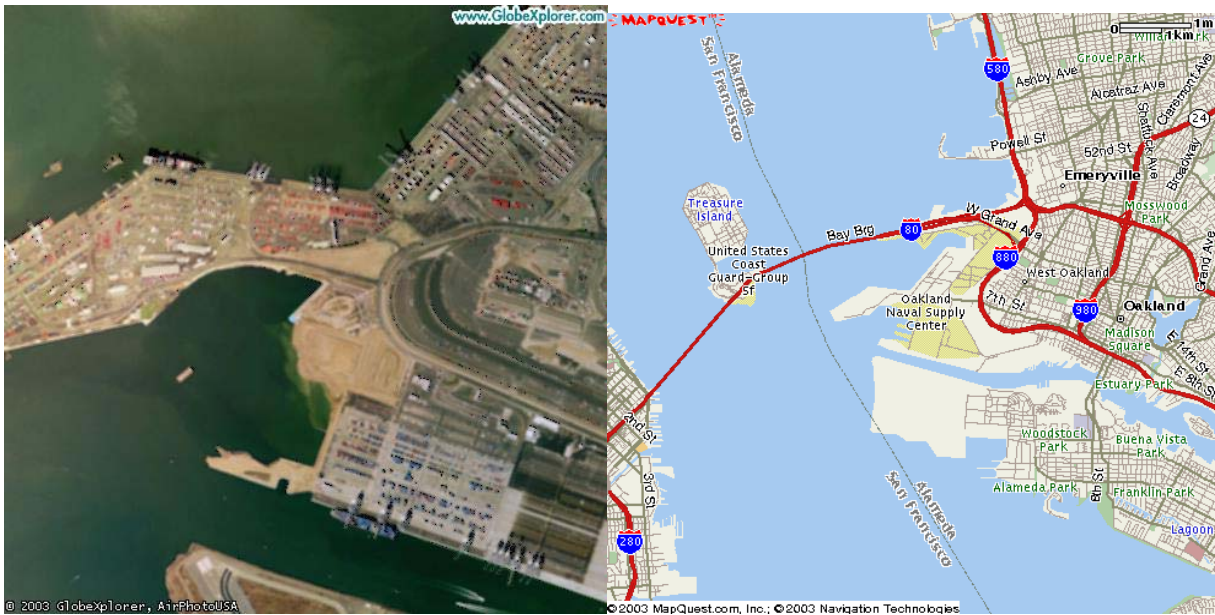
Figure A.45. Aerial Map and Street Map to Port of Oakland

(via www.globexplorer.com & www.mapquest.com)
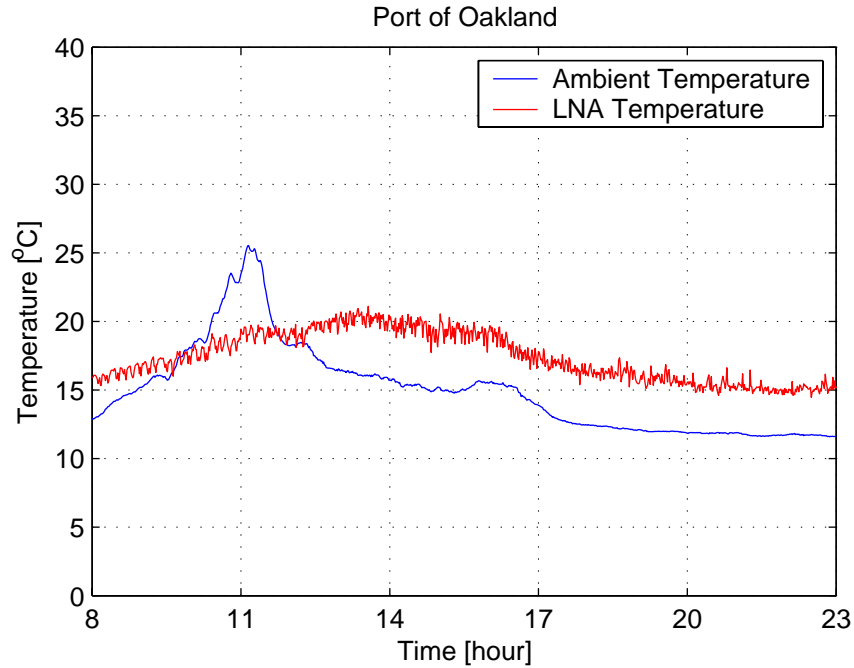
Figure A.46. Temperature Variation during Measurements at Port of Oakland

Data Observation

Band		Comments
GPS L1 (Fig A.47)	Temporal analysis	The average received power was almost always between -113.5 ~ -112.7 dBm/MHz, below the thermal noise floor for all measurement time periods. At 16:08, there were man-made signals detected by the vertical horn antenna, which is approximately 0.5 dB higher than the rest of the data and supposed to have originated from a single source in the San Francisco downtown area.
	Spectral analysis	The average received power was between -113.7 ~ -110.8 dBm/MHz, below the thermal noise floor for the most of the measurement frequencies. The highest power, -110.8 dBm/MHz, was measured at 1575.5 MHz, which is the GPS signal from the GPS satellites.
	Angular analysis	The average received power was between -113.5 ~ -112.8 dBm/MHz, below the thermal noise floor for all measurement angles. The highest power, -112.8 dBm/MHz, was measured at 225 degrees, which is corresponding to the San Francisco downtown area.
	Statistical analysis	Man-made signals were present in less than 0.01 % of the measurement data with a maximum power of -100.5 dBm/MHz.

111

UNI-S (Fig A.48)	Temporal analysis	The average received power was -113.0 ~ -91.5 dBm/MHz, above the thermal noise floor for the most of the measurement time periods. During the daytime, it was relatively quiet but it increased sharply after 19:00. The highest power, -91.5 dBm/MHz, was measured at 10:30. Man-made signals were continuous in time, except one quiet moment at 16:00, which probably originated from multiple sources in the San Francisco Downtown area.
	Spectral analysis	The average received power was variable and high, -113.7 ~ -82.5 dBm/MHz and above the thermal noise floor in approximately 50 % of the frequencies. The highest power, -62.8 dBm/MHz, was measured at 2051.4 MHz. Man-made signals were discontinuous in frequency, and approximately 50 % of the frequencies were quiet. The relatively narrow band man-made signals with less than 10 MHz bandwidth were measured at 2034, 2040, 2068 and 2101 MHz, and the wide band man-made signals with more than 10 MHz bandwidth were measured at 2051 and 2084 MHz.
	Angular analysis	The average received power was variable and high, -111.7 ~ -91.1 dBm/MHz, and above the thermal noise floor in approximately 50 % of the angles. The highest power, -91.1 dBm/MHz, was measured at 240 degrees which is corresponding to the San Francisco downtown area. Man-made signals were continuous in the angle between 150 and 300 degrees.
	Statistical analysis	Man-made signals were clearly indicated. They were present 2.77 % of the measurement data with a maximum power of -76.7 dBm/MHz.
ISM 2.4 (Fig A.49)	Temporal analysis	The average received power was variable and high, -95.6 ~ -72.7 dBm/MHz, above the thermal noise floor for all measurement time periods. The highest power, -72.7 dBm/MHz, was measured at 16:48. Man-made signals were continuous in time and probably originated from multiple sources, including WiFi transmitters especially in the San Francisco downtown area.
	Spectral analysis	The average received power was variable and high, -109.2 ~ -70.3 dBm/MHz, above the thermal noise floor for all measurement frequencies. The highest power, -70.3 dBm/MHz, was measured at 2426.5 MHz. Man-made signals were continuous in frequency. The relatively high power wide band man-made signals with more than 10 MHz bandwidth were measured at 2410 ~ 2430 MHz and 2450 ~ 2465 MHz.
	Angular analysis	The average received power was variable and high, -102.6 ~ -68.6 dBm/MHz, above the thermal noise floor for all measurement angles. The highest power, -68.6 dBm/MHz, was measured at 270 degrees corresponding to the San Francisco downtown area. Man-made signals were continuous in angle.
	Statistical analysis	Man-made signals were prevalent. They were present 43.30 % of the measurement data with a maximum power of -49.9 dBm/MHz.
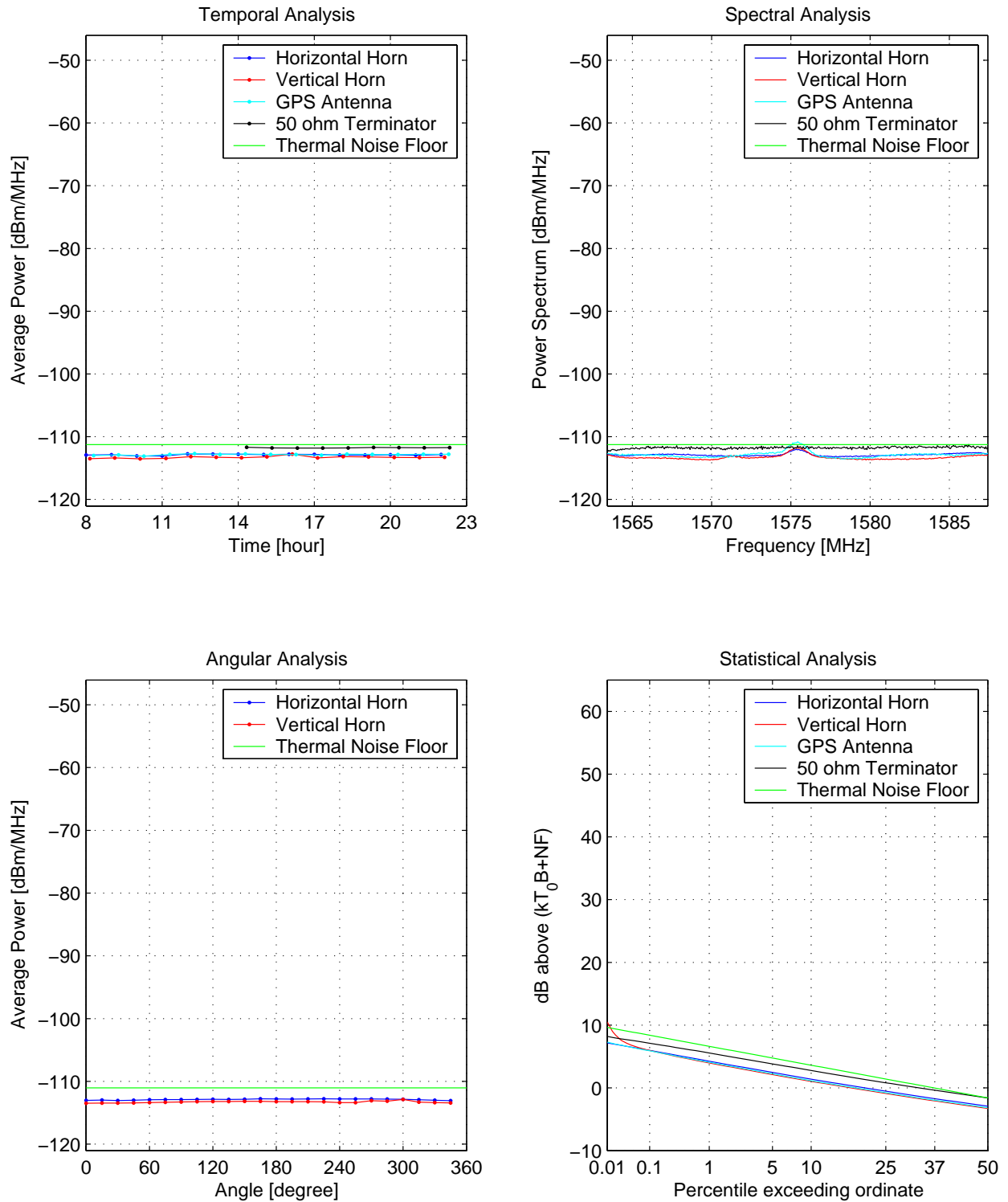
Figure A.47. Spectrum Measurements at Port of Oakland (GPS L1)
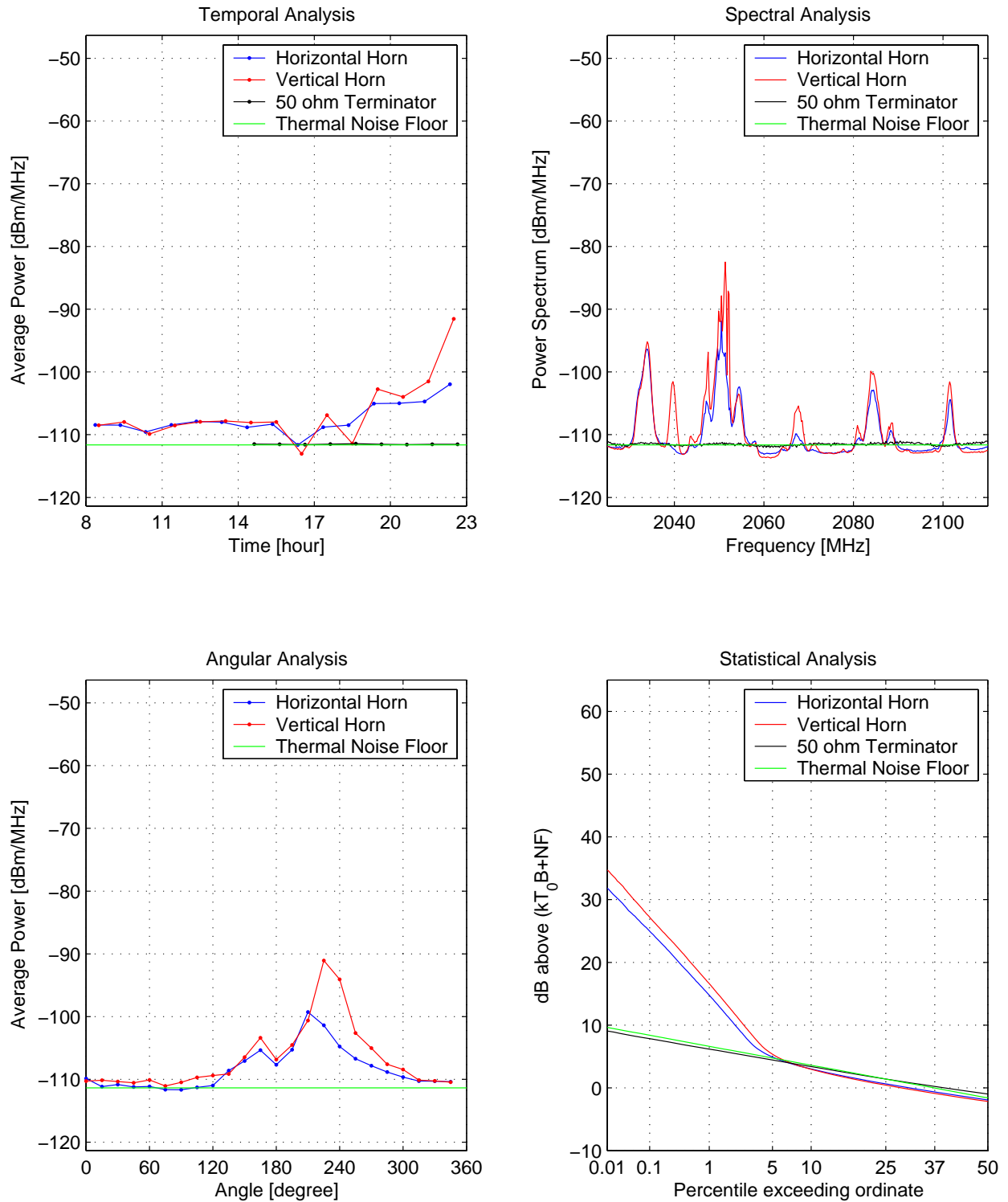
Figure A.48. Spectrum Measurements at Port of Oakland (UNI-S)
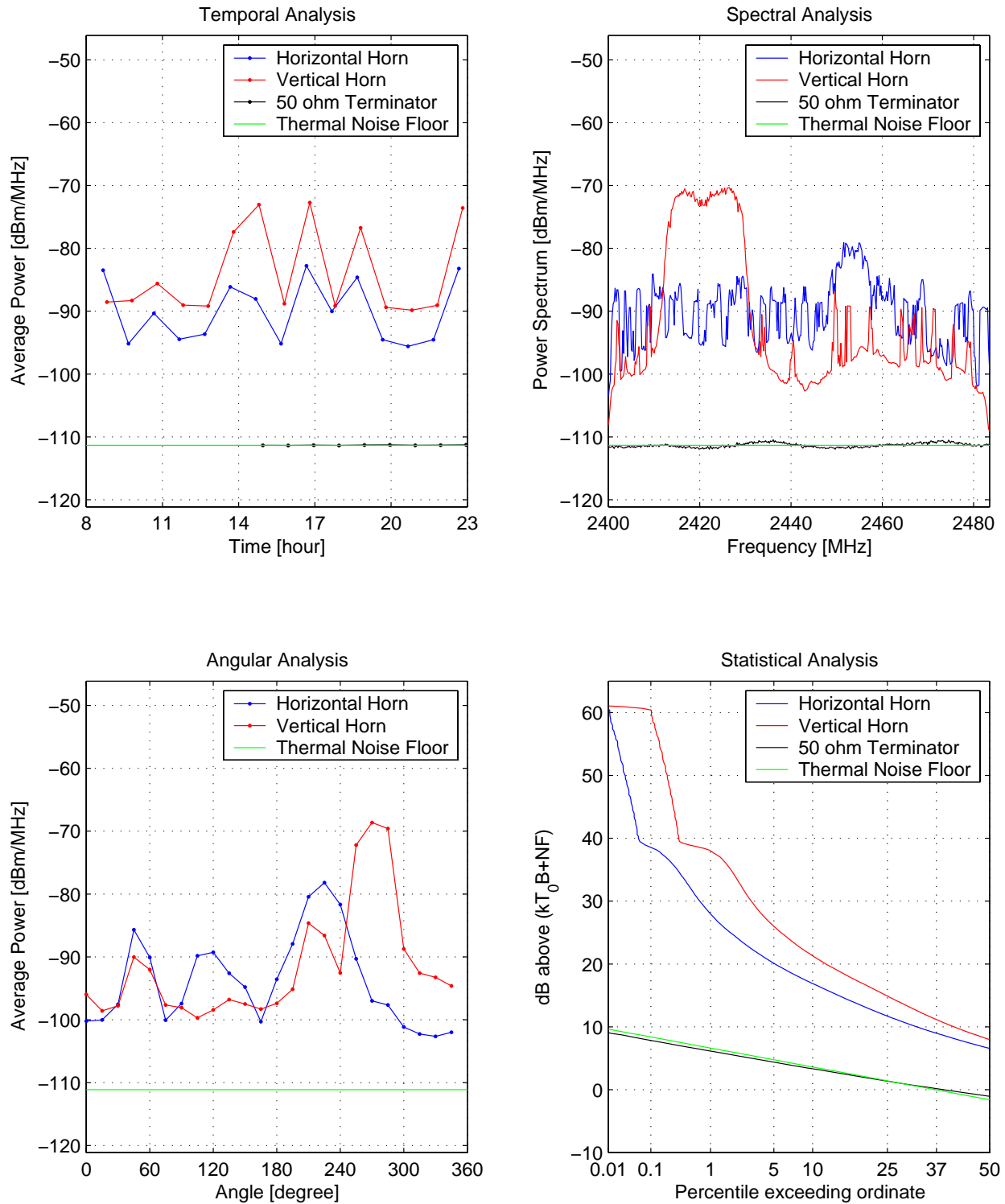
Figure A.49. Spectrum Measurements at Port of Oakland (ISM 2.4)

(This page was left intentionally blank)

Appendix A.8: Coyote Point Marina

Site Description

The Coyote Point Marina is a recreational harbor located within the Coyote Point Recreation Area. It faces the San Francisco Bay and is bordered by a public golf course. Table A.8 and Figures A.50 through A.53 depict the measurement site location and conditions. The LSSM was located at the corner of the harbor area overlooking the array of the docked boats. Major objects in close proximity to the LSSM were the single story yacht club house (10 m away, north), the array of boats (50 m away, east), the harbor facility buildings (100 m away, south), and the hill (50 m away, west). The distance to the pathway was 1 m but the pedestrian traffic was very low for all day. Weather was sunny and windy with occasional clouds. WiFi activity (channel number = 2, SNR = 48) was detected during the site survey.

Time	Location	Weather	Distance to Building	Distance to Pathway	WiFi Channel	Address
Aug 28 0700 ~ Aug 28 2300	N37.59 W122.32	Sunny Windy	10 m	1 m	Channel 2 SNR = 48	1966 Coyote Point Drive San Mateo CA 94401

Table A.8. Measurement Site Conditions (Coyote Point Marina)
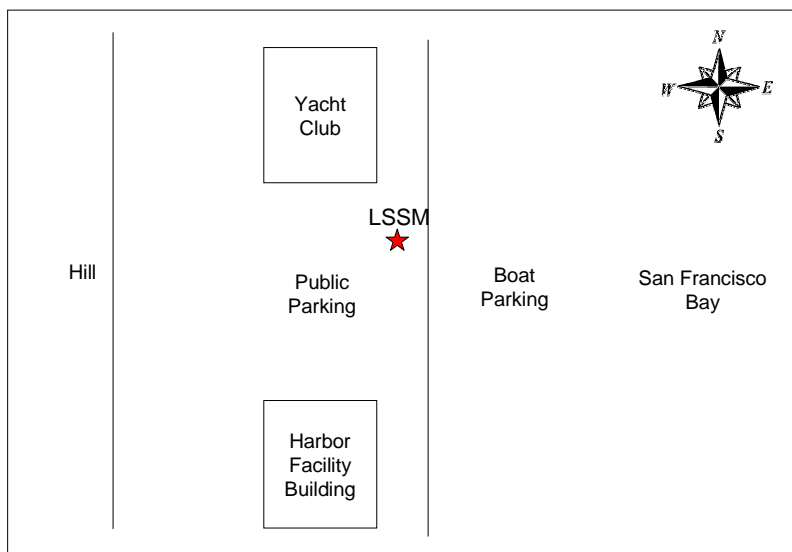
Figure A.50. Location of LSSM at Coyote Point Marina

Figure A.51. Photo of Spectrum Survey at Coyote Point Marina
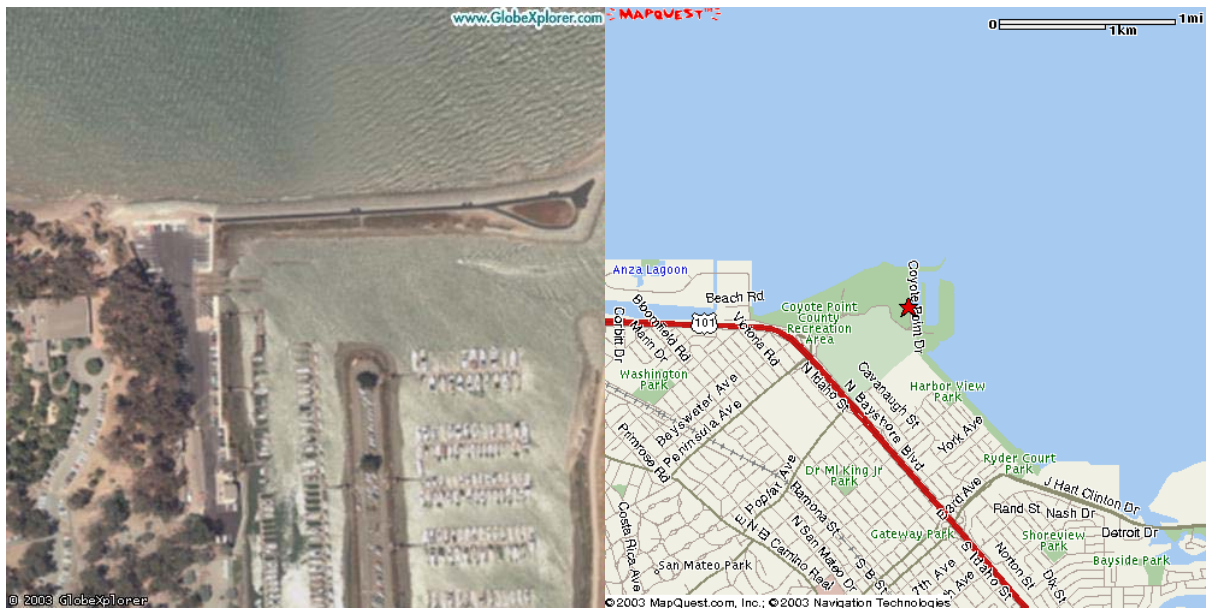
Figure A.52. Aerial Map and Street Map to Coyote Point Marina

(via www. globexplorer. com & www. mapquest. com)
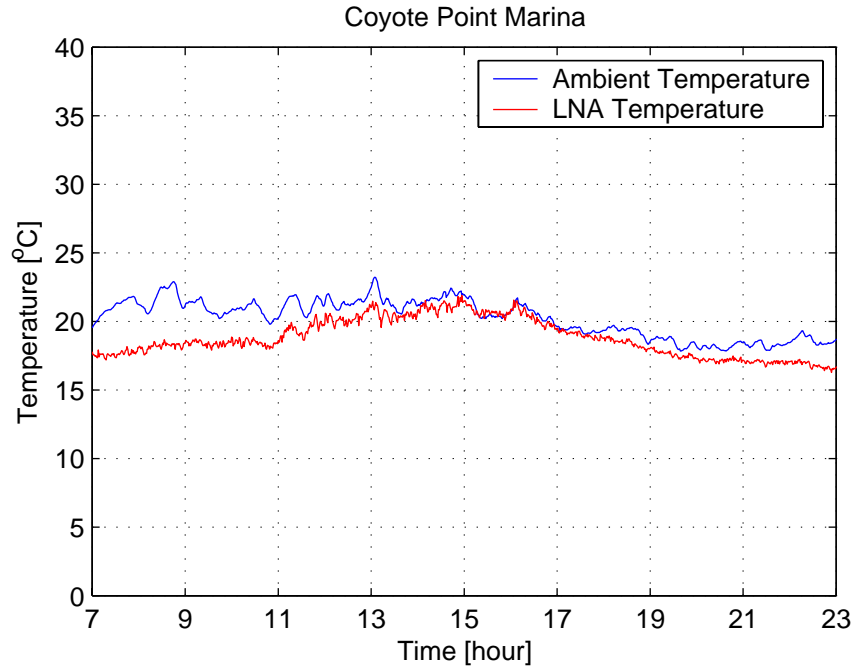
Figure A.53. Temperature Variation During Measurements at Coyote Point Marina

Data Observation

Band		Comments
GPS L1 (Fig A.54)	Temporal analysis	The average received power was between -112.5 ~ -111.7 dBm/MHz, below the thermal noise floor for all measurement time periods. The highest power, -111.7 dBm/MHz, was measured at 17:00.
	Spectral analysis	The average received power was between -113.0 ~ -110.4 dBm/MHz, below the thermal noise floor for the most of the measurement frequencies. The highest power, -110.4 dBm/MHz, was measured at 1575.5 MHz, which is the GPS signal from the GPS satellites.
	Angular analysis	The average received power was between -112.7 ~ -111.3 dBm/MHz, below the thermal noise floor for all measurement angles. The highest power, -111.3 dBm/MHz, was measured at 255 degrees, which corresponds to the hill. This is because the antennas observed less of the sky, and more of the hill whose temperature is higher than the sky temperature.
	Statistical analysis	No man-made signal except the GPS signal was detected.
UNI-S (Fig A.55)	Temporal analysis	The average received power was between -112.1 ~ -107.7 dBm/MHz, at the thermal noise floor for all measurement time periods. The highest power, -107.7 dBm/MHz, was measured at 18:20. Man-made signals were observed only in 11, 18 and 22 hours and probably originated from a single source with the multiple frequencies in the yacht club house.

	Spectral analysis	The average received power was between -112.9 and -101.7 dBm/MHz, at the thermal noise floor for all measurement frequencies. The highest power, -101.7 dBm/MHz, was measured at 2093.2 MHz. Man-made signals were observed only in 2030 MHz, 2068 MHz, and 2093 MHz.
	Angular analysis	The average received power was between -112.4 and -107.4 dBm/MHz, at the thermal noise floor for all measurement frequencies. The highest power, -107.4 dBm/MHz, was measured at 345 degrees corresponding to the yacht club house. Man-made signals were observed only in 150 ~ 165 degrees corresponding to the parked boats where numerous electronic equipments are installed,, as well as at an angle corresponding to the yacht club house.
	Statistical analysis	Man-made signals were clearly indicated. They were present 0.40 % of the measurement data with a maximum power of -87.2 dBm/MHz.
ISM 2.4 (Fig A.56)	Temporal analysis	The average received power was variable and high, -104.3 ~ -74.3 dBm/MHz, above the thermal noise floor for all measurement time periods. The highest power, -74.3 dBm/MHz, was measured at 18:40. Man-made signals were continuous in time and probably originated from the WiFi hub detected during the site survey and the multiple sources in the yacht club house and the parked boats.
	Spectral analysis	The average received power was variable and high, -111.8 ~ -69.2 dBm/MHz, above the thermal noise floor for all measurement frequencies. The highest power, -69.2 dBm/MHz, was measured at 2456.2 MHz. Man-made signals were continuous in frequency. The relatively high power wide band man-made signals with more than 10 MHz bandwidth were measured at 2410 ~ 2425 MHz and 2450 ~ 2465 MHz.
	Angular analysis	The average received power was variable and high, -108.8 ~ -71.0 dBm/MHz, above the thermal noise floor for all measurement angles. The highest power, -71.0 dBm/MHz, was measured at 165 degrees corresponding to the harbor facility building. Man-made signals were continuous in angle. Relatively high power was monitored in 120 ~ 180 degrees corresponding to the parked boats and 300 ~ 330 corresponding to the yacht club house.
	Statistical analysis	Man-made signals were prevalent. They were present 22.31 % of the measurement data with a maximum power of -50.2 dBm/MHz.
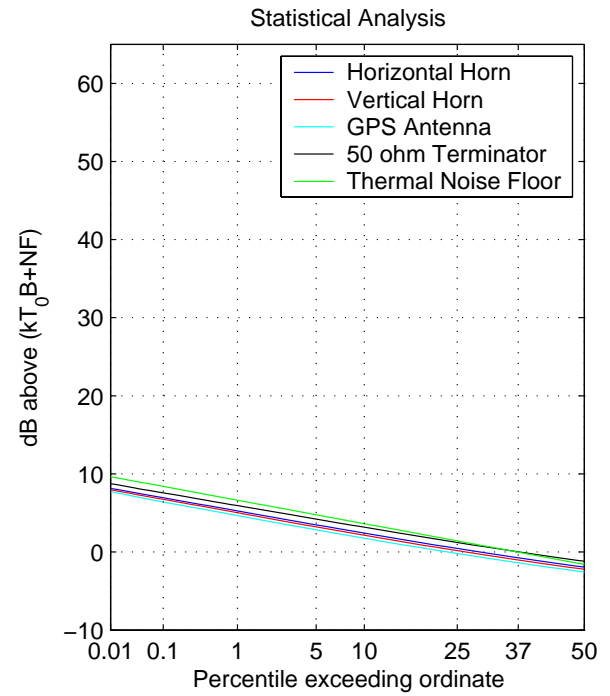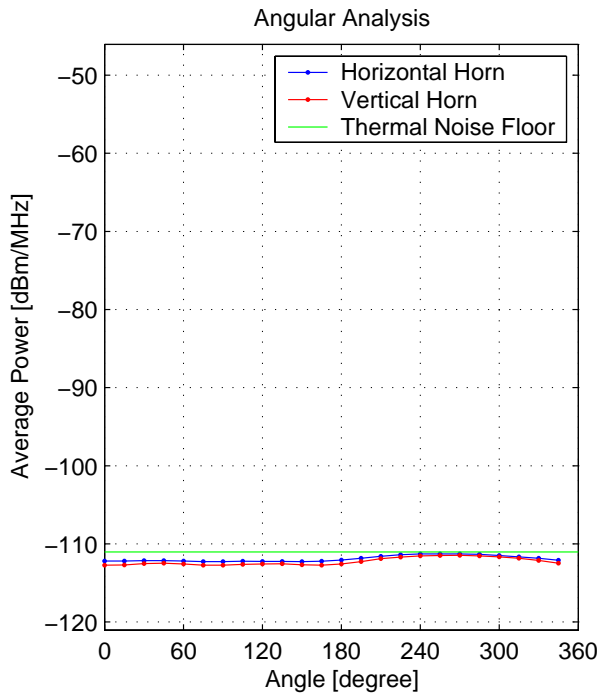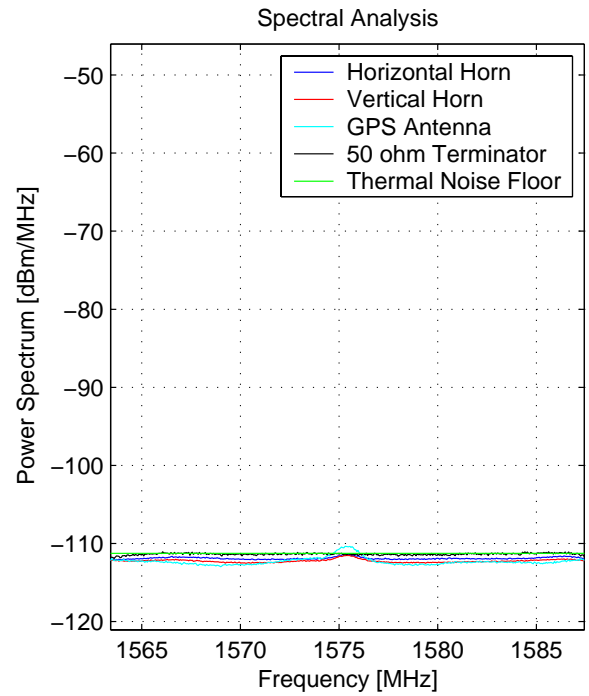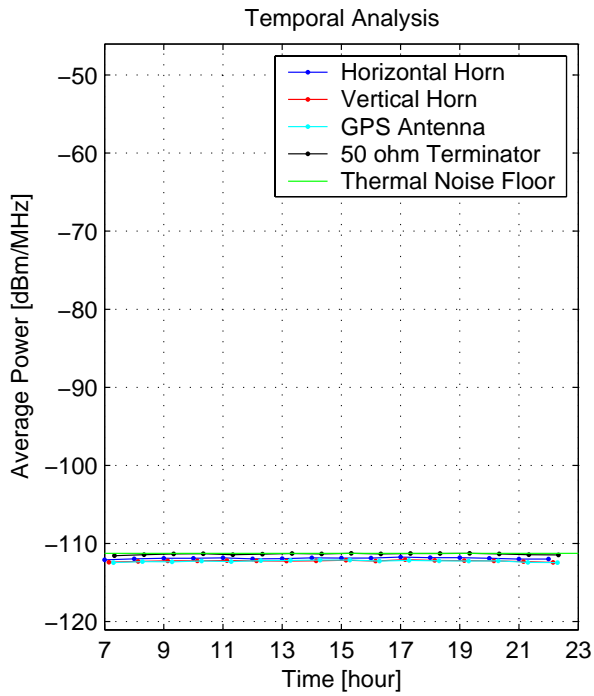
Figure A.54. Spectrum Measurements at Coyote Point Marina (GPS L1)
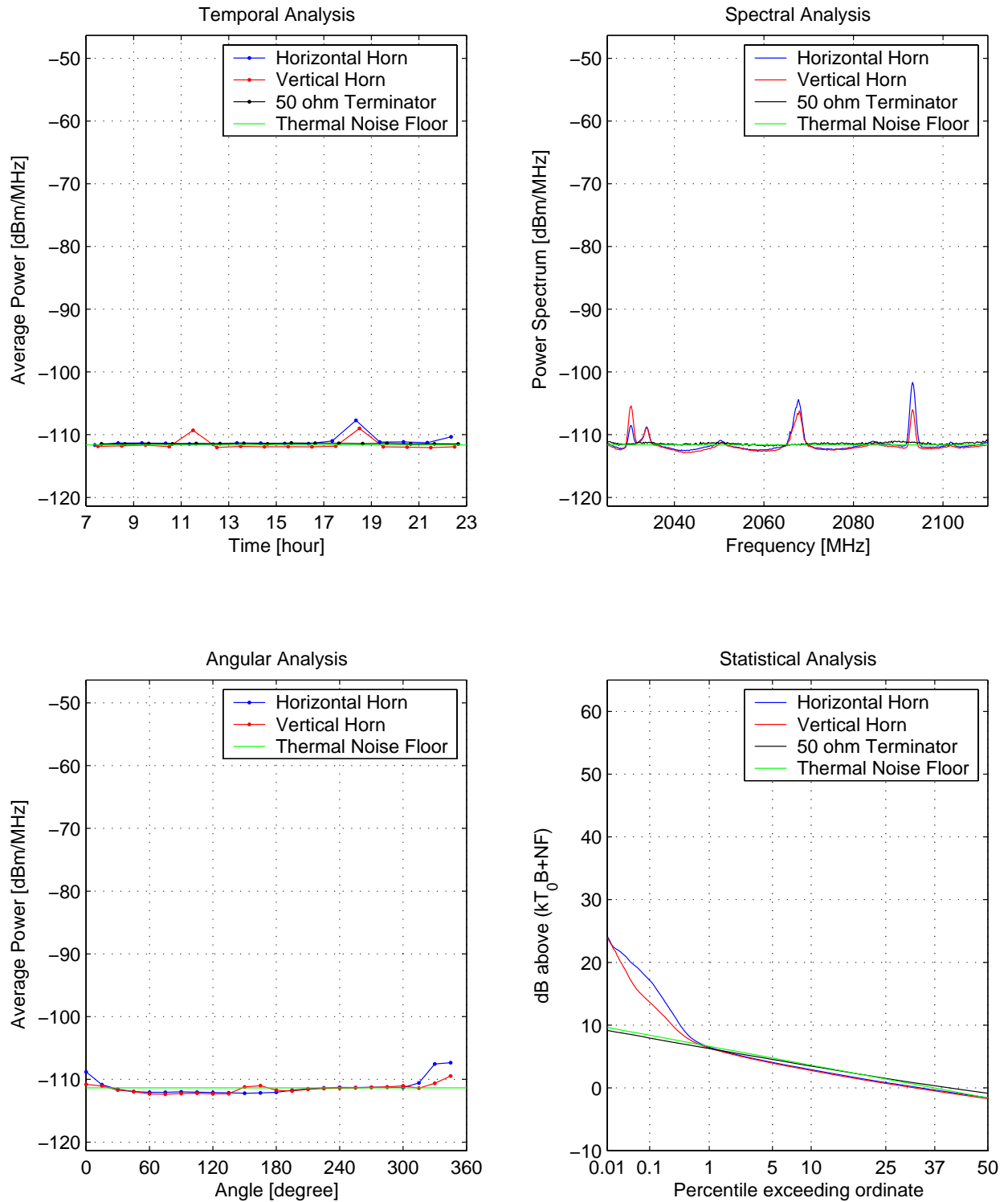
Figure A.55. Spectrum Measurements at Coyote Point Marina (UNI-S)
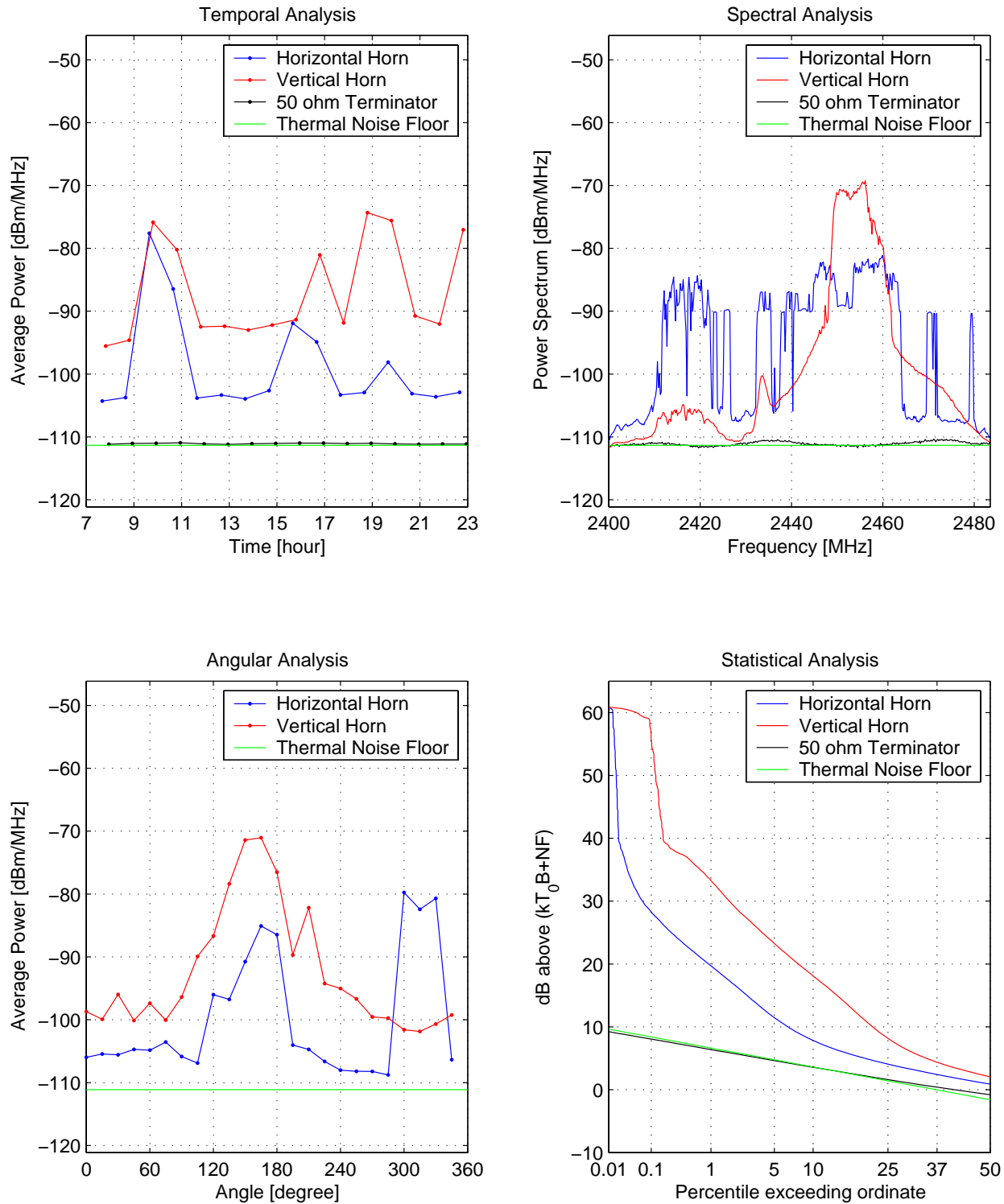
Figure A.56. Spectrum Measurements at Coyote Point Marina (ISM 2.4)

(This page was left intentionally blank)

Appendix B: Passive Sensor Band Survey Measurement Data

Appendix B.1: Oconee County Airport, Clemson, South Carolina (Site 1)

Date: 9/12/03
Map of Location: See Figure B.1
Noteworthy Results:

- Spectral trends: In general, uniform in frequency; spectral peaks at 23.41, 23.43, 23.35, 23.69, 23.85, 24.03, 24.07, 24.02, and 24.12 GHz mainly in the direction of an antenna bed between 1 and 2 p.m. at power levels ranging from 8 to 15 dB above the measured noise floor (Figures B.2, B.6, B.10, B.12, B.13, and B.16).
- Angular trends: Between 8:30 and 9:30 p.m., angular peaks occurred in the general direction of bodies of water (Figures B.3, B.7, and B.11). See map on figure B.1.
- Temporal trends: Lower power levels in the morning hours, temporal peaks occurred between 3 and 5 p.m. (Figures B.4, B.8, B.14, and B.17).
- An anomalous feature of resonances at 23.36, 23.40, and 23.50 GHz appear in this data set.
- Pre-measurement calibrated gain: 47.2 dB; Post-measurement calibrated gain: 46.4 dB.
- Figures B.5, B.9, B.15, and B.18 depict a statistical analysis.
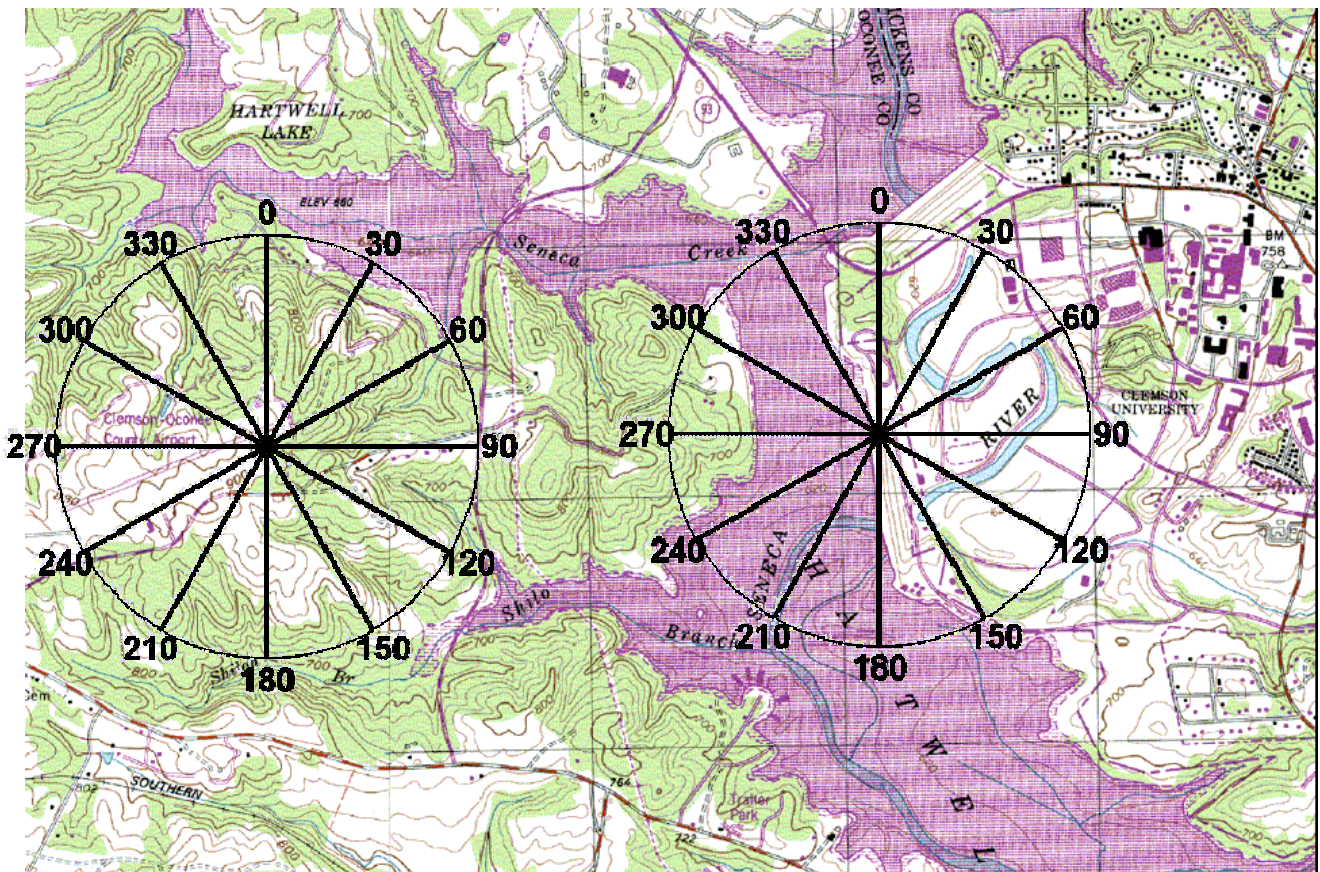
Figure B.1.
Map of Oconee County Airport (Left) and Lake Hartwell Dike (Right) Measurement Sites
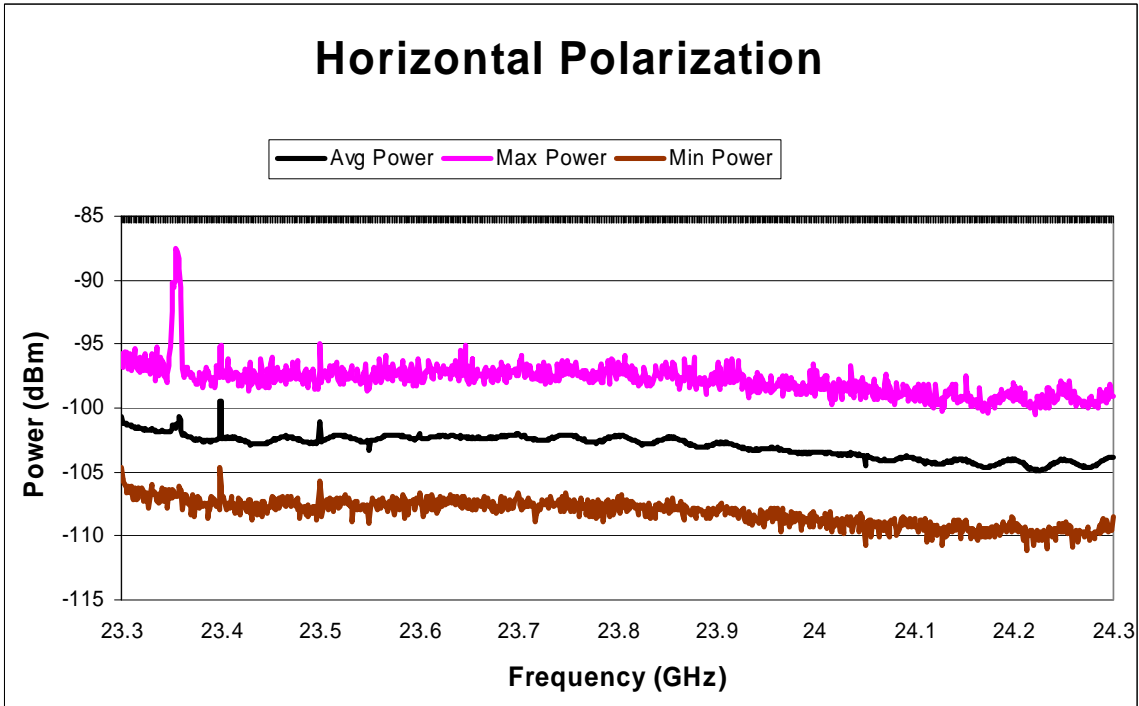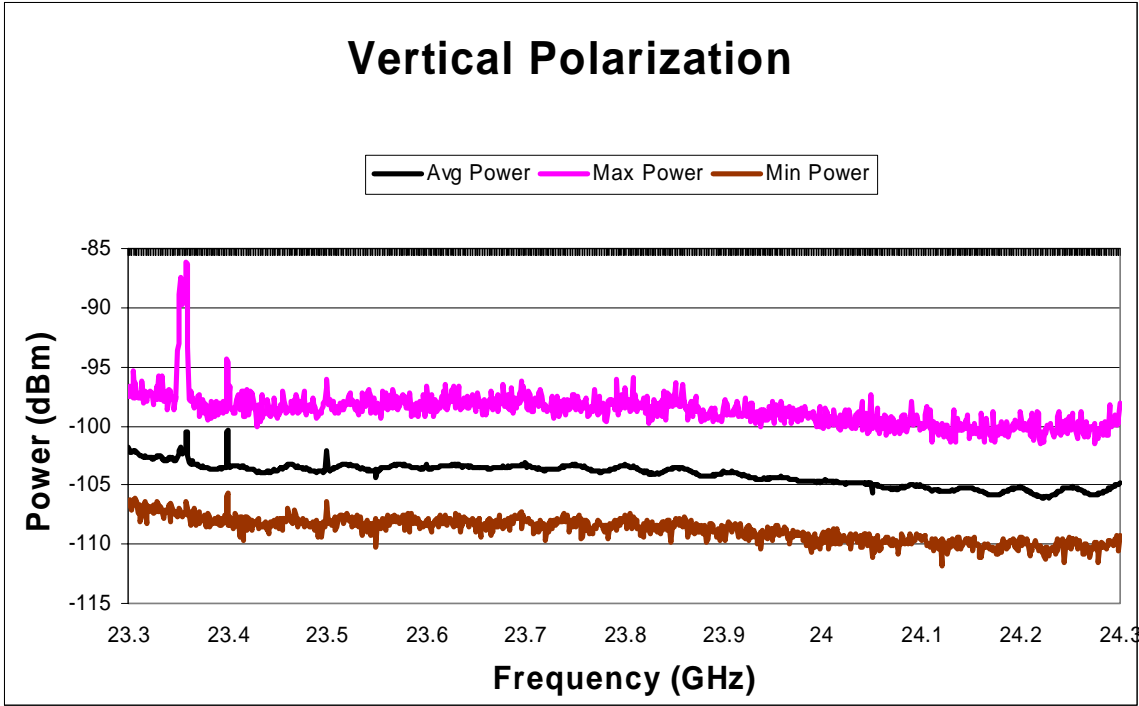
Figure B.2. Oconee County Airport: Zero Degree Elevation, Spectral Analysis
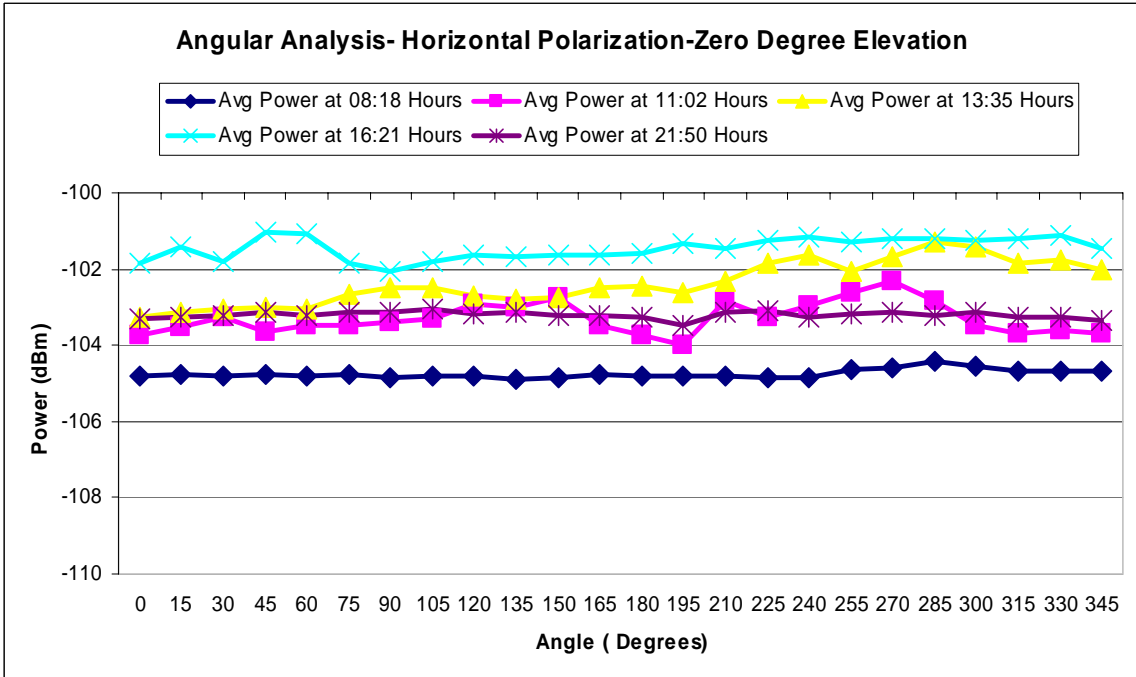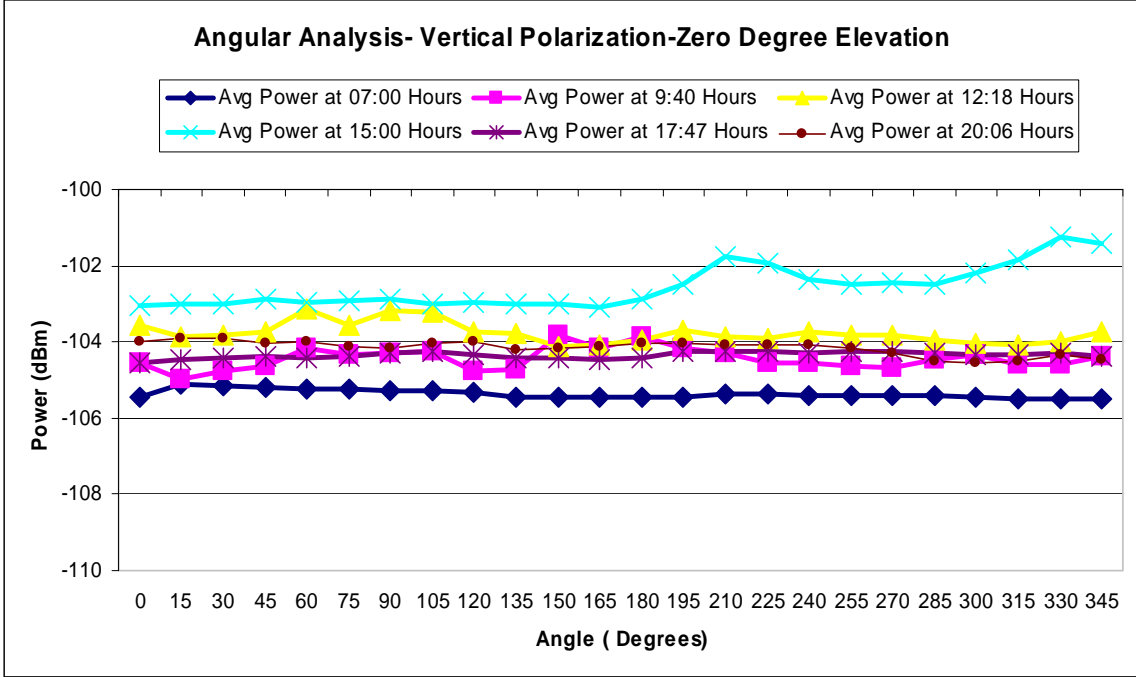
Figure B.3. Oconee County Airport: Zero Degree Elevation, Angular Analysis

127
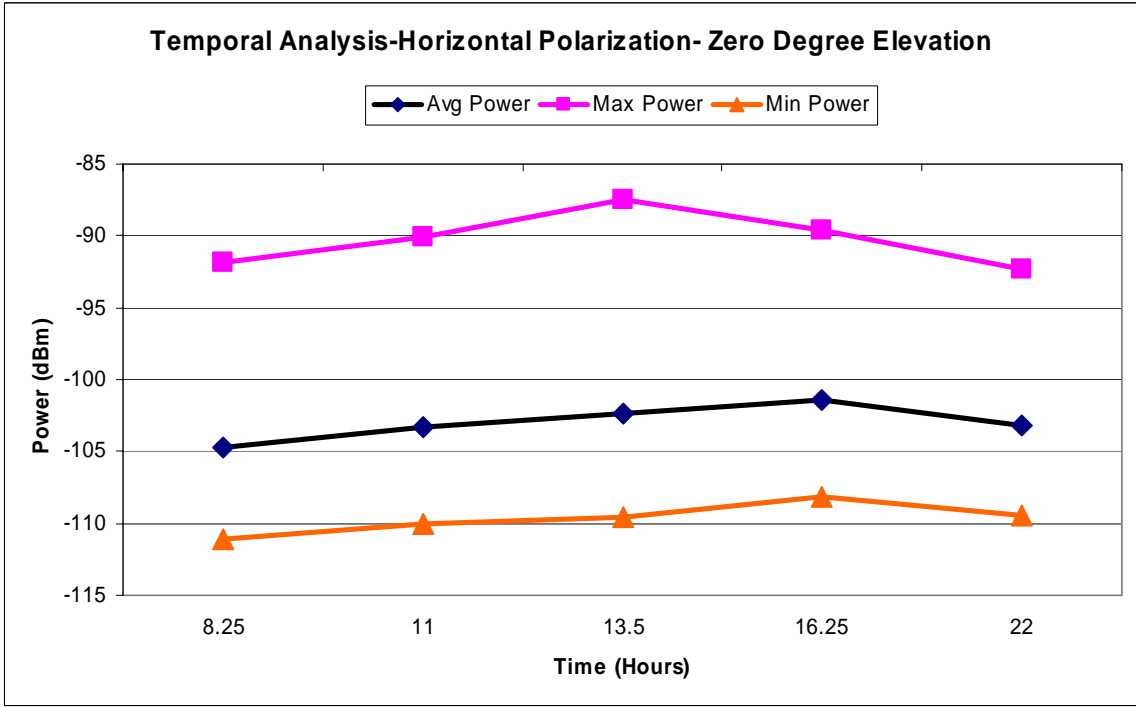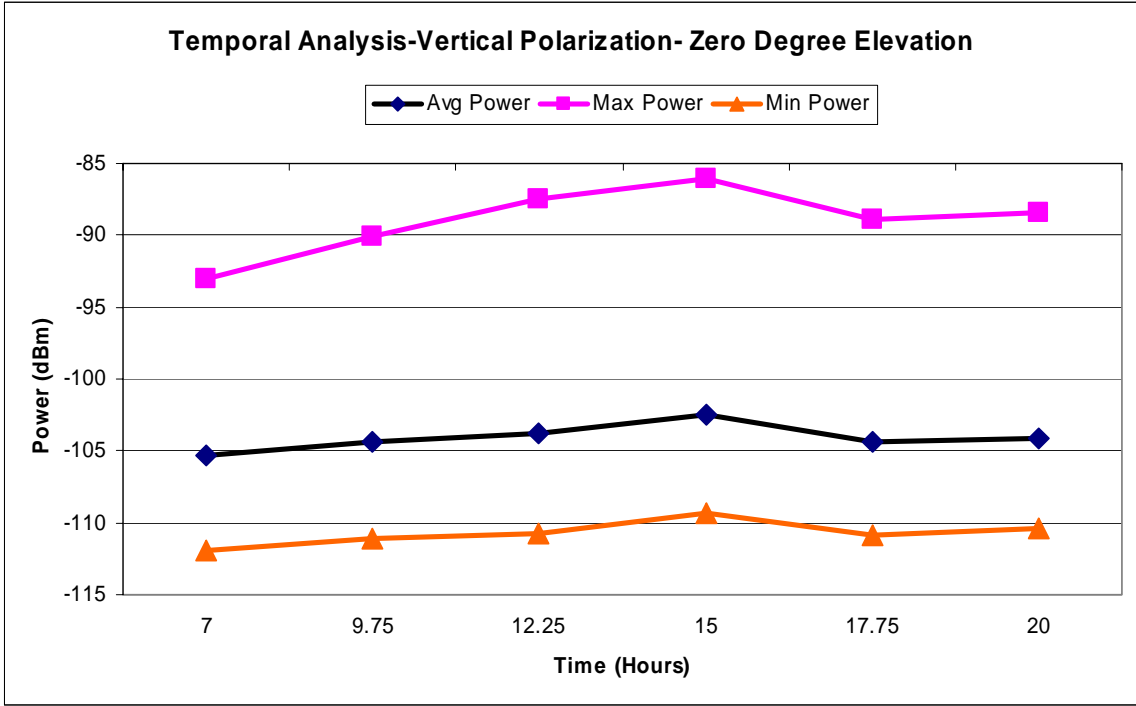
Figure B.4. Oconee County Airport: Zero Degree Elevation, Temporal Analysis
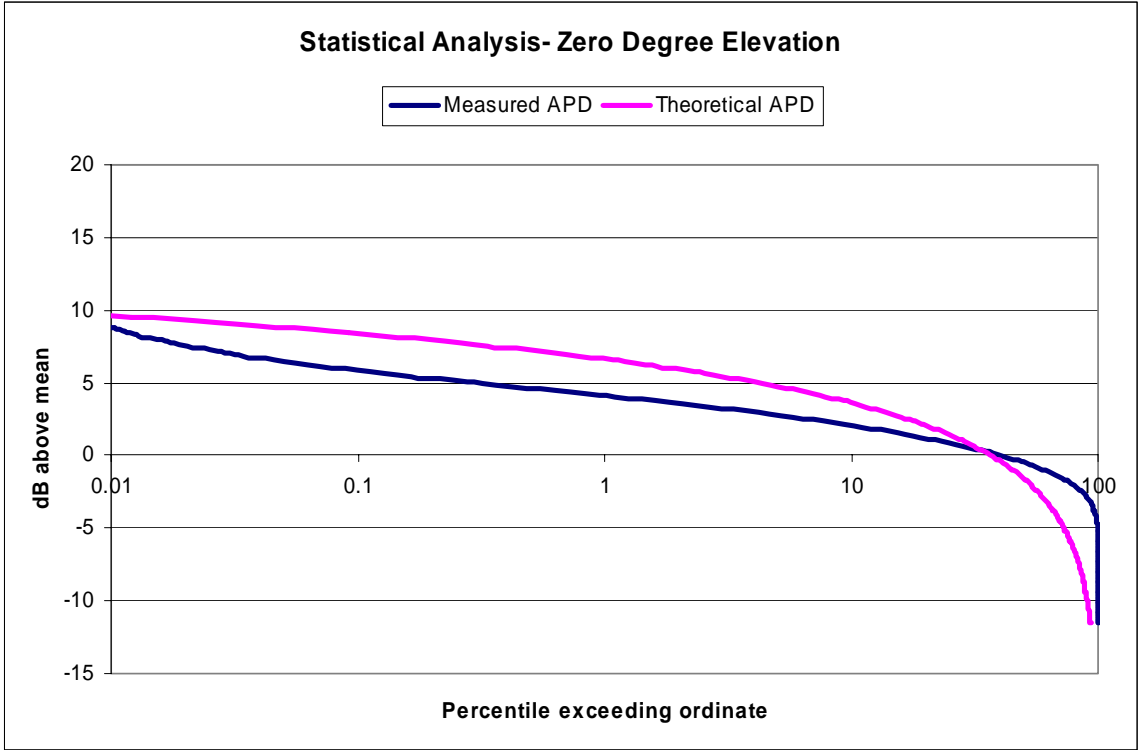
Figure B.5. Oconee County Airport: Zero Degree Elevation, Statistical Analysis
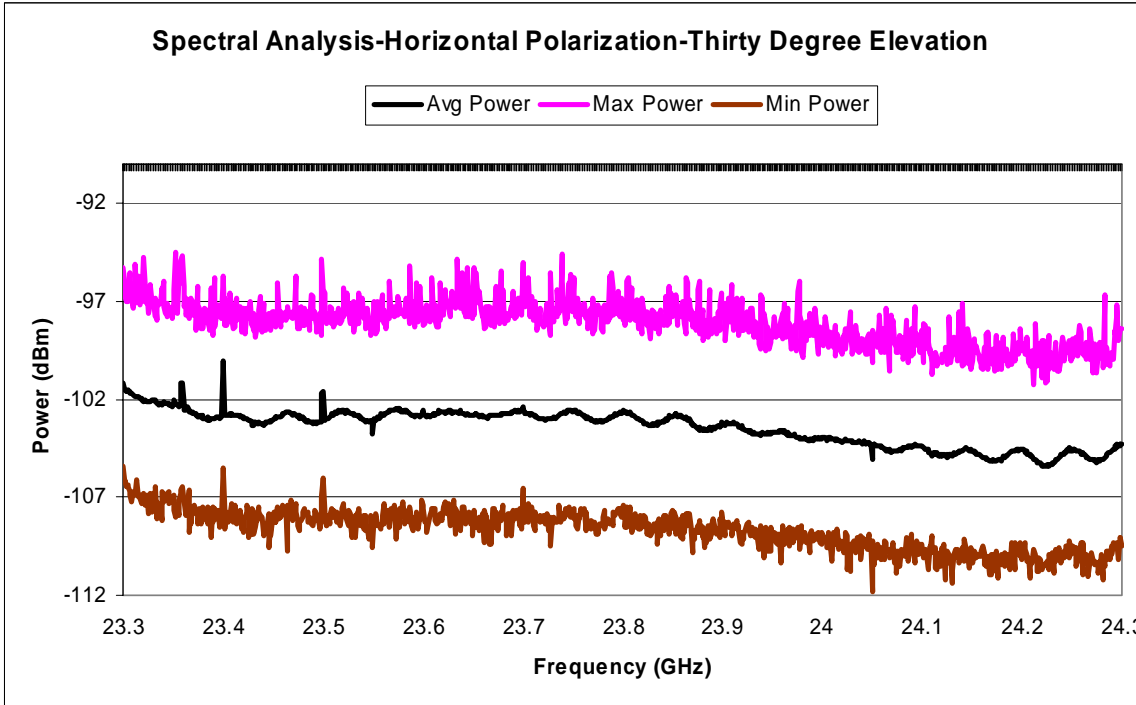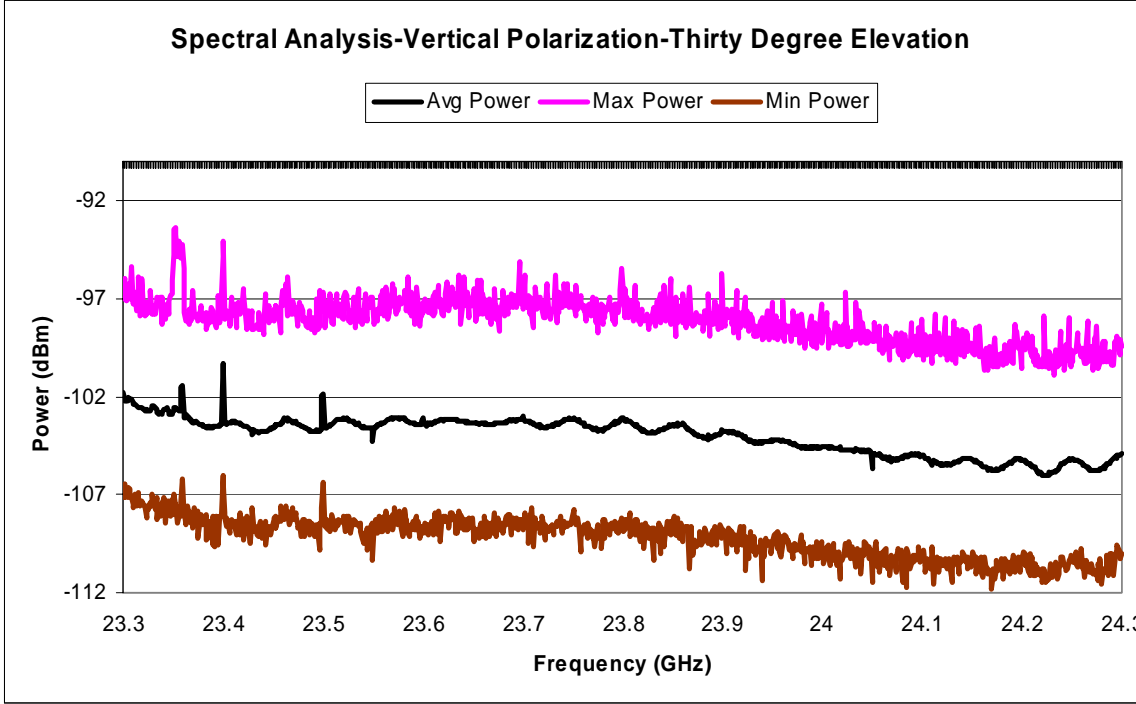
Figure B.6. Oconee County Airport: Thirty Degree Elevation, Spectral Analysis
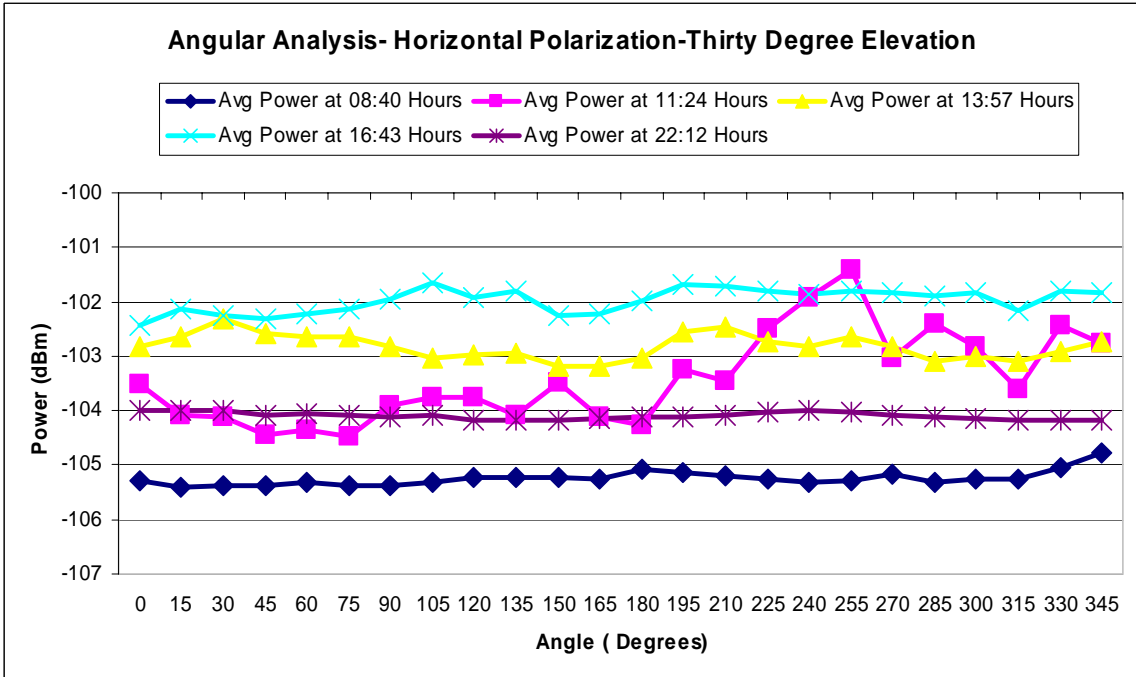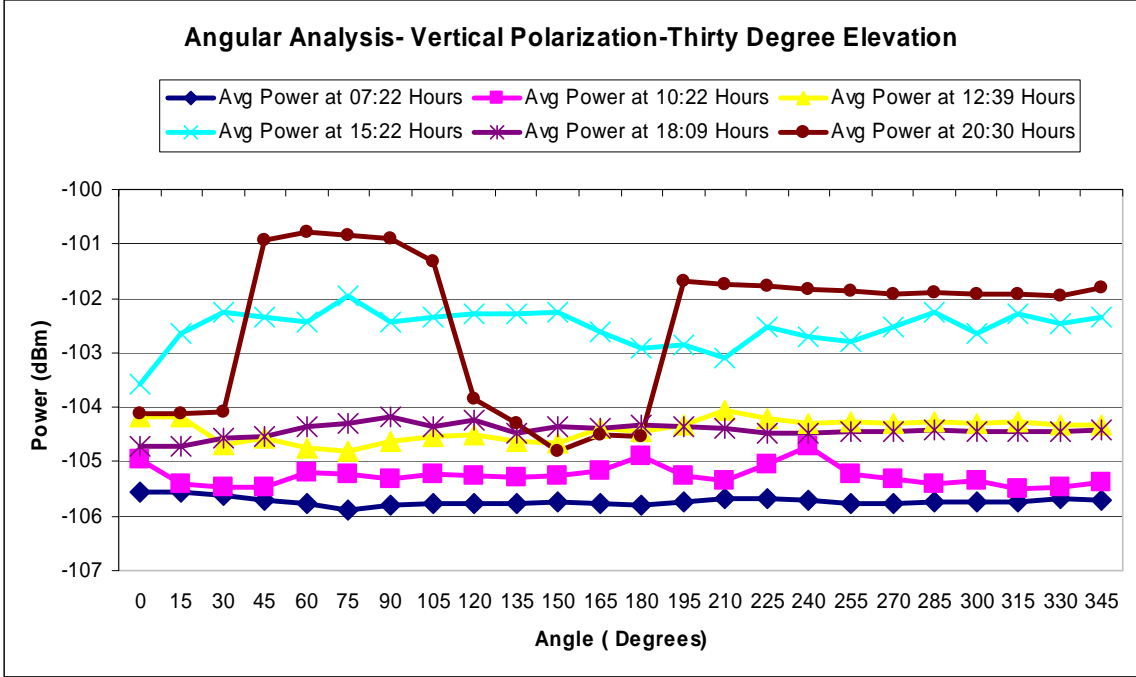
Figure B.7. Oconee County Airport: Thirty Degree Elevation, Angular Analysis

131
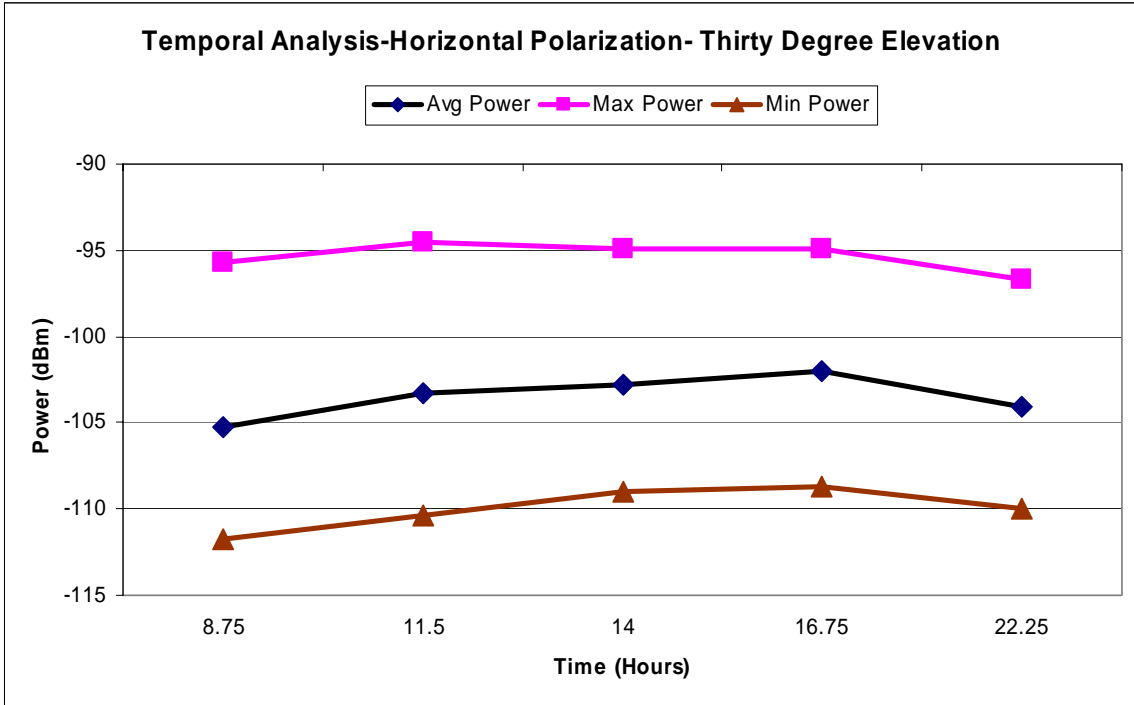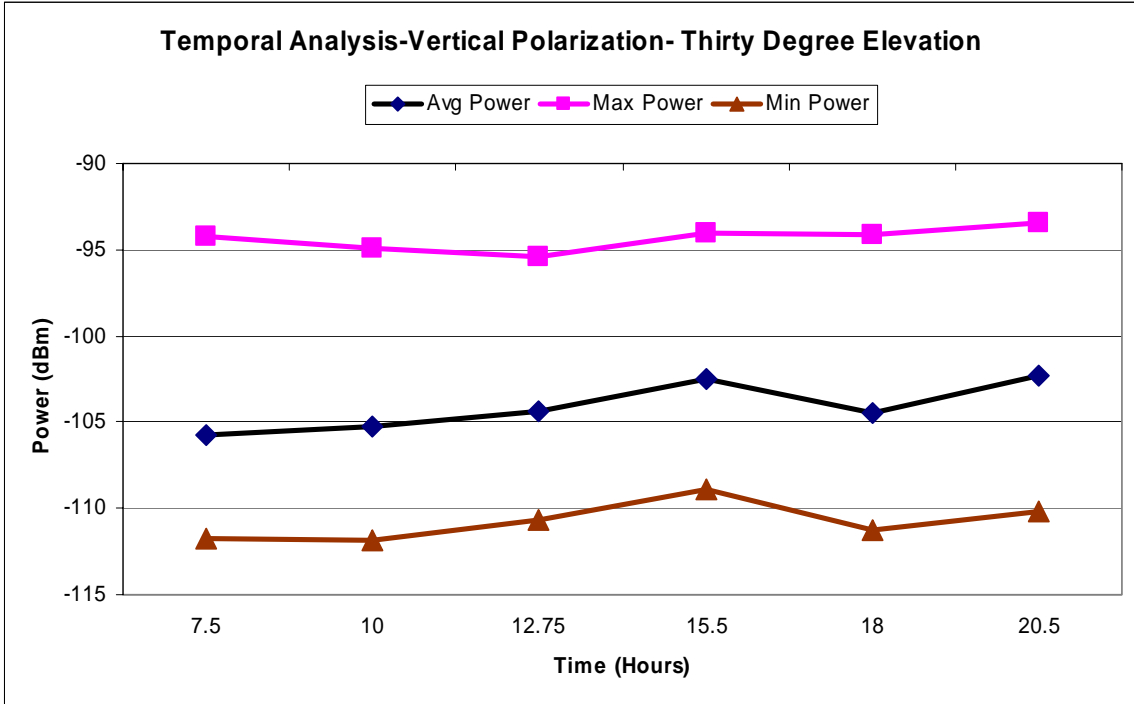
Figure B.8. Oconee County Airport: Thirty Degree Elevation, Temporal Analysis
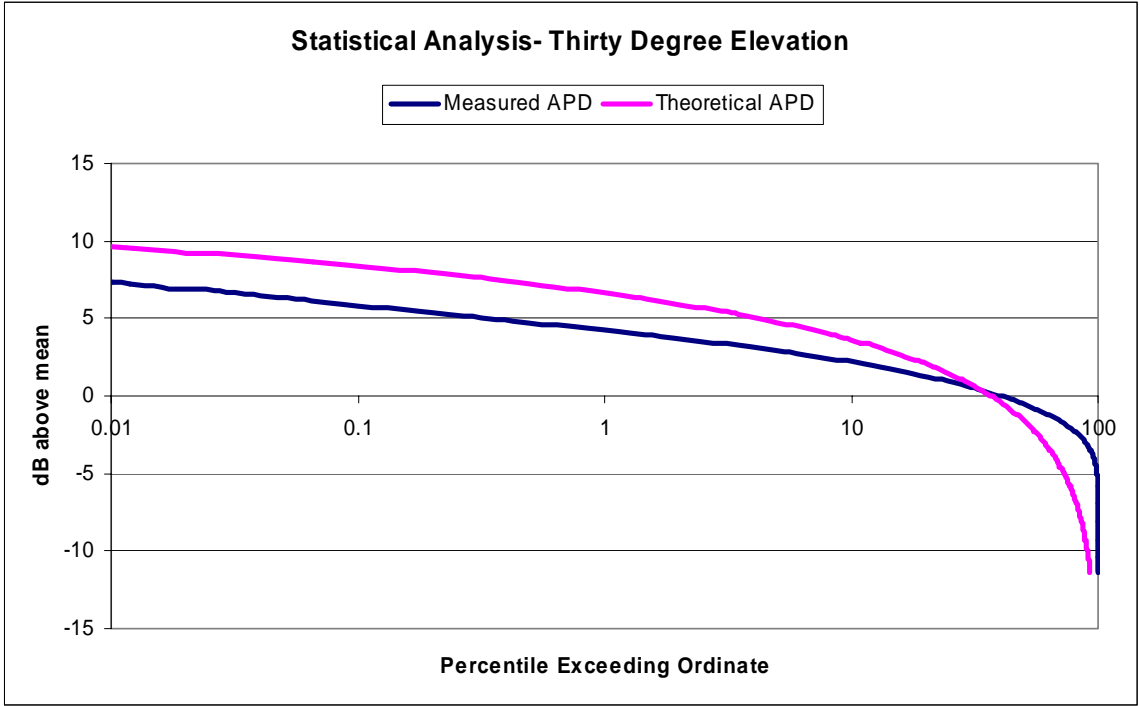
Figure B.9. Oconee County Airport: Thirty Degree Elevation, Statistical Analysis
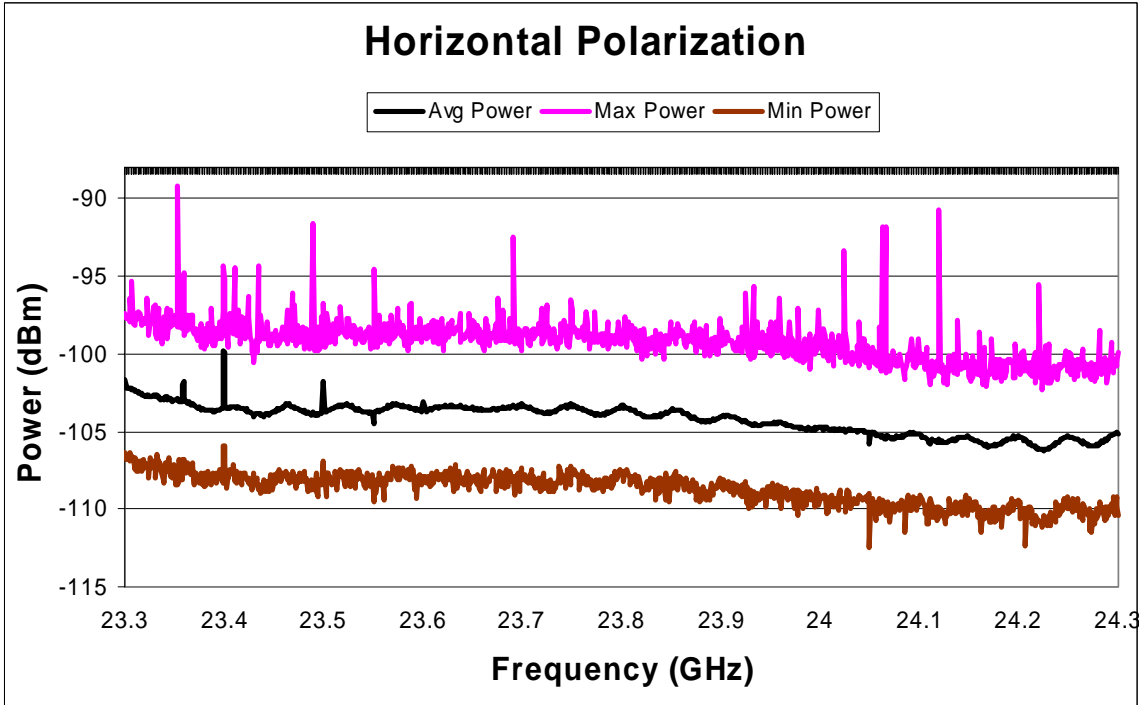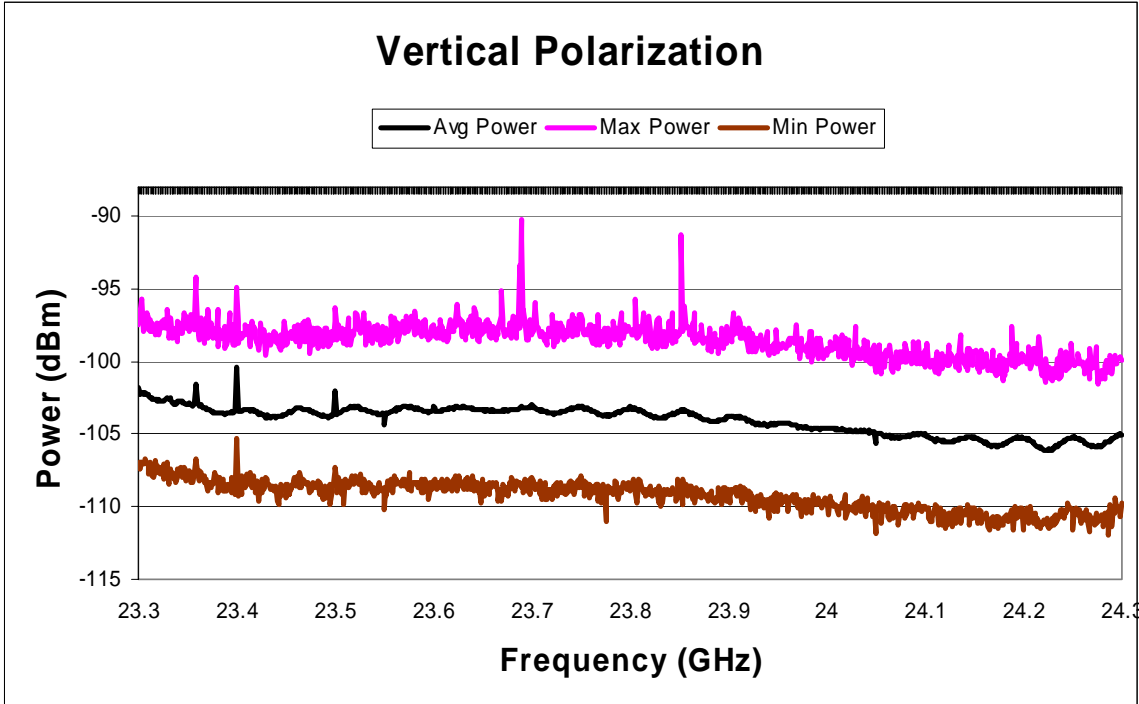
Figure B.10. Oconee County Airport: Sixty Degree Elevation, Spectral Analysis
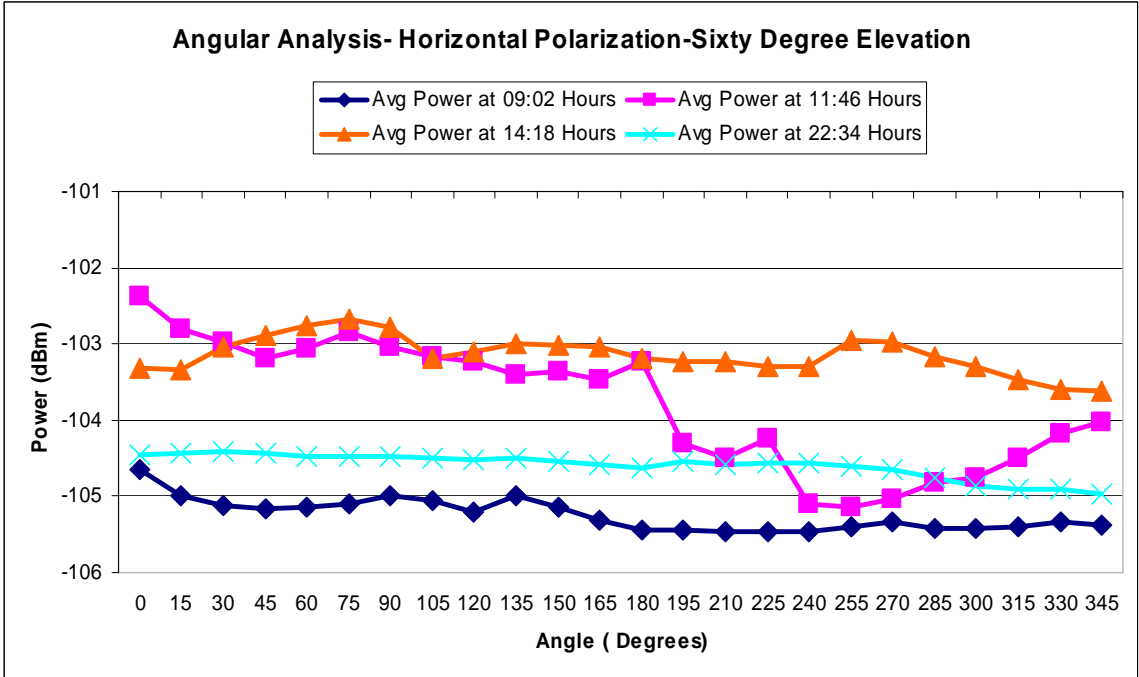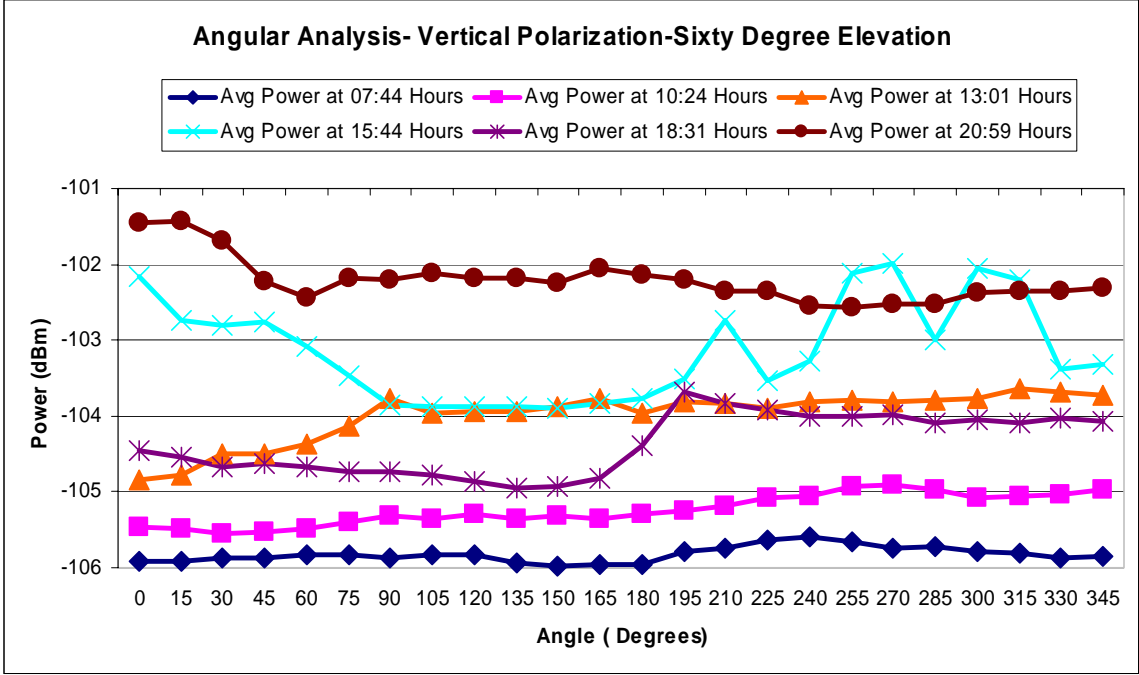
Figure B.11. Oconee County Airport: Sixty Degree Elevation, Angular Analysis
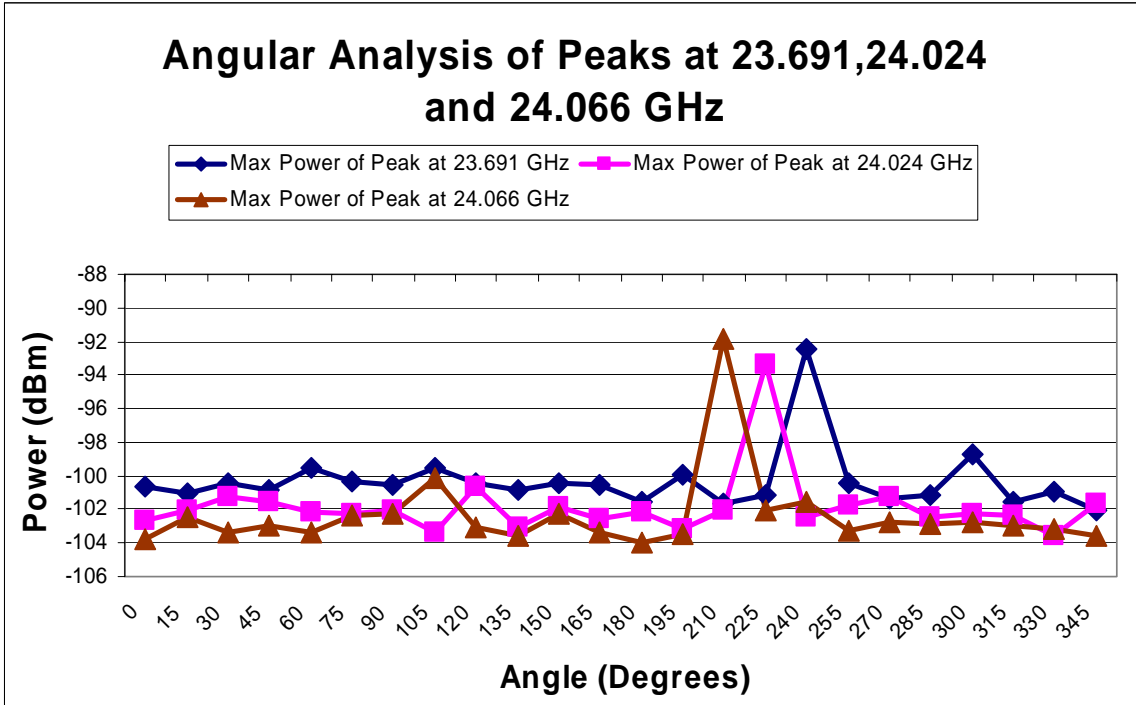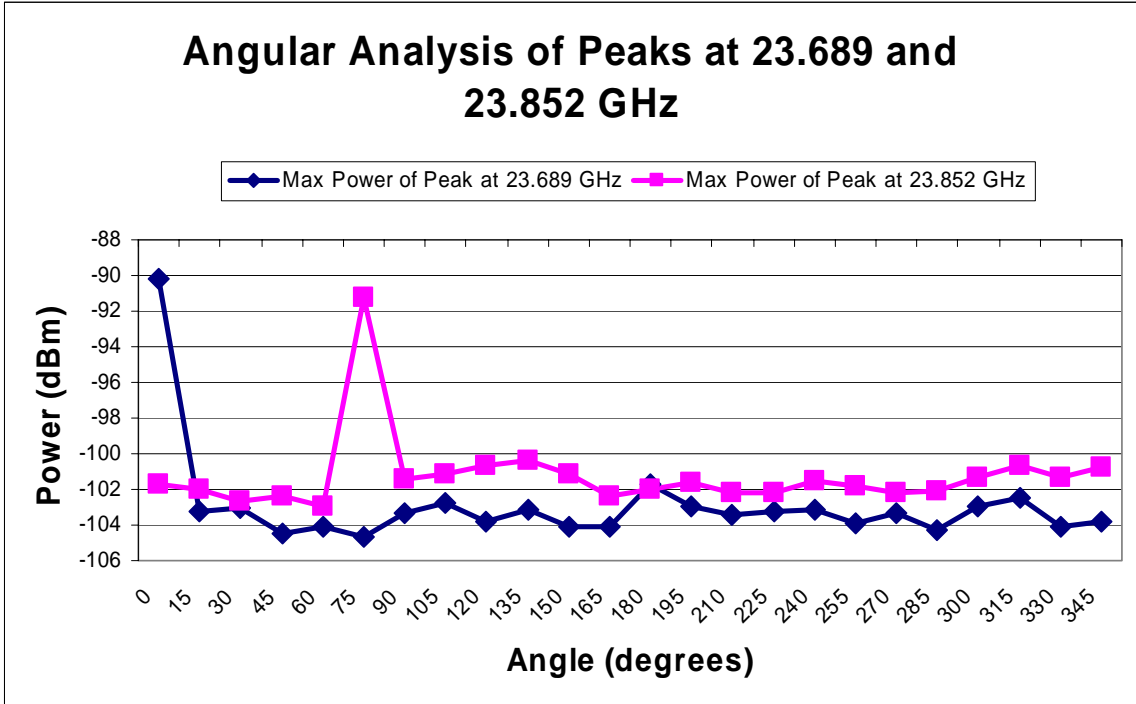
Figure B.12. Oconee County Airport: Sixty Degree Elevation, Angular Analysis

136

Angular Analysis of peaks at 23.353, 23.389 and 24.12 GHz

Angular Analysis of Peaks at 23.399, 23.41 and 23.434 GHz
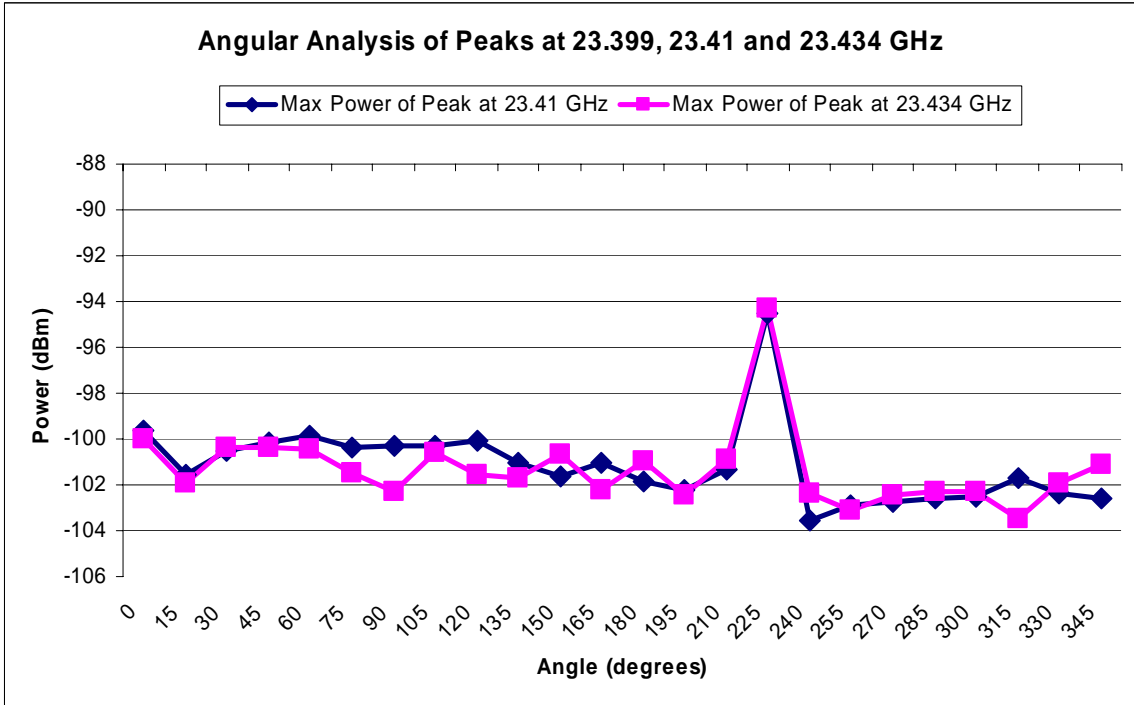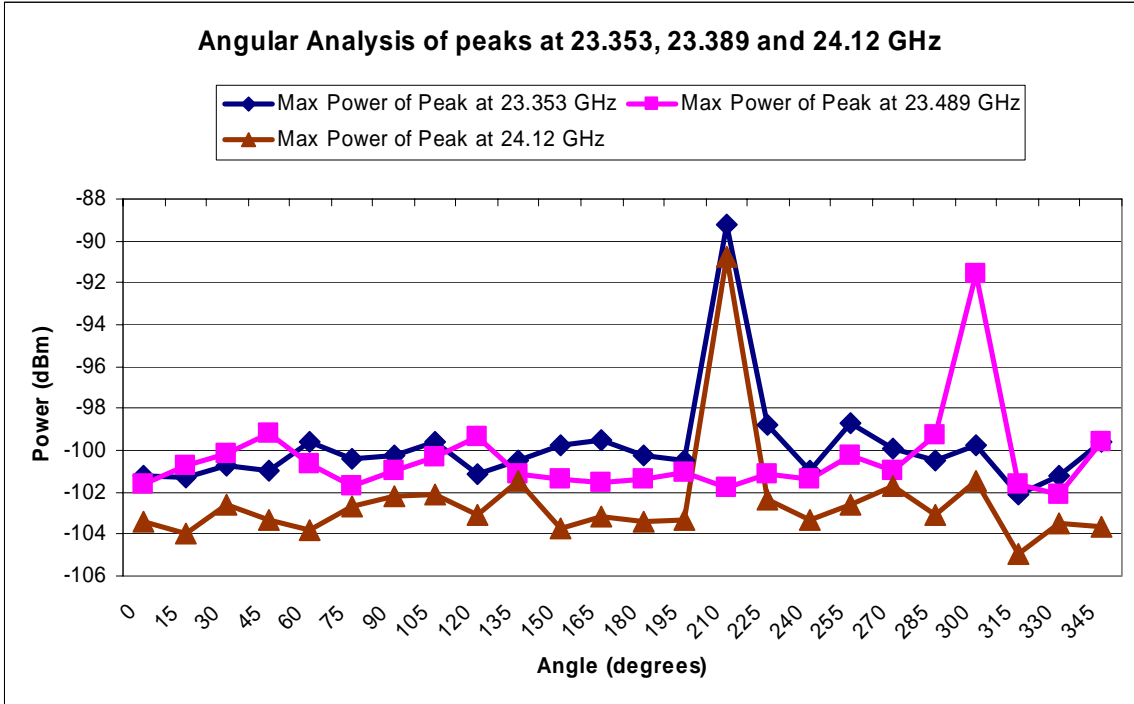
Figure B.13. Oconee County Airport: Sixty Degree Elevation, Angular Analysis
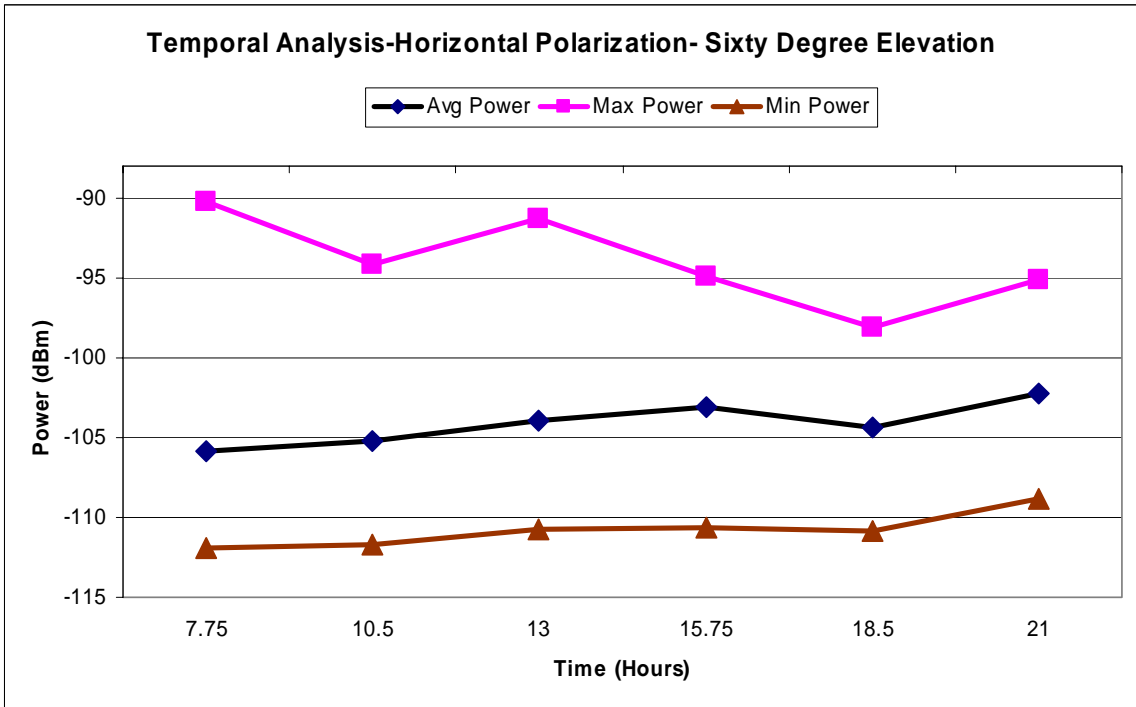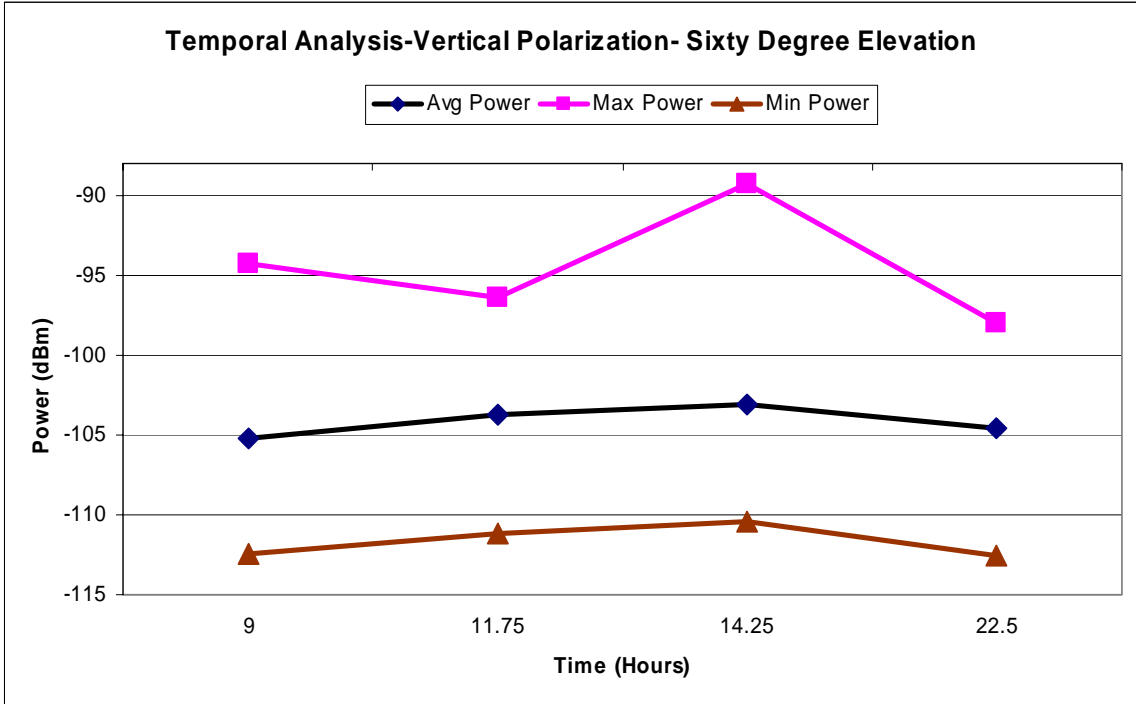
Figure B.14. Oconee County Airport: Sixty Degree Elevation, Temporal Analysis
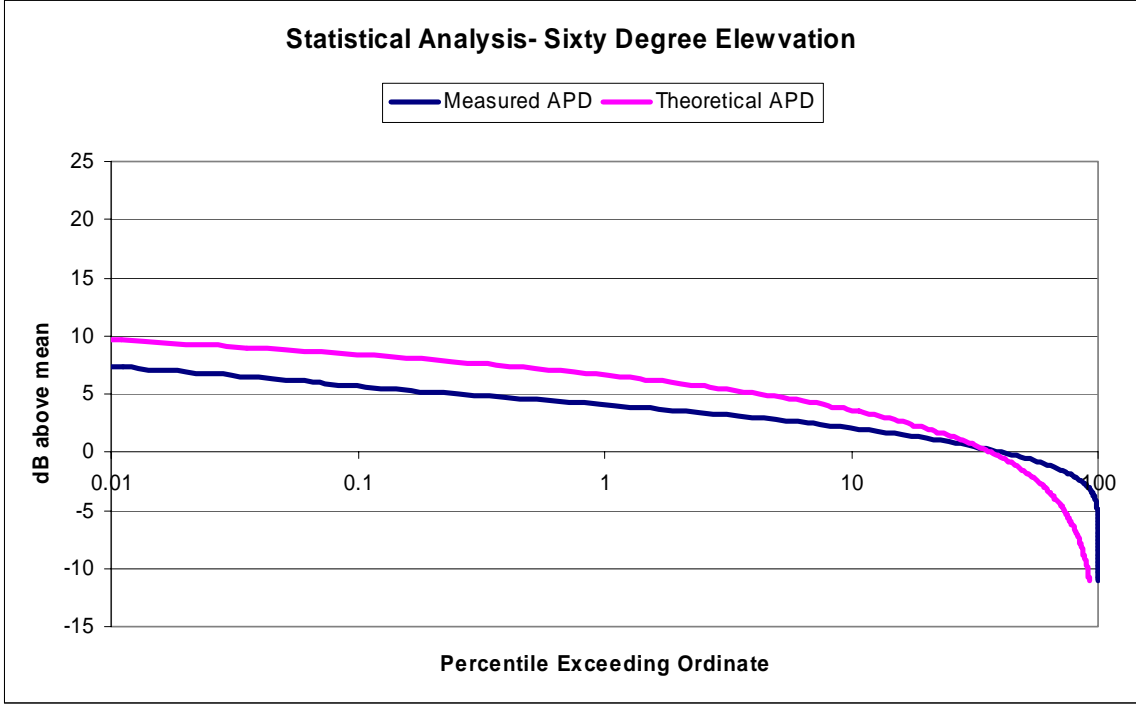
Figure B.15. Oconee County Airport: Sixty Degree Elevation, Statistical Analysis
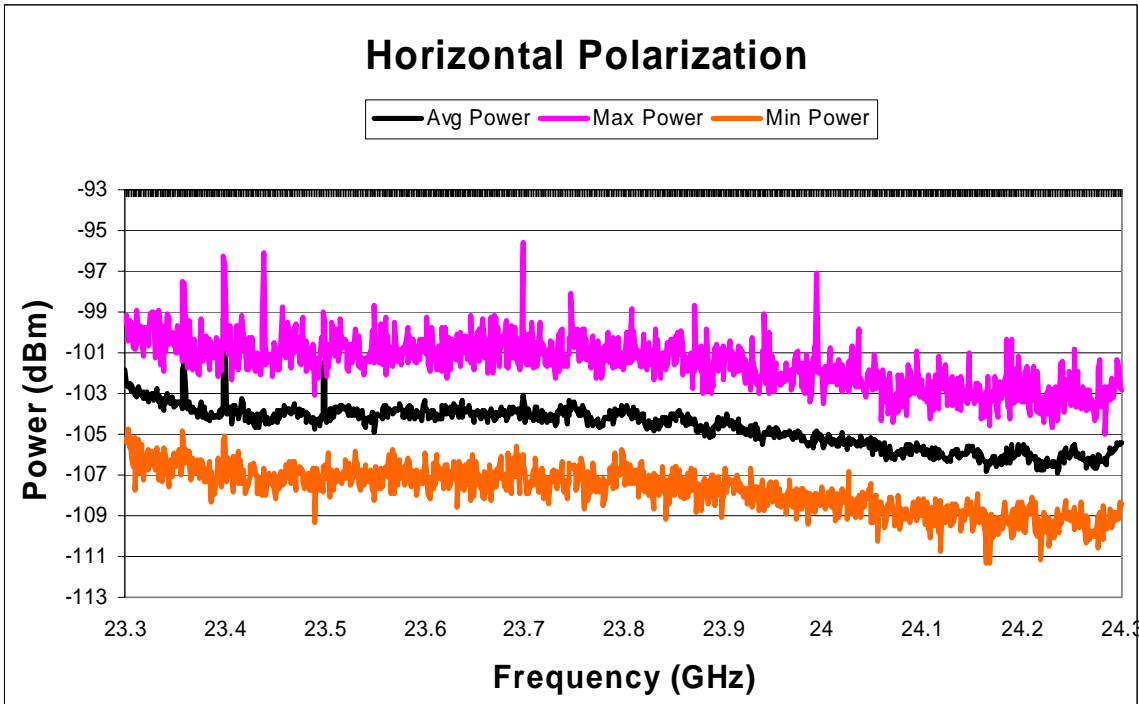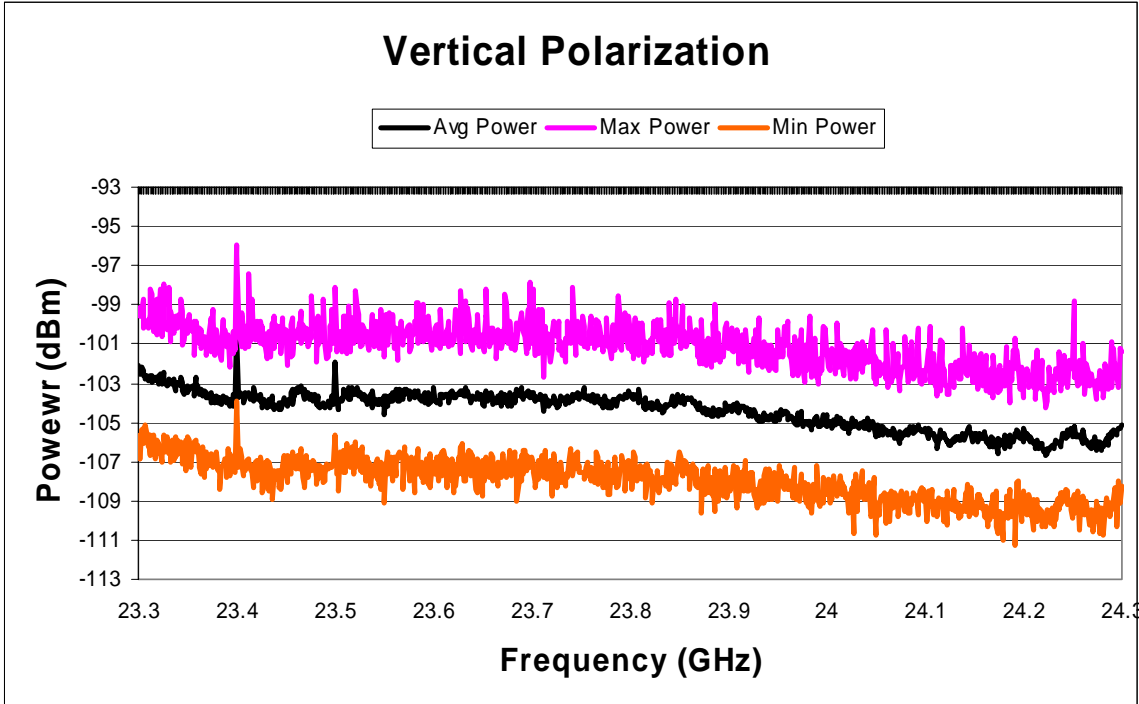
Figure B.16. Oconee County Airport: Ninety Degree Elevation, Spectral Analysis
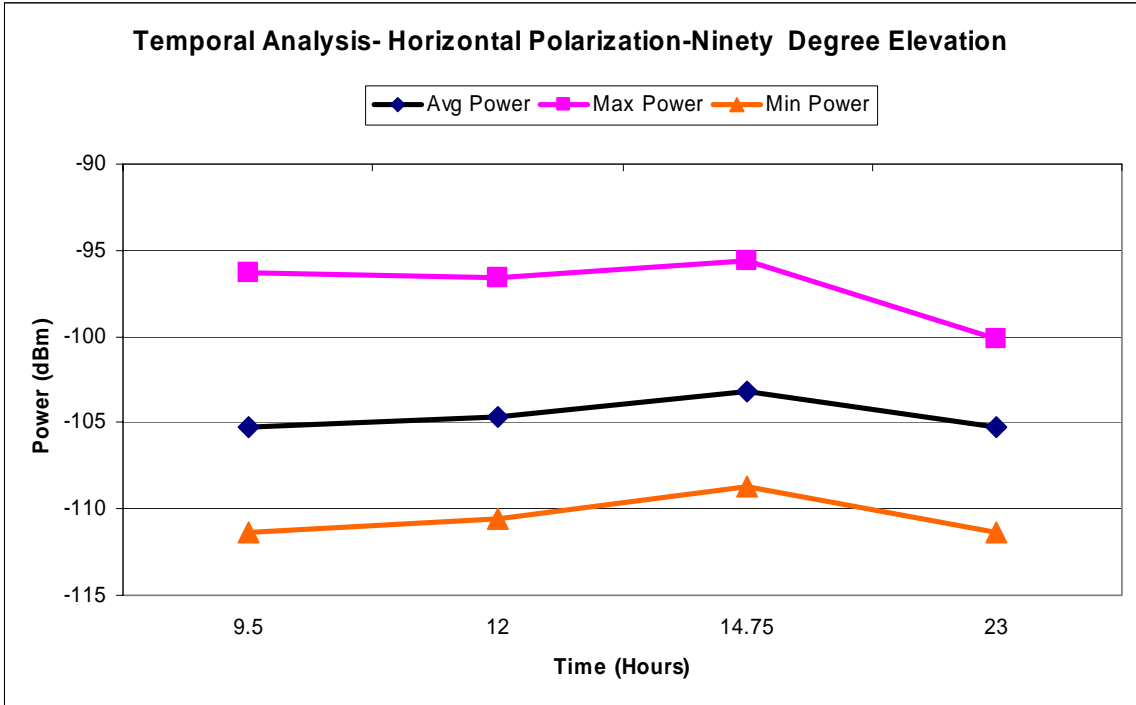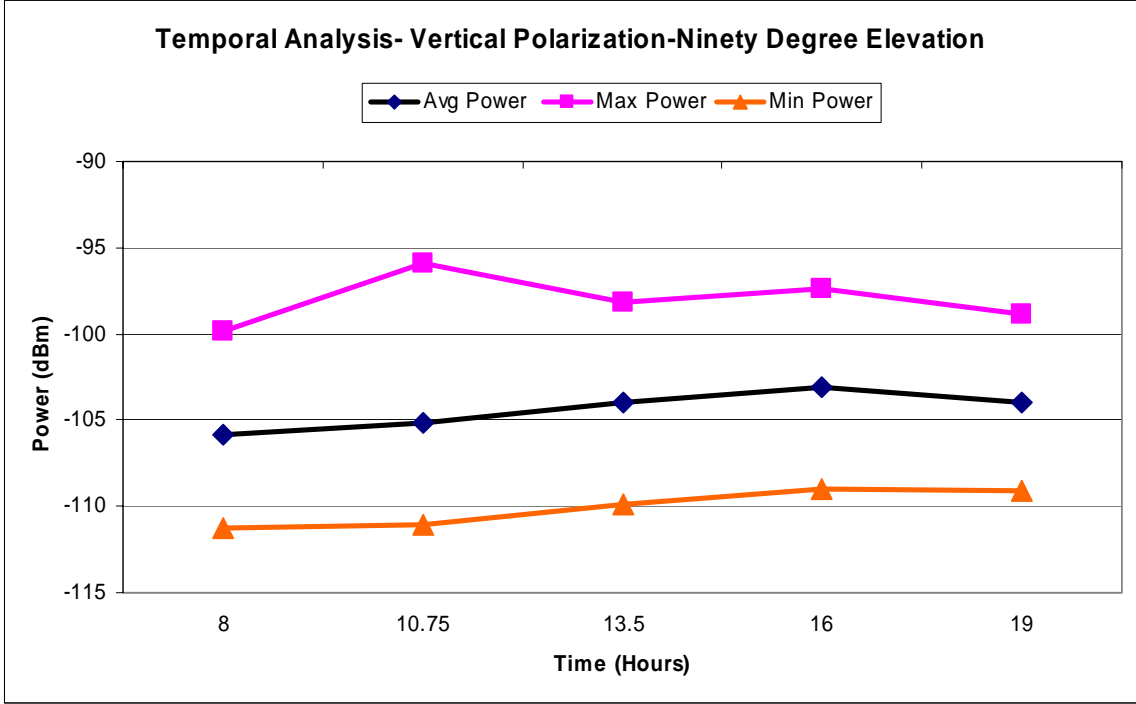
Figure B.17. Oconee County Airport: Ninety Degree Elevation, Temporal Analysis

141
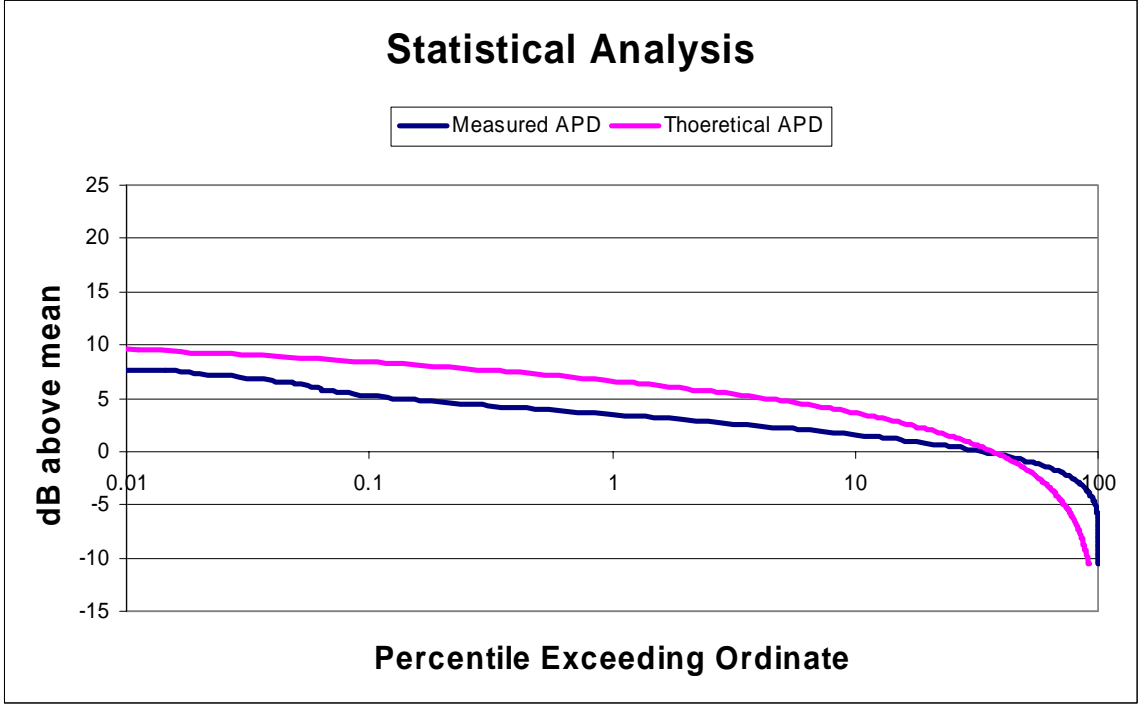
Figure B.18. Oconee County Airport: Ninety Degree Elevation, Statistical Analysis

Appendix B.2: Lake Hartwell Dike, Clemson, South Carolina (Site 2)

Date: 9/17/03
Map of Location: See Figure B.19
Noteworthy Results:

- Spectral trends: Uniform in frequency within 2 dB. Between 24.05 and 24.1 GHz, there is a spectral artifact. We have verified experimentally that this artifact is introduced by the input attenuator in the spectrum analyzer, not the ambient noise floor. See Figures B.20, B.24, B.28, and B.32.
- Angular trends: Angular peaks occur in the afternoon and evening between 0 and 60 degrees as marked on the map (Figure B.19)   See Figures B.21, B.25, and B.29.
- Temporal trends: Lower power level in the morning hours, temporal peak occurs at 7 p.m. See Figures B.22, B.26, B.30, and B.33.
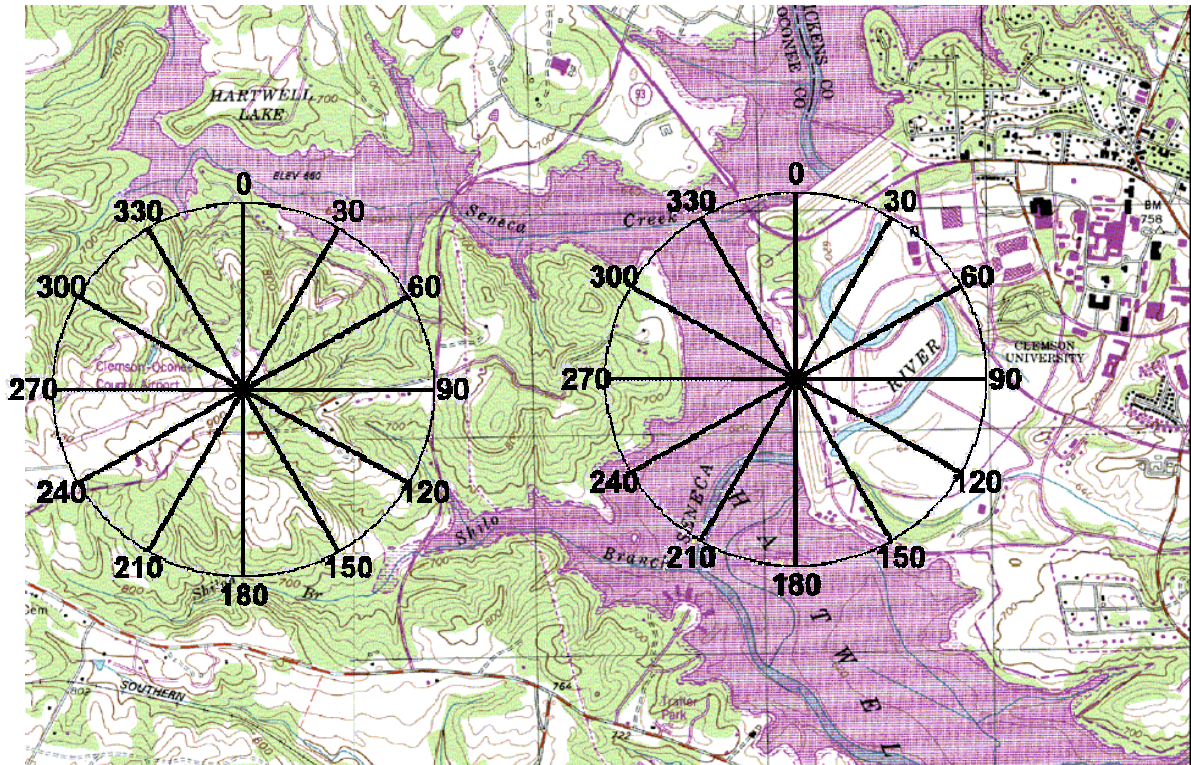
Figure B.19.
Map of Oconee County Airport (Left) and Lake Hartwell Dike (Right) Measurement Sites

- Pre-measurement calibrated gain: 81.8 dB. Post-measurement calibrated gain: 74.0 dB. The reason for the discrepancy between these two calibrations was an anomalous change in DC bias current. All day at the measurement site and during the pre-measurement calibration, the DC bias current was 162 mA to the receiver front-end. In the post-measurement calibration, the DC bias changed to 177 mA and the gain decreased. The change in gain can be attributed to the change in DC bias current to the amplifiers, and therefore the pre-measurement gain of 81.8 dB is used in computing the received power. This choice is corroborated by the noise level observed on the

spectrum analyzer for this set of measurements. We believe that a bad solder joint was the source of this problem.

- Figures B.23, B.27, B.31, and B.34 depict a statistical analysis.
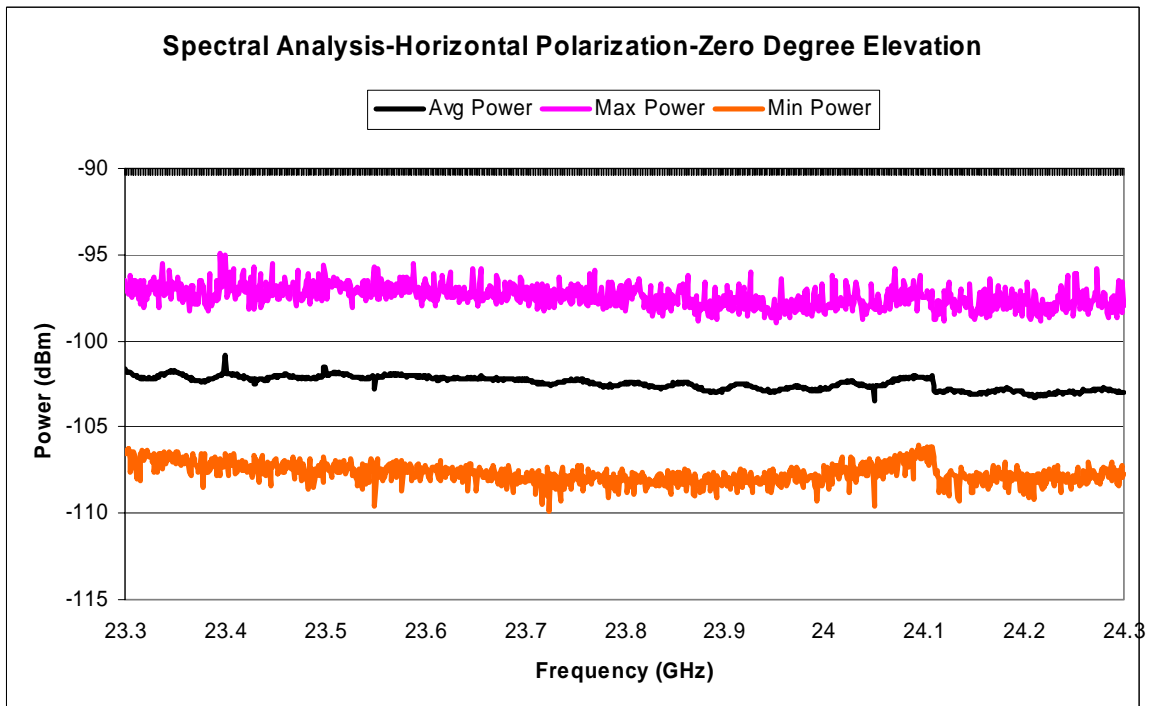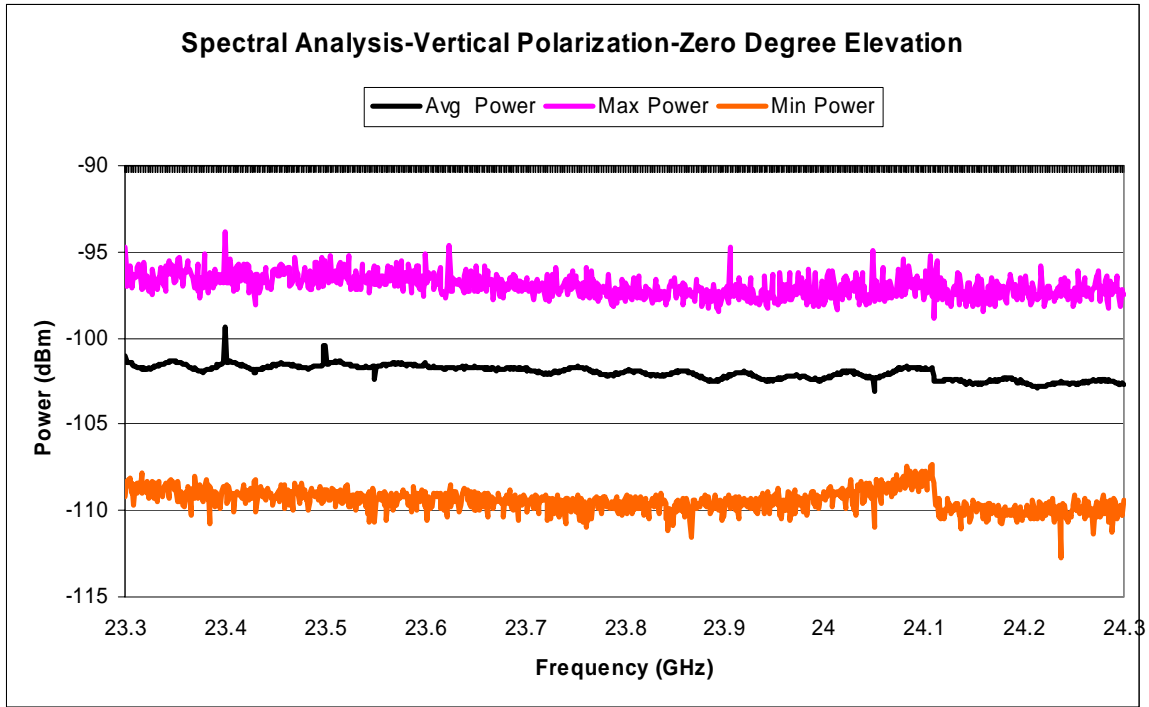
Figure B.20. Lake Hartwell Dike: Zero Degree Elevation, Spectral Analysis
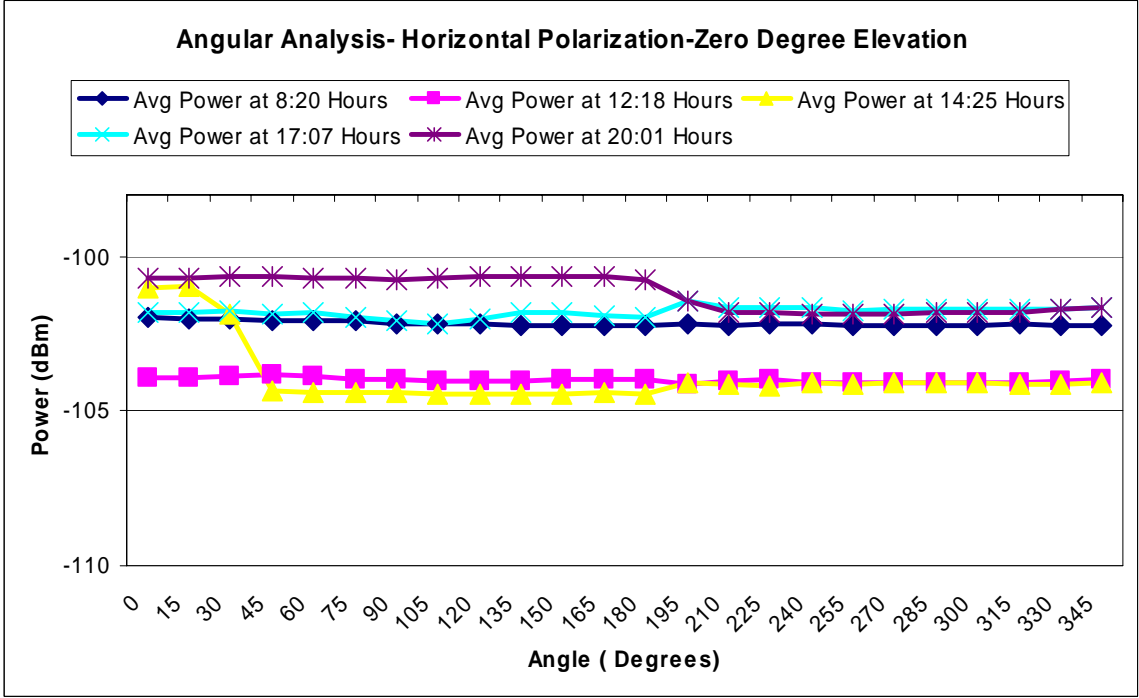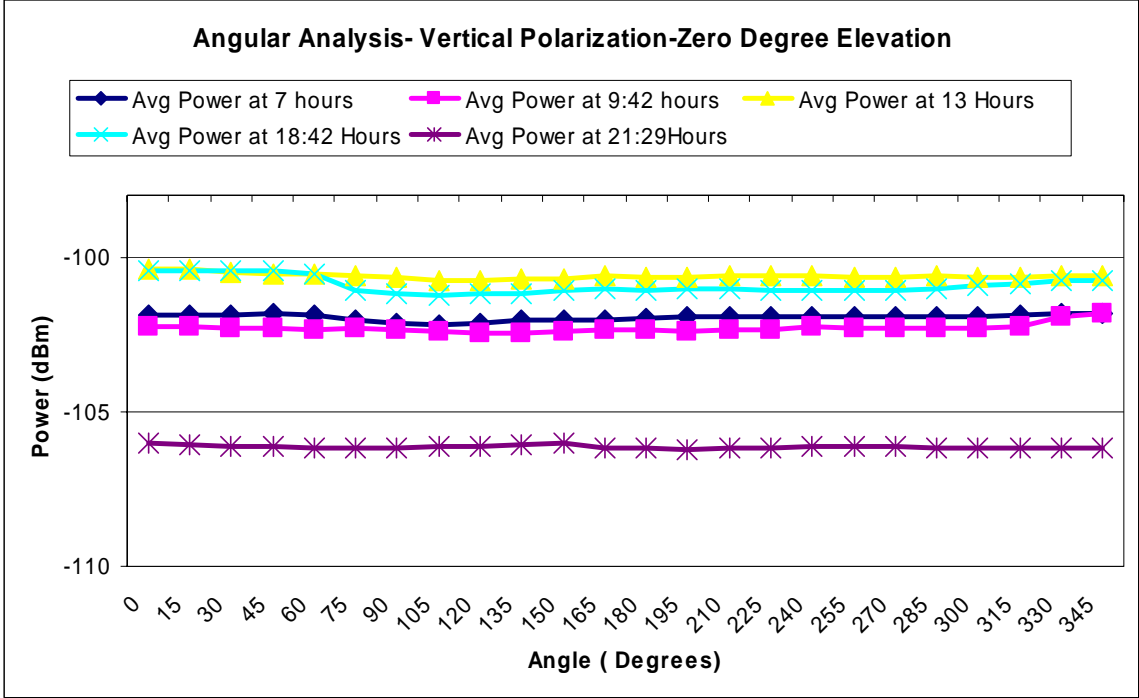
Figure B.21. Lake Hartwell Dike: Zero Degree Elevation, Angular Analysis

Temporal Analysis-Vertical Polarization- Zero Degree Elevation

Temporal Analysis- Horizontal Polarization- Thirty Degree Elevation
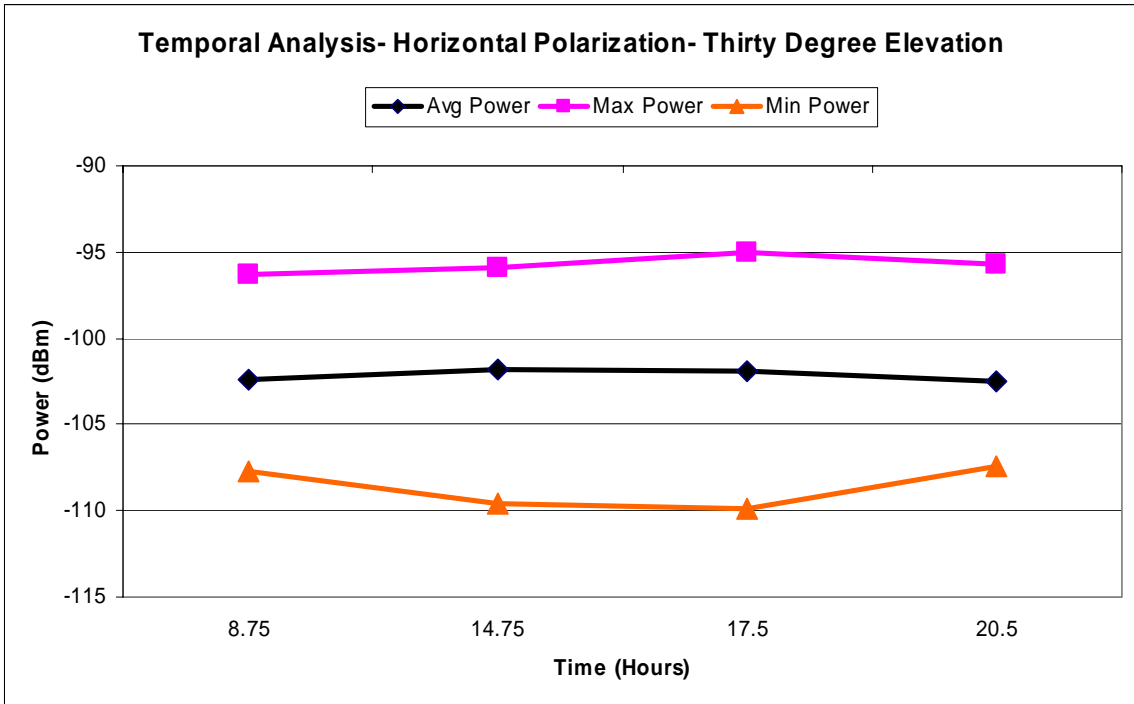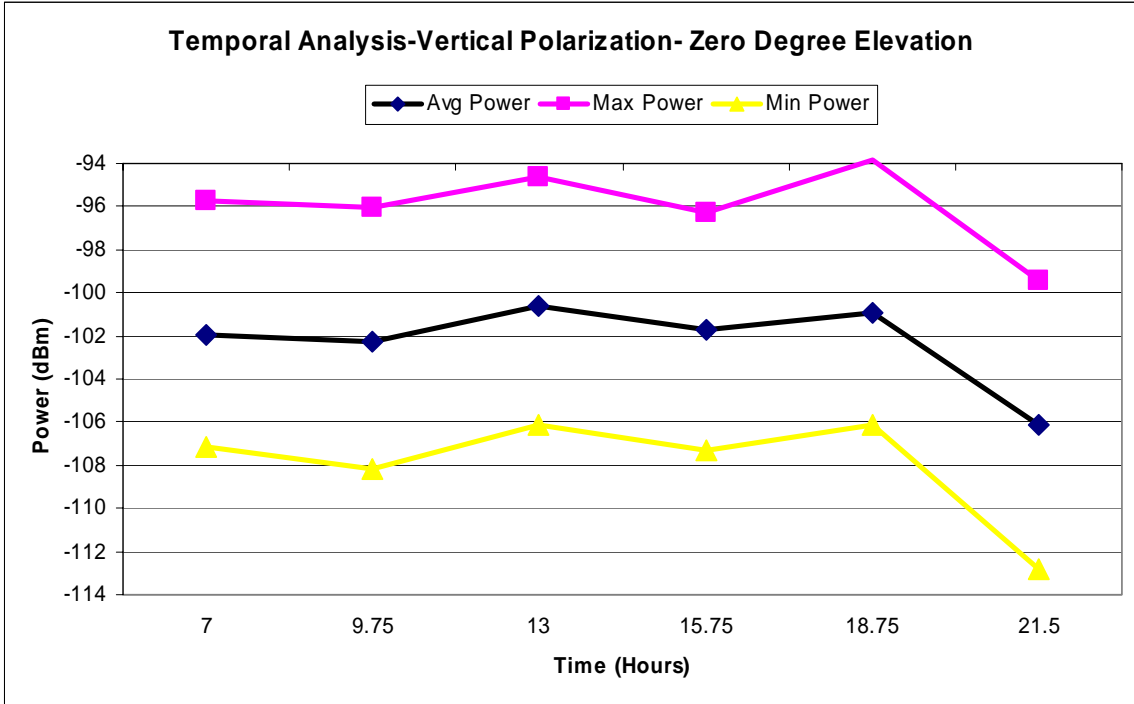
Figure B.22. Lake Hartwell Dike: Zero Degree Elevation, Temporal Analysis

146
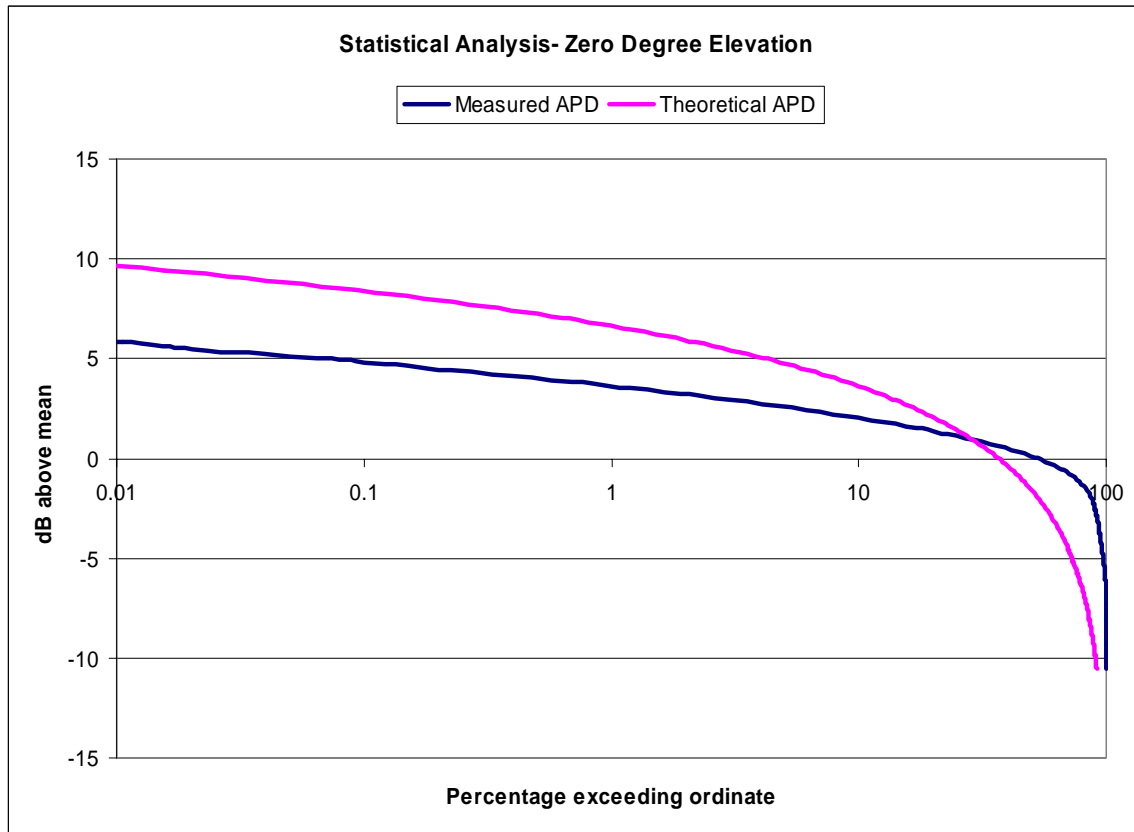
Figure B.23. Lake Hartwell Dike: Zero Degree Elevation, Statistical Analysis
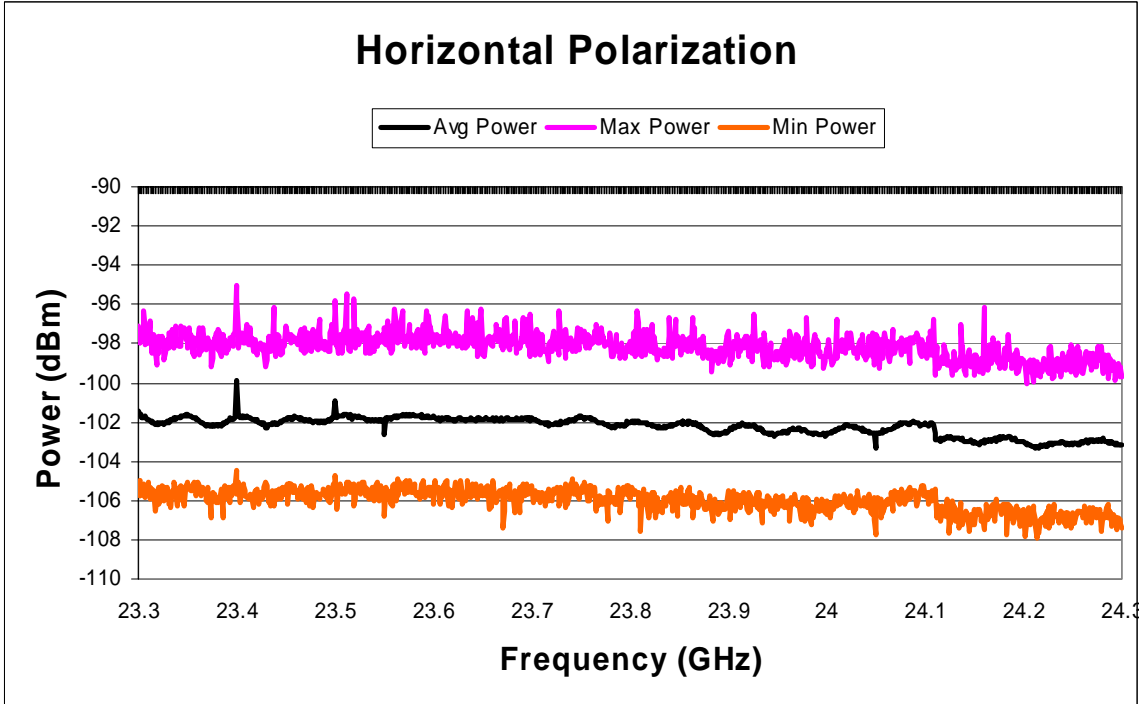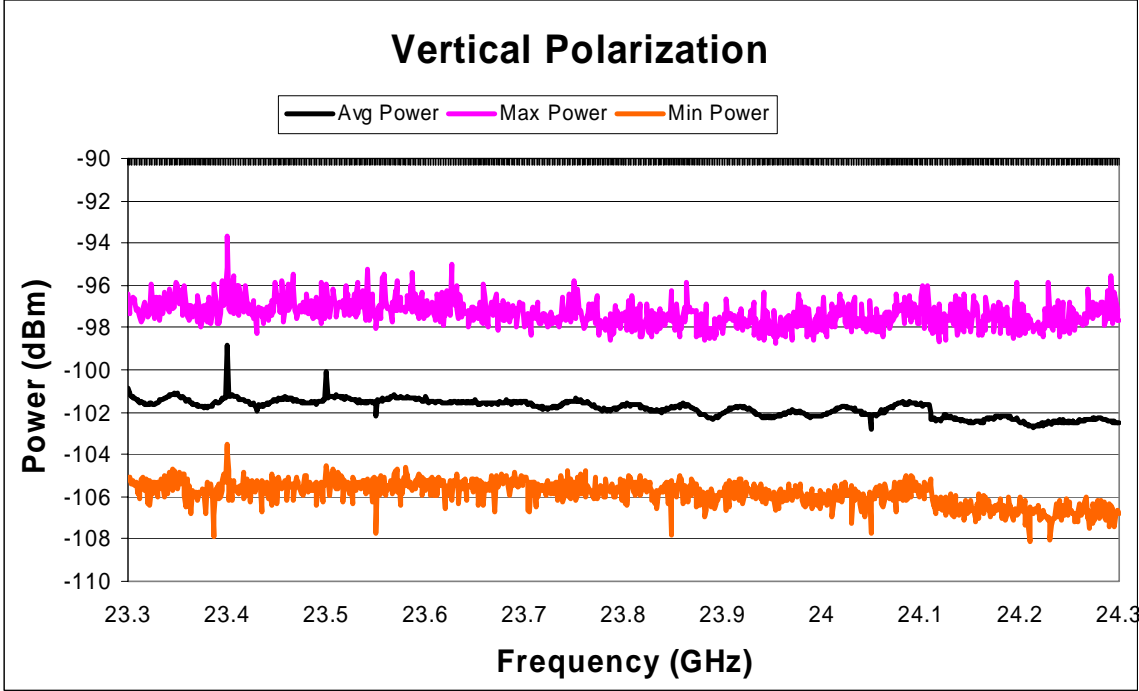
Figure B.24. Lake Hartwell Dike: Thirty Degree Elevation, Spectral Analysis

148
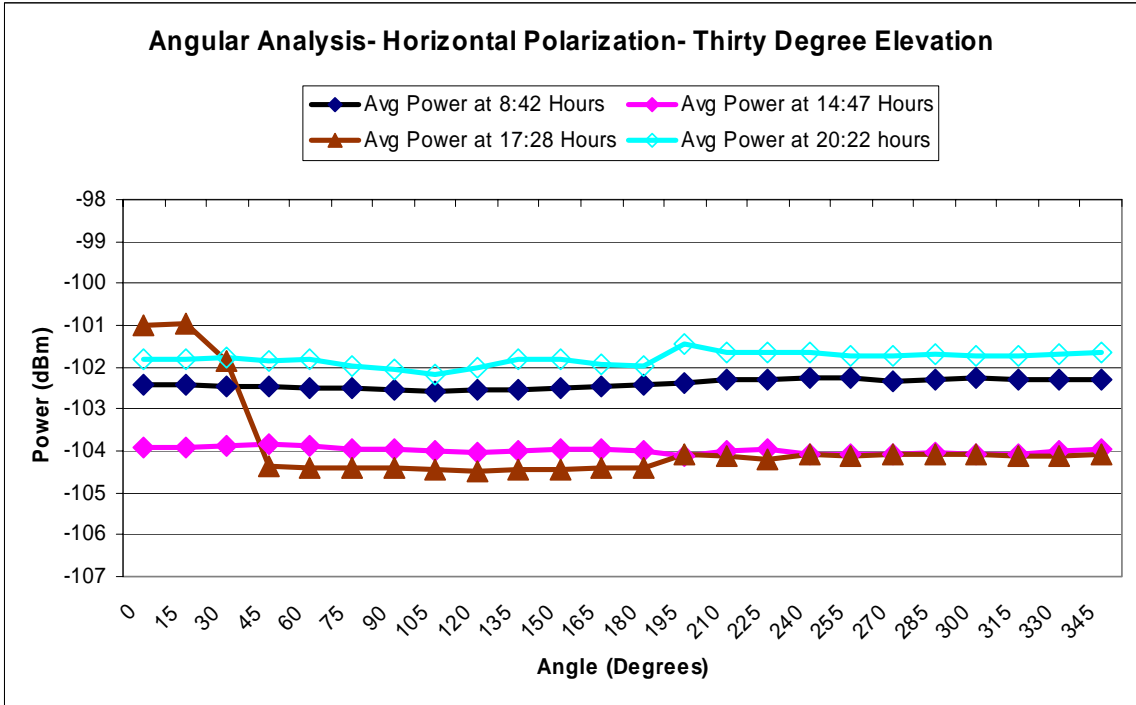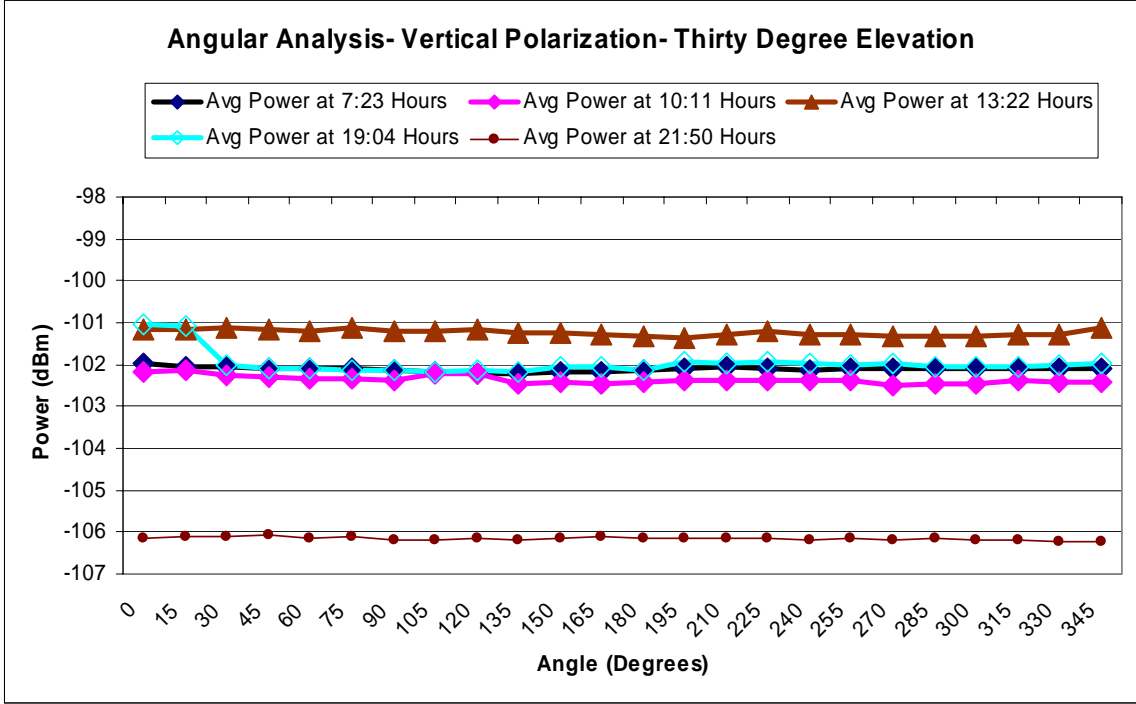
Figure B.25. Lake Hartwell Dike: Thirty Degree Elevation, Angular Analysis

149
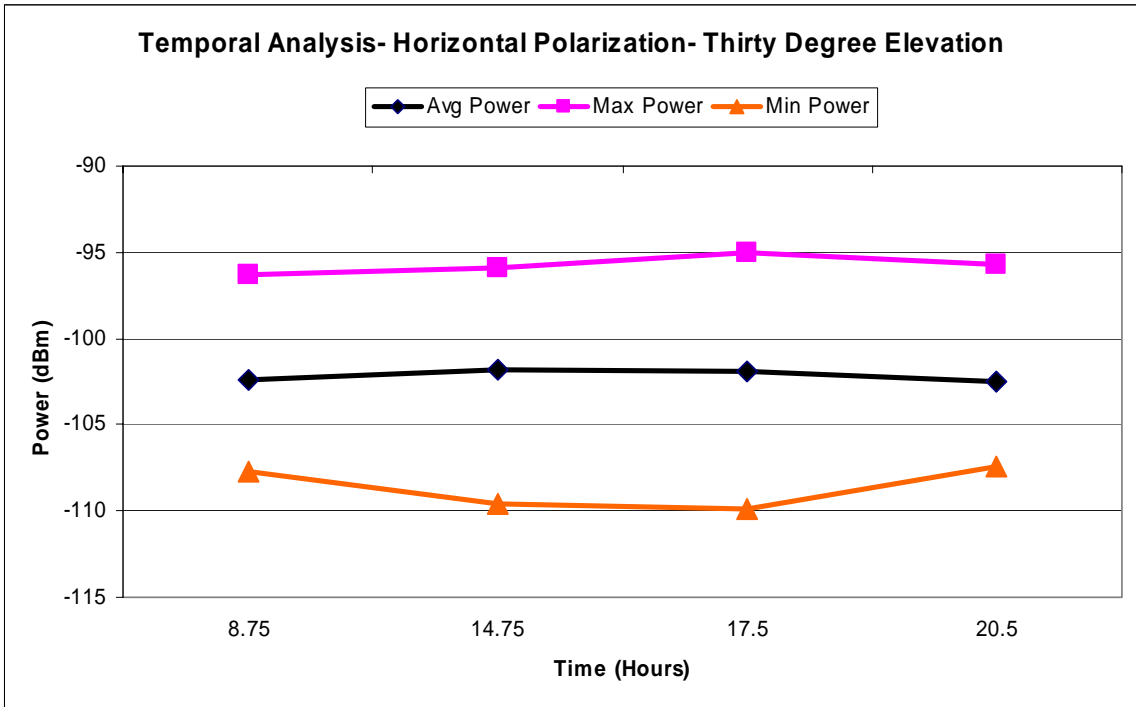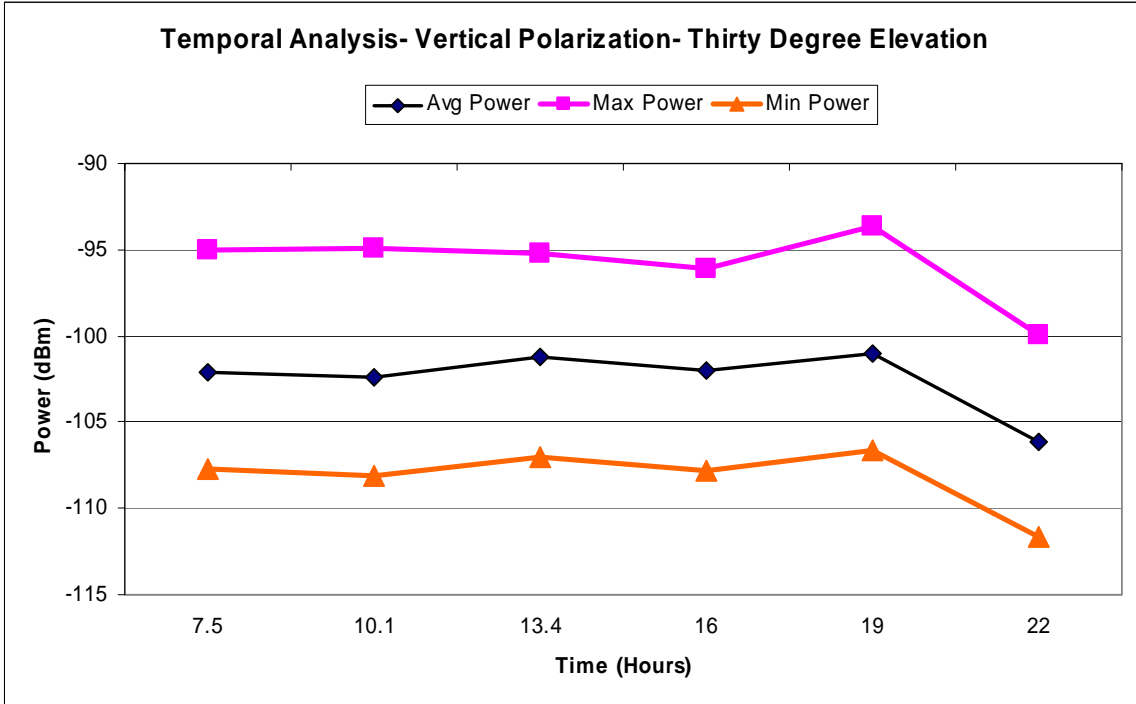
Figure B. 26 Lake Hartwell Dike: Thirty Degree Elevation, Temporal Analysis
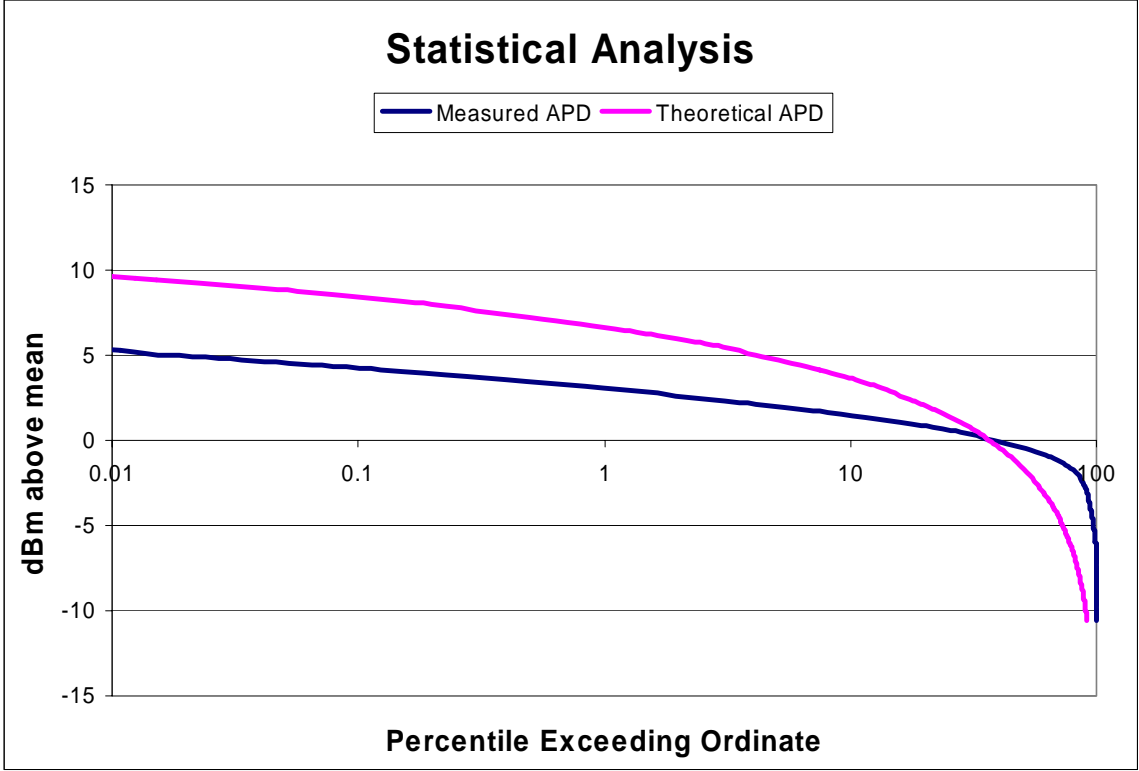
Figure B.27. Lake Hartwell Dike: Thirty Degree Elevation, Statistical Analysis

151
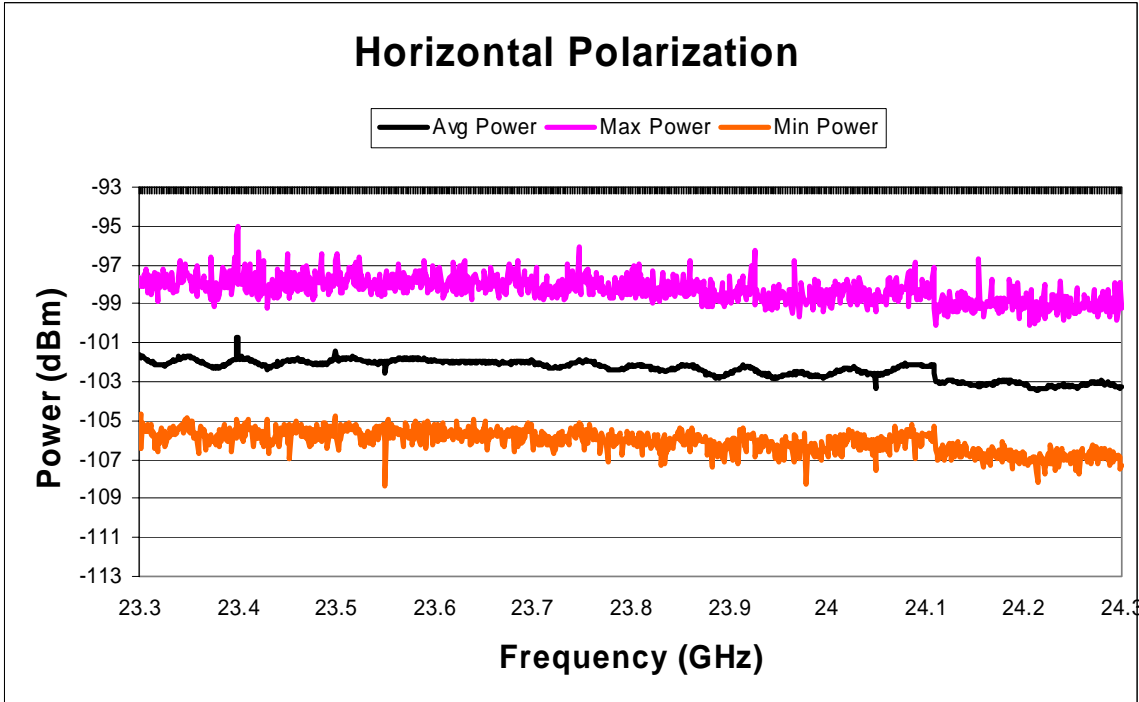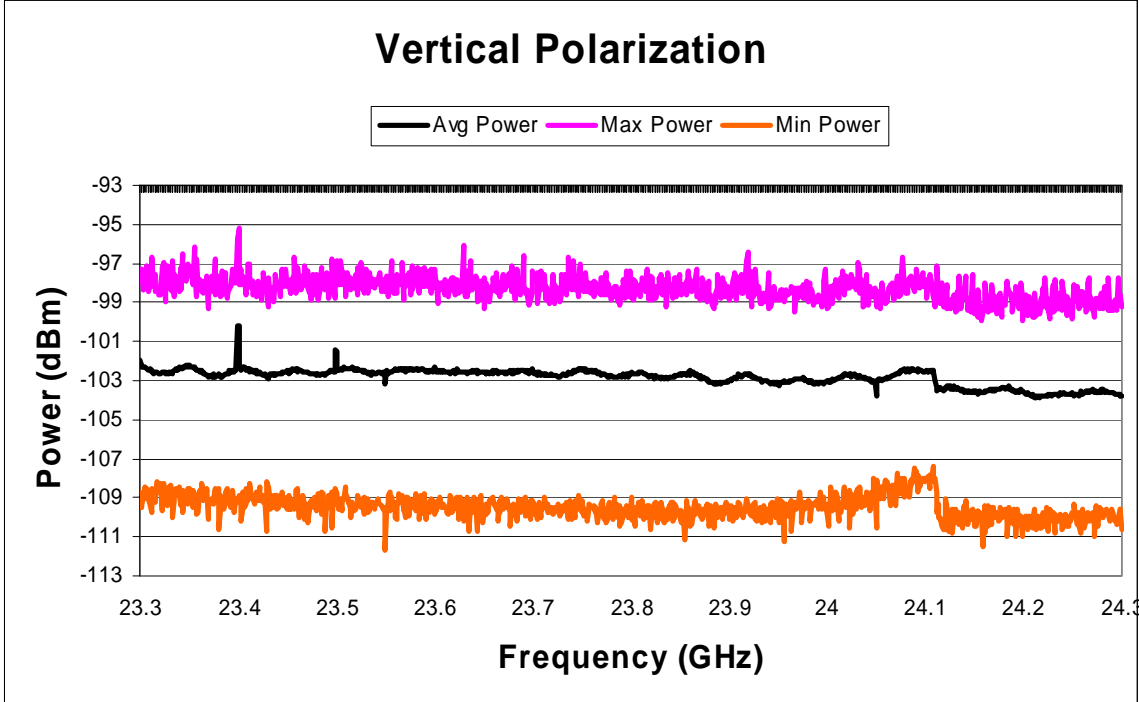
Figure B.28. Lake Hartwell Dike: Sixty Degree Elevation, Spectral Analysis

Angular Analysis- Vertical Polarization- Sixty Degree Elevation

Angular Analysis- Horizontal Polarization- Sixty Degree Elevation
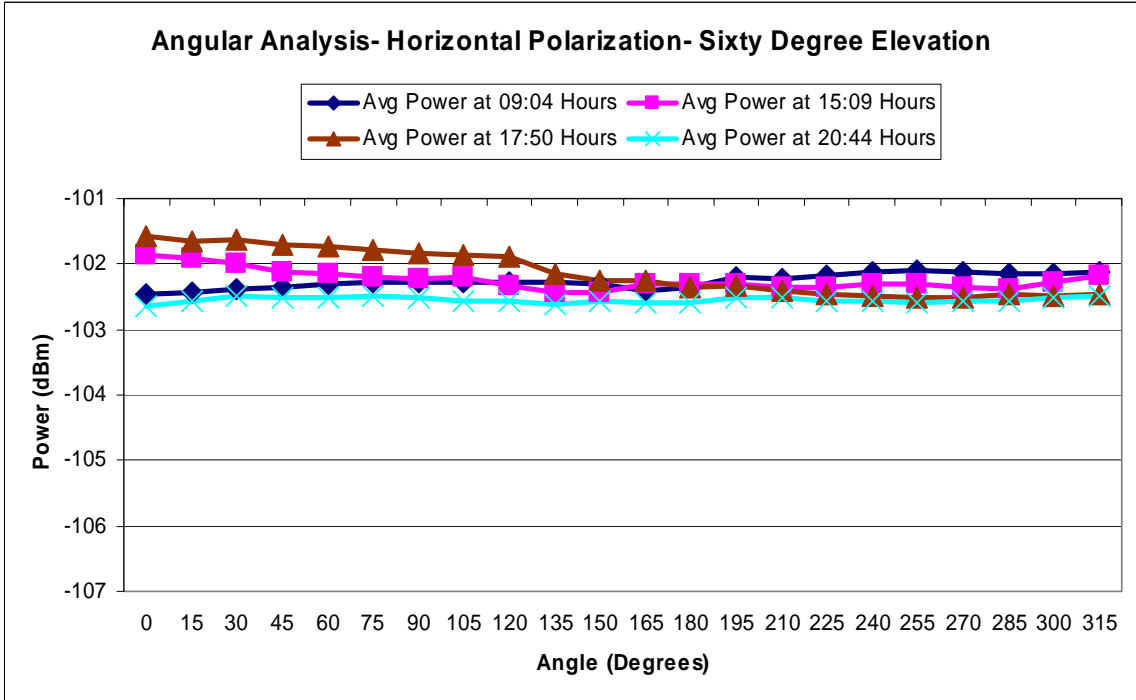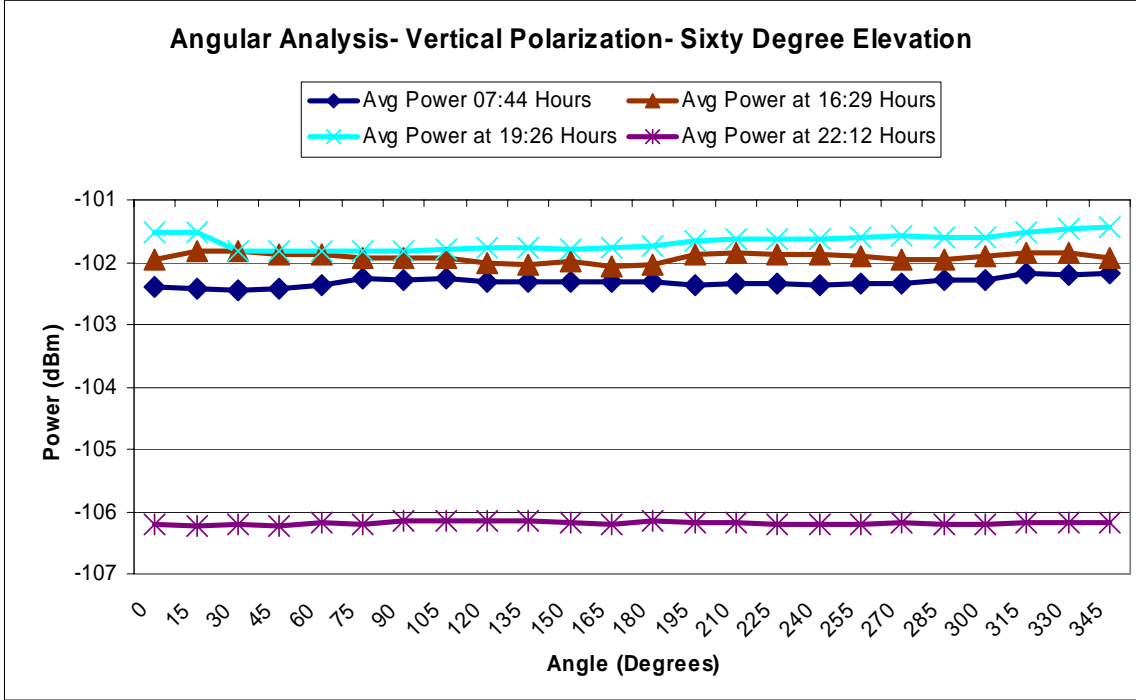
Figure B.29. Lake Hartwell Dike: Sixty Degree Elevation, Angular Analysis
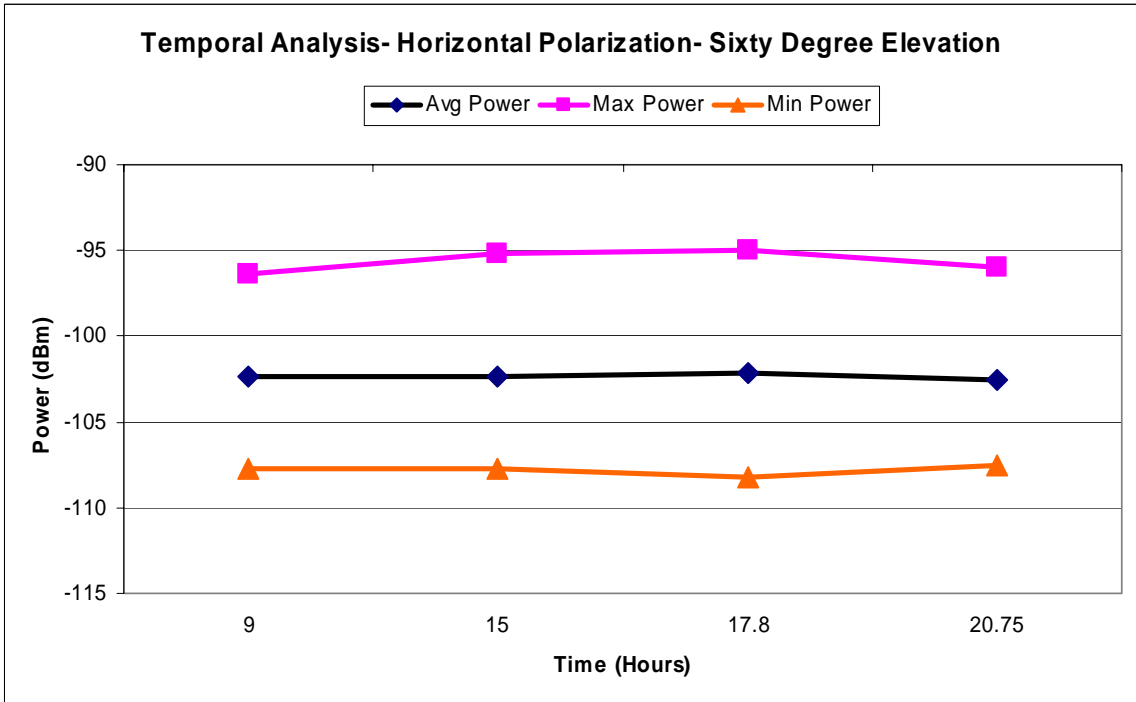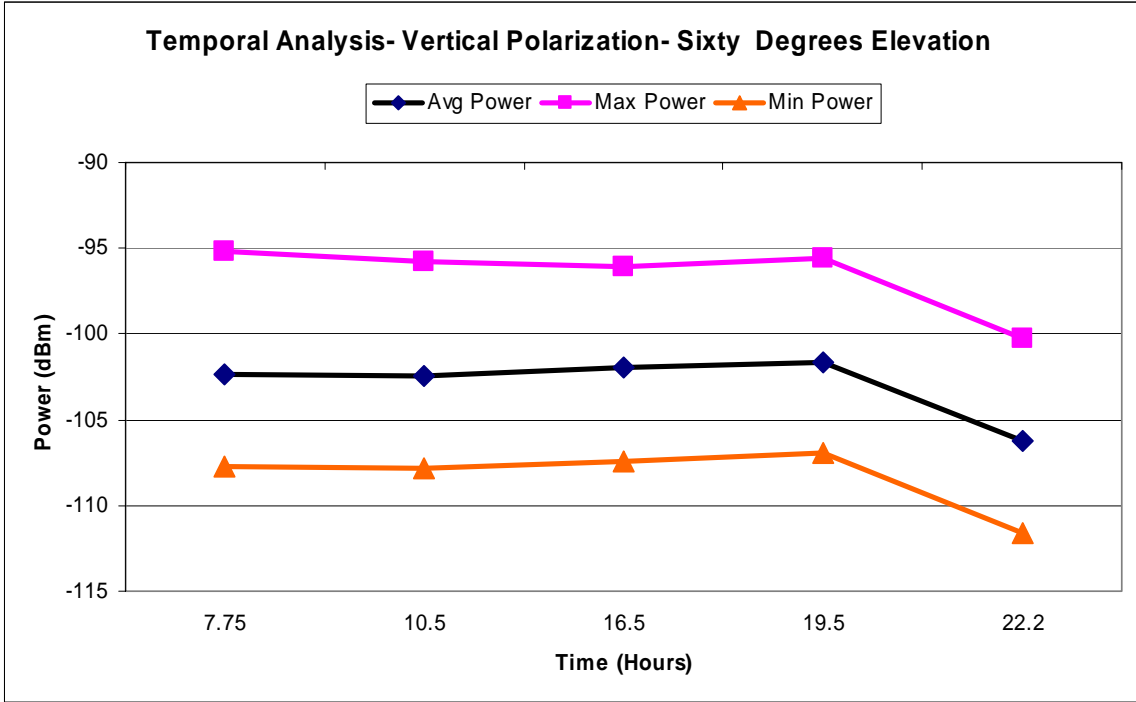
Figure B.30. Lake Hartwell Dike: Sixty Degree Elevation, Temporal Analysis

154
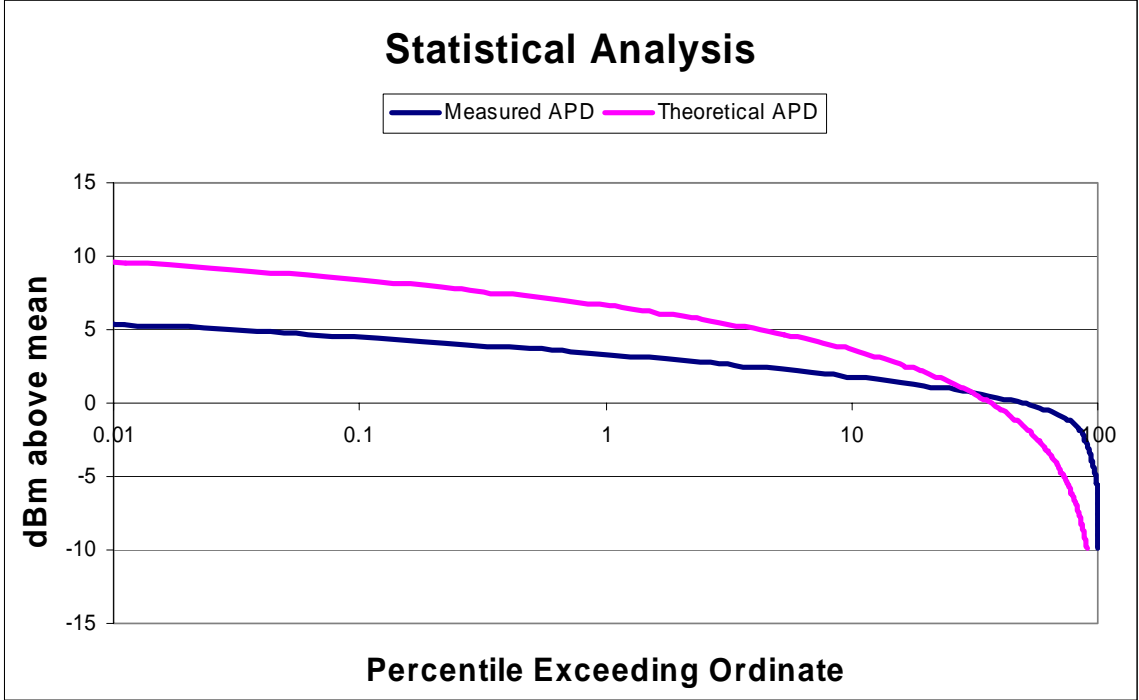
Figure B.31. Lake Hartwell Dike: Sixty Degree Elevation, Statistical Analysis
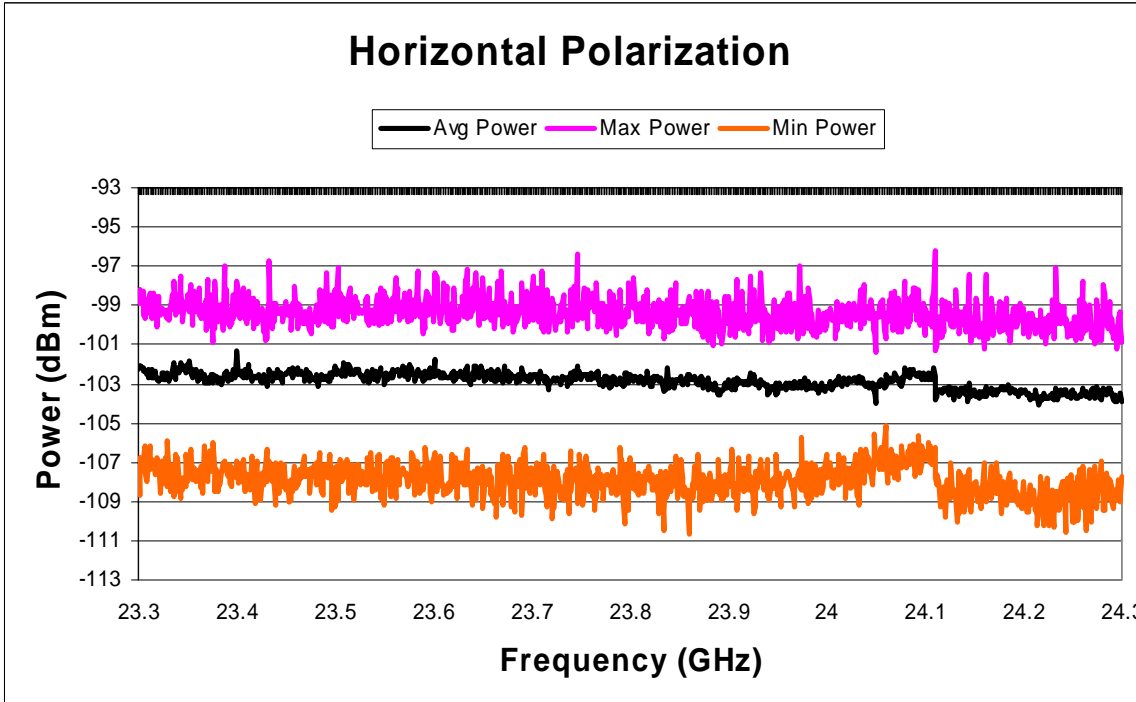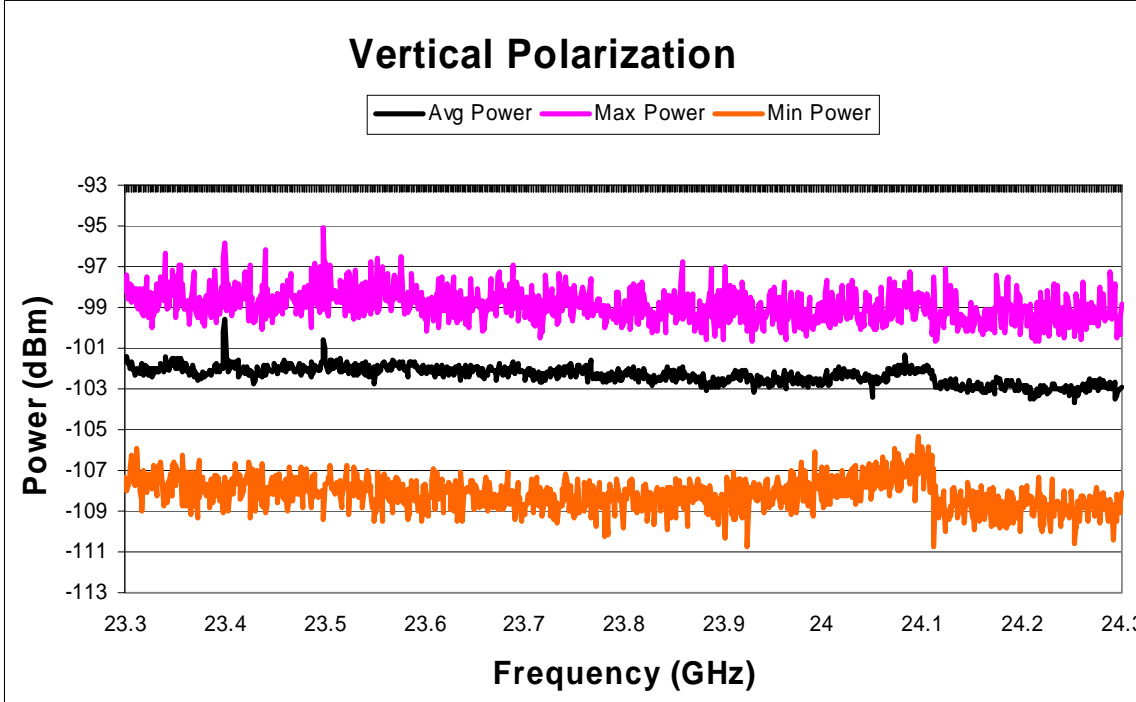
Figure B.32. Lake Hartwell Dike: Ninety Degree Elevation, Spectral Analysis
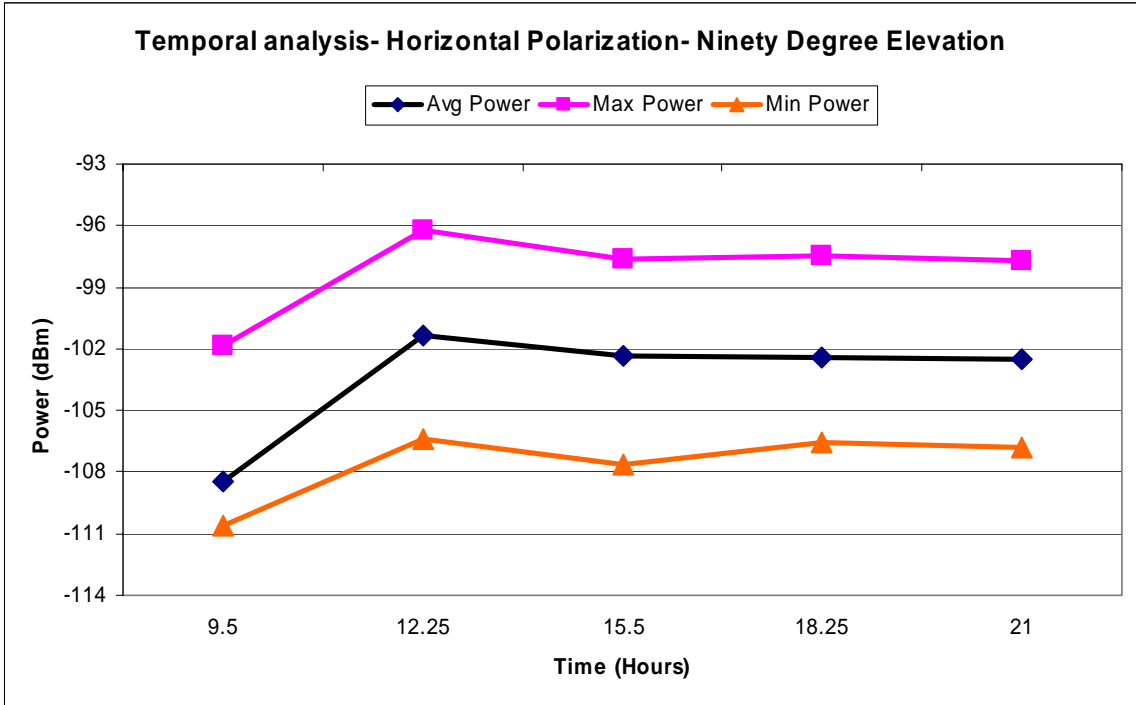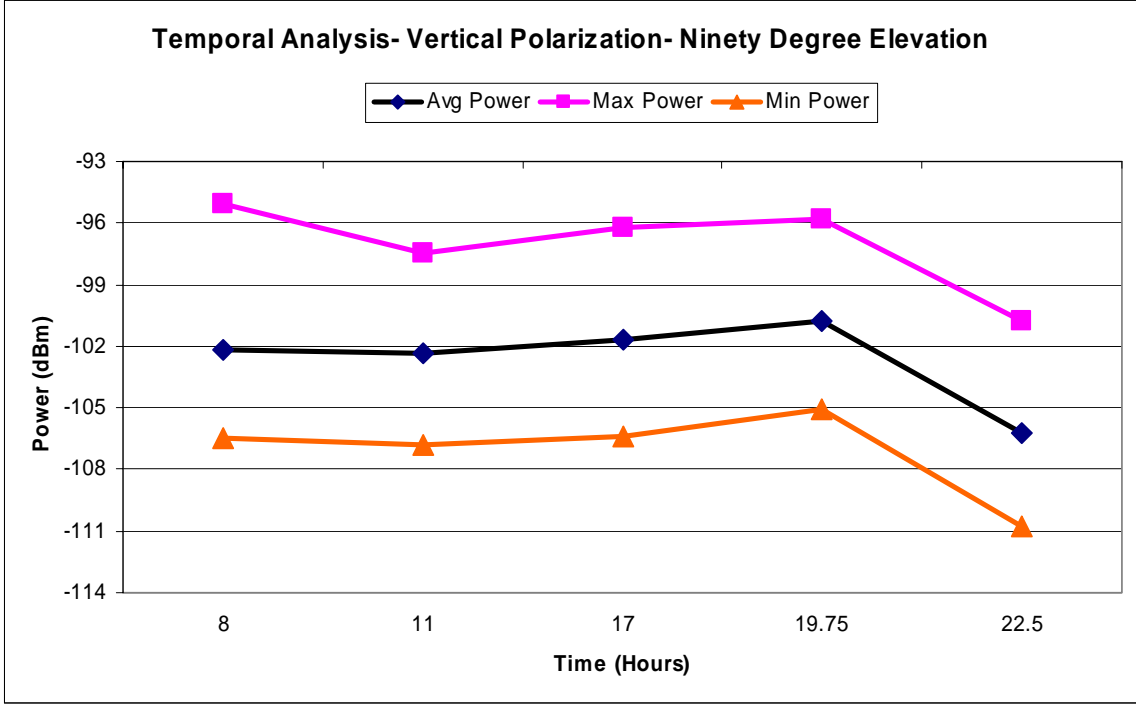
Figure B.33. Lake Hartwell Dike: Ninety Degree Elevation, Temporal Analysis
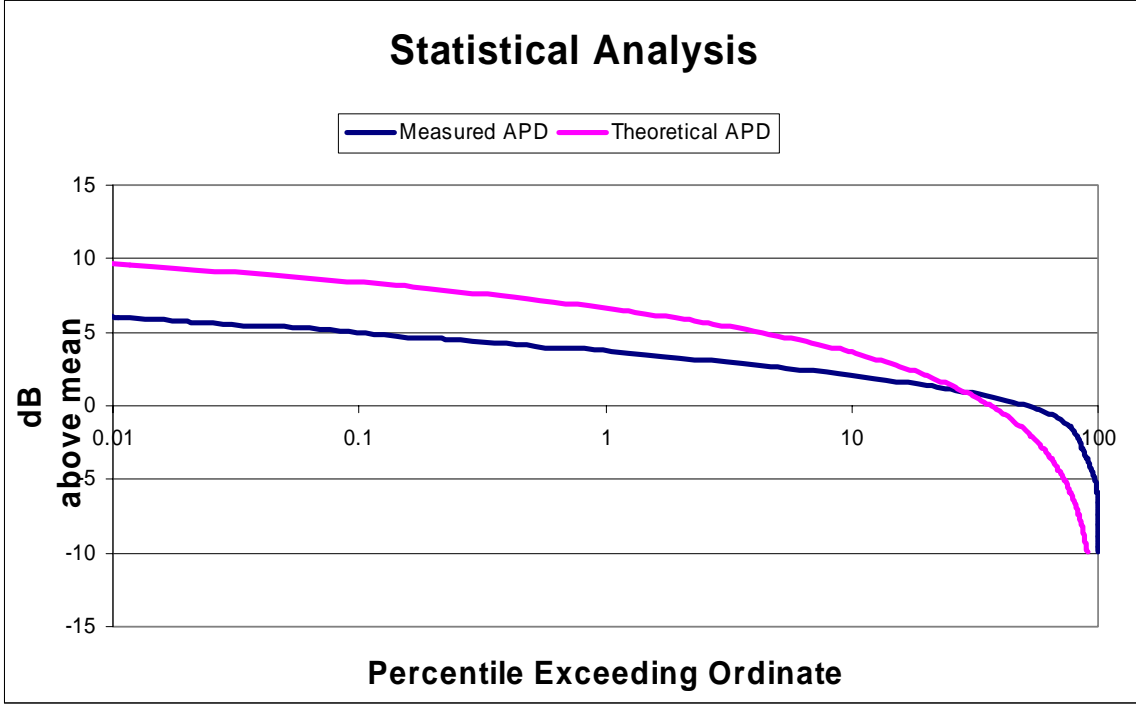
Figure B.34. Lake Hartwell Dike: Ninety Degree Elevation, Statistical Analysis

Appendix B.3: Blue Ridge Parkway, North Carolina (Site 3)

Date: 9/19/03
Map of Location: See Figure B.35
Noteworthy Results:

- Spectral trends: Uniform in frequency within 2 dB. Between 24.05 and 24.1 GHz, there is a spectral artifact. It has been verified experimentally that this artifact was generated by the input attenuation in the spectrum analyzer, not the ambient noise floor. See Figures B. 36, B.40, B.44, and B.48.
- Angular trends: Uniform in angle within 2 dB. See Figures B.37, B.41, and B.45.
- Temporal trends: Temporal peak occurs at noon, otherwise uniform within 2 dB. See Figures B.38, B.42, B.46, and B.49.
- Pre-measurement calibrated gain: 74.0 dB; Post-measurement calibrated gain: 83.8 dB. The reason for the discrepancy between these two calibrations was an anomalous change in DC bias current discussed in the description of the measurement at Site 2.
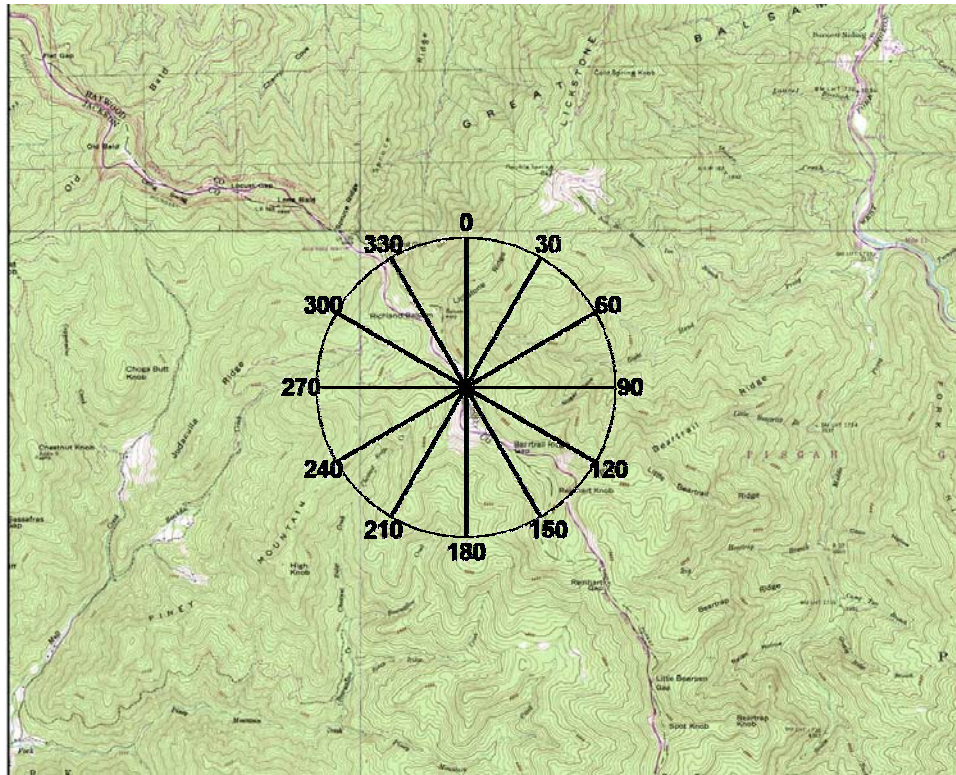
Figure B.35. Map of Blue Ridge Parkway Measurement Site
(Note the lack of man-made structures in the immediate vicinity of the measurement site)

- The power levels in this measurement are roughly 10 dB above that of the previous measurements, and the spectral artifact due to the attenuator at the input of the spectrum analyzer is emphasized to a greater extent than previous sites. The lower gain discussed above causes the noise power due to the attenuator to dominate the measured noise floor. The scope of this project

is to measure the man-made interference sources. The man-made sources from all other sites listed were at a level of -97 dBm or above. The average observed noise floor of this measurement site existed at this -97 dBm level as can be seen from the figures. Therefore, the ability to detect man-made sources was modestly impaired by this shift in system noise floor.

- Figures B.39, B.43, B.47, and B.50 depict a statistical analysis.
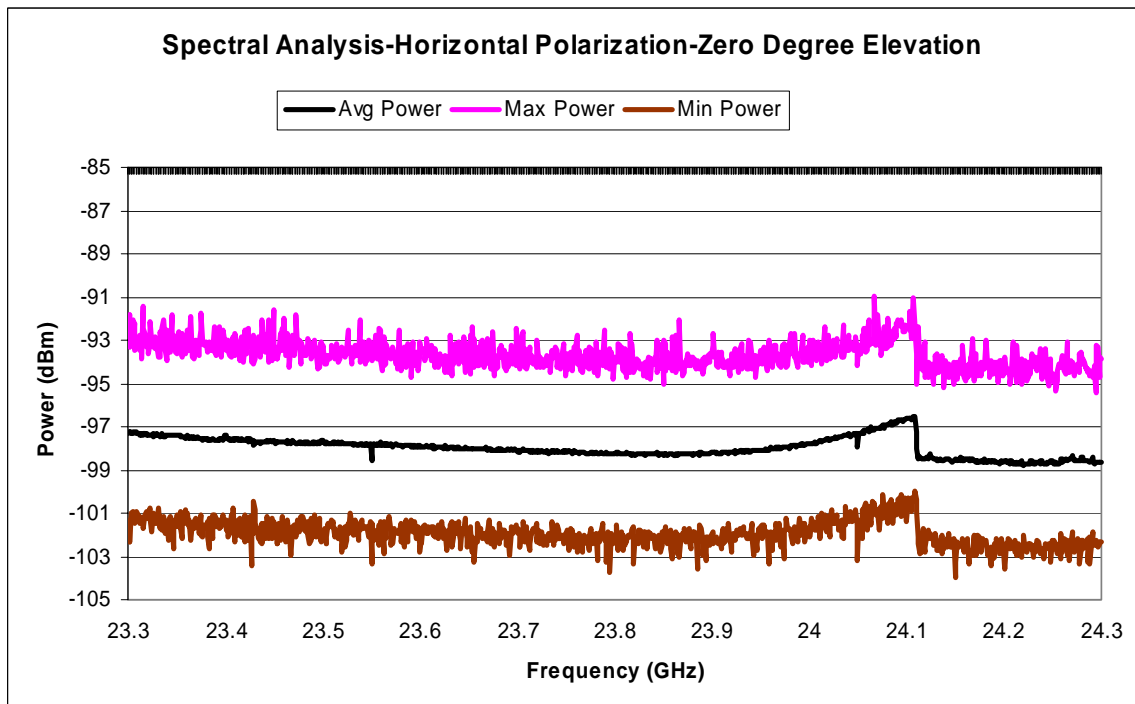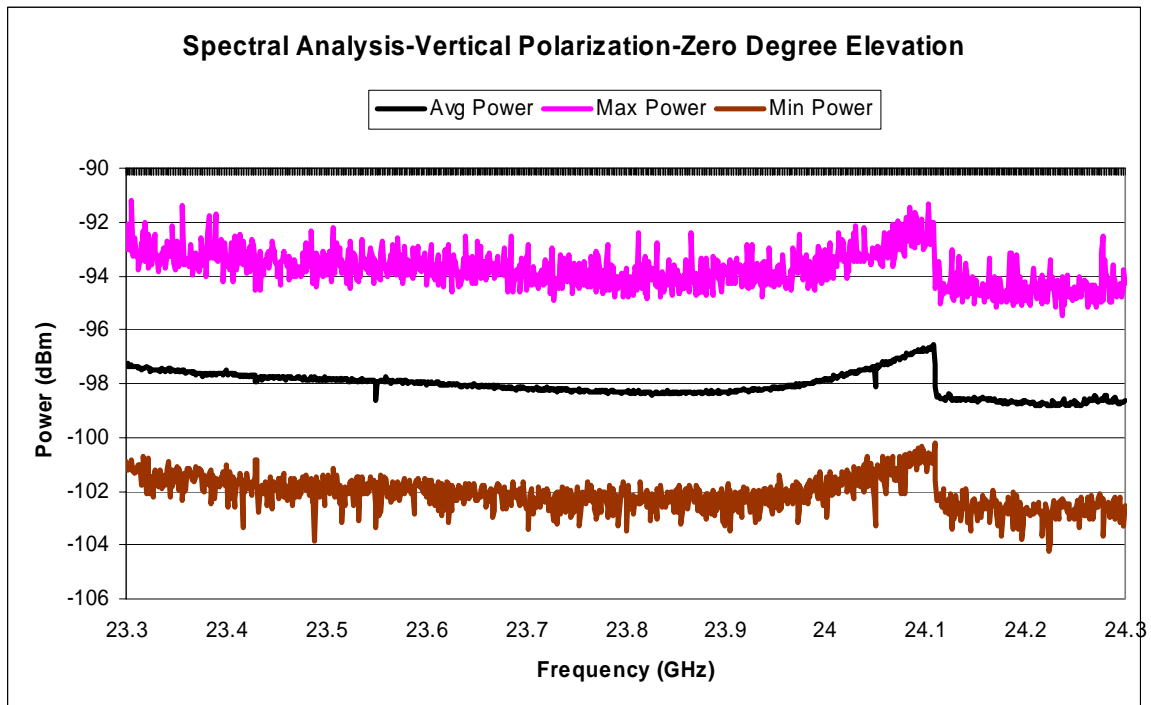
Figure B.36. Blue Ridge Parkway: Zero Degree Elevation, Spectral Analysis

161
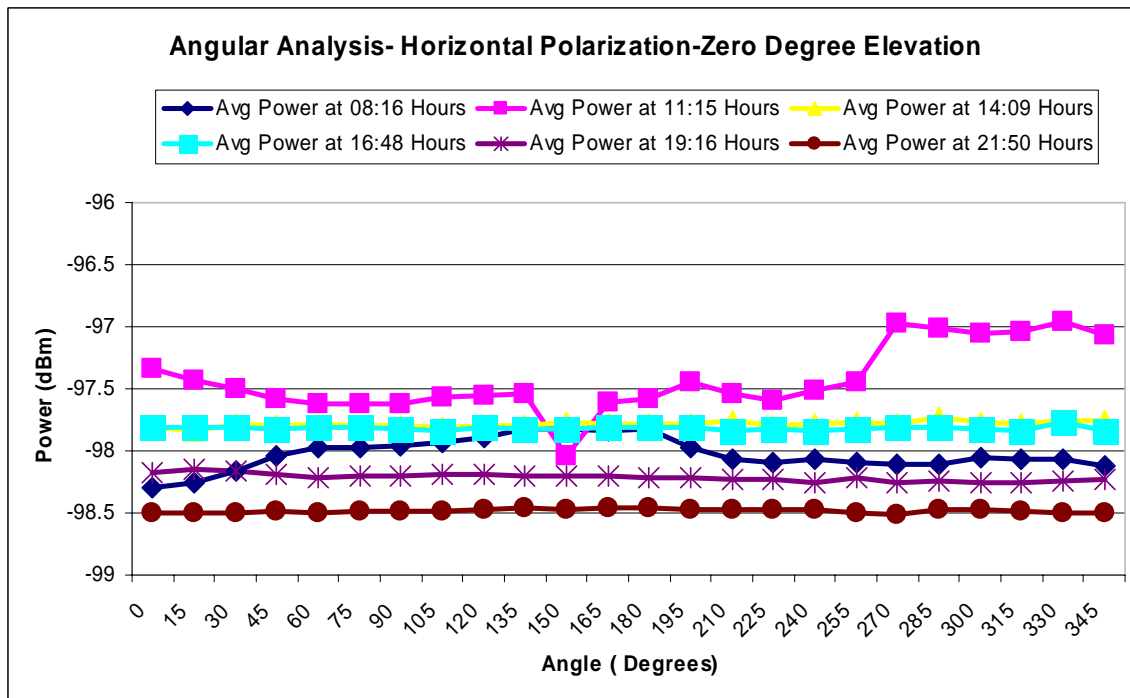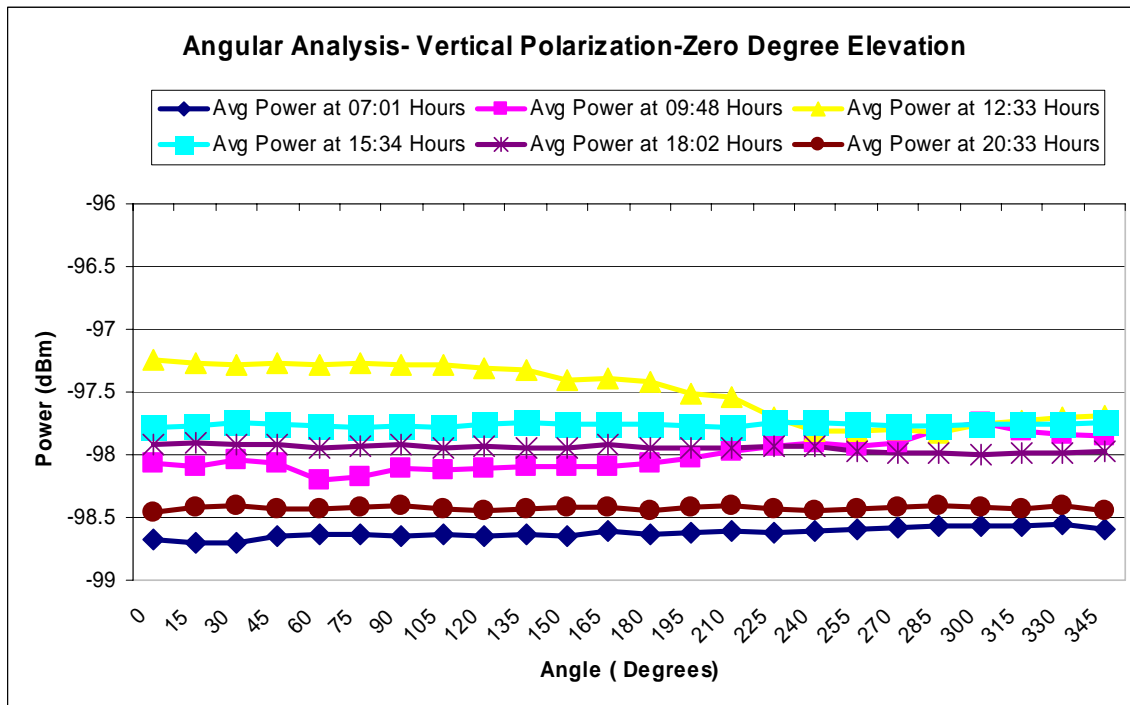
Figure B.37. Blue Ridge Parkway: Zero Degree Elevation, Angular Analysis
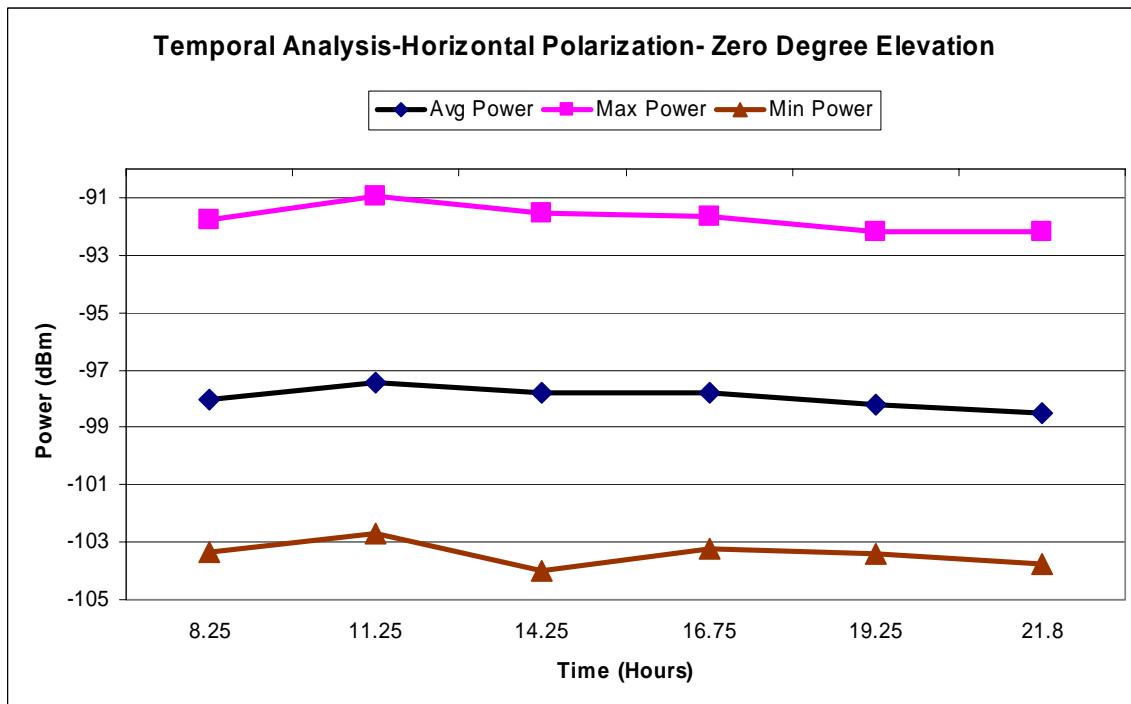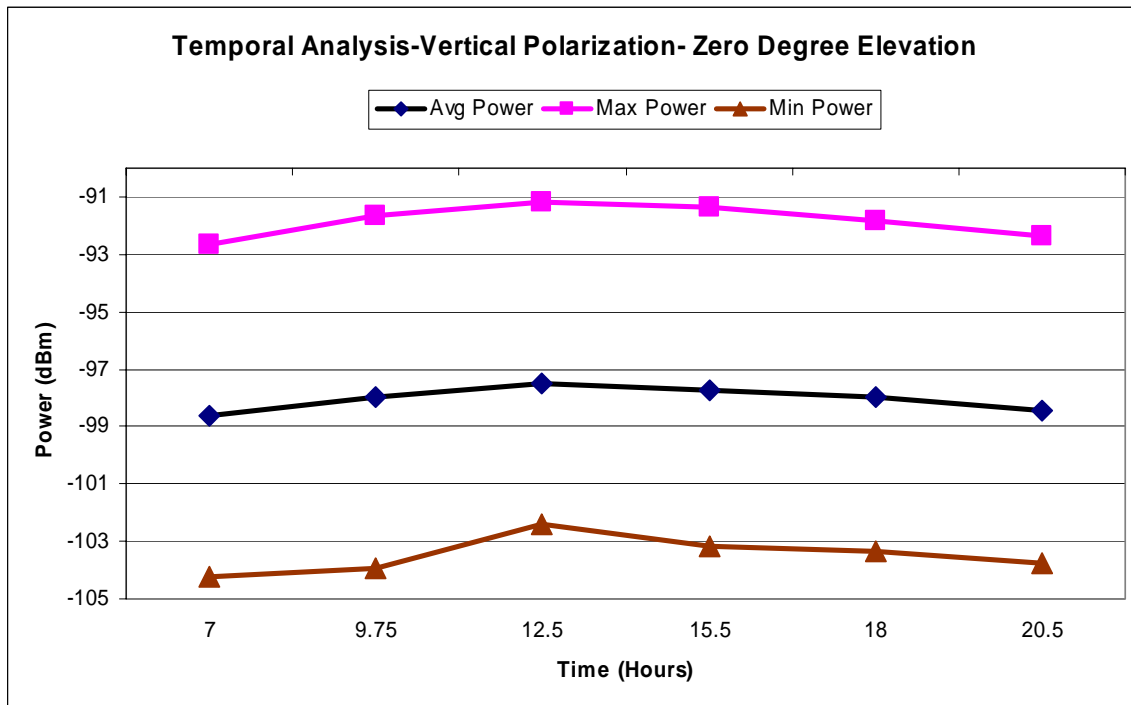
Figure B.38. Blue Ridge Parkway: Zero Degree Elevation, Temporal Analysis

163
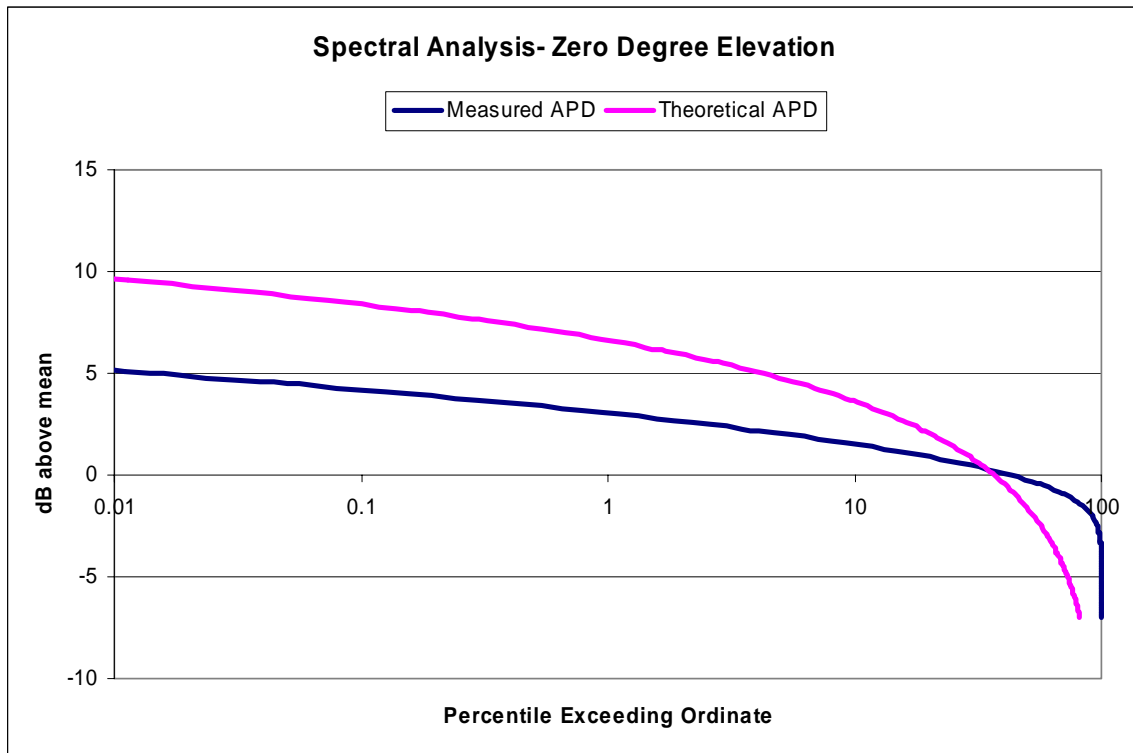
Figure B.39. Blue Ridge Parkway: Zero Degree Elevation, Statistical Analysis
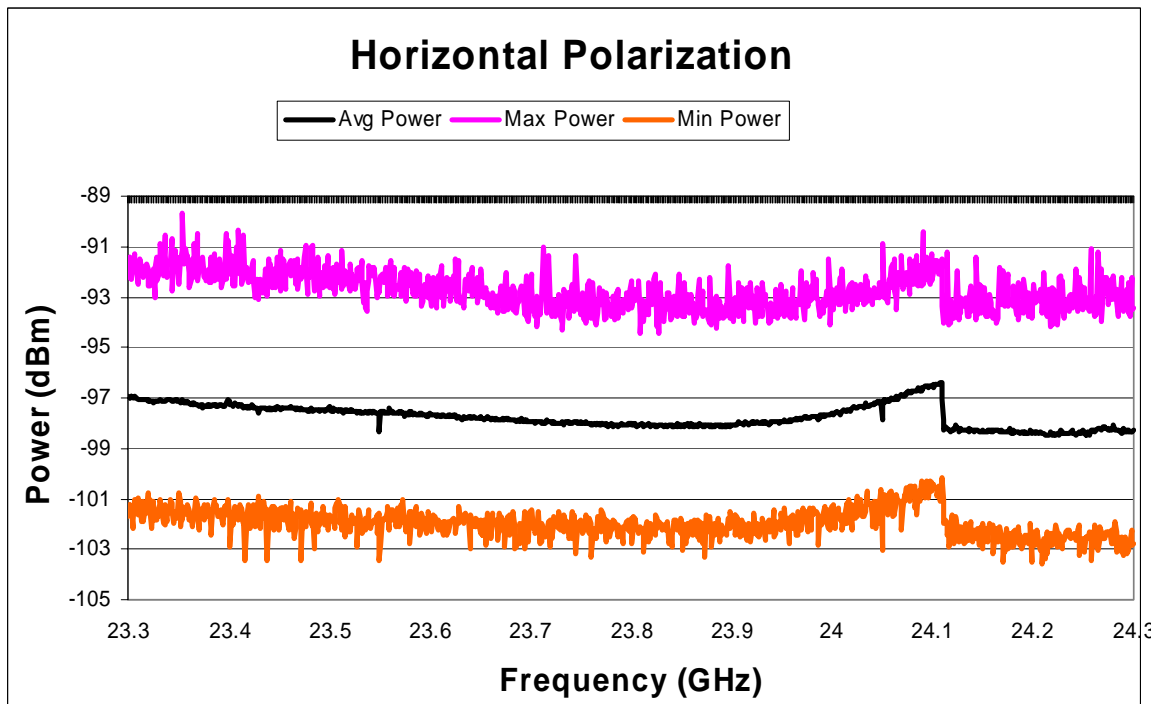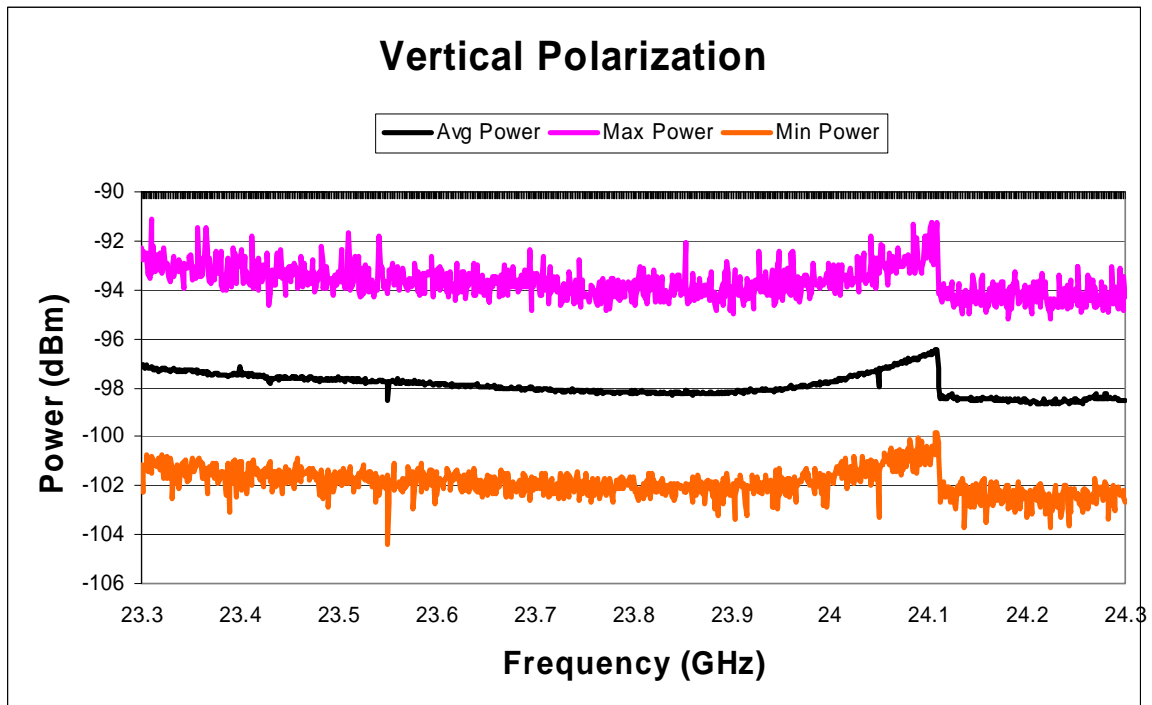
Figure B.40. Blue Ridge Parkway: Thirty Degree Elevation, Spectral Analysis

Angular Analysis- Vertical Polarization-Zero Degree Elevation

Angular Analysis- Horizontal Polarization-Zero Degree Elevation
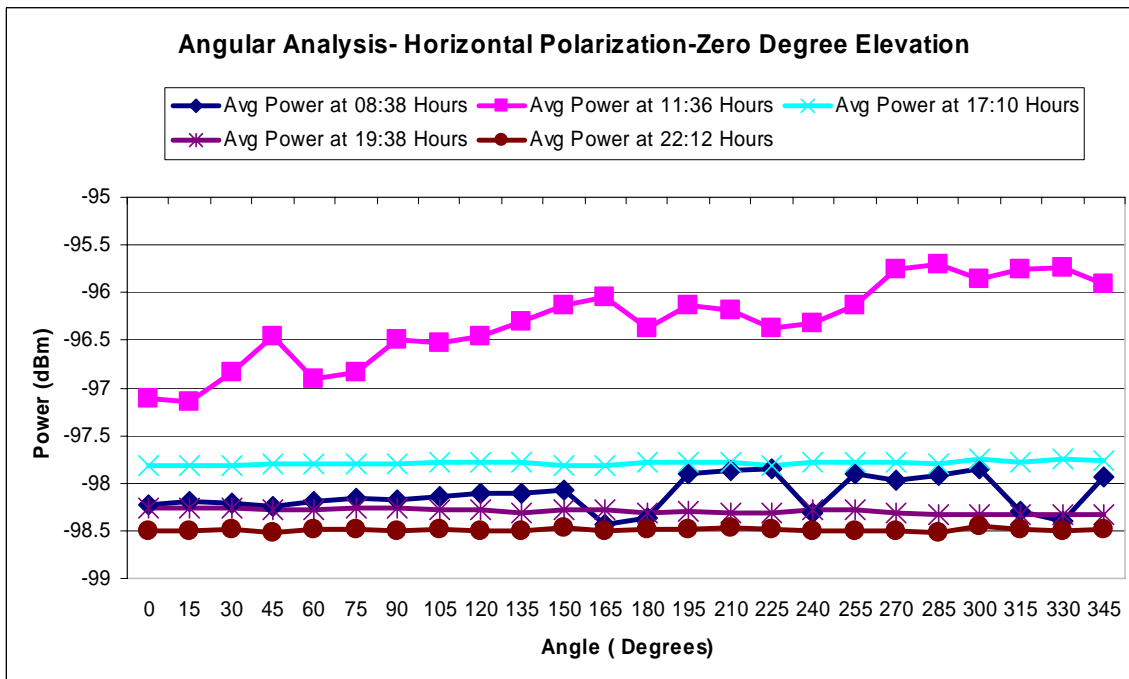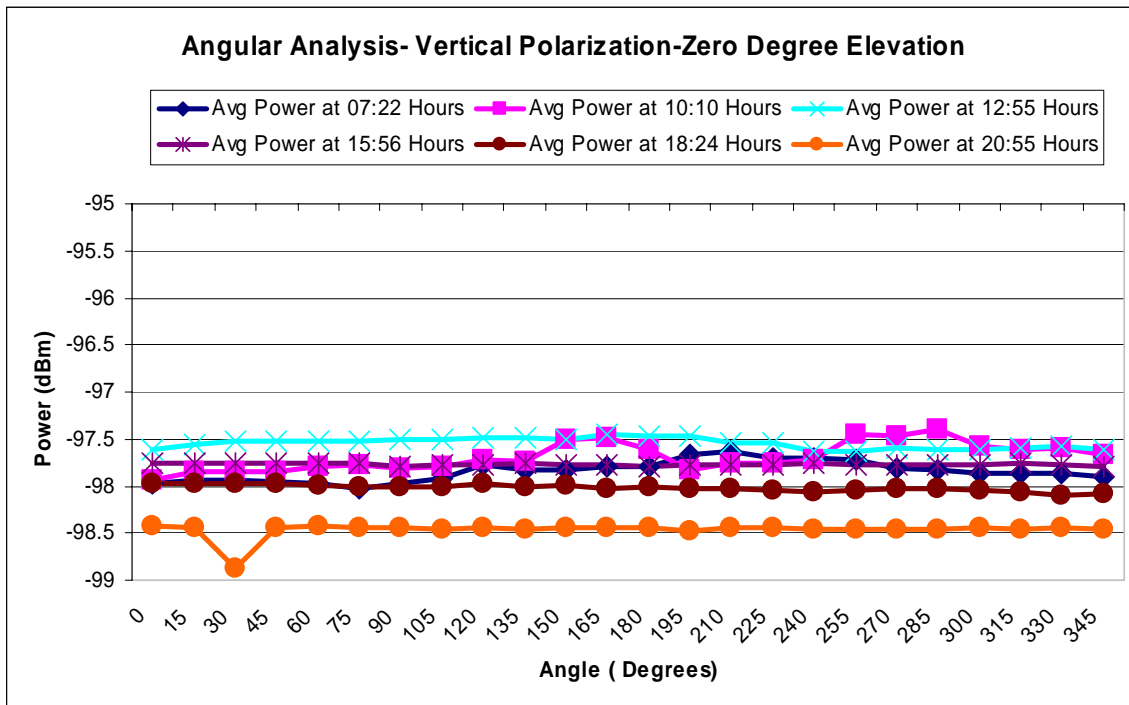
Figure B.41. Blue Ridge Parkway: Thirty Degree Elevation, Angular Analysis

166
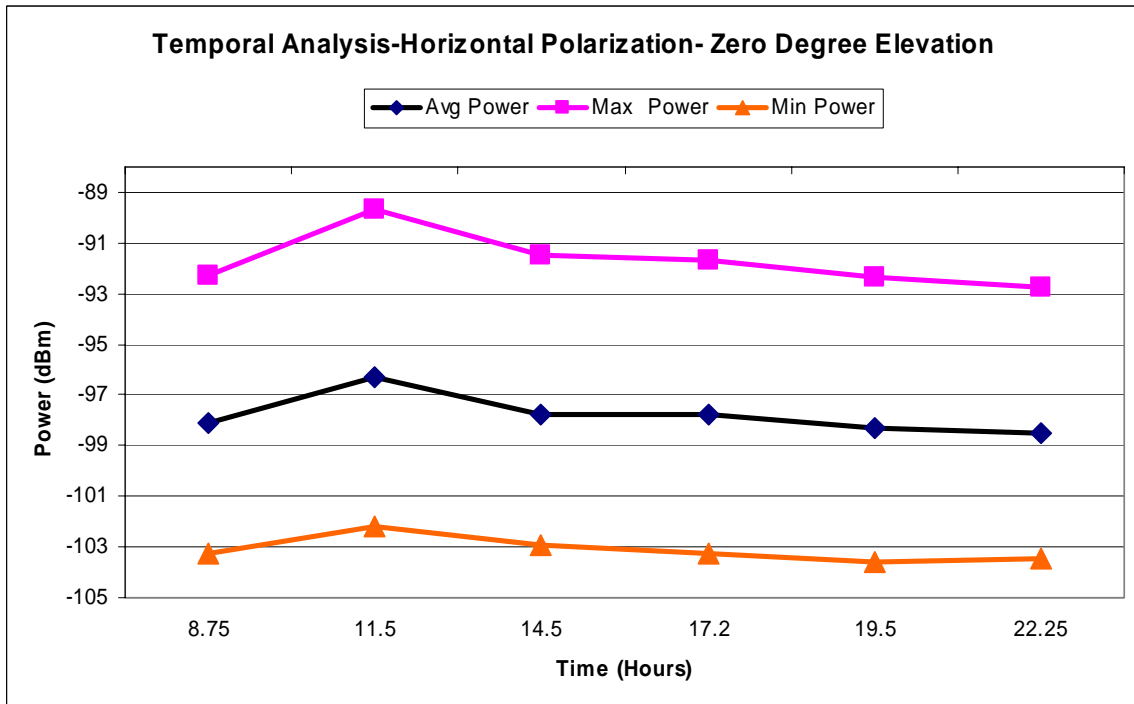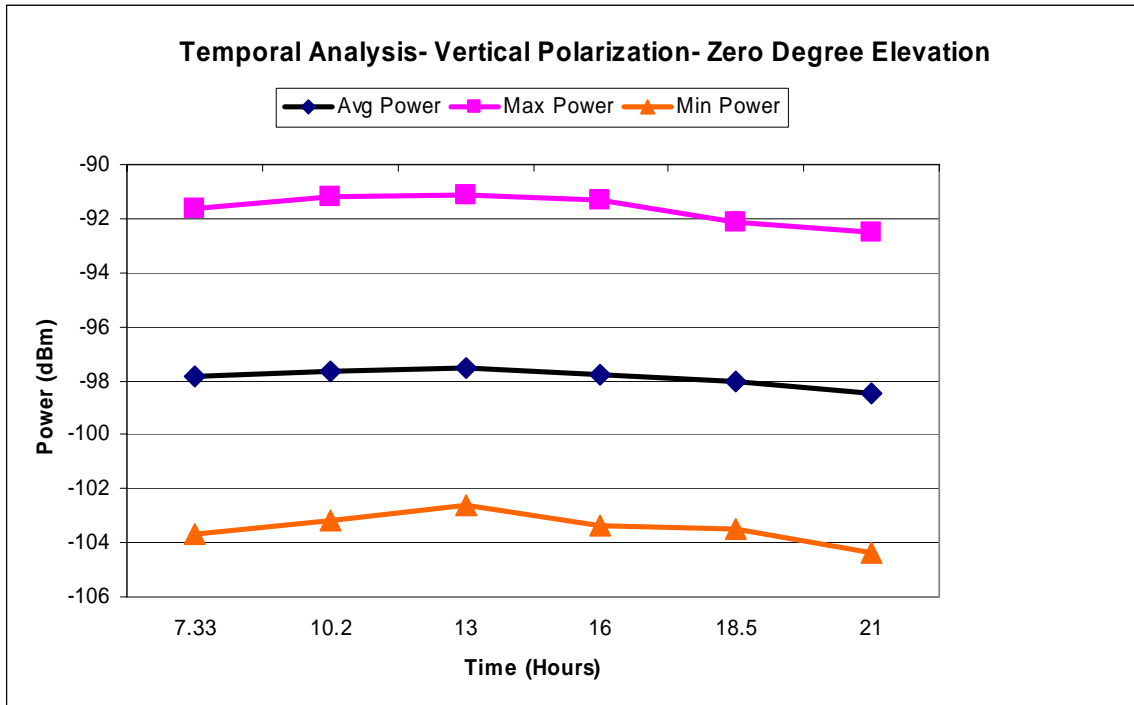
Figure B.42. Blue Ridge Parkway: Thirty Degree Elevation, Temporal Analysis
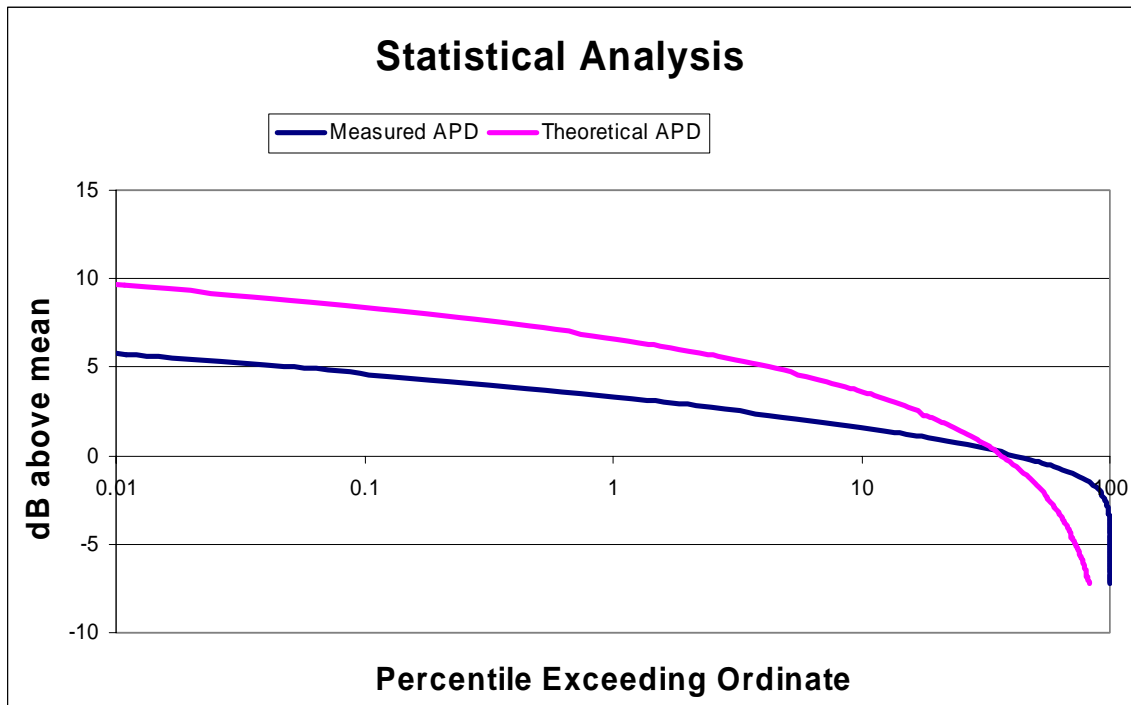
Figure B.43. Blue Ridge Parkway: Thirty Degree Elevation, Statistical Analysis
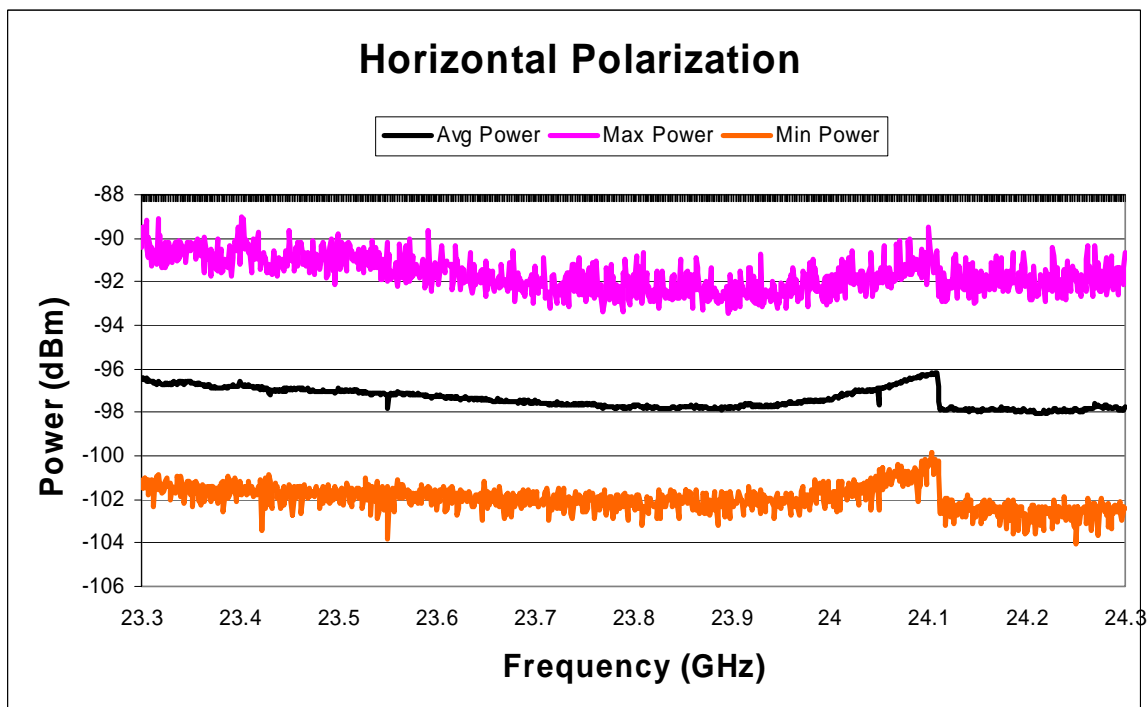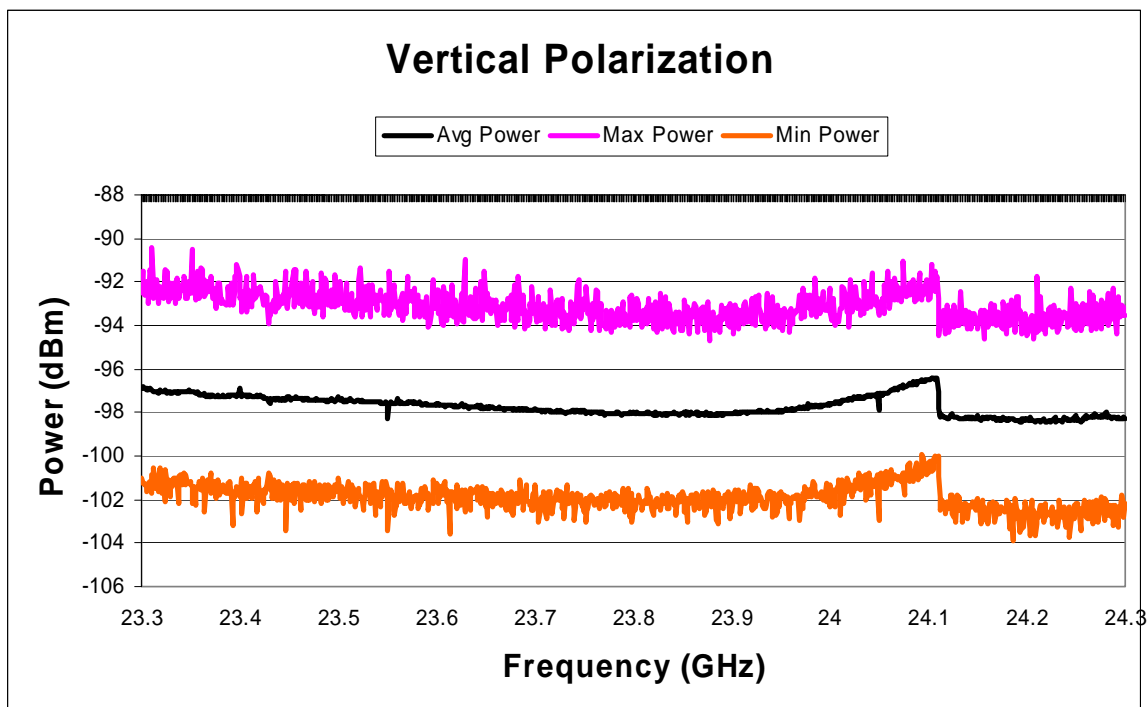
Figure B.44. Blue Ridge Parkway: Sixty Degree Elevation, Spectral Analysis

169
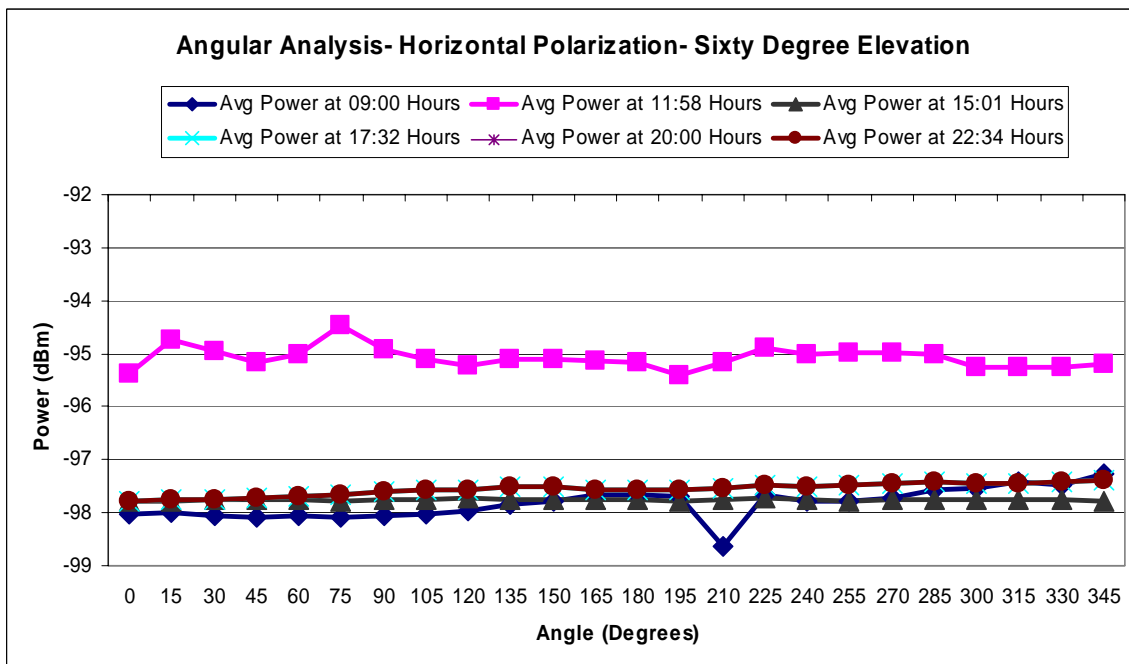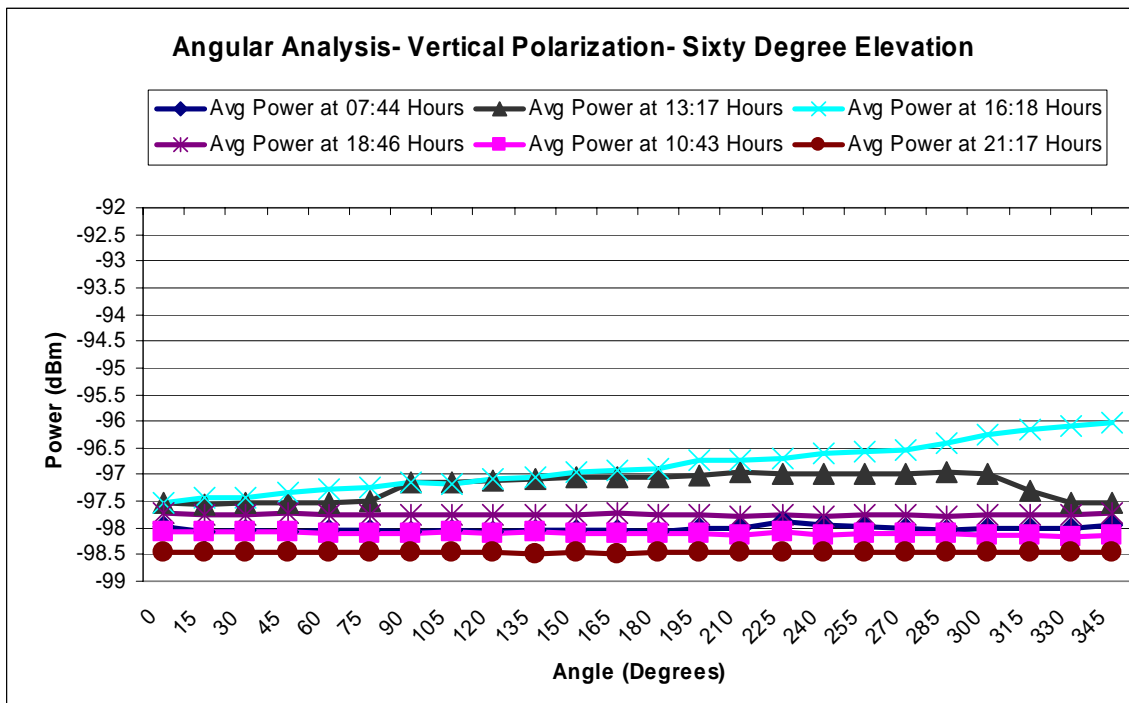
Figure B.45. Blue Ridge Parkway: Sixty Degree Elevation, Angular Analysis
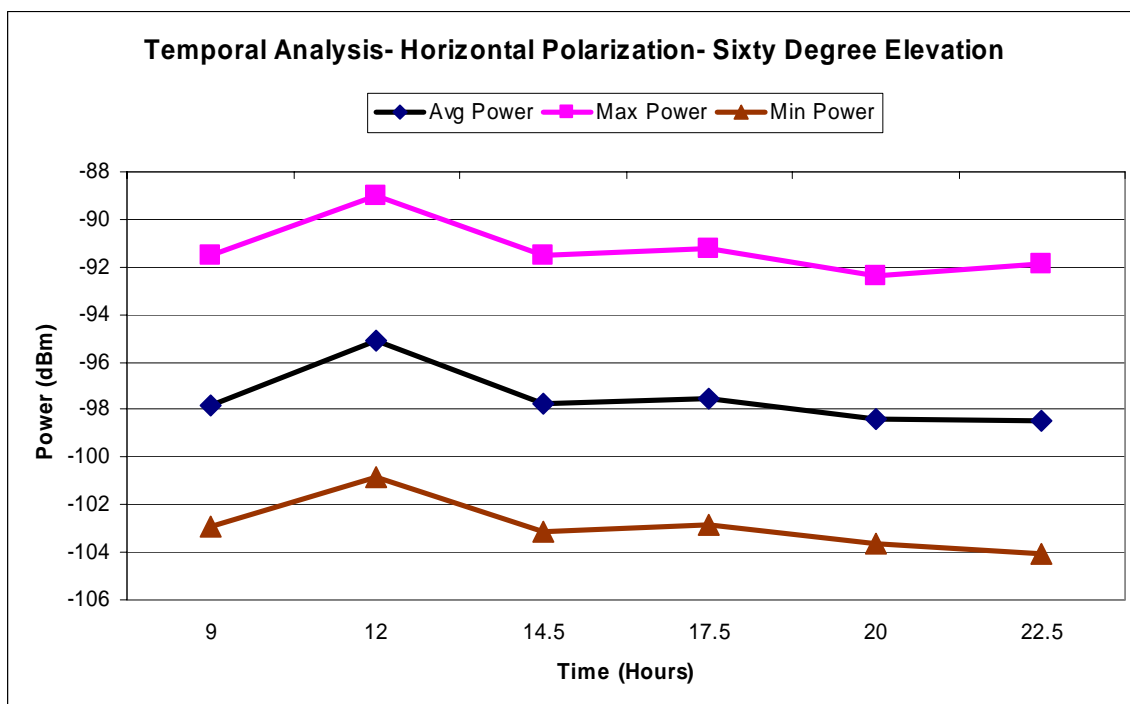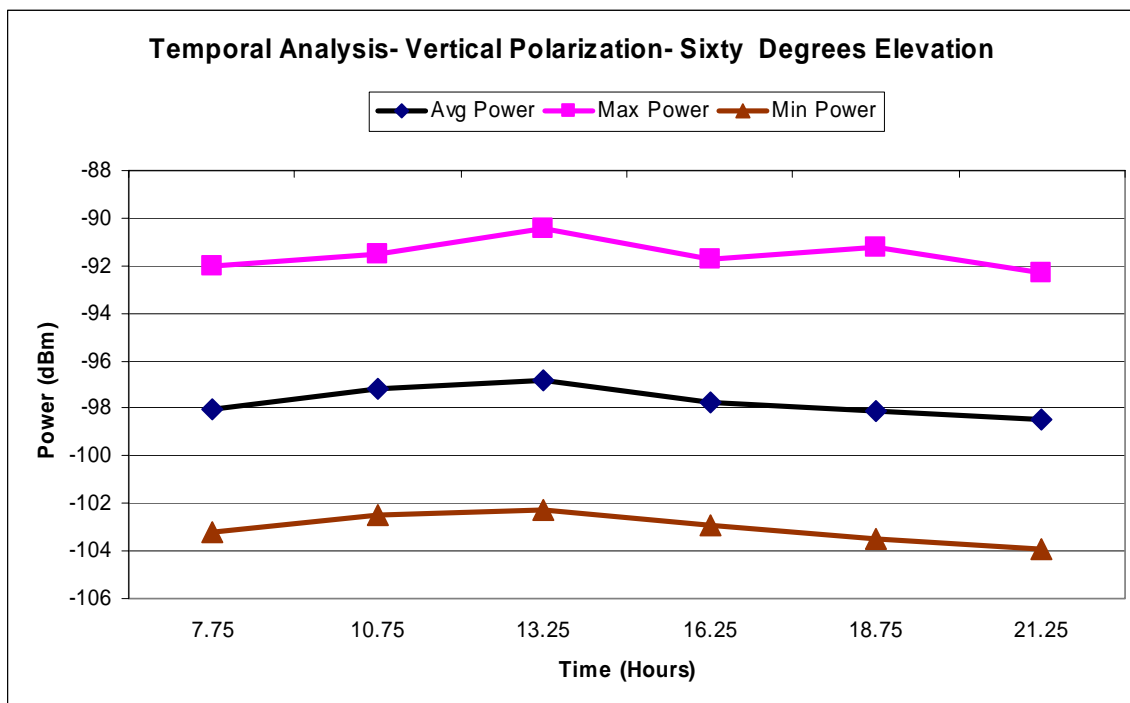
Figure B.46. Blue Ridge Parkway: Sixty Degree Elevation, Temporal Analysis

171
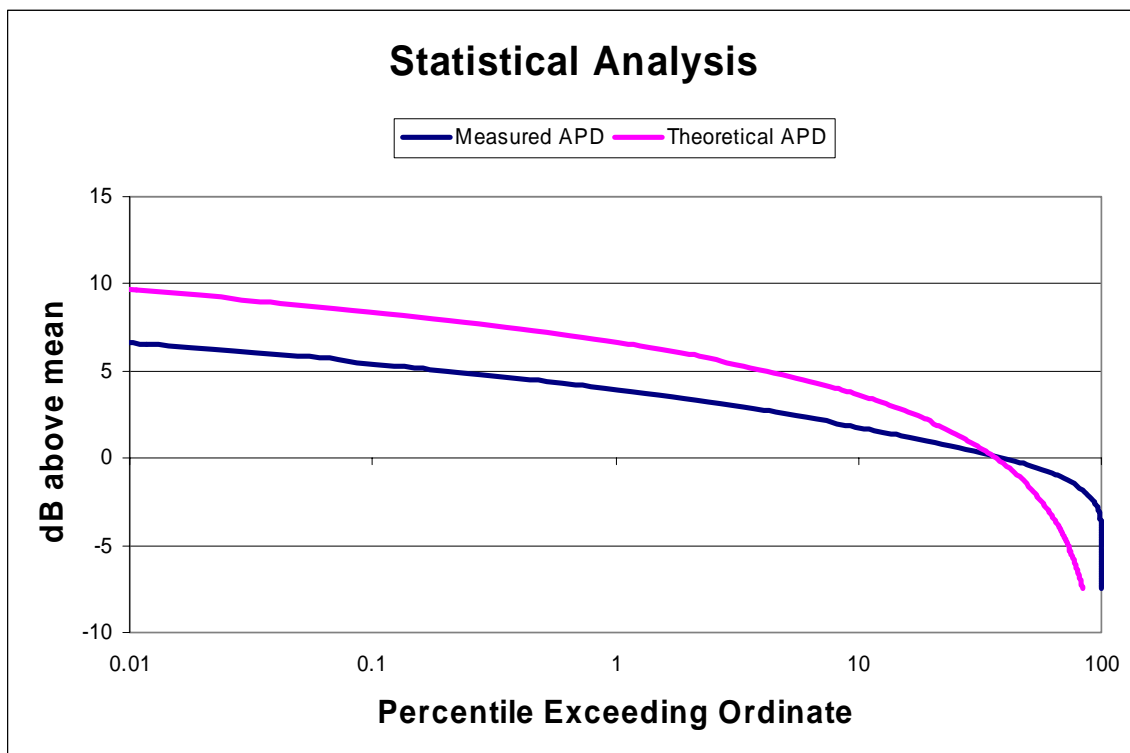
Figure B.47. Blue Ridge Parkway: Sixty Degree Elevation, Statistical Analysis
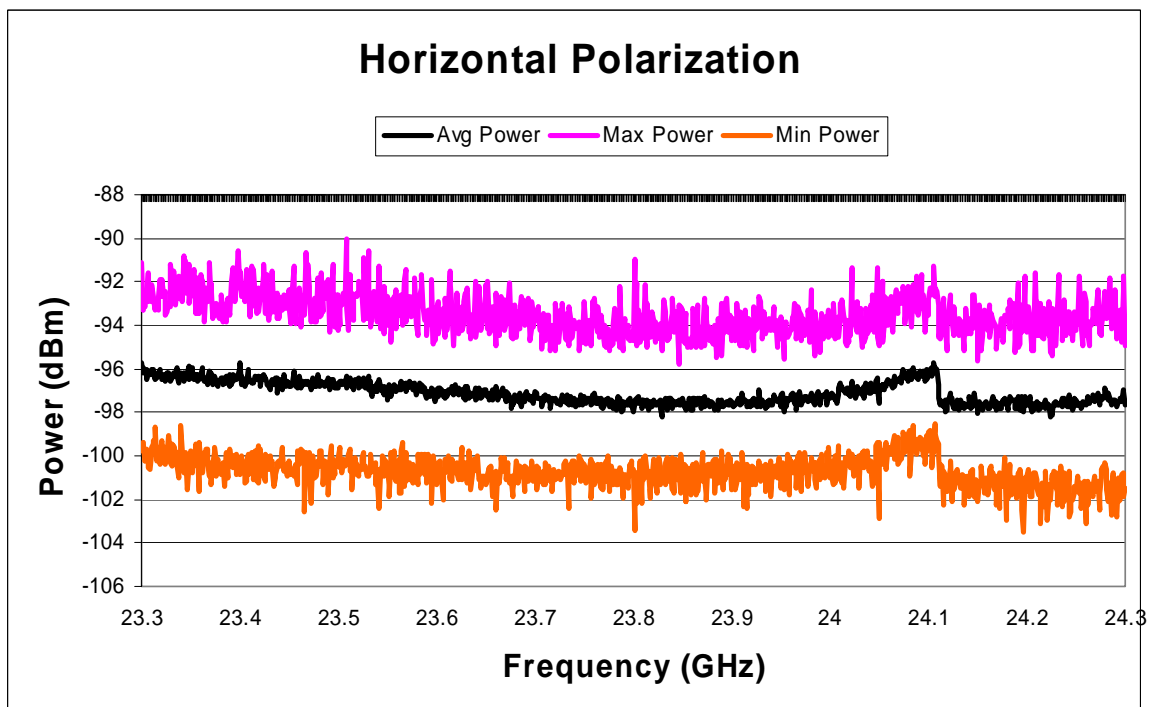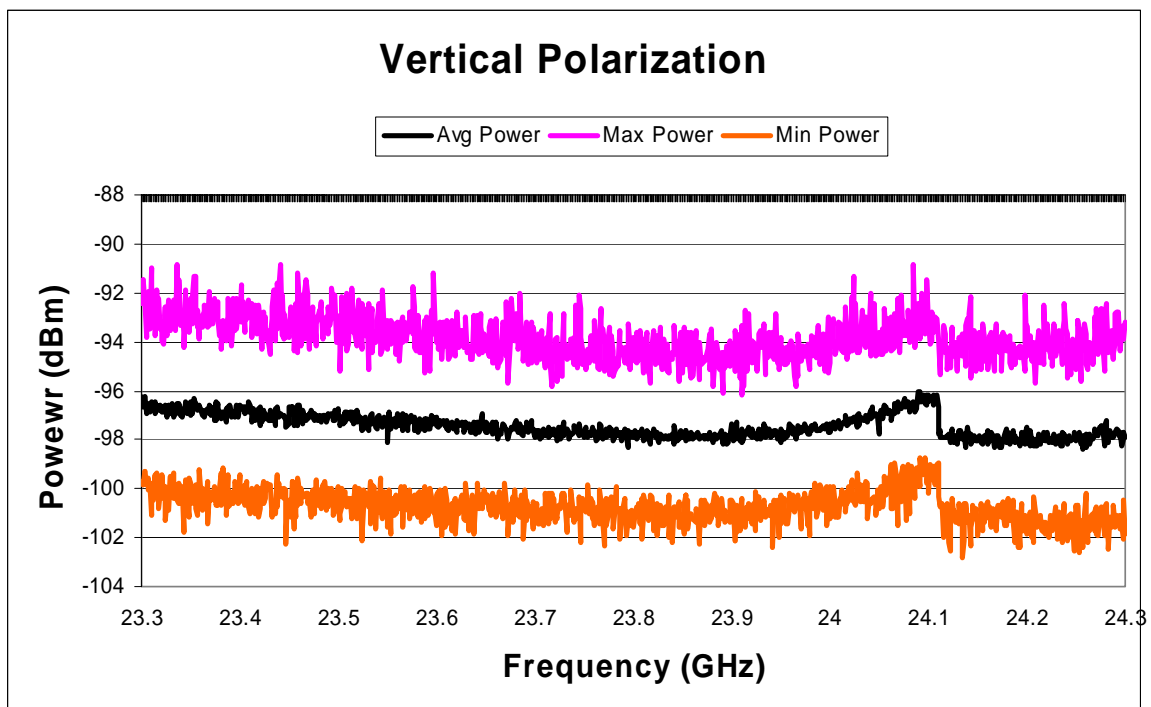
Figure B.48. Blue Ridge Parkway: Ninety Degree Elevation, Spectral Analysis

Temporal Analysis- Vertical Polarization-Ninety Degree Elevation

Temporal Analysis- Horizontal Polarization-Ninety Degree Elevation
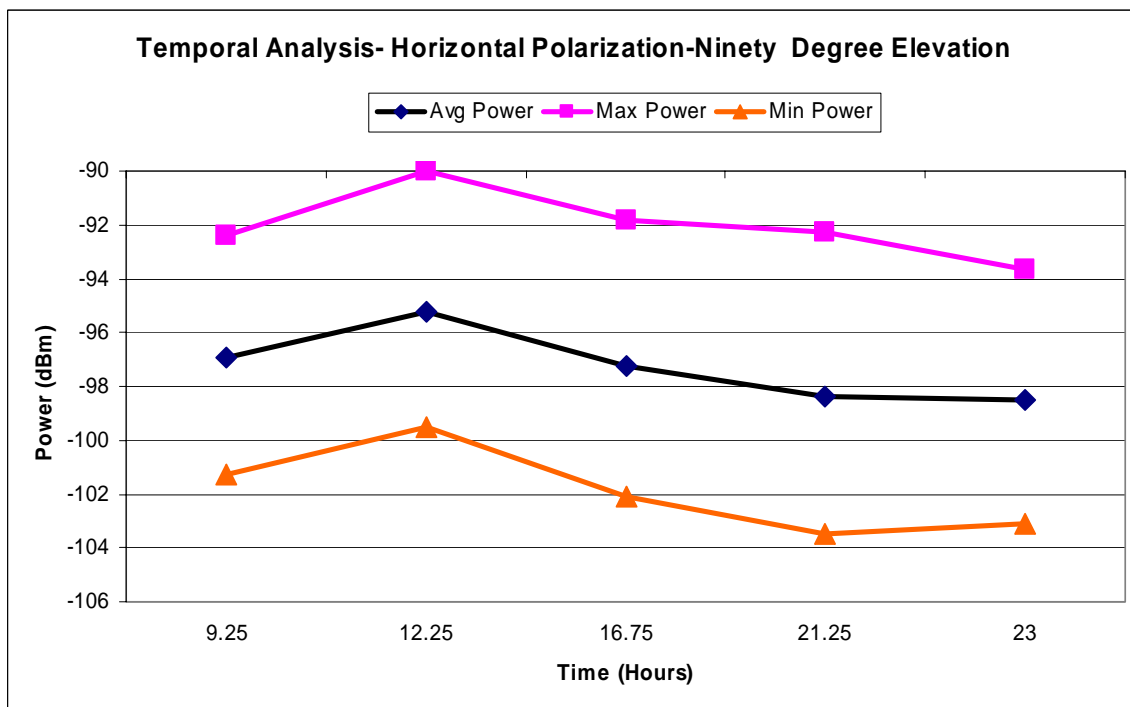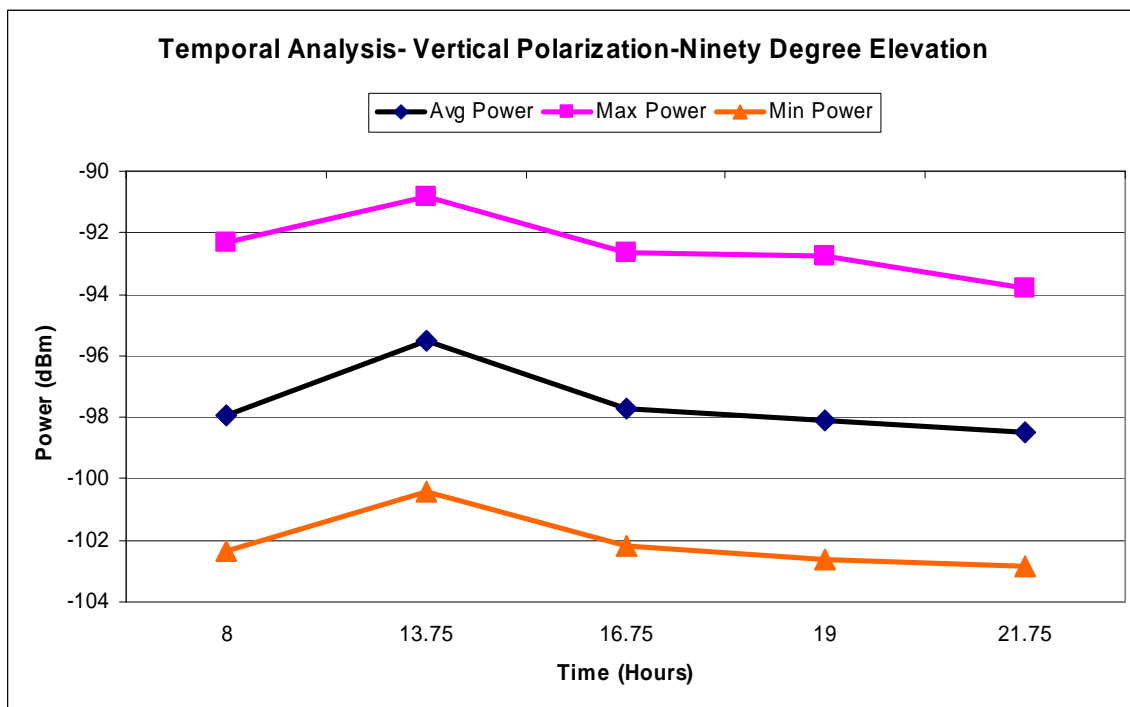
Figure B.49. Blue Ridge Parkway: Ninety Degree Elevation. Temporal Analysis.
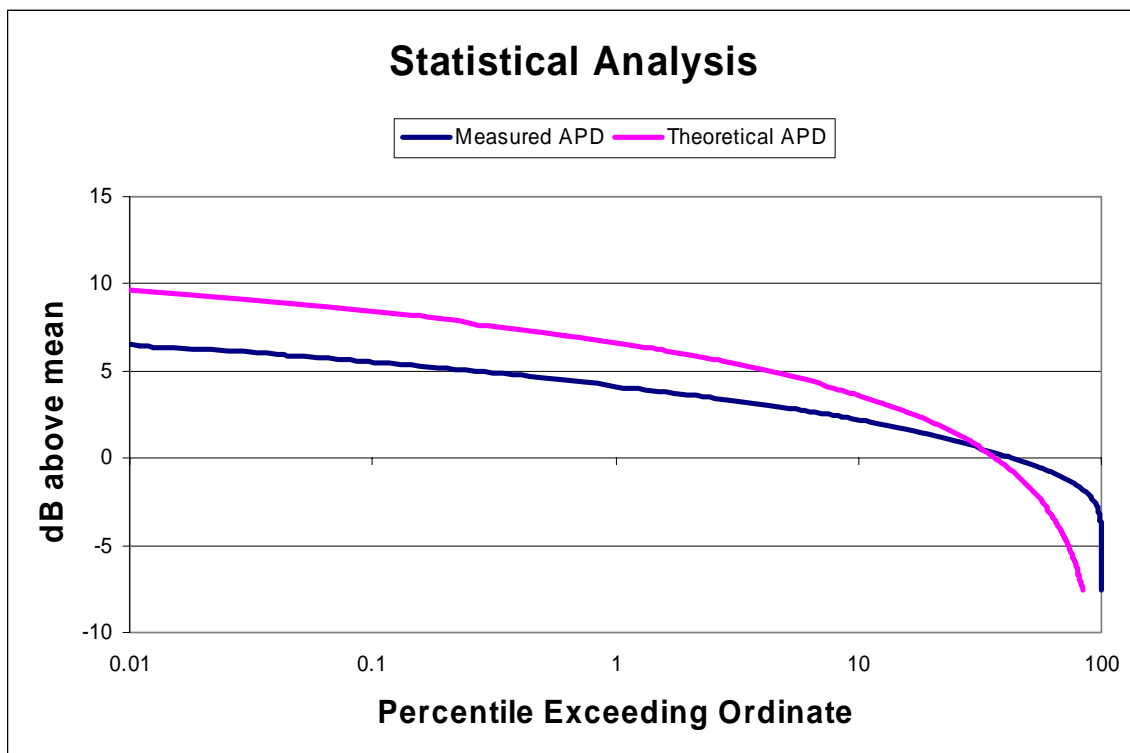
Figure B.50. Blue Ridge Parkway: Ninety Degree Elevation, Statistical Analysis

(This page was left intentionally blank)

Appendix B.4: Hartsfield-Jackson Airport, Atlanta, Georgia (Site 4)

Date: 9/24/03
Map of Location: See Figure B.51
Noteworthy Results:

- Spectral trends: Uniform in frequency within 2 dB with the exception of spectral peak at 23.38 GHz occurring in the direction of the control tower antenna bed measured at 3 separate times during the morning (Fig. B.54). Between 24.05 and 24.1 GHz, there is a spectral artifact. It has been verified experimentally that this artifact was generated by the input attenuation in the spectrum analyzer, not the ambient noise floor. See Figures B.52, B.57, B.61, and B.65.
- Angular trends: Uniform in angle within 2 dB. See Figures B.53, B.54, B.58, and B.62,
- Temporal trends: Measurement ended at 12:30 P.M.; temporal peak occurs at 7 a.m. See Figures B.55, B.59, and B. 63.
- Pre-measurement gain: 83.8 dB; Post-measurement gain: not measured because of damage to system.
- Figures B.56, B.60, B.64, and B.67 depict a statistical analysis.
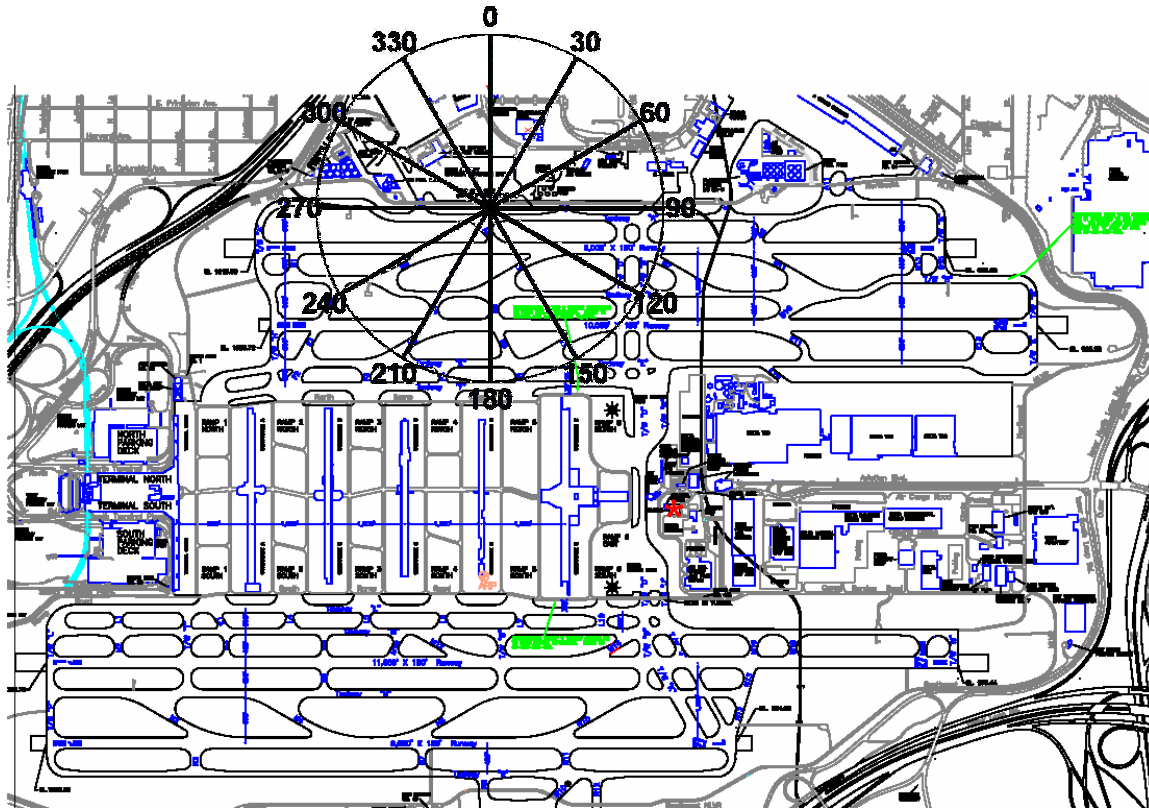
Figure B.51. Map of first Hartsfield-Jackson Airport Measurement Site
(Asterisk denotes control tower from which a manmade signal was detected)
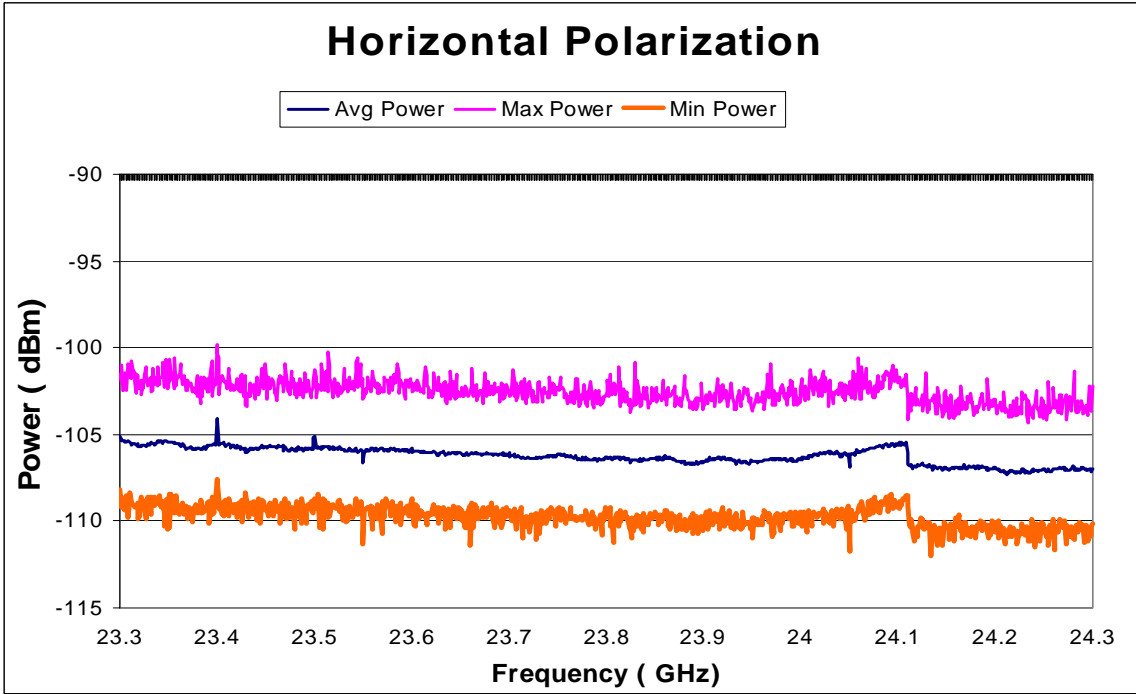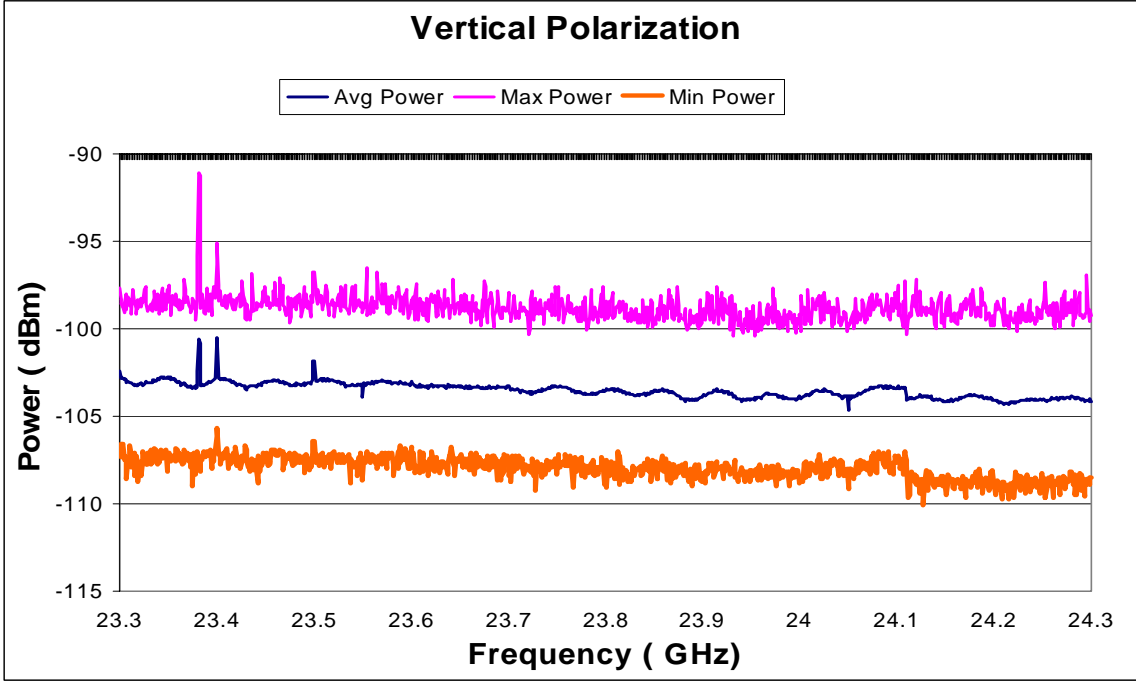
Figure B.52. Hartsfield-Jackson Airport (9/24/03): Zero Degree Elevation, Spectral Analysis
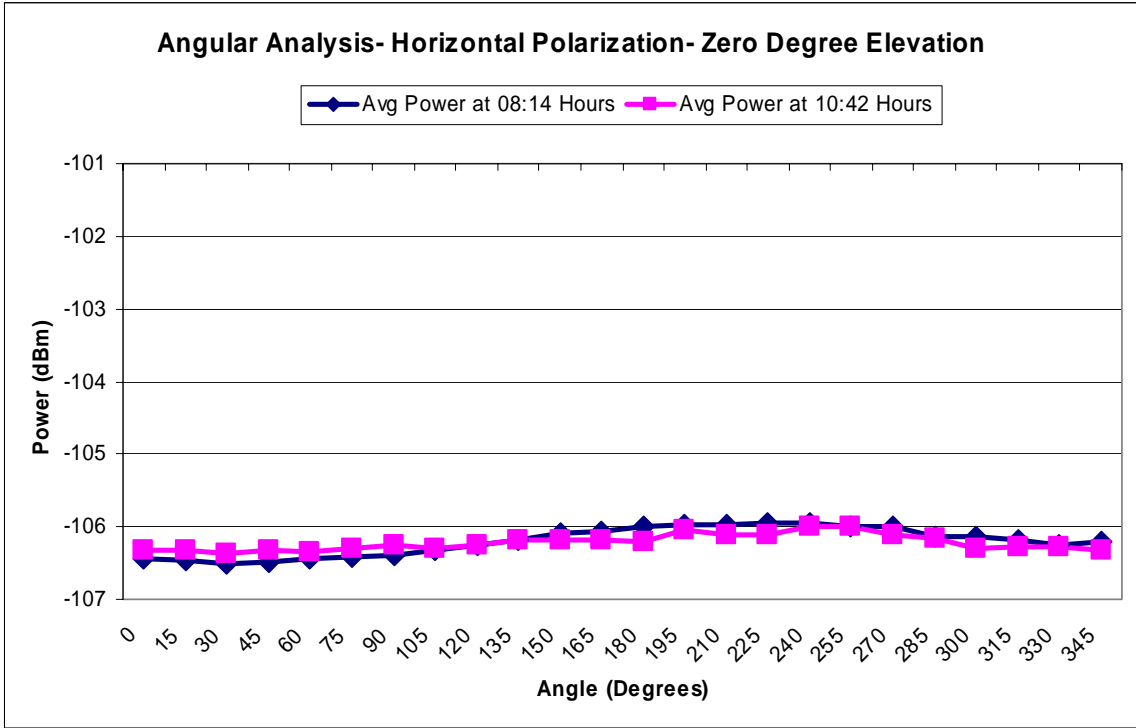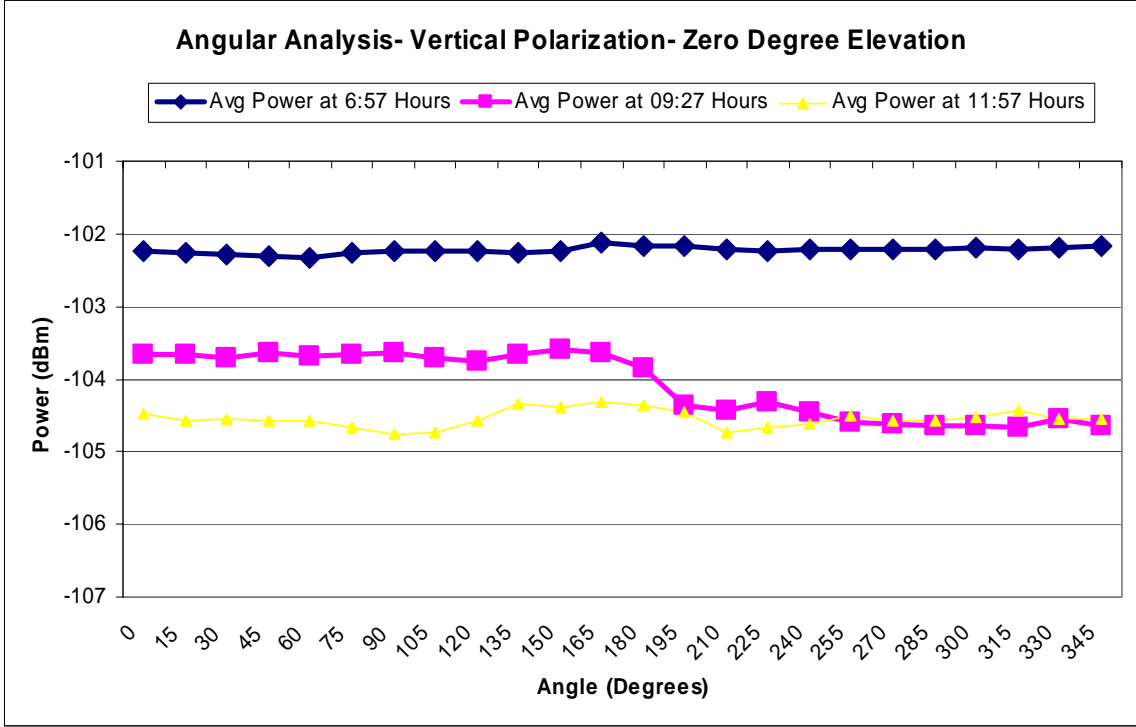
Figure B.53. Hartsfield-Jackson Airport (9/24/03): Zero Degree Elevation, Angular Analysis

179
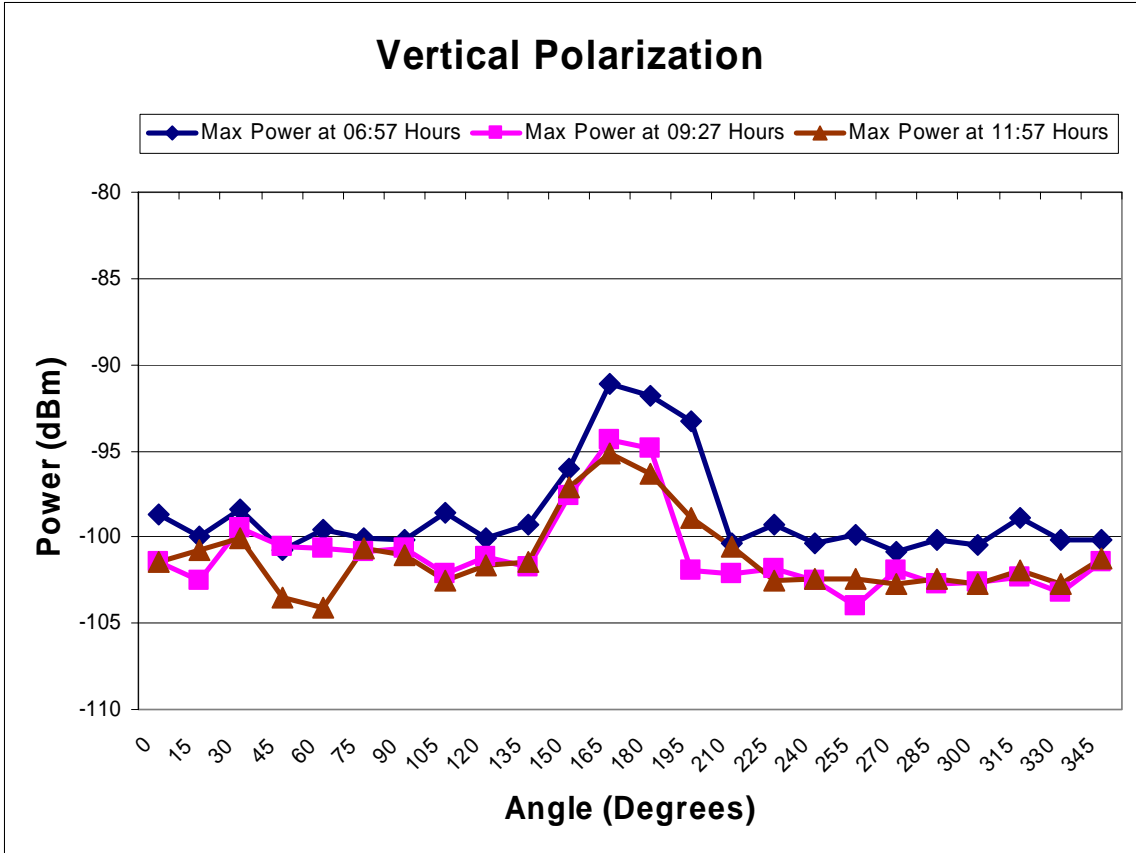
Figure B.54. Hartsfield-Jackson Airport (9/24/03): Zero Degree Elevati,.
Angular Analysis of Peak at 23.38 GHz
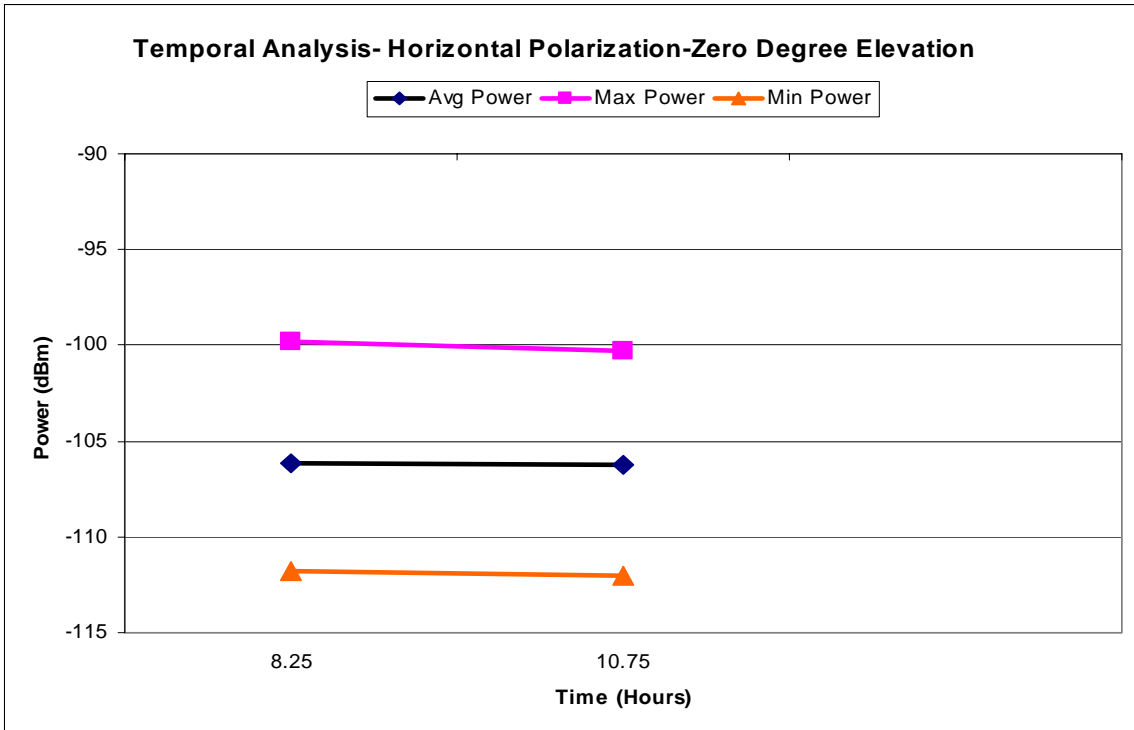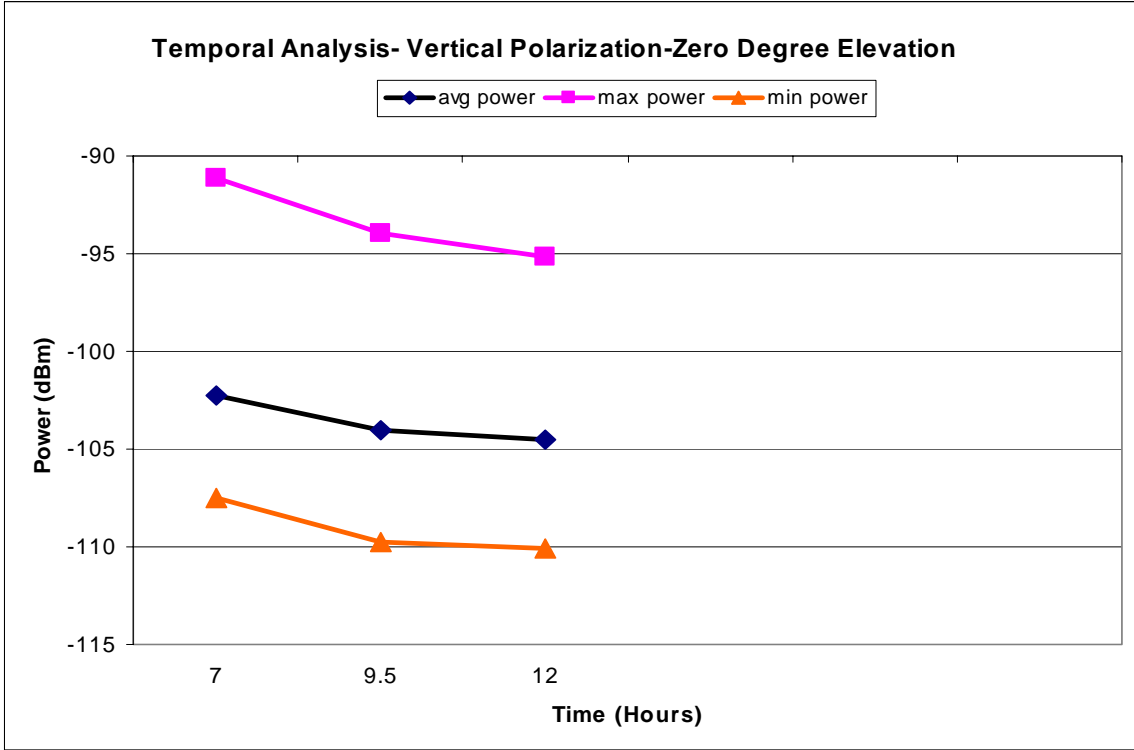
Figure B.55. Hartsfield-Jackson Airport (9/24/03): Zero Degree Elevation, Temporal Analysis
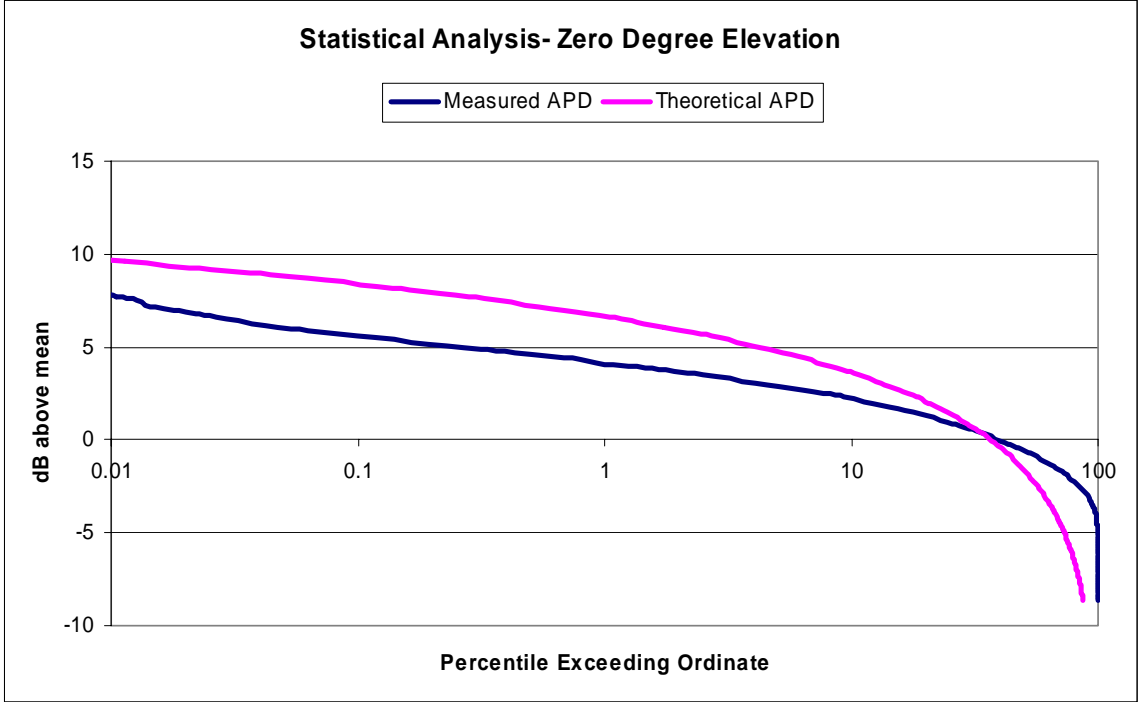
Figure B.56. Hartsfield-Jackson Airport (9/24/03): Zero Degree Elevation, Statistical Analysis
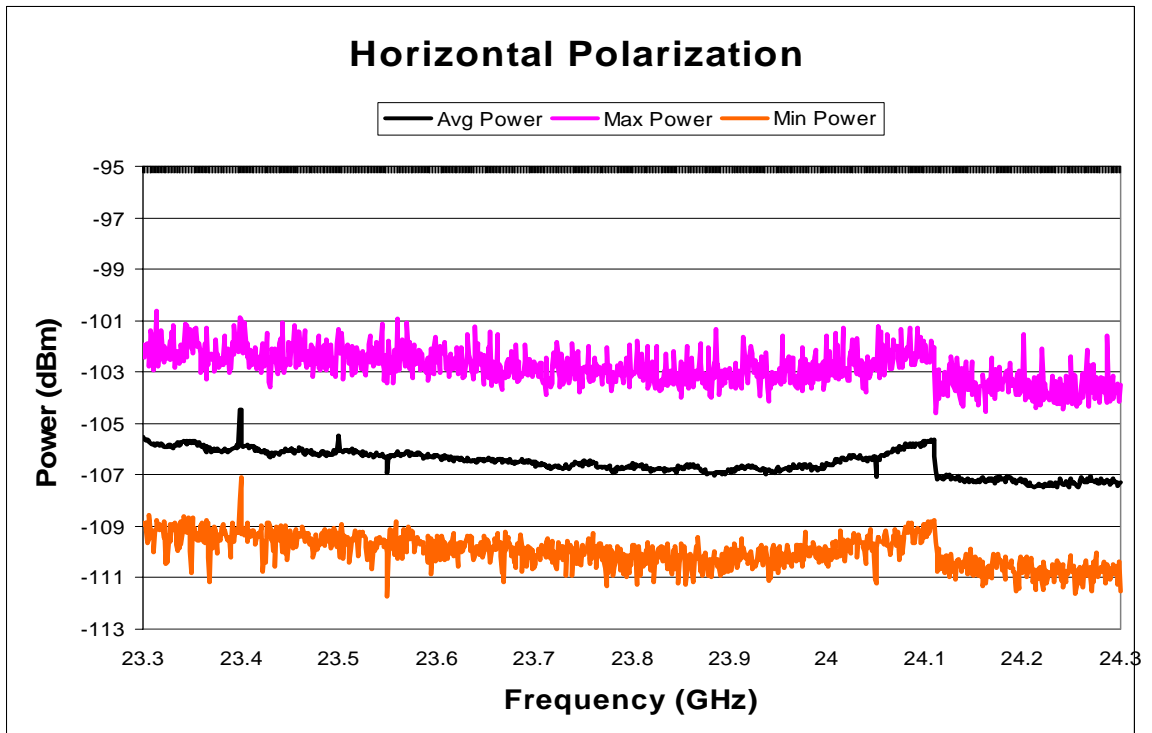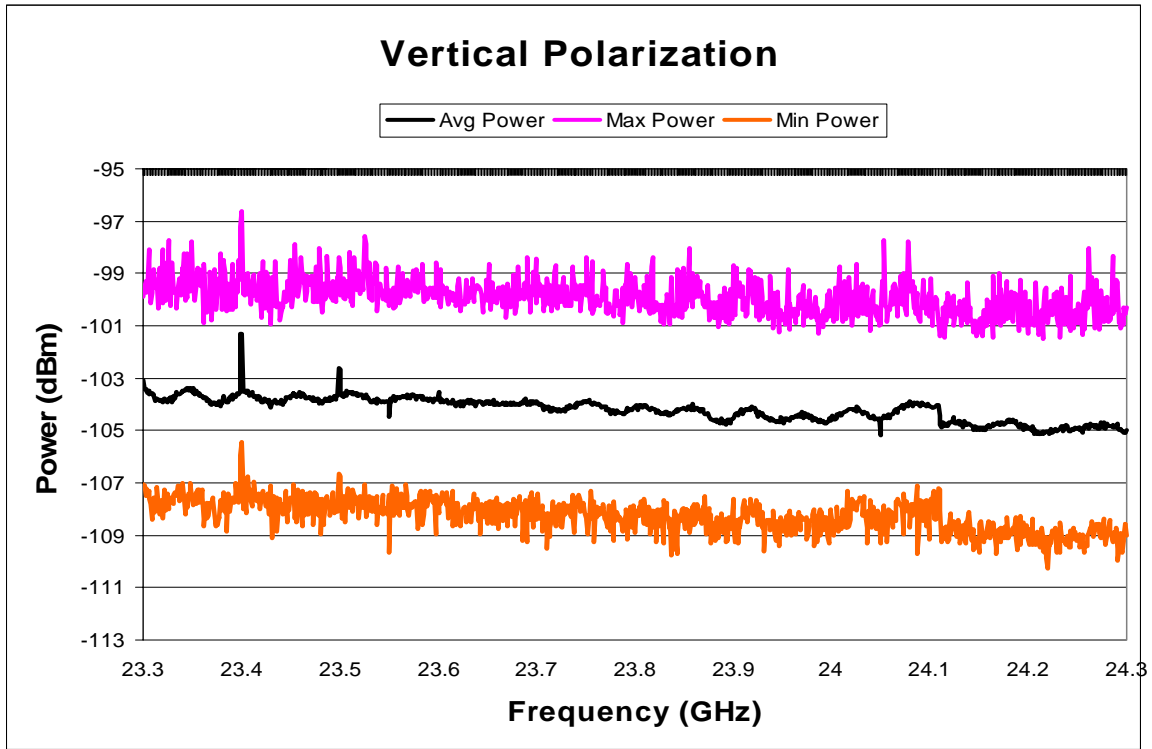
Figure B.57. Hartsfield-Jackson Airport (9/24/03): Thirty Degree Elevation, Spectral Analysis

183
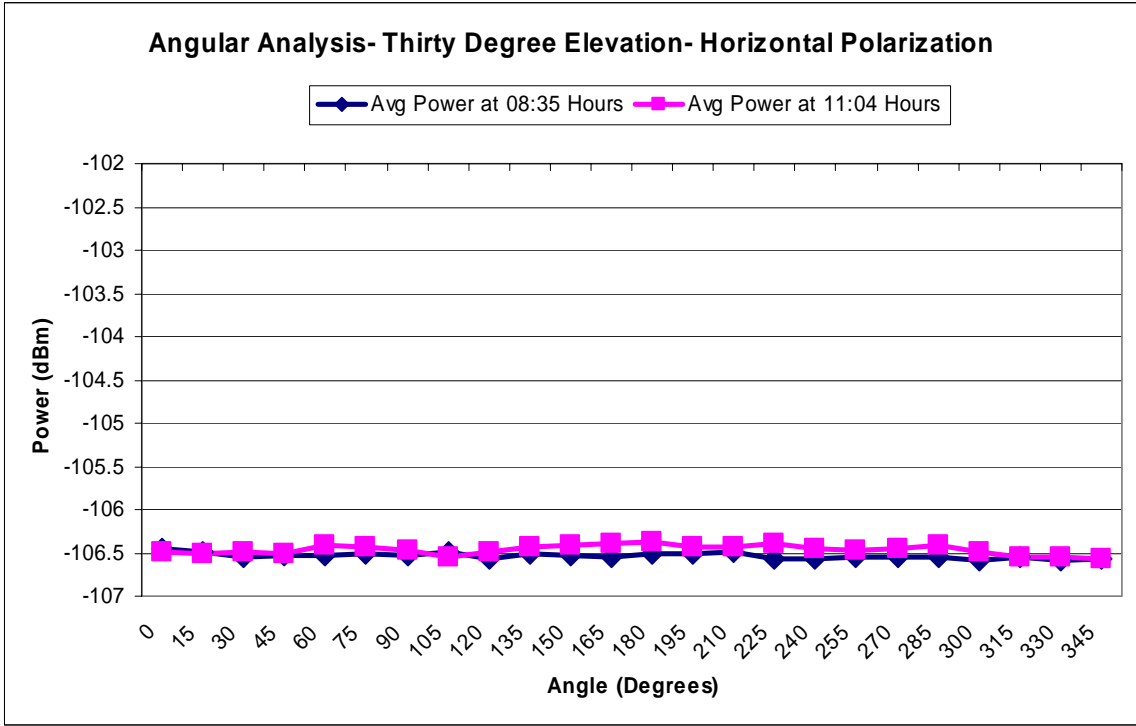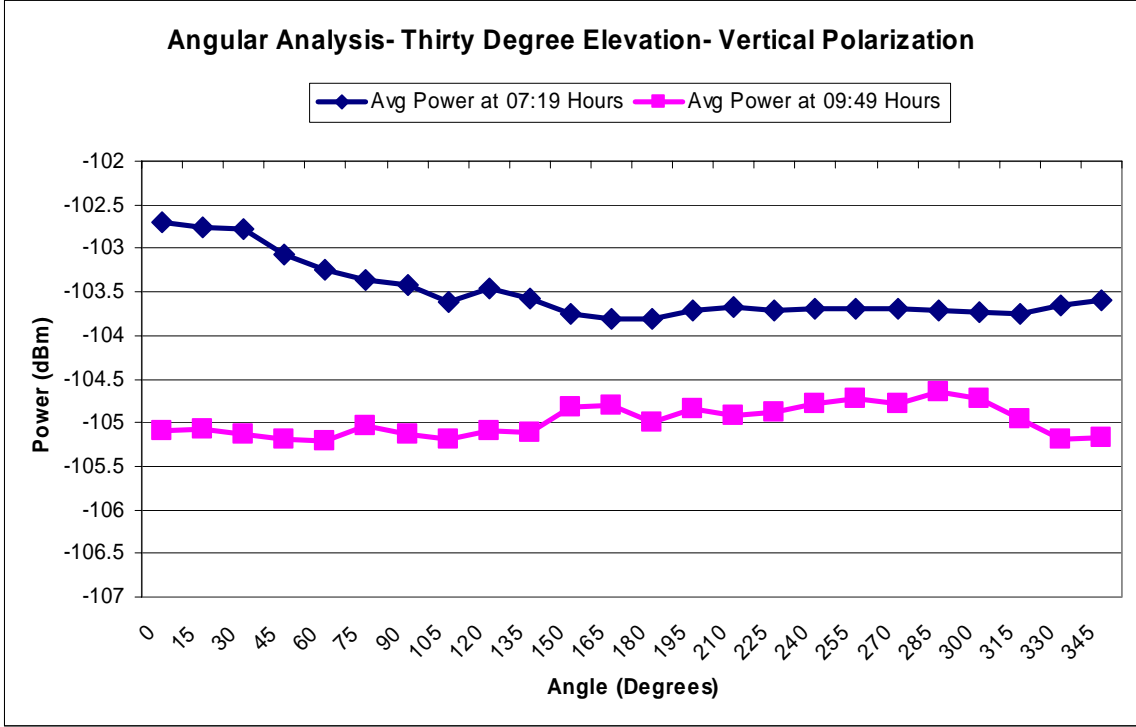
Figure B.58. Hartsfield-Jackson Airport (9/24/03): Thirty Degree Elevation, Angular Analysis
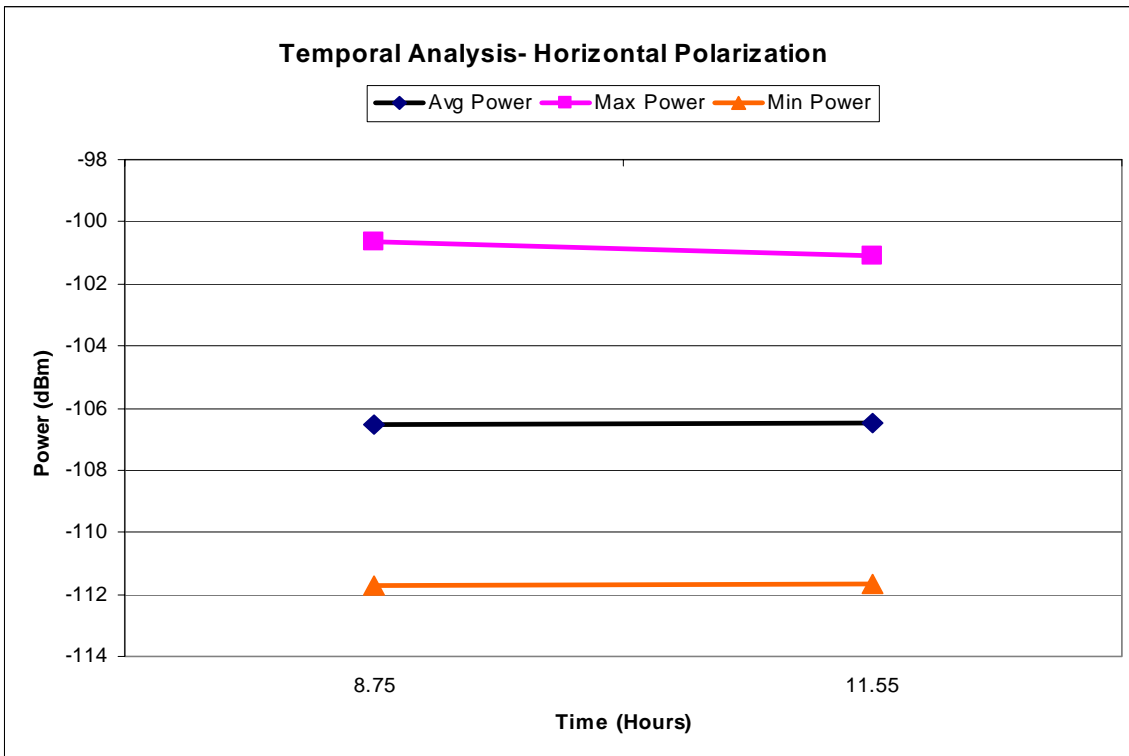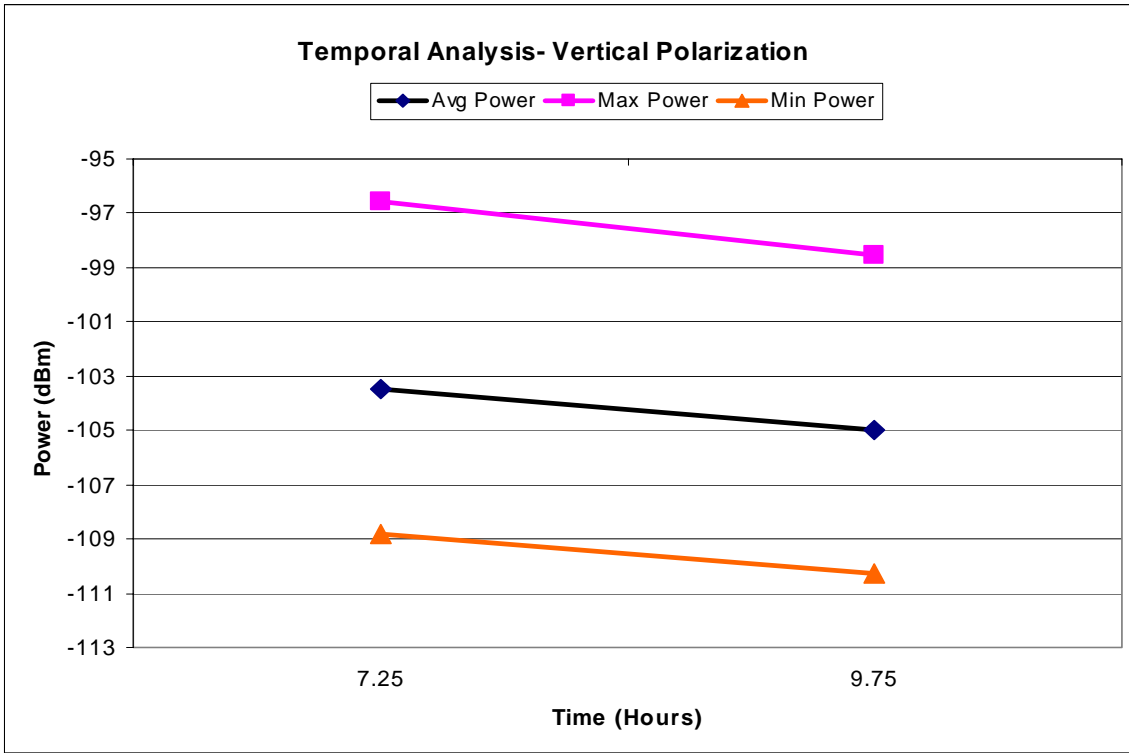
Figure B. 59. Hartsfield-Jackson Airport (9/24/03): Thirty Degree Elevation, Temporal Analysis
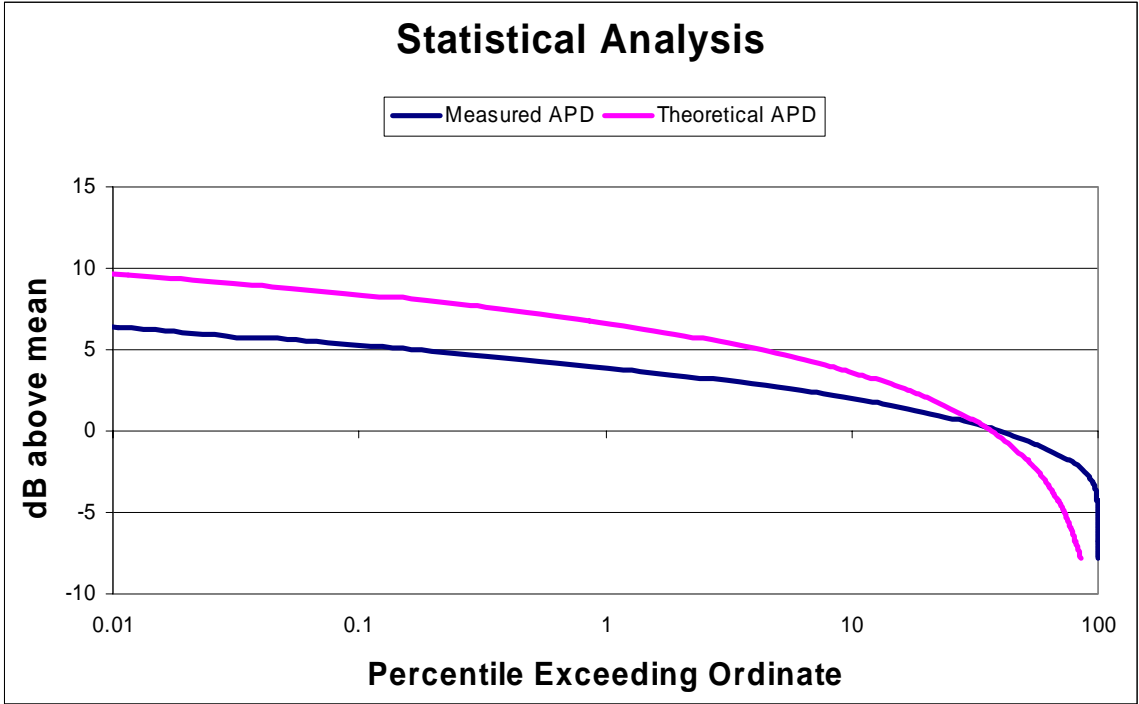
Figure B.60. Hartsfield-Jackson Airport (9/24/03): Thirty Degree Elevation, Statistical Analysis
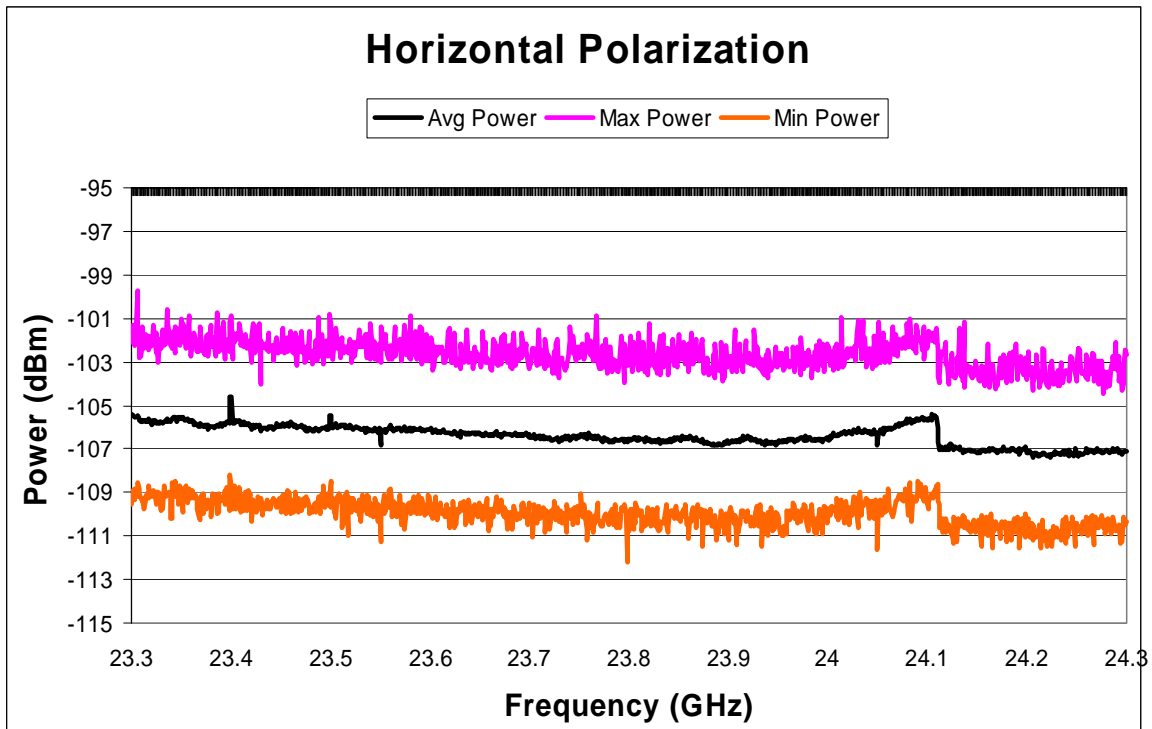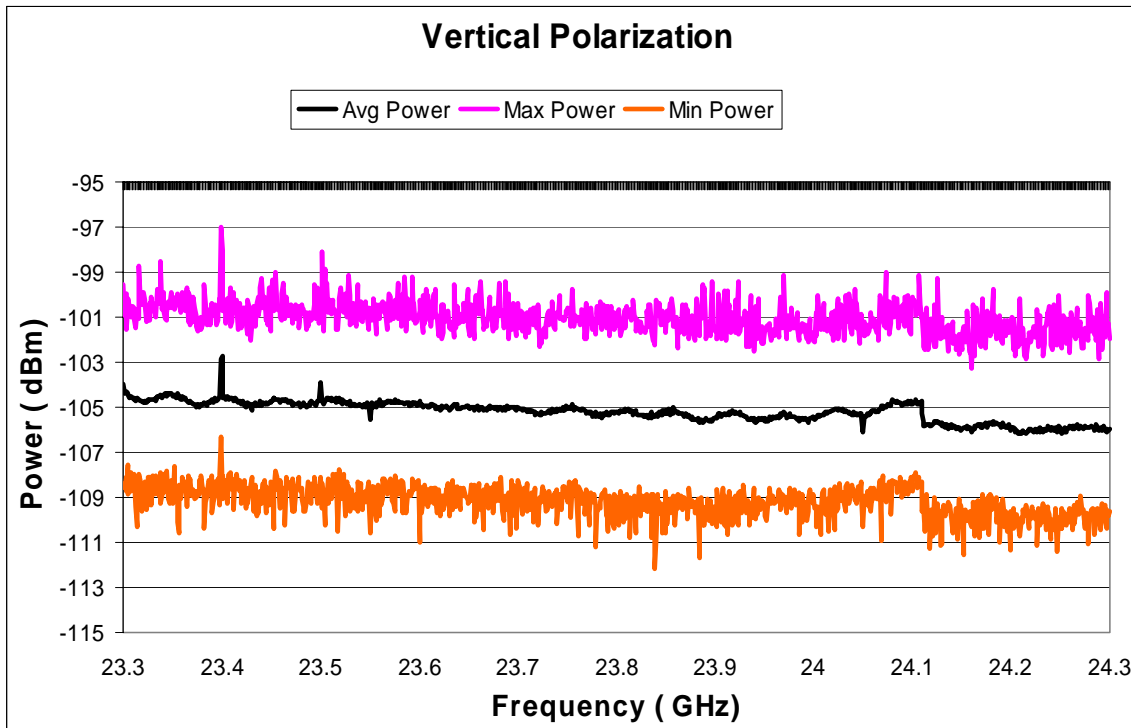
Figure B.61. Hartsfield-Jackson Airport (9/24/03): Sixty Degree Elevation, Spectral Analysis

187

Angular Analysis- Vertical Polarization- Sixty Degree Elevation

Angular Analysis- Horizontal Polarization- Sixty Degree Elevation
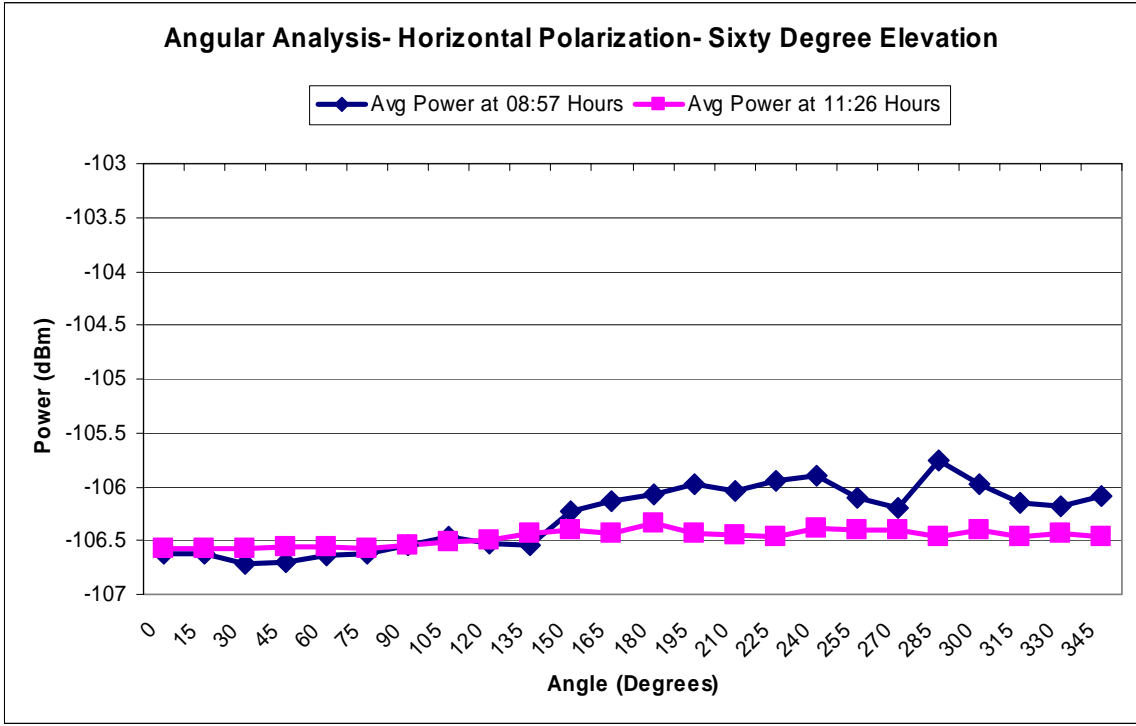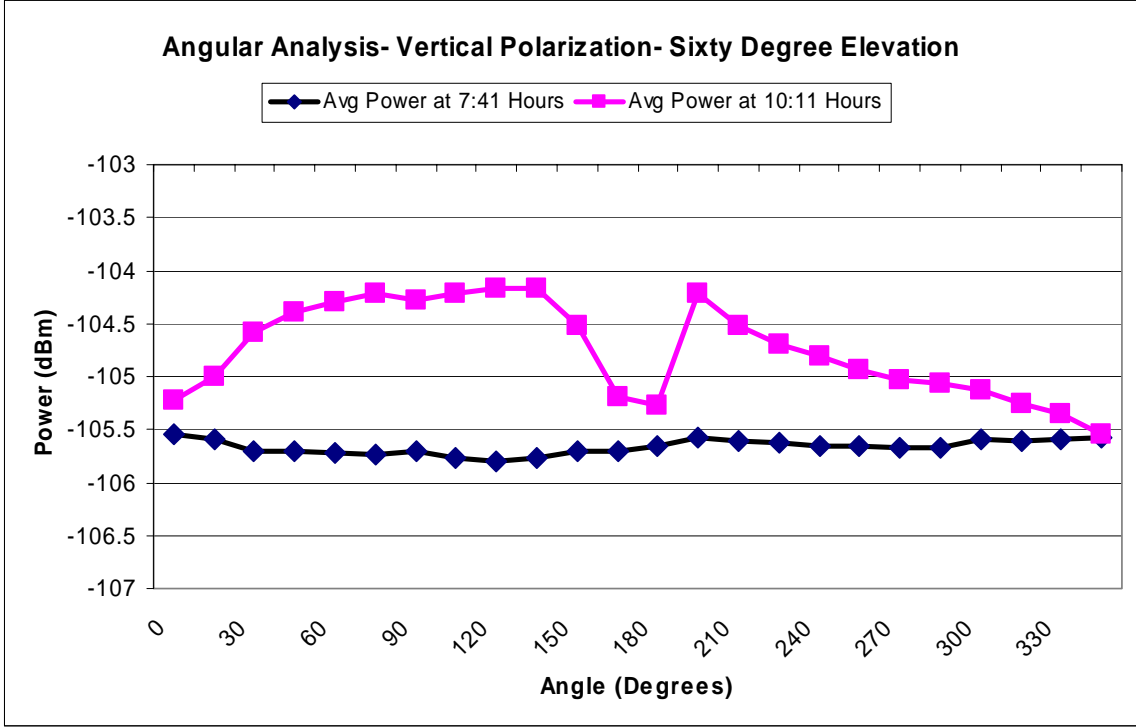
Figure B.62. Hartsfield-Jackson Airport (9/24/03): Sixty Degree Elevation, Angular Analysis

188
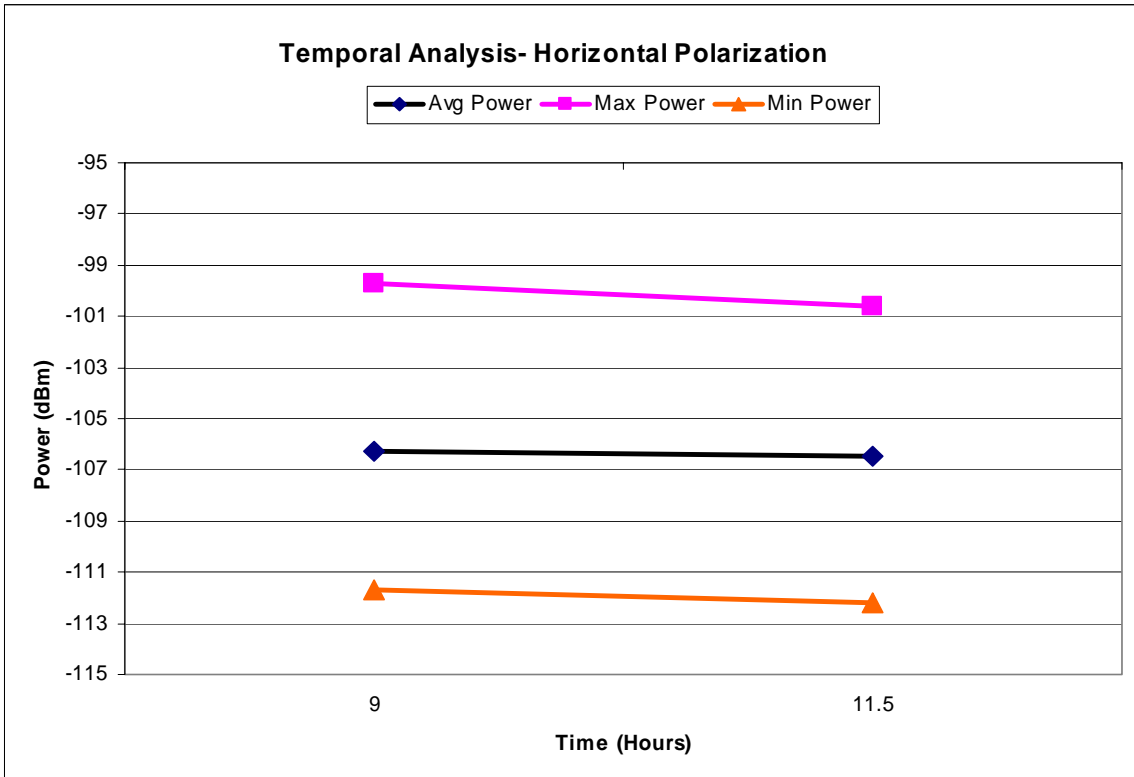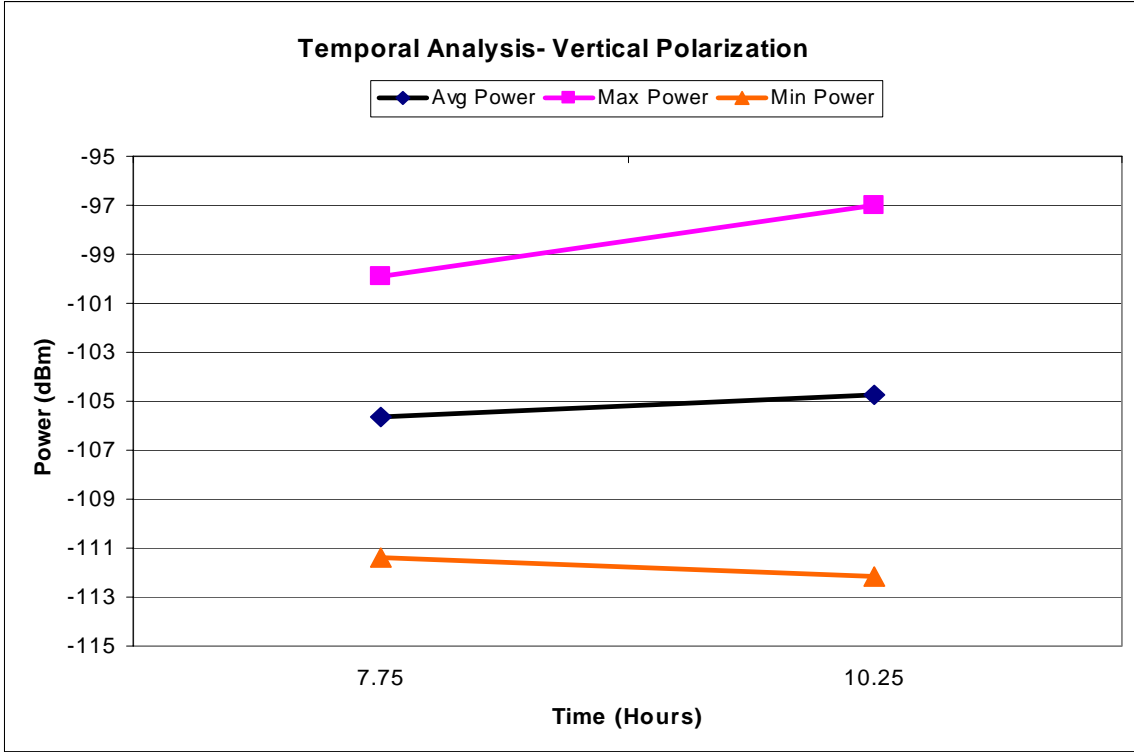
Figure B.63. Hartsfield-Jackson Airport (9/24/03): Sixty Degree Elevation, Temporal Analysis

189
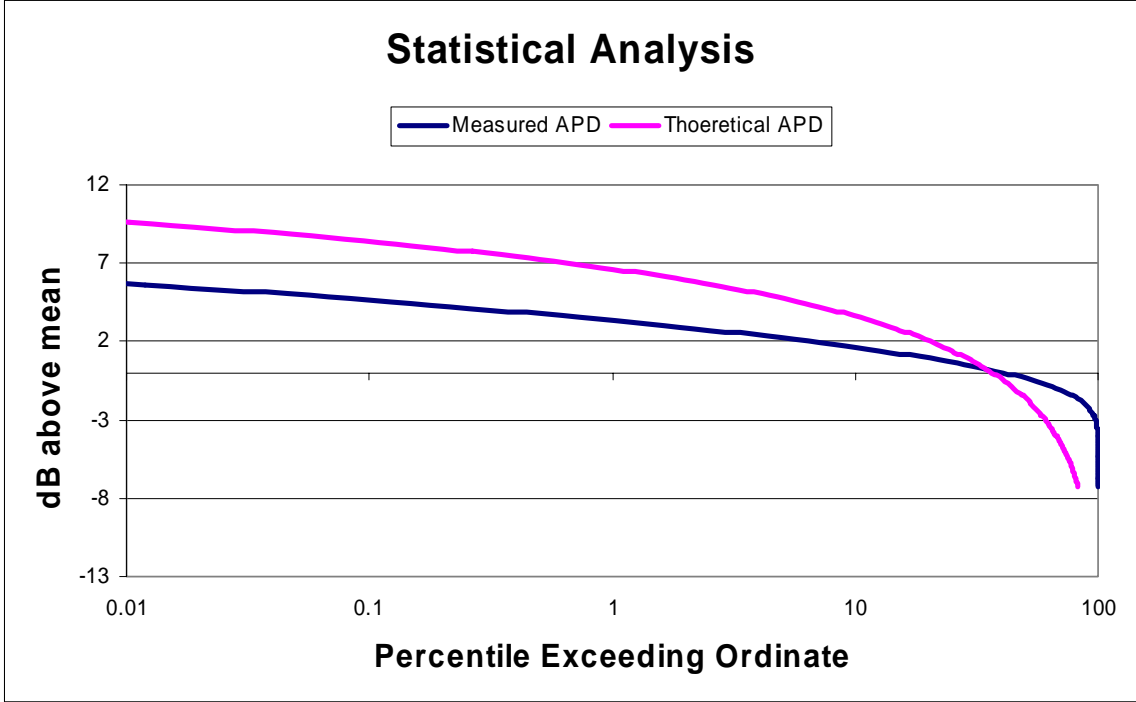
Figure B.64. Hartsfield-Jackson Airport (9/24/03): Sixty Degree Elevation, Statistical Analysis
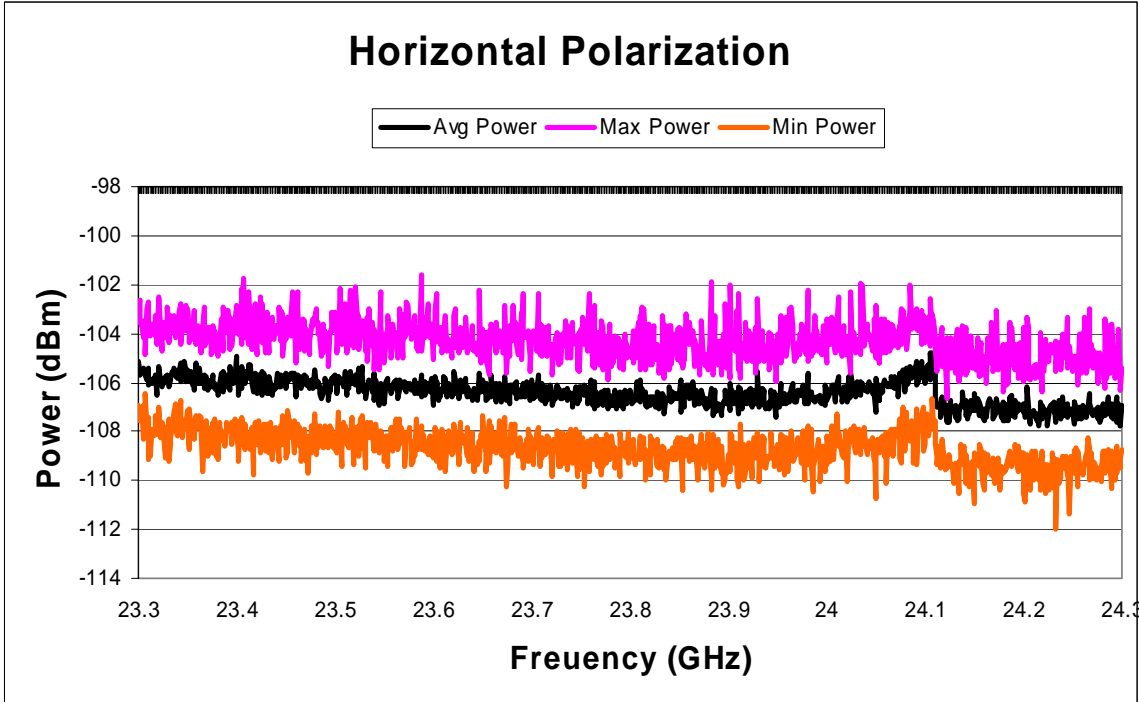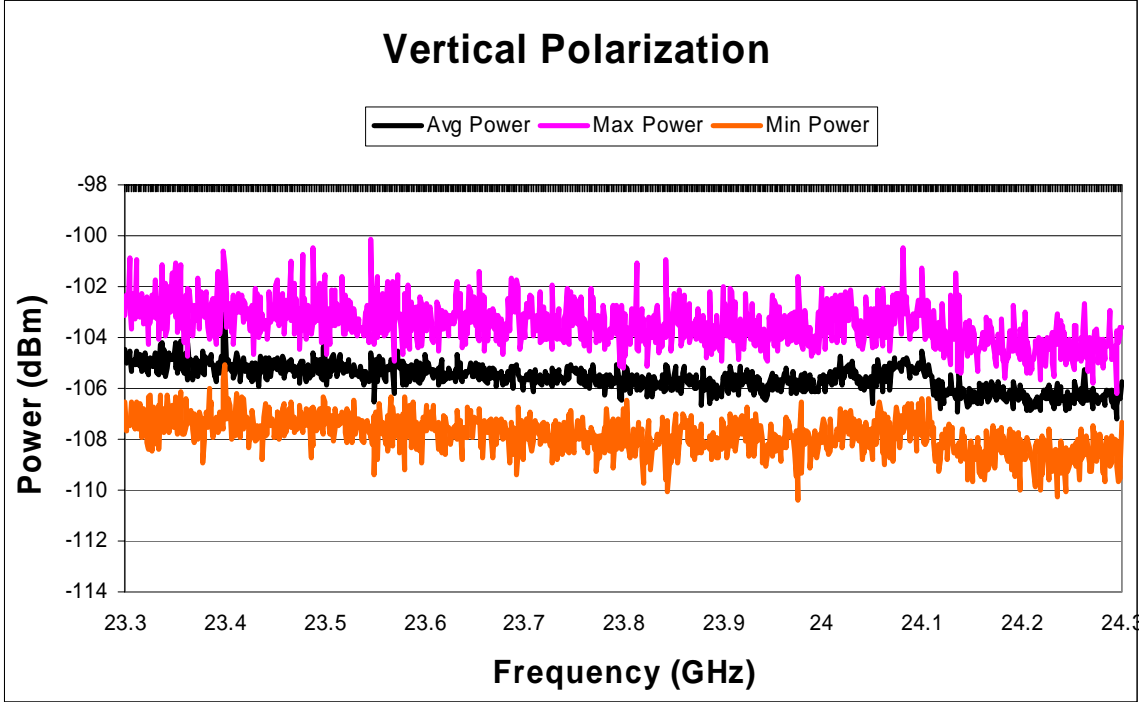
Figure B.65. Hartsfield-Jackson Airport (9/24/03): Ninety Degree Elevation, Spectral Analysis
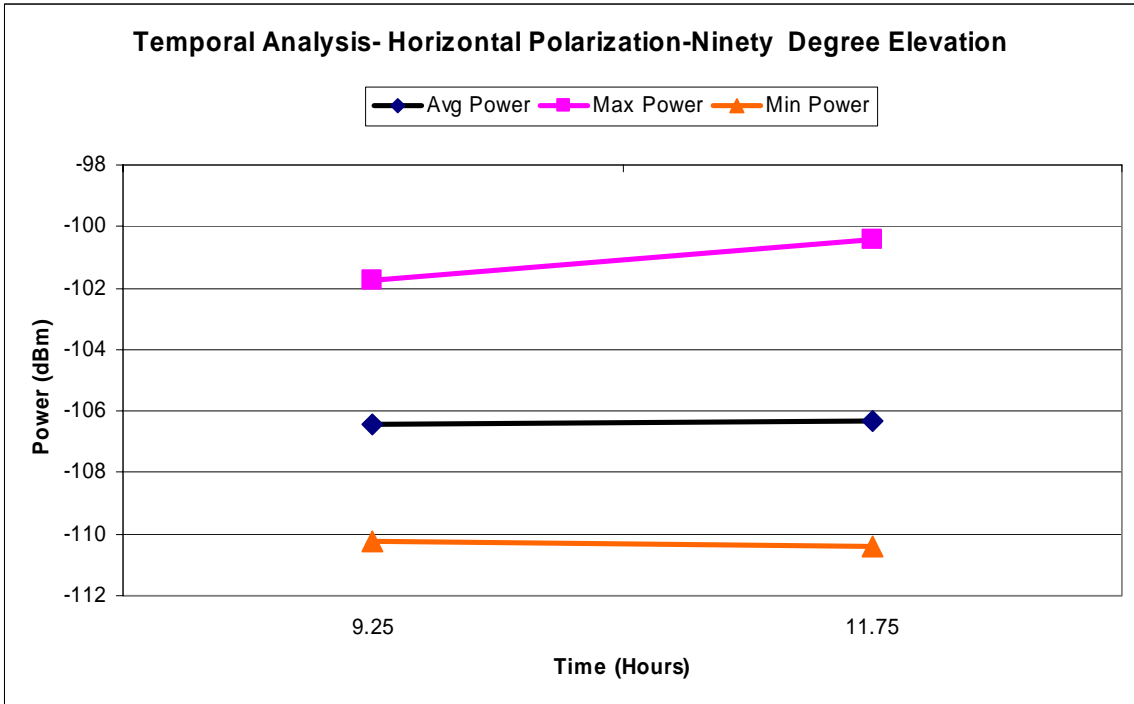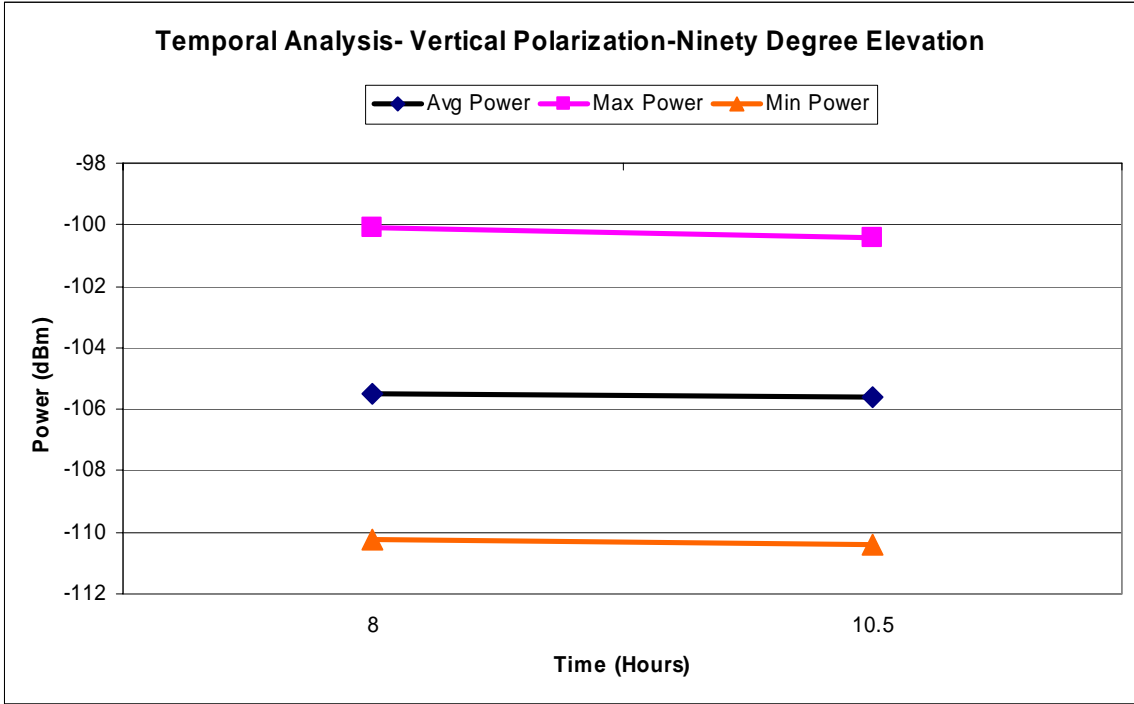
Figure B.66. Hartsfield-Jackson Airport (9/24/03): Ninety Degree Elevation, Temporal Analysis
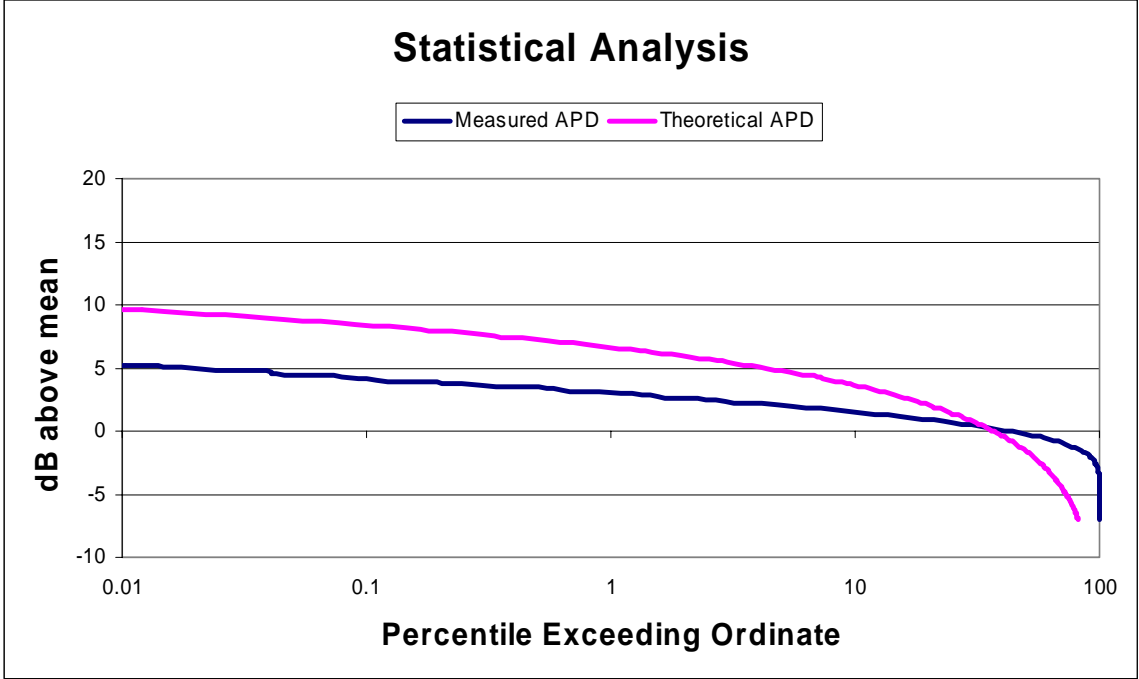
Figure B.67. Hartsfield-Jackson Airport (9/24/03): Ninety Degree Elevation, Statistical Analysis

(This page was left intentionally blank)

Appendix B.5: Hartsfield-Jackson Airport, Atlanta, Georgia (Site 4 Revisited)

Date: 10/22/03
Map of Location: See Figure B.68
Noteworthy Results

- Because of the shortened day due to the cable break, this site was repeated. Operating protocol (accompaniment by a paid escort) for measurement on the Airport grounds forced us to leave the system unattended for a period of an hour at noon. This unmonitored period contributed to the cable failure which might have been avoided if an attendant had been present. Consequently, this second set of measurements was performed from the roof of the Renaissance Hotel immediately outside airport limits near the original site.
- Spectral trends: Uniform in frequency within 2 dB. See Figures B. 69, B.72, B.75, and B. 78.
- Angular trends: Uniform in angle within 2 dB, with the exception of lower power levels which occur in the direction of a building in close proximity of the measurement. See Figures B.70, B.73, and B.76.
- Temporal trends: Uniform in time within 2 dB   See Figures B.71, B.74, B.77, and B.79.
- Pre-measurement calibrated gain: 43.1 dB: Post-measurement gain: 42.9 dB.
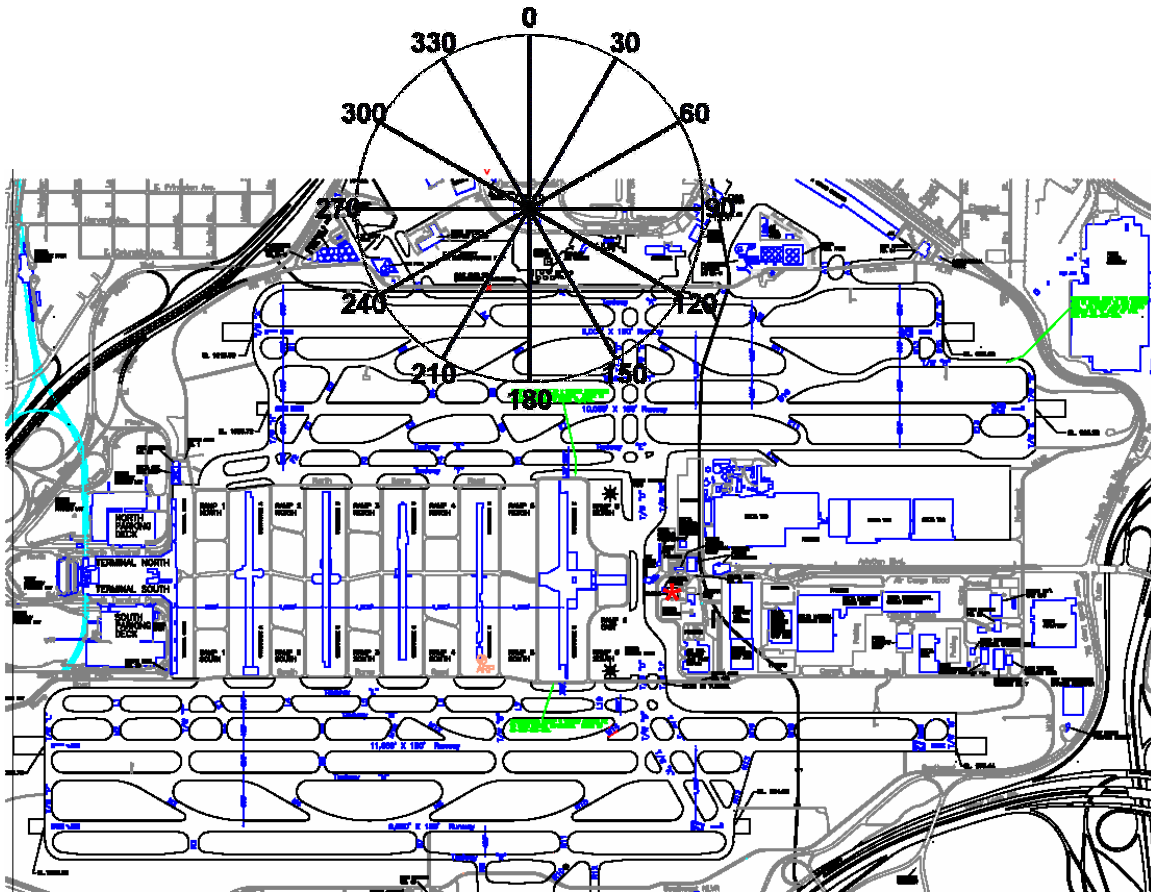
Figure B.68 Map of second Hartsfield-Jackson Airport
(Asterisk denotes control tower)
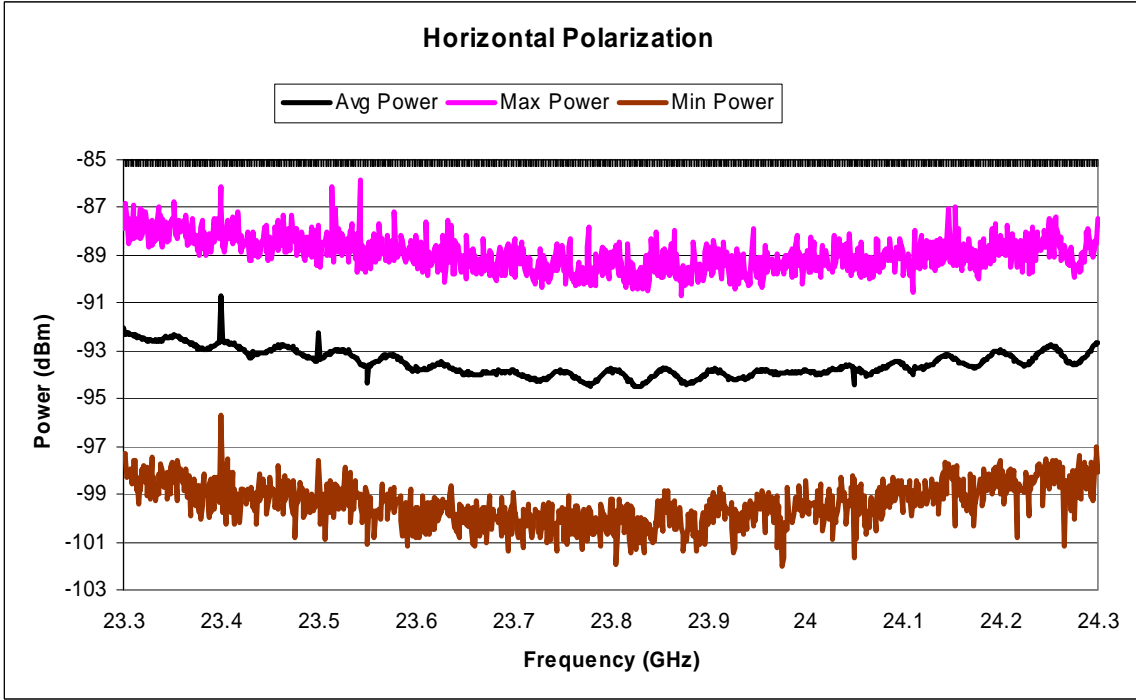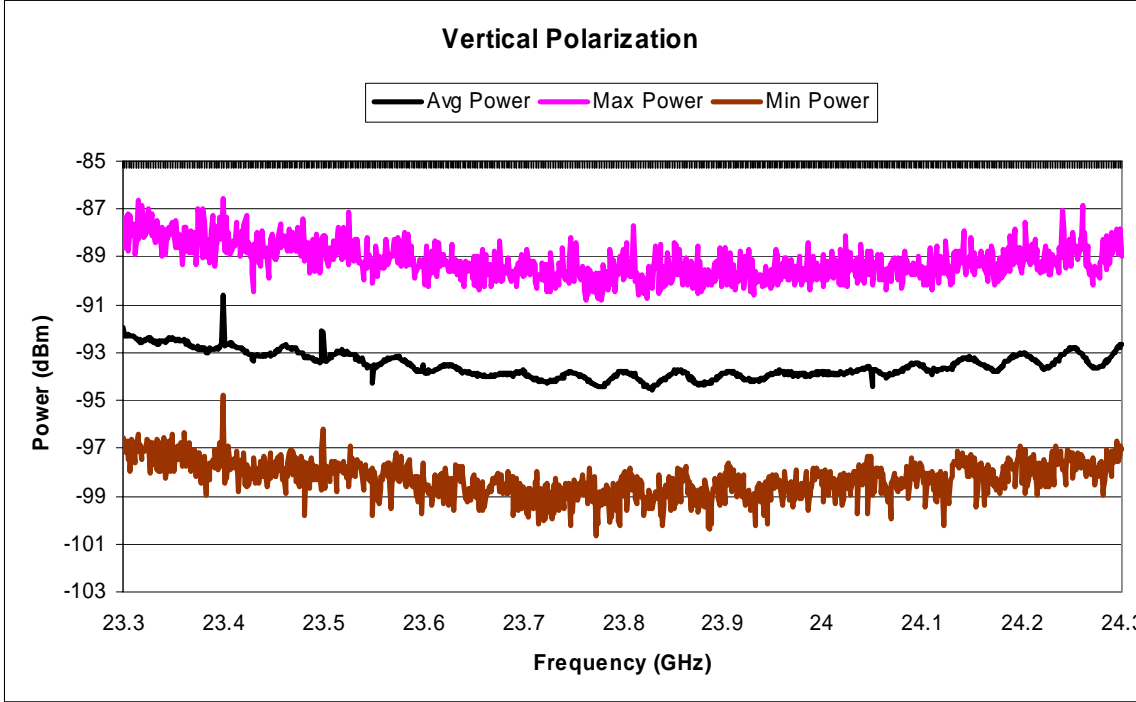
Figure B.69. Hartsfield-Jackson Airport(10/22/03): Zero Degree Elevation, Spectral Analysis
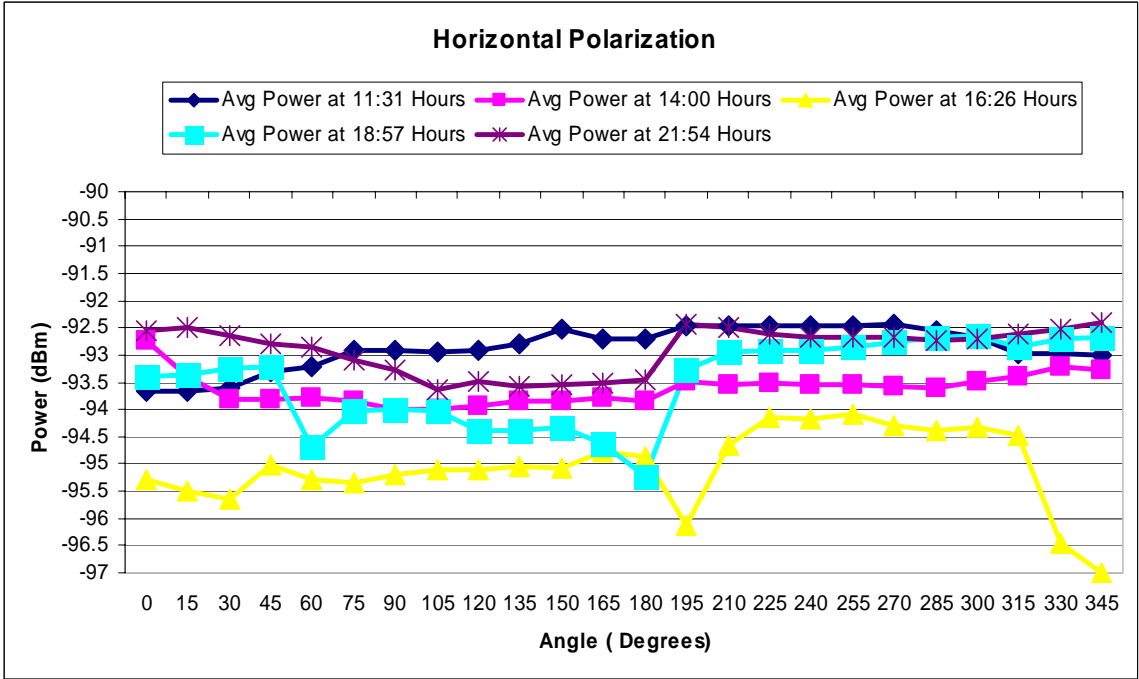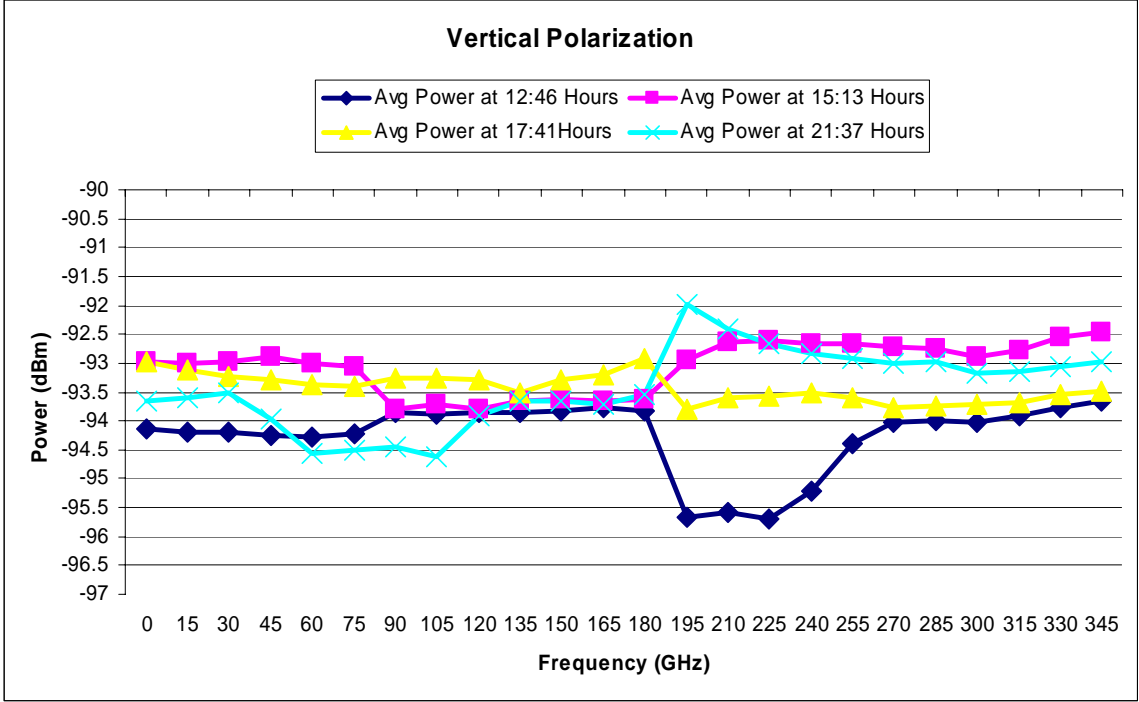
Figure B.70. Hartsfield-Jackson Airport (10/22/03): Zero Degree Elevation, Angular Analysis
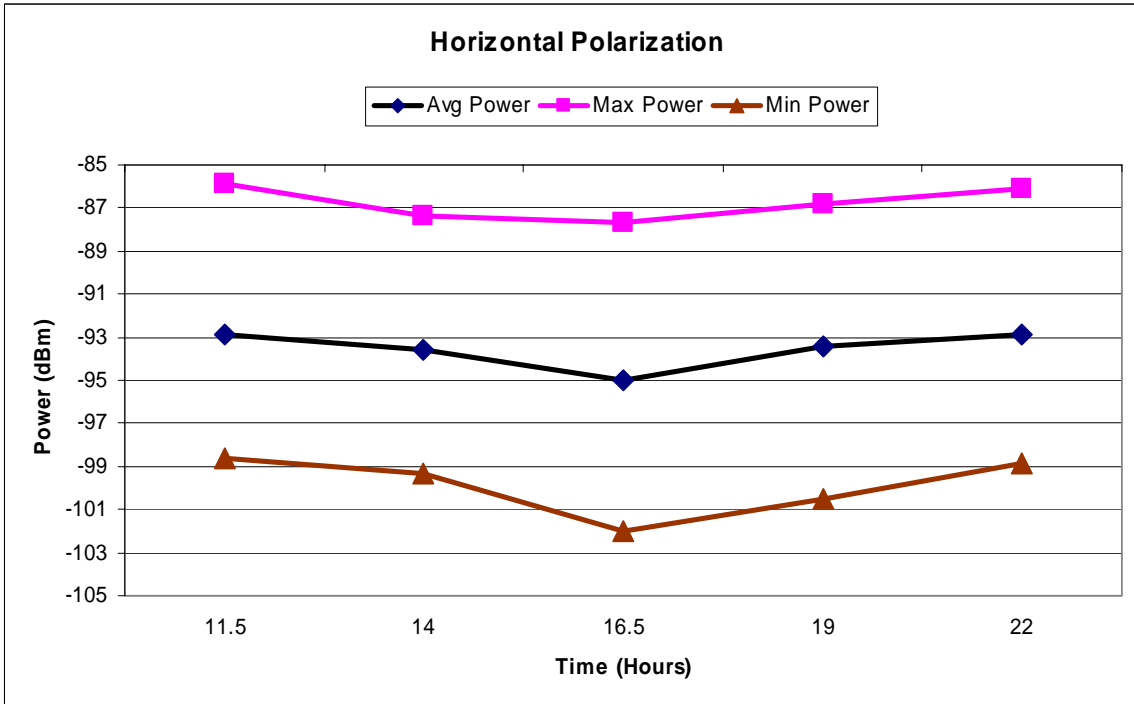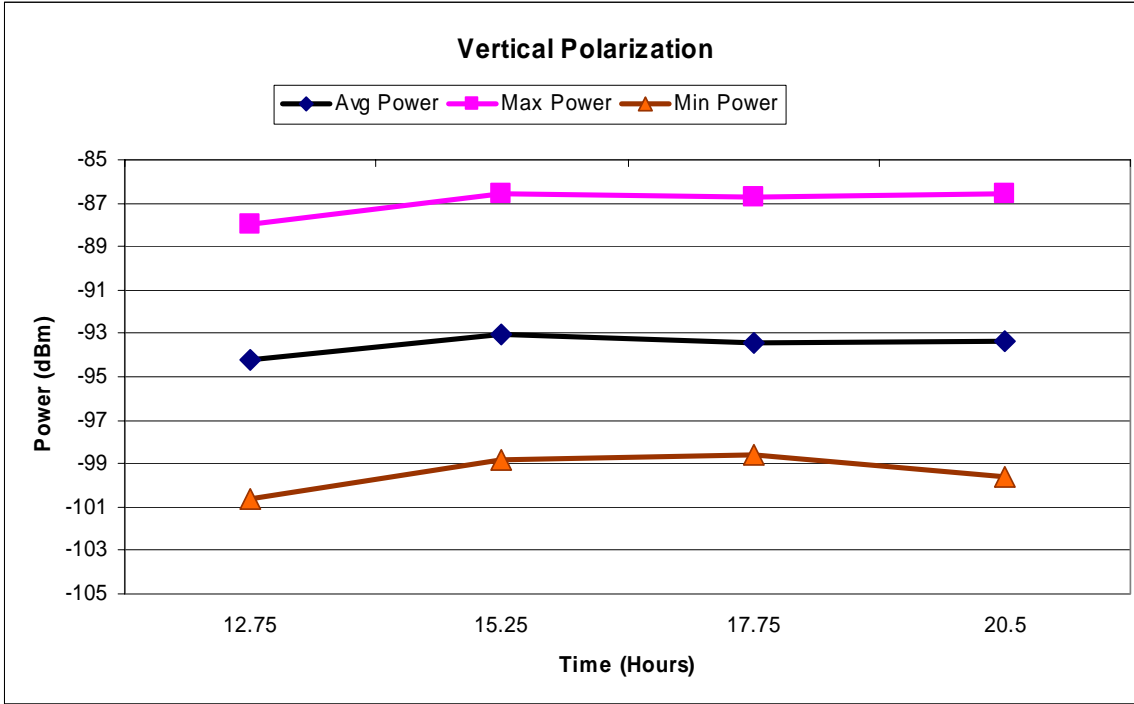
Figure B.71. Hartsfield-Jackson Airport (10/22/03): Zero Degree Elevation, Temporal Analysis
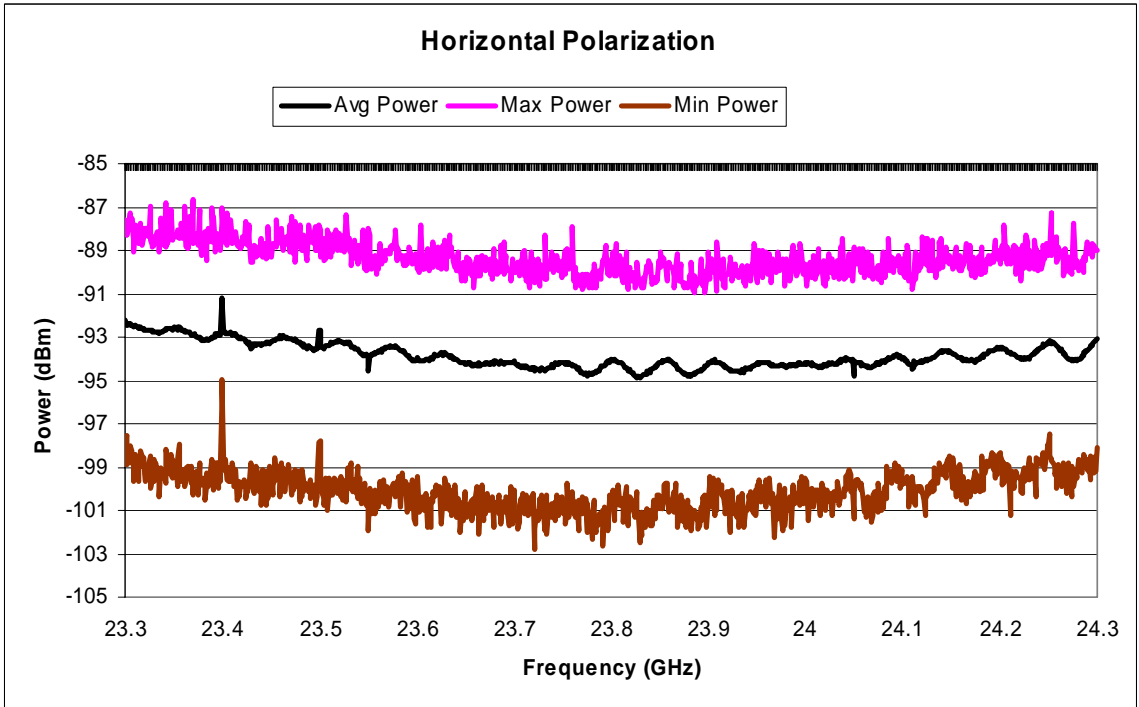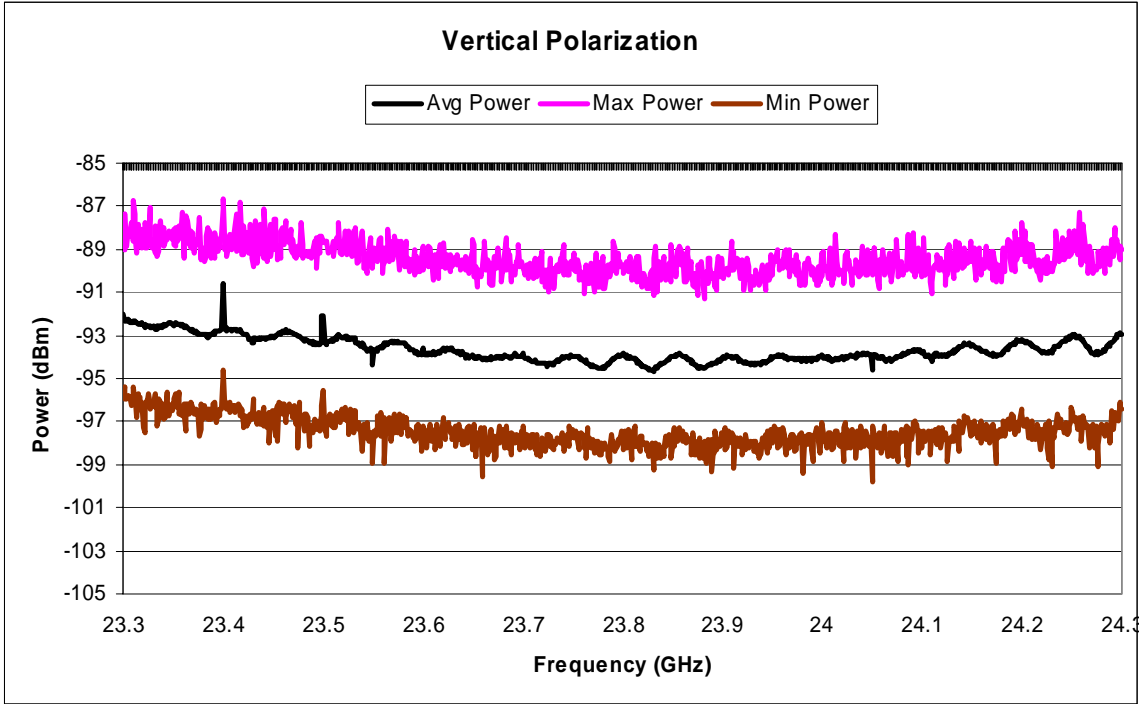
Figure B.72. Hartsfield-Jackson Airport(10/22/03): Thirty Degree Elevation, Spectral Analysis
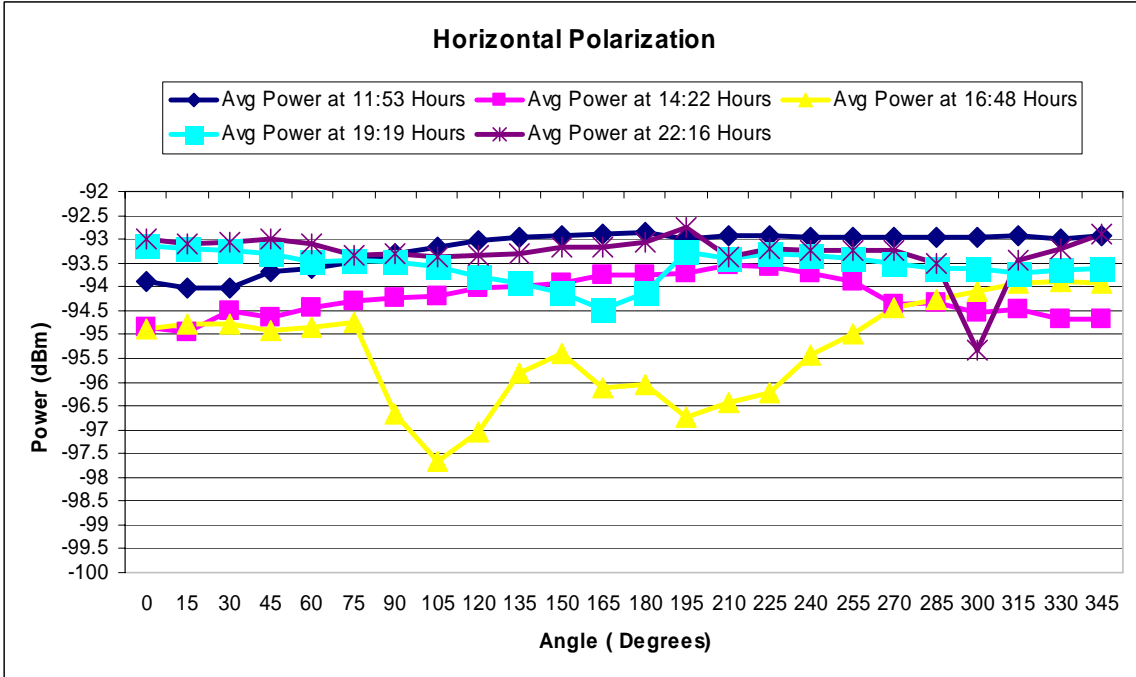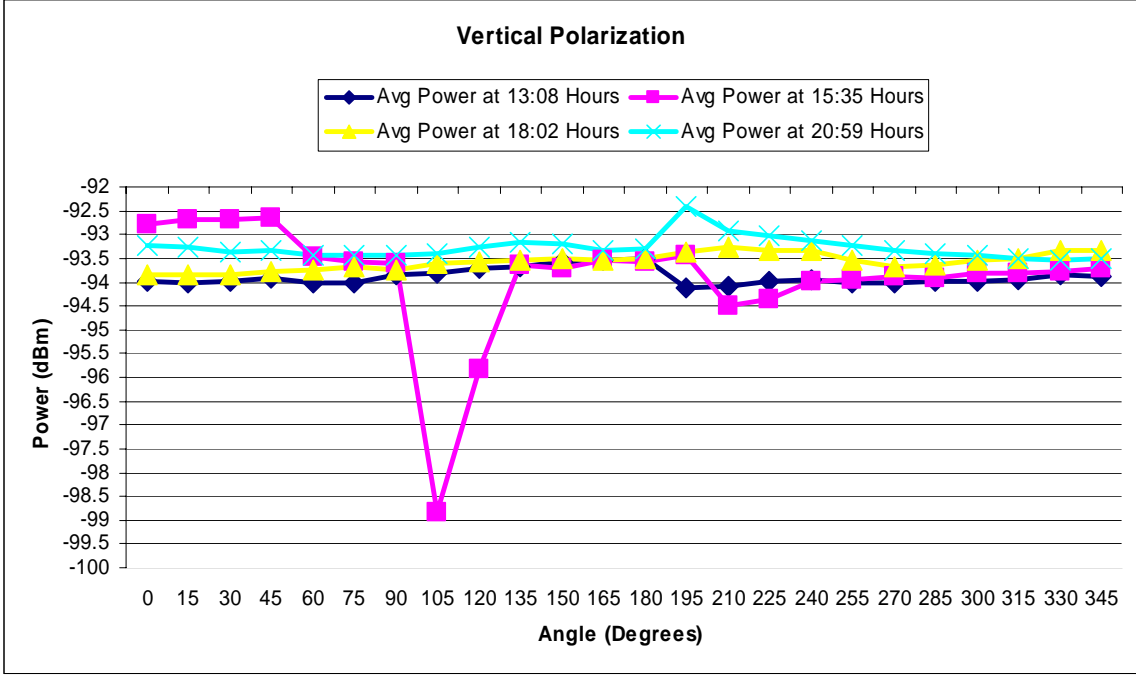
Figure B.73. Hartsfield-Jackson Airport (10/22/03): Thirty Degree Elevation, Angular Analysis
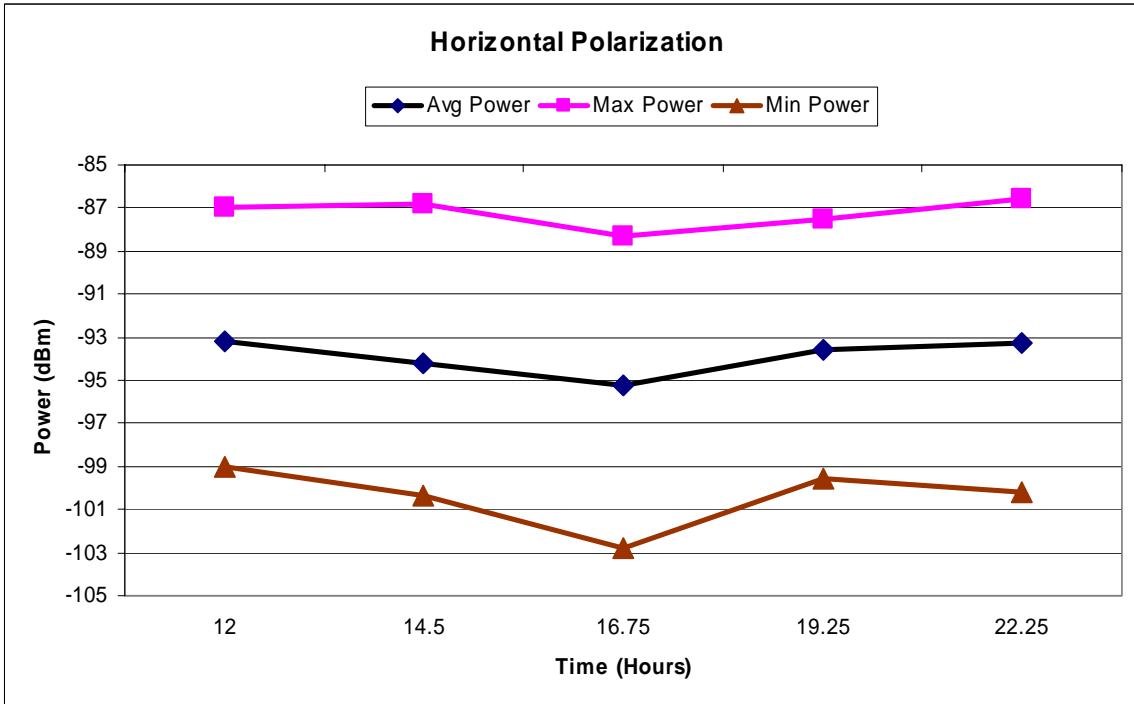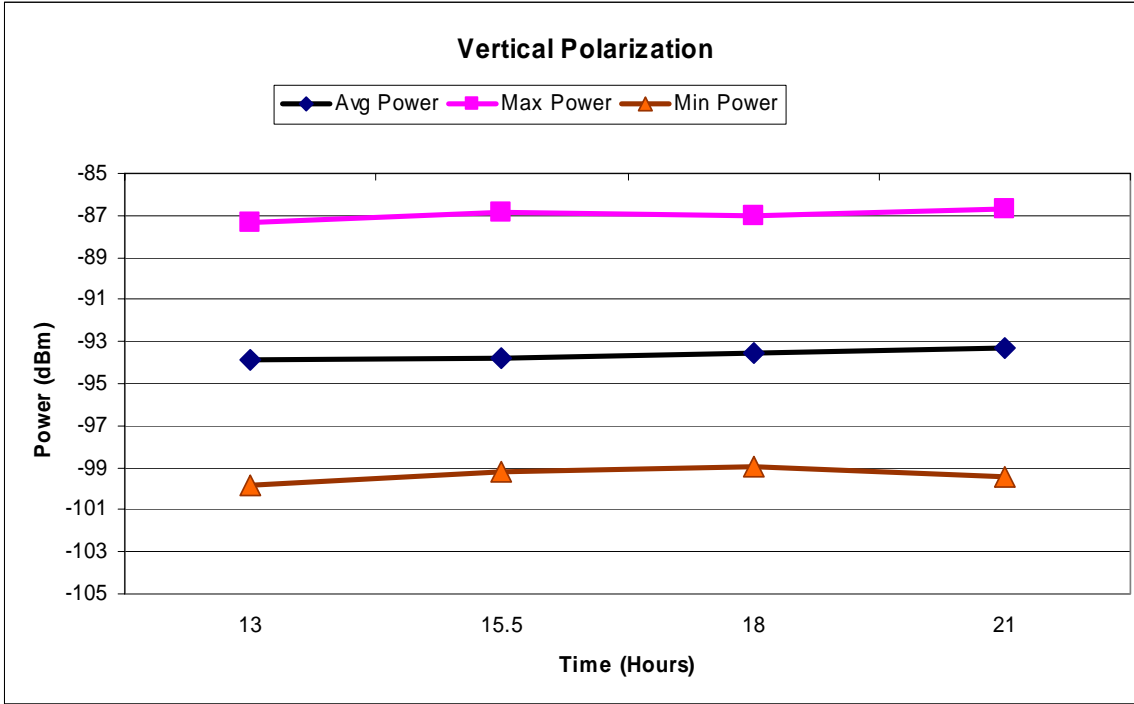
Figure B.74. Hartsfield-Jackson Airport (10/22/03): Thirty Degree Elevation, Temporal Analysis
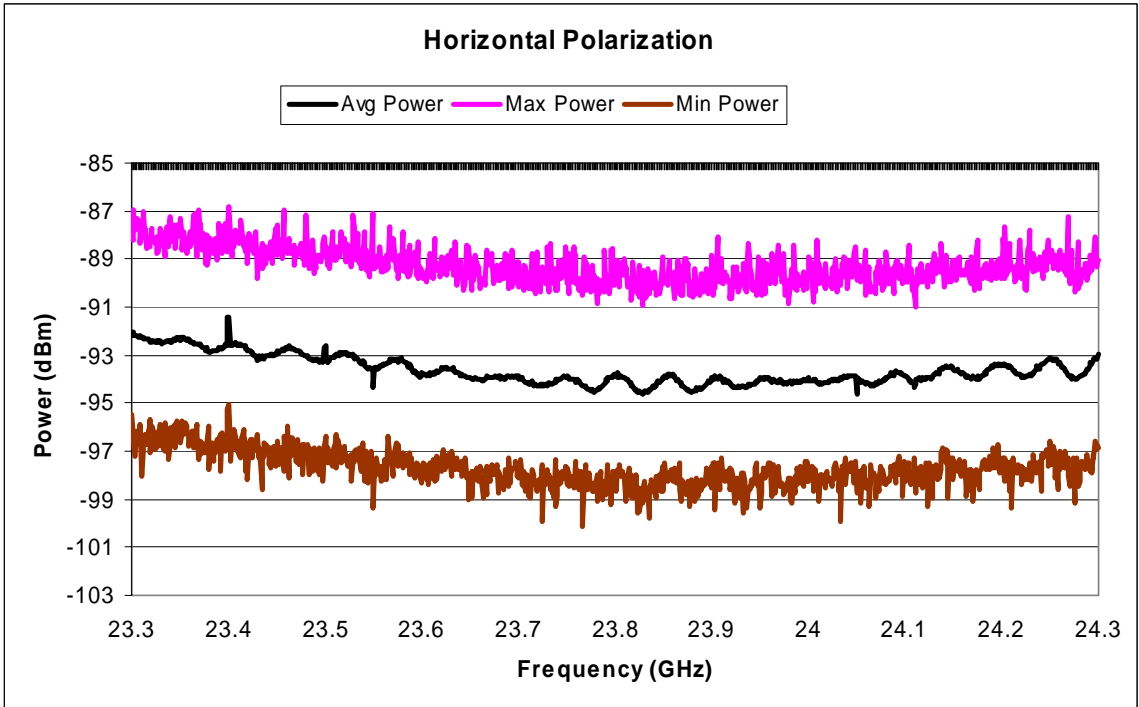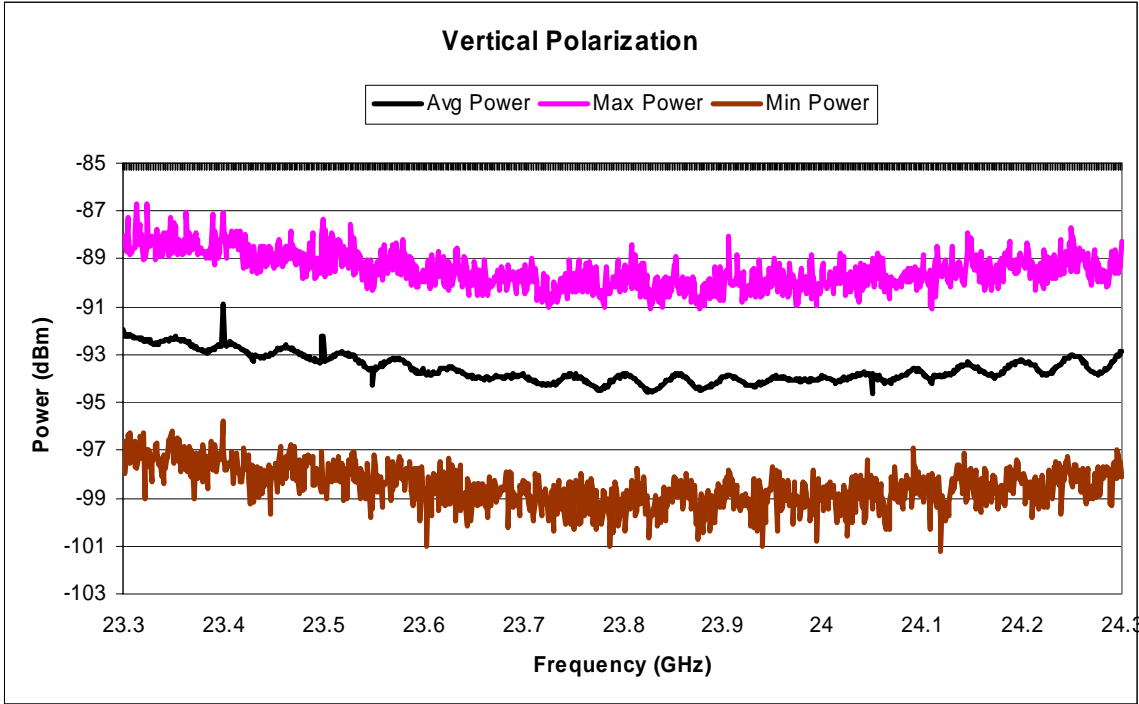
Figure B.75. Hartsfield-Jackson Airport (10/22/03): Sixty Degree Elevation, Spectral Analysis
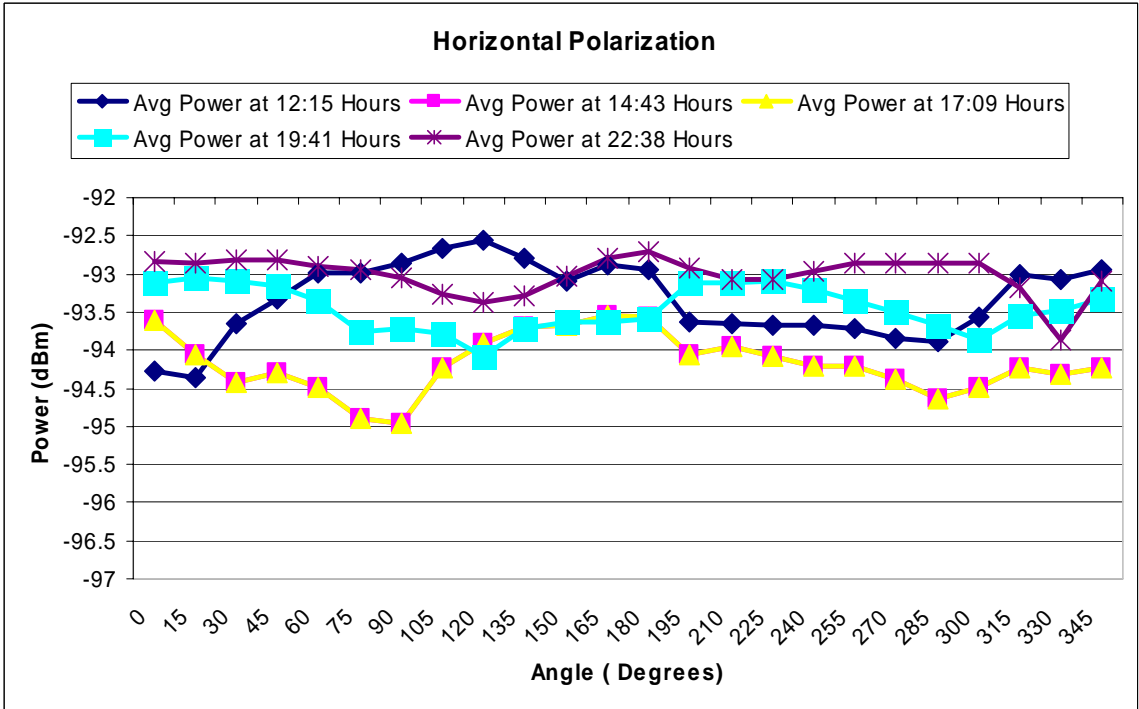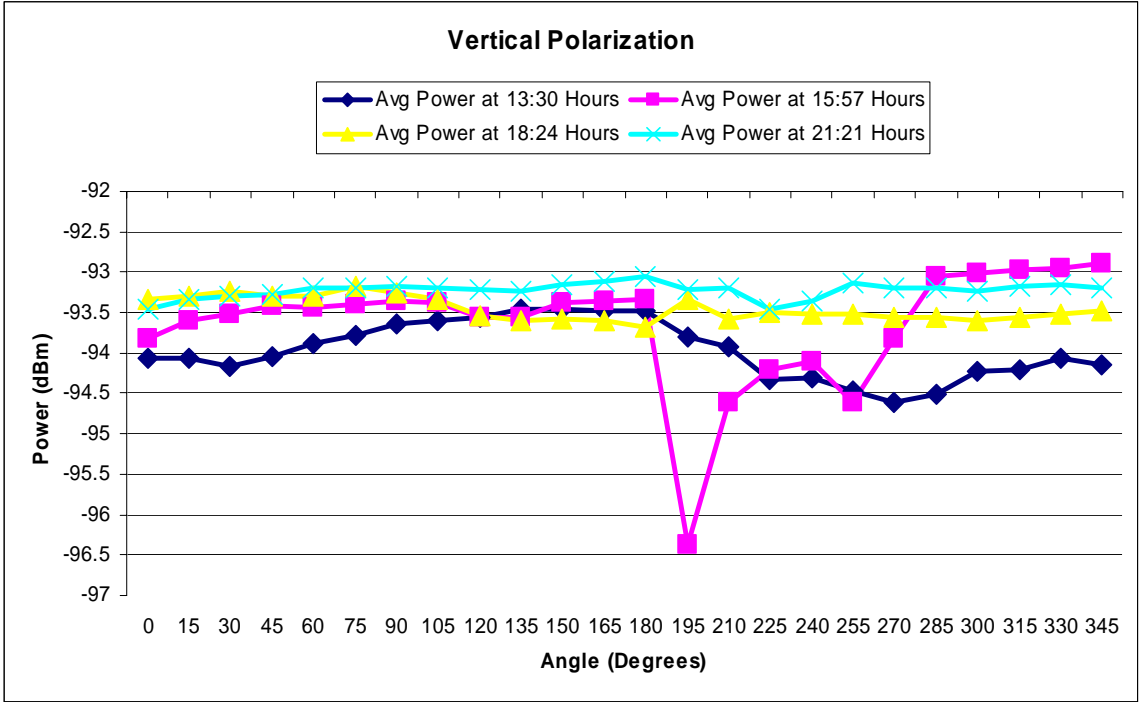
Figure B.76. Hartsfield-Jackson Airport (10/22/03): Sixty Degree Elevation, Angular Analysis
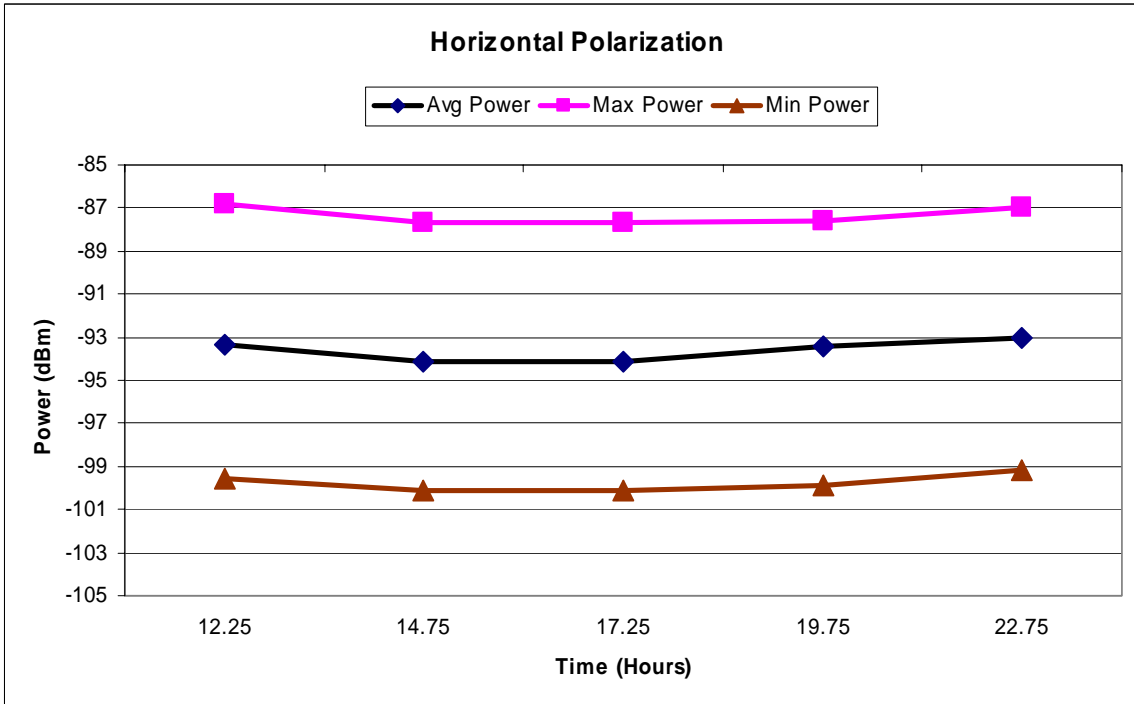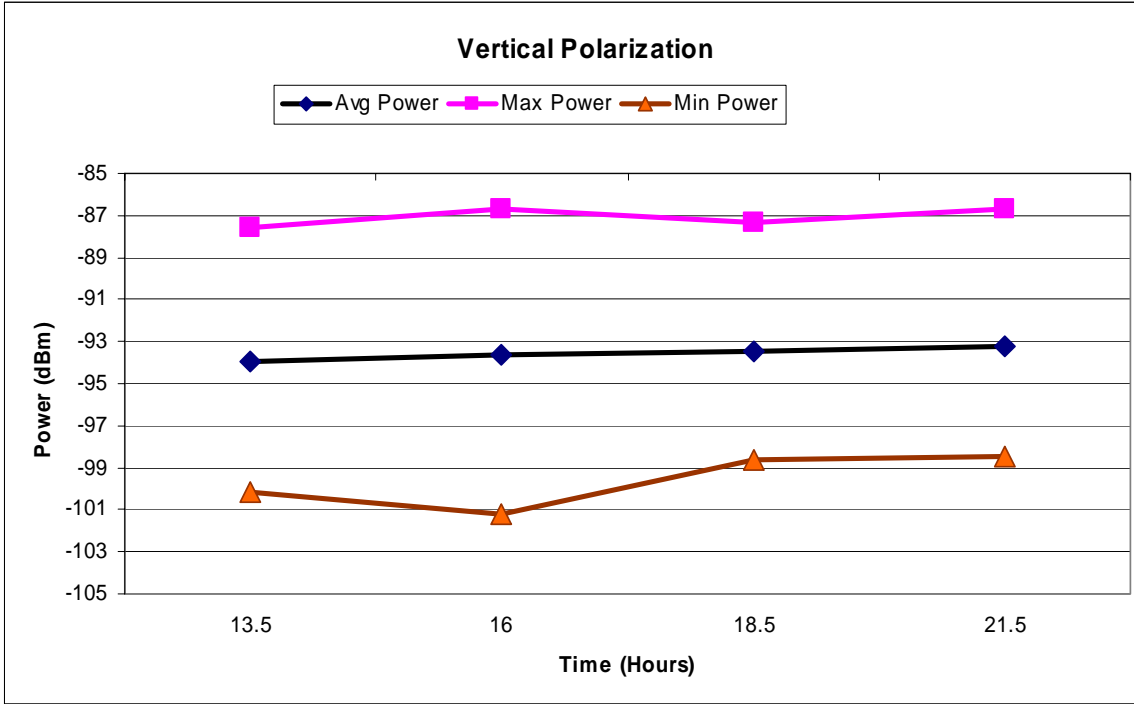
Figure B.77. Hartsfield-Jackson Airport (10/22/03): Sixty Degree Elevation, Temporal Analysis
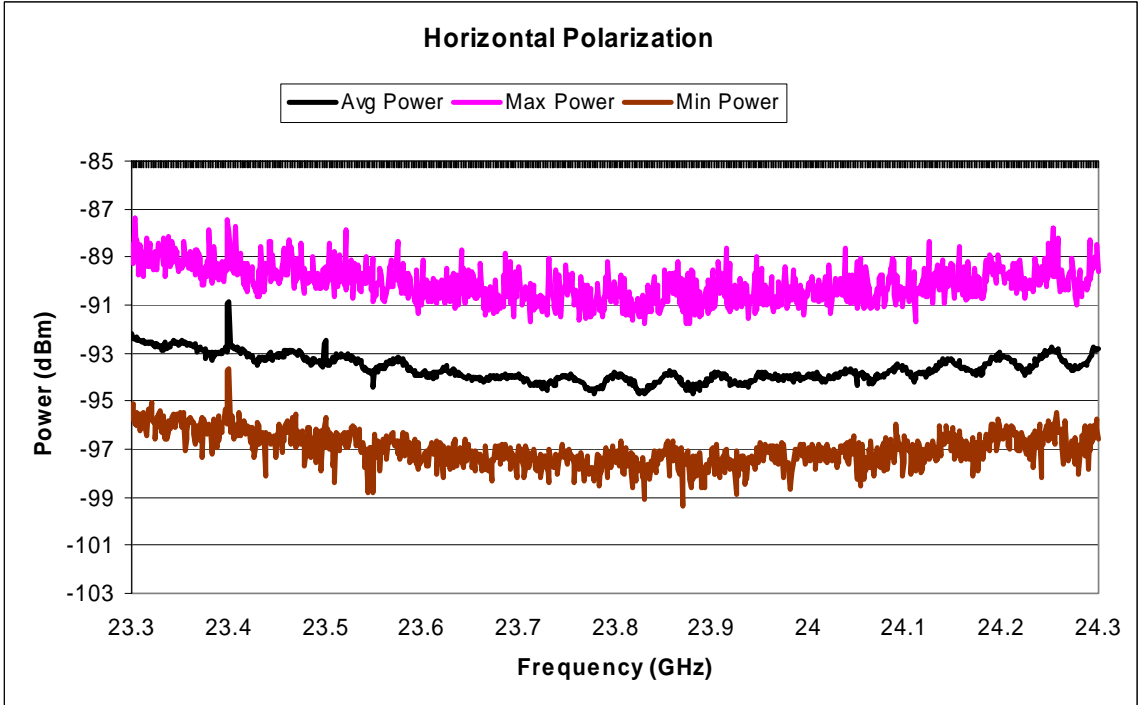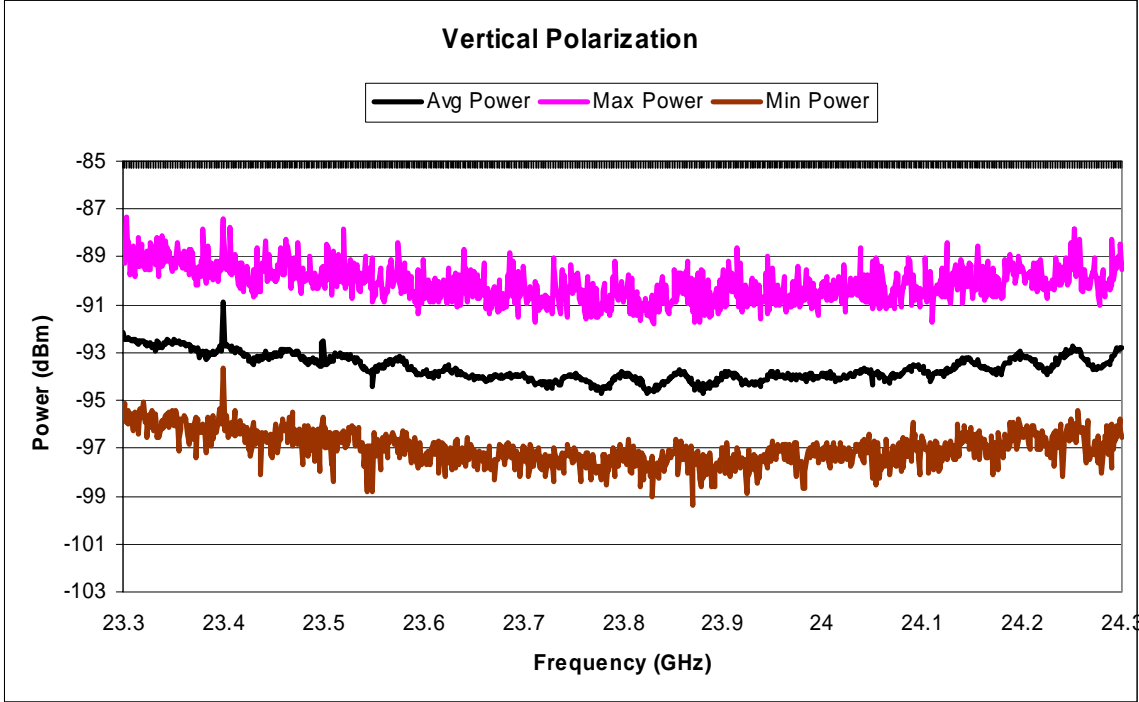
Figure B.78. Hartsfield-Jackson Airport (10/22/03): Ninety Degree Elevation, Spectral Analysis
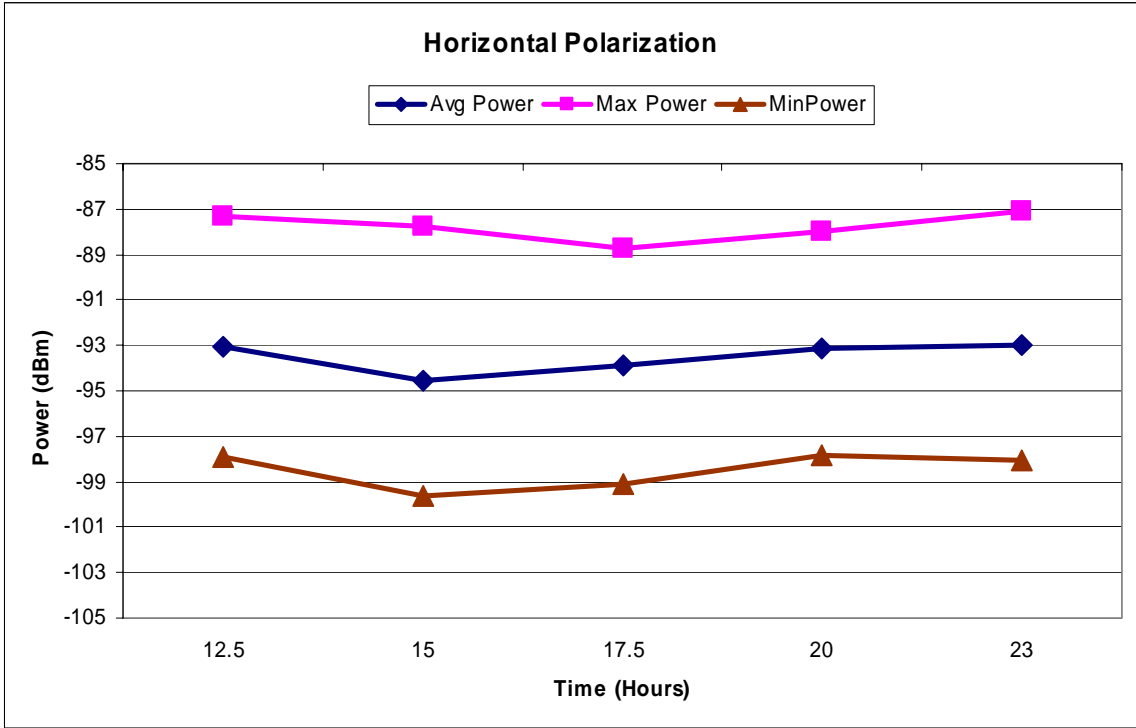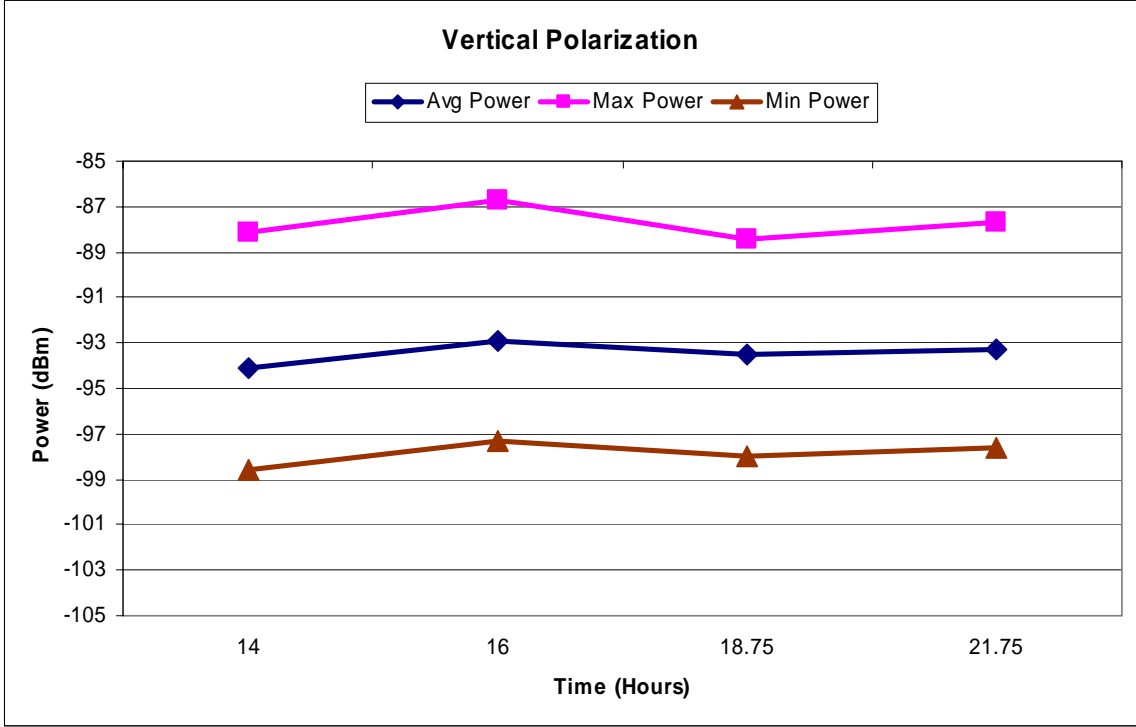
Figure B.79. Hartsfield-Jackson Airport (10/22/03): Ninety Degree Elevation, Temporal Analysis

Appendix B.6: Interstate 85 rest area, Anderson, South Carolina (Site 5)

Date: 4/16/04
Map of Location: See Figure B.80
Noteworthy Results:

- Spectral trends: In general, uniform in frequency; spectral peaks at 23.371 GHz, 23.559 GHz, 23.561 GHz, 23.576 GHz, 23.947 GHz, 23.999 GHz, 24.14 GHz. See Figures B.81, B.83, B.85, B.87, B.89, B.91 and B.93.
- Angular trends: Manmade peaks seem to occur in direction of interstate traffic. See Figures B.82, B.86, andB.90.
- Temporal trends: Increases throughout the day; peak occurs in the early evening. See Figures B.84, B.88, B.92, and B.94.
- An anomalous feature of resonance at 23.40 GHz appears in this data set.
- Pre-measurement calibrated gain: 41.3 dB; Post-measurement calibrated gain: 45.3 dB. The discrepancy is due to the absence of the resonances in the post-measurement calibration. It has been verified that these resonances were present the entire day of measurements.
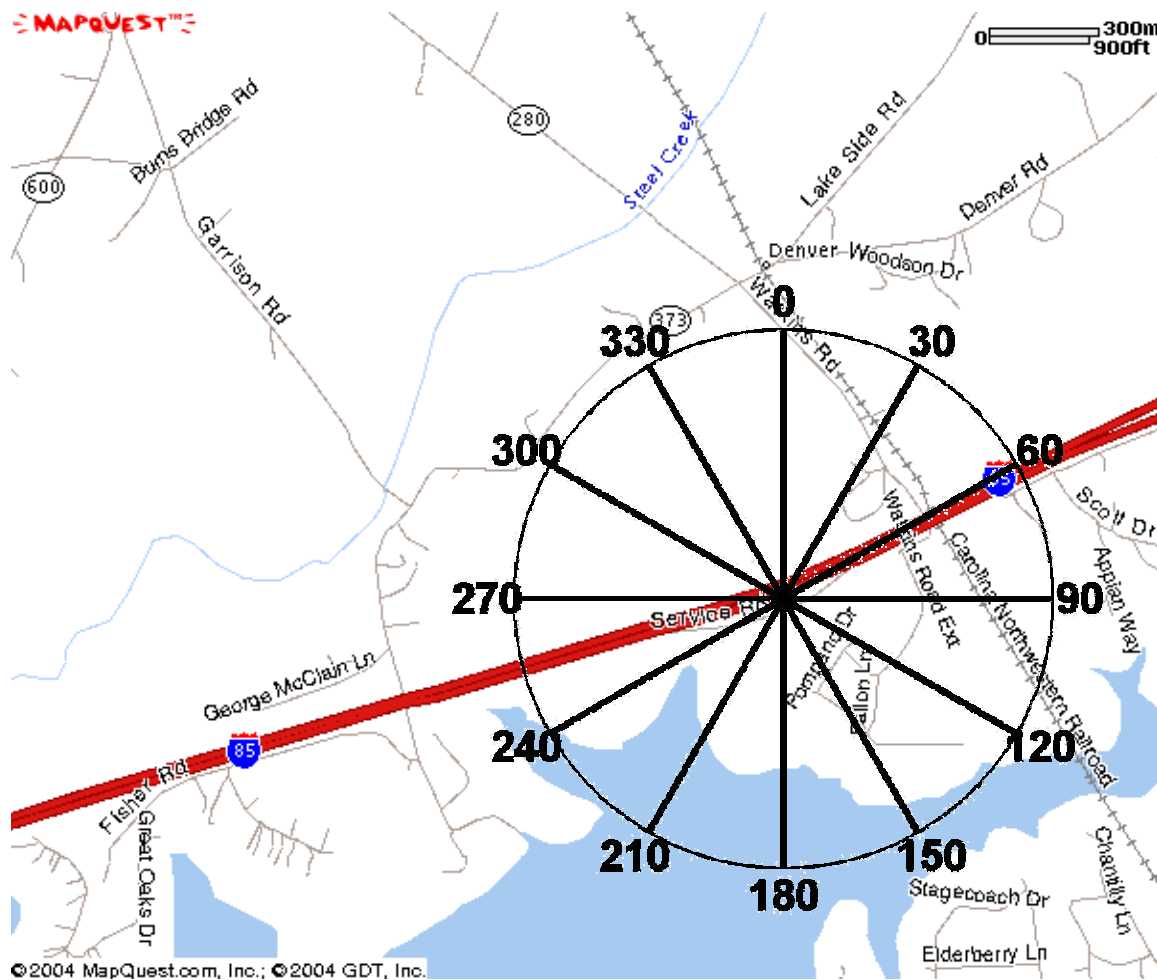
Figure B.80. Map of Interstate 85 in Anderson, South Carolina
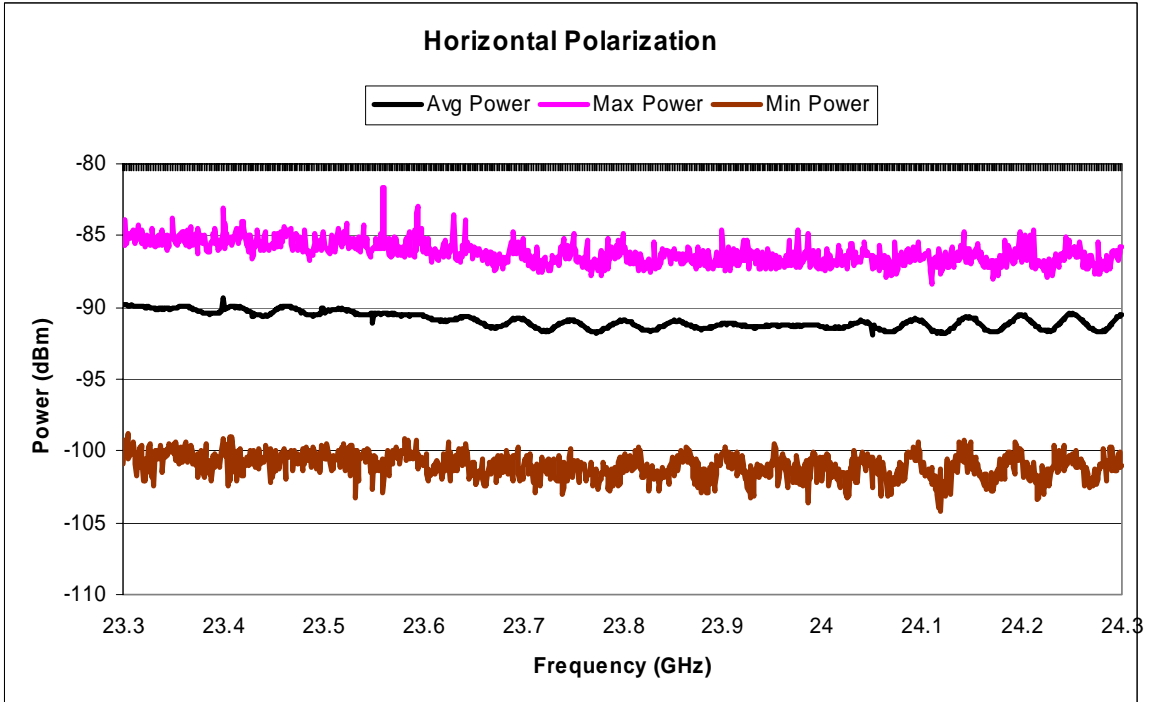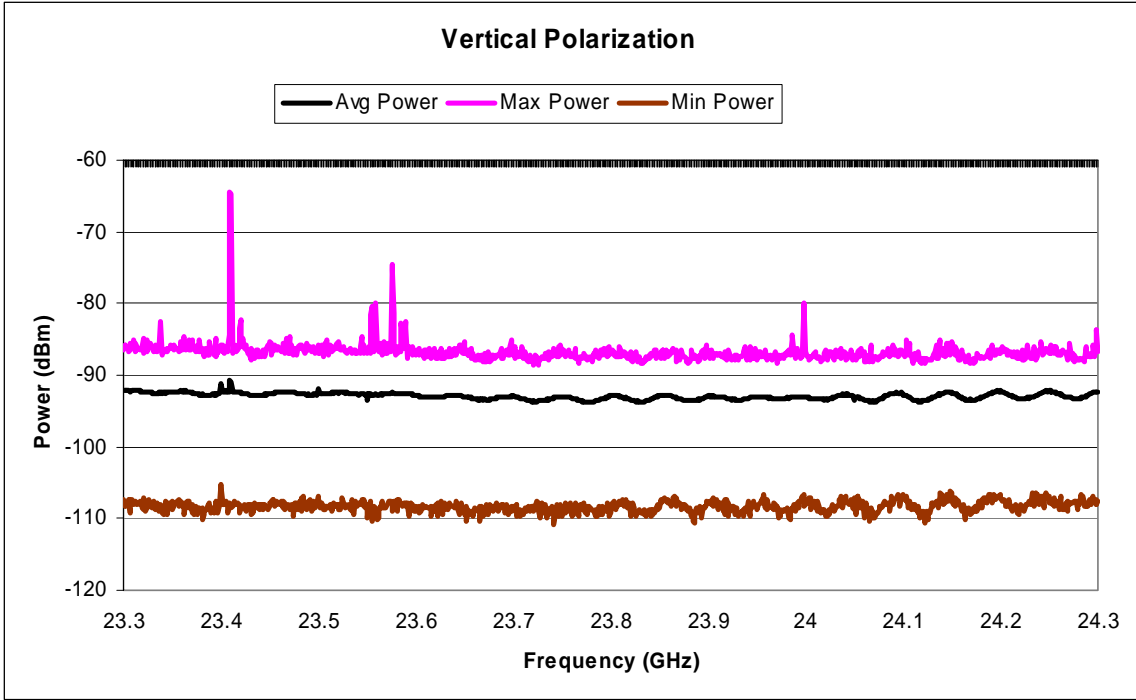
Figure B.81. I-85 Anderson: Zero Degree Elevation, Spectral Analysis
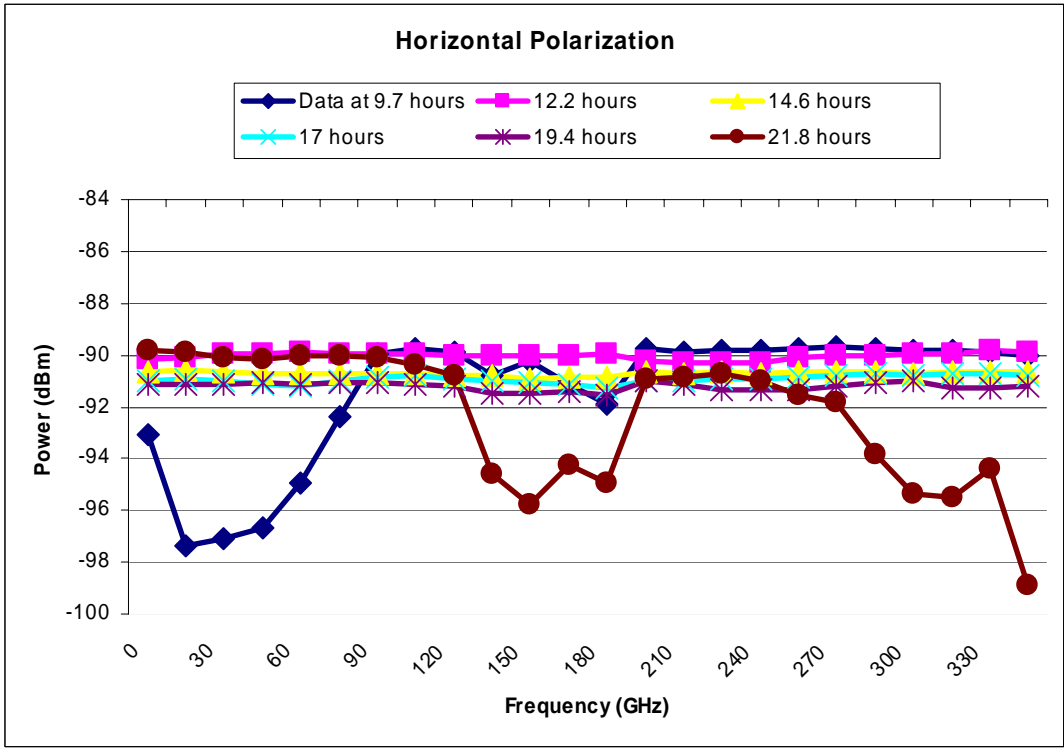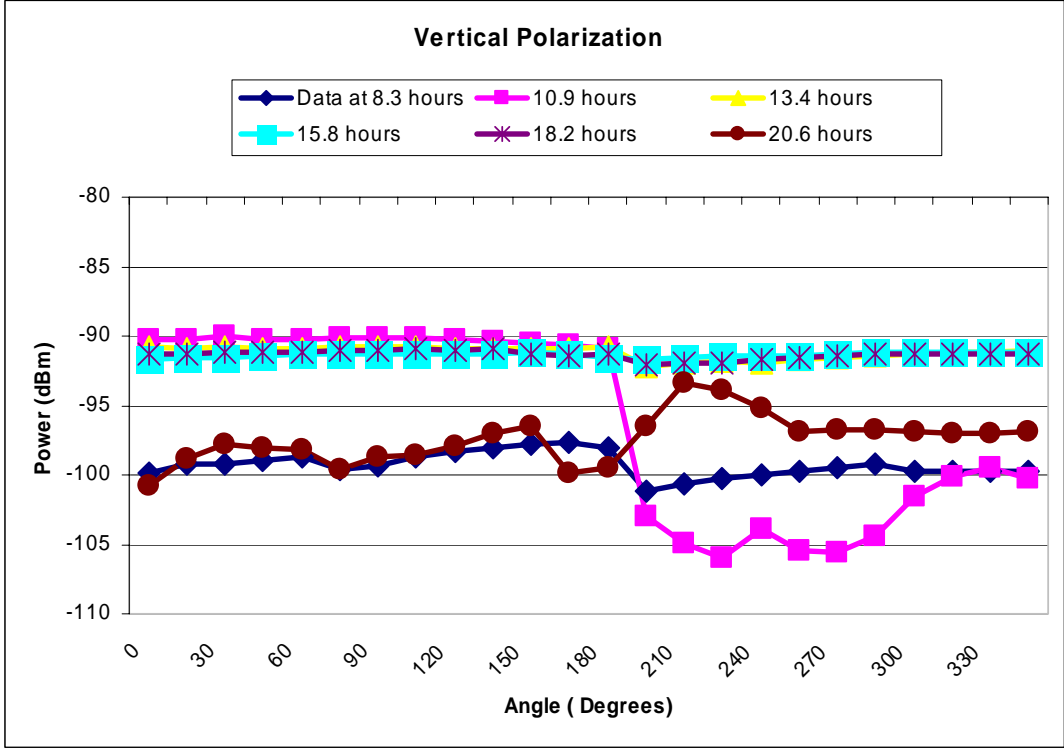
Figure B.82. I-85 Anderson: Zero Degree Elevation, Angular Analysis
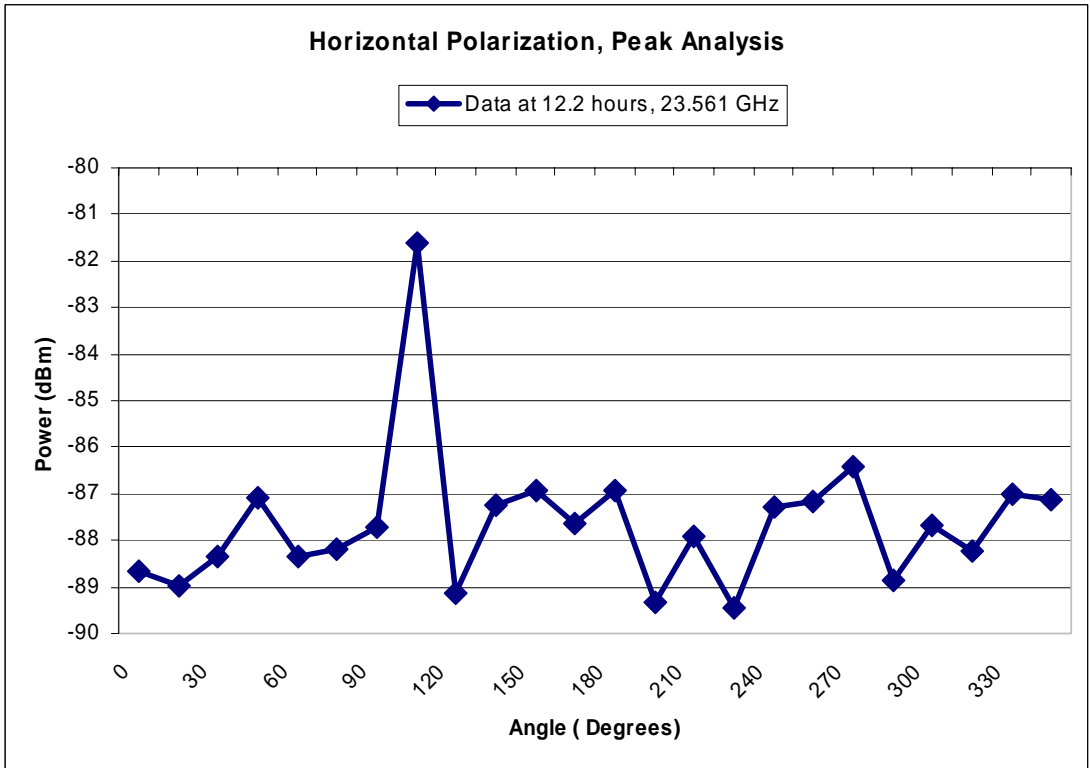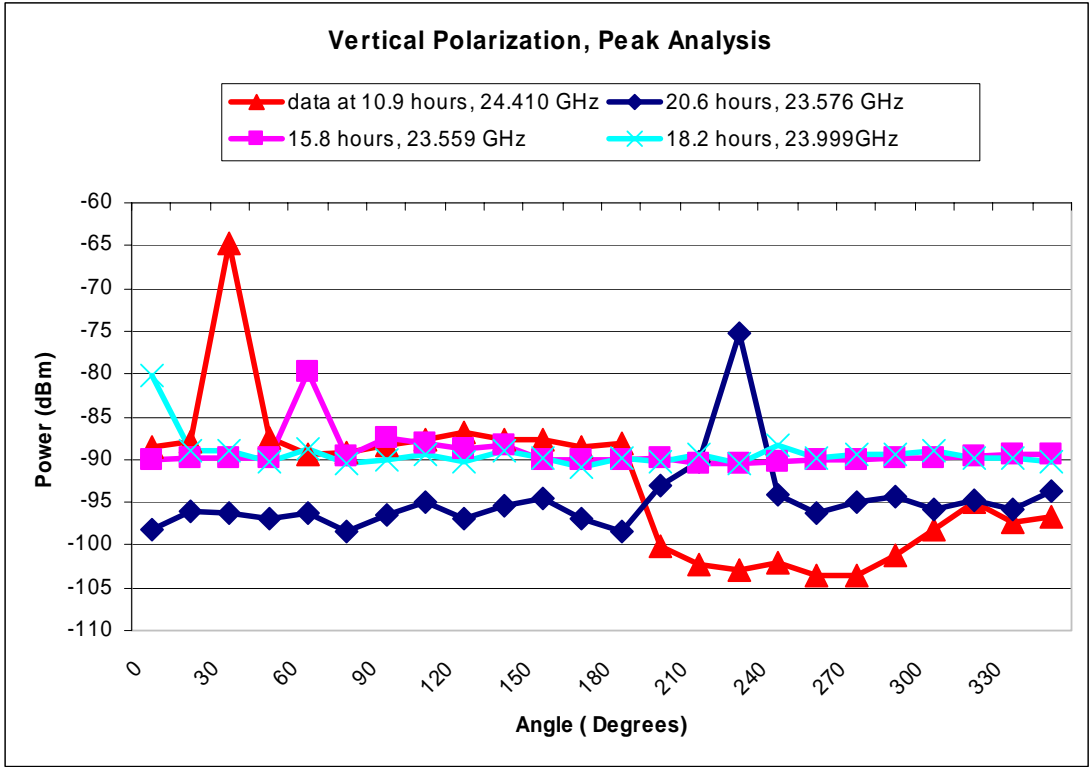
Figure B.83. I-85 Anderson: Zero Degree Elevation, Angular Analysis of Spectral Peaks

210
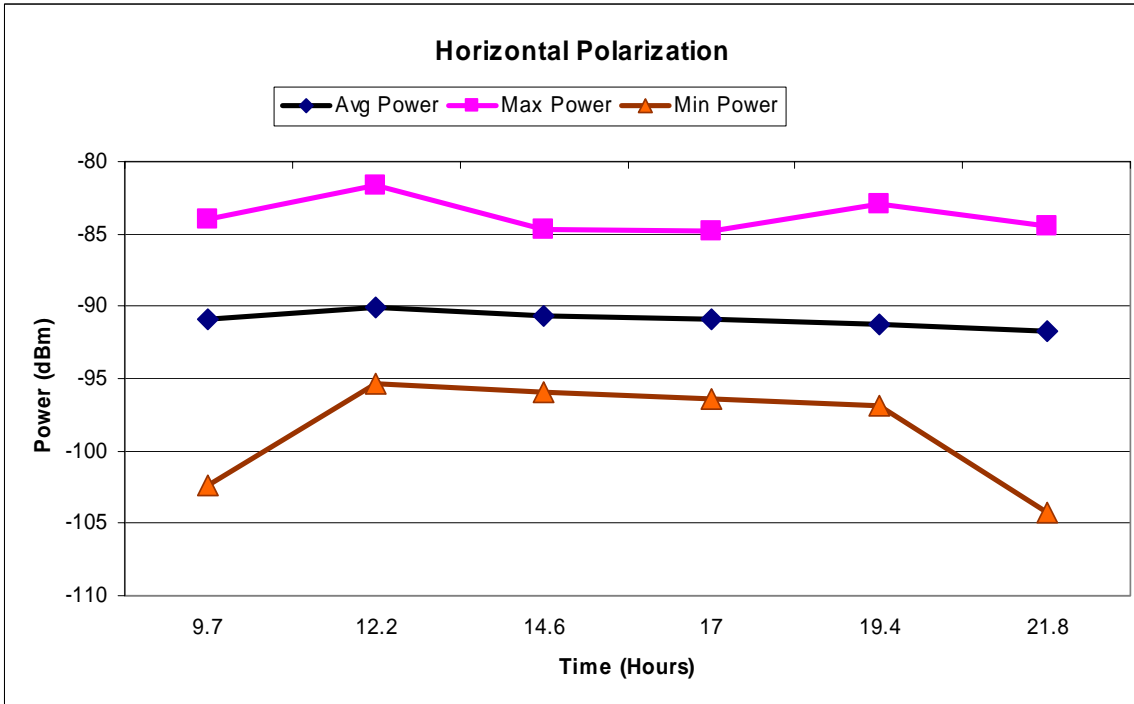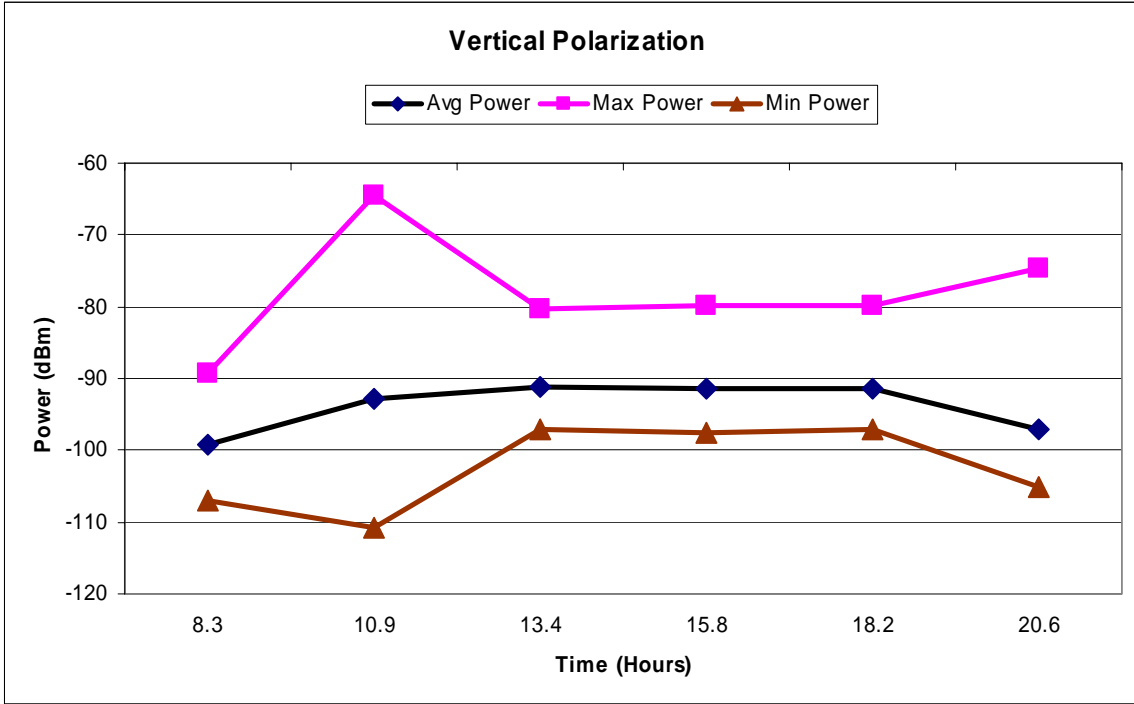
Figure B.84. I-85 Anderson: Zero Degree Elevation, Temporal Analysis
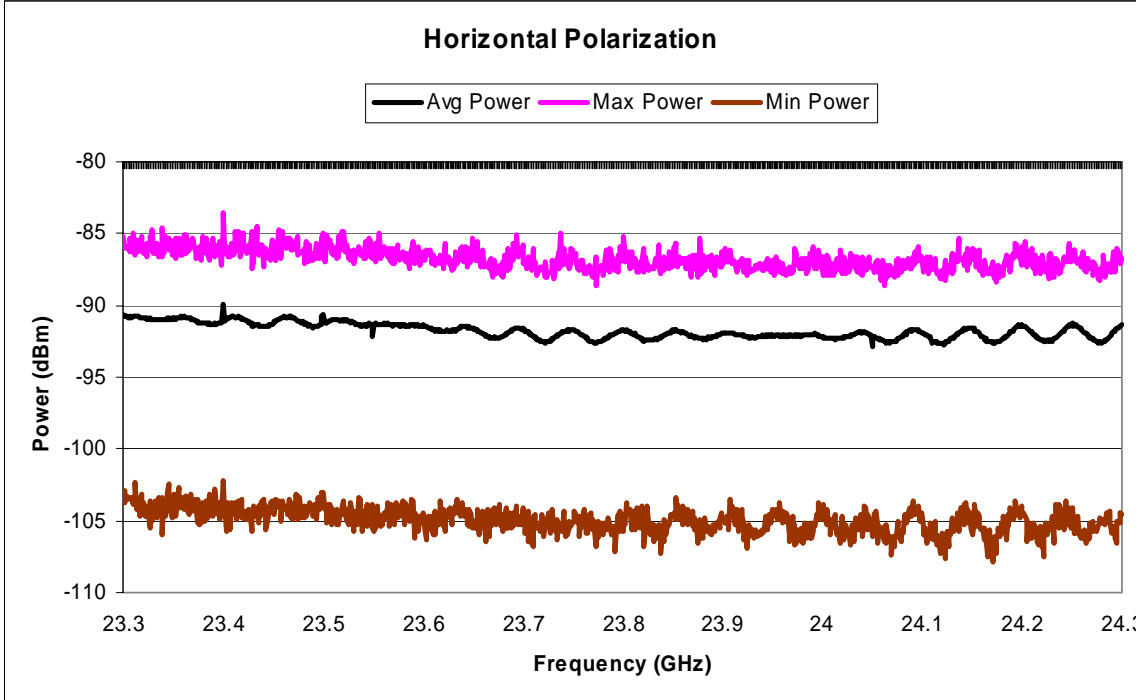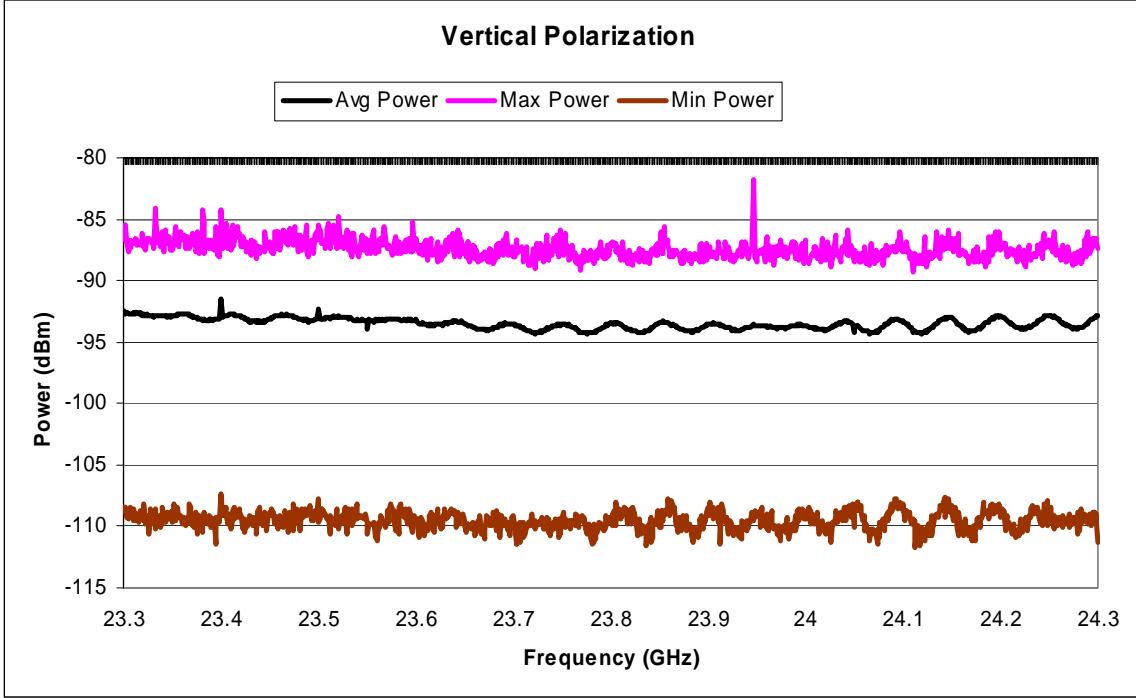
Figure B.85. I-85 Anderson: Thirty Degree Elevation, Spectral Analysis
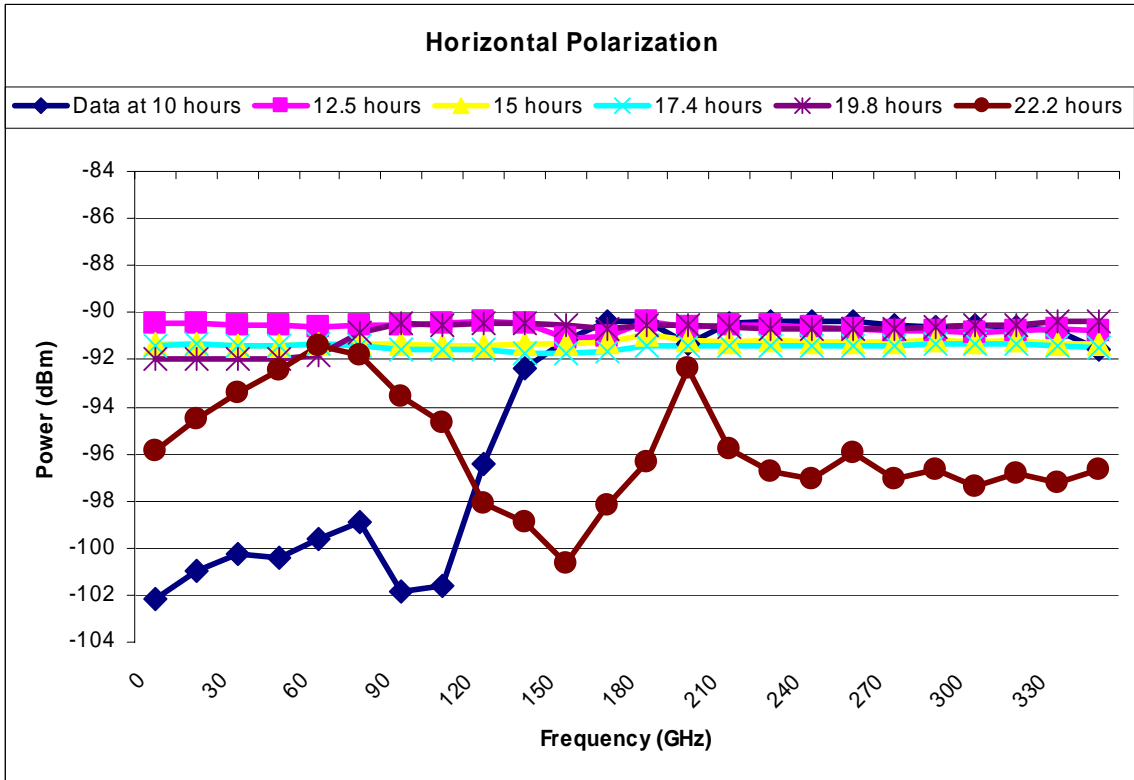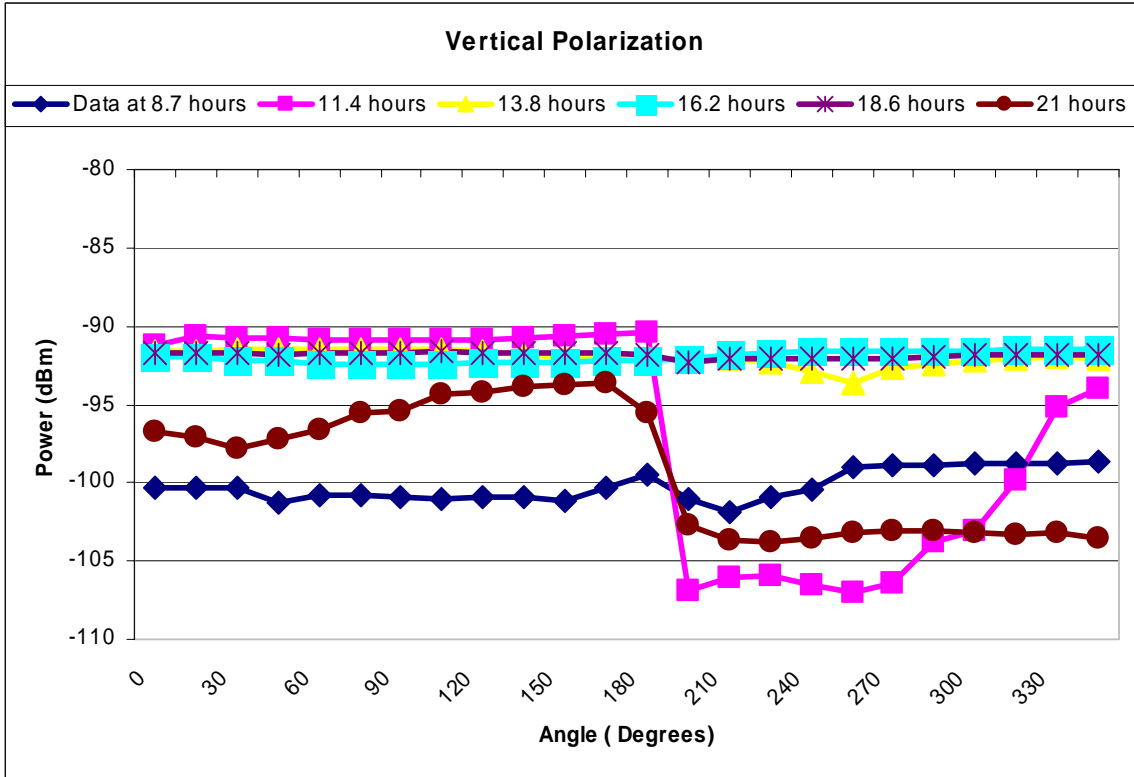
Figure B.86. I-85 Anderson: Thirty Degree Elevation, Angular Analysis
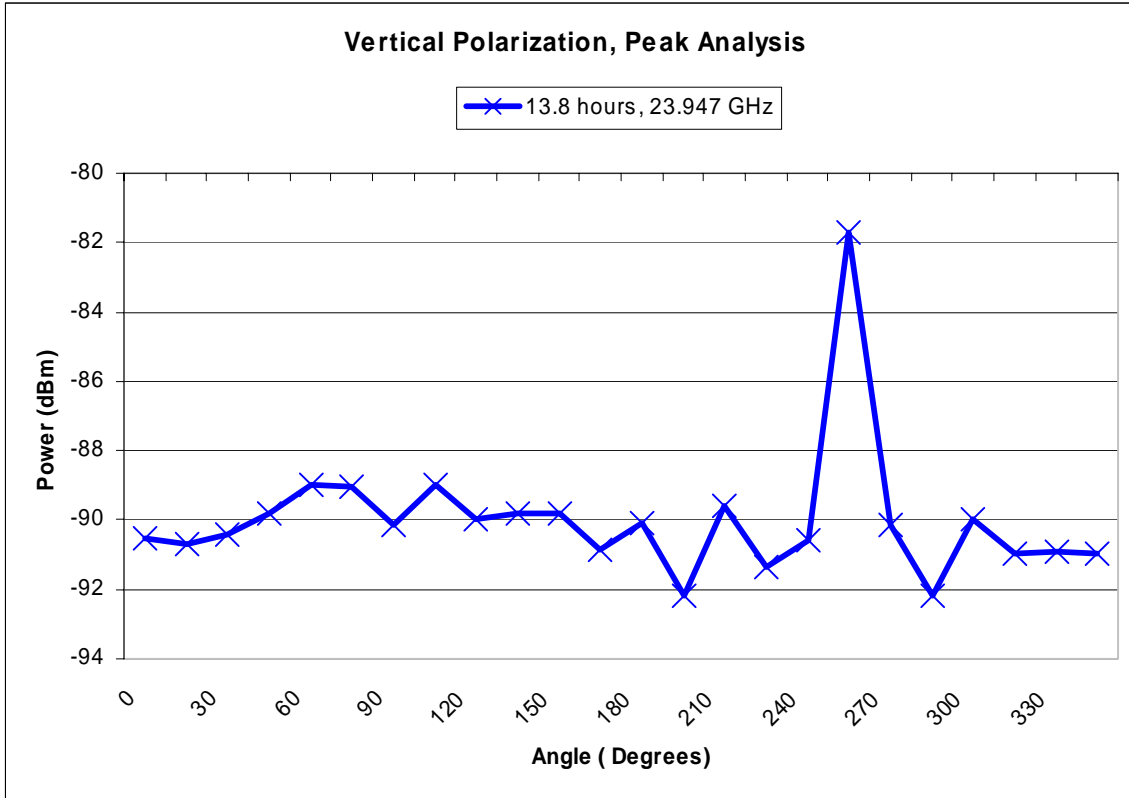
Figure B.87. I-85 Anderson: Thirty Degree Elevation, Angular Analysis of Spectral Peak
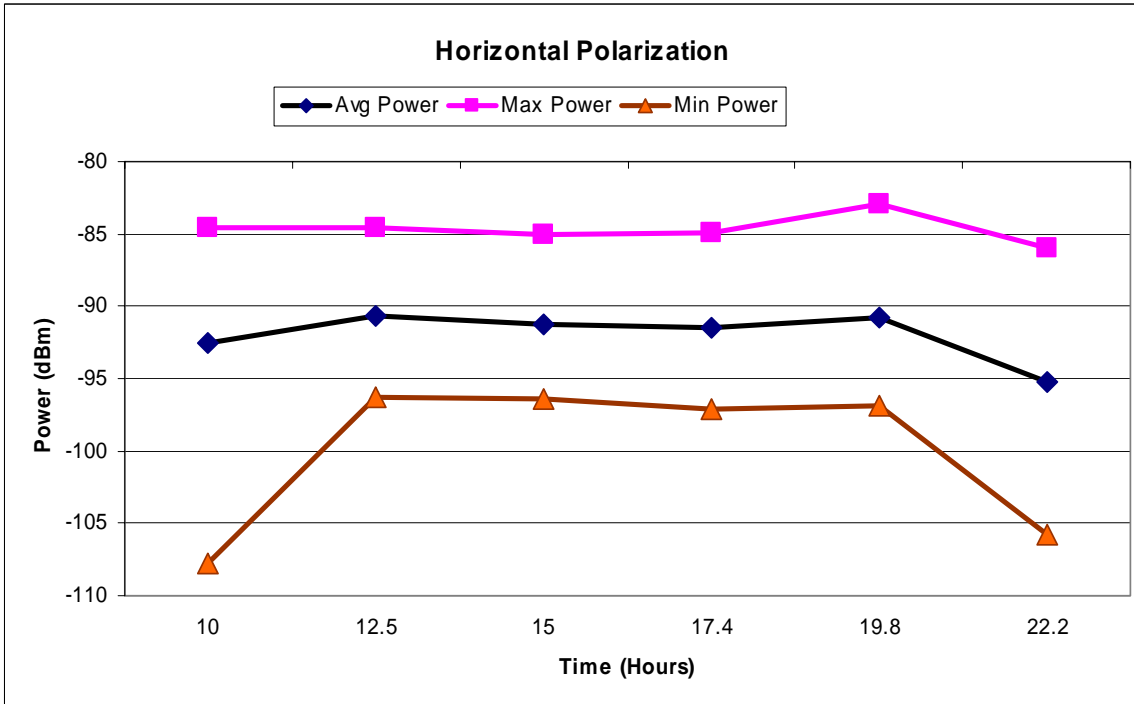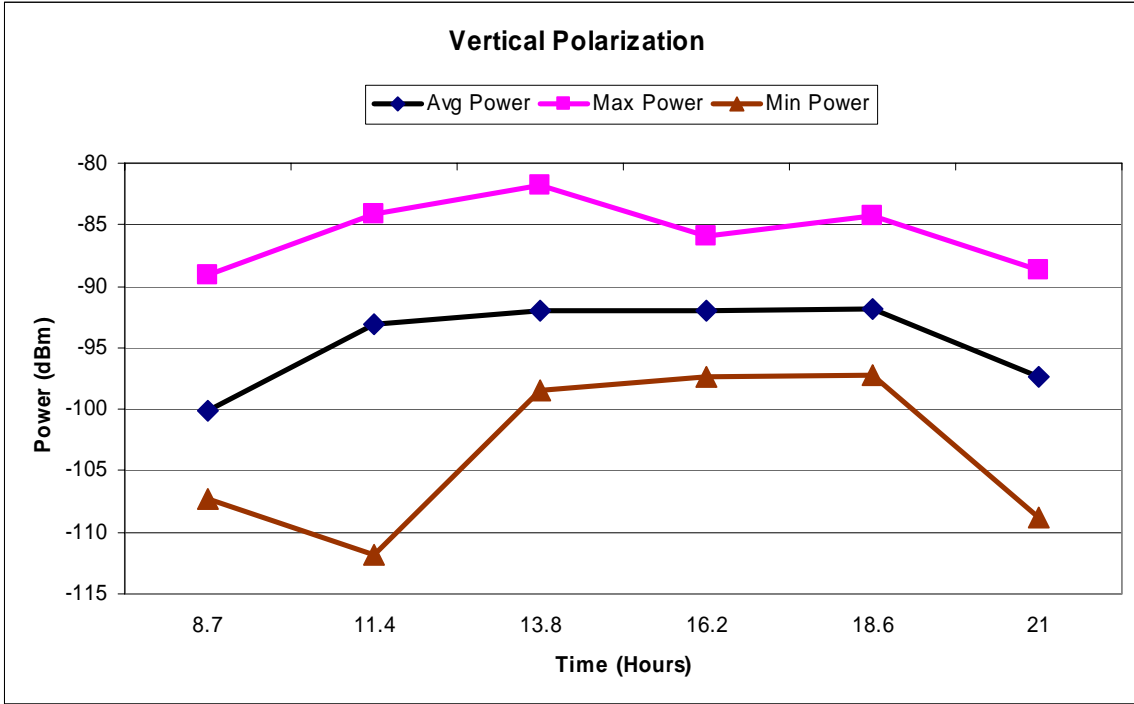
Figure B.88. I-85 Anderson: Thirty Degree Elevation, Temporal Analysis

215
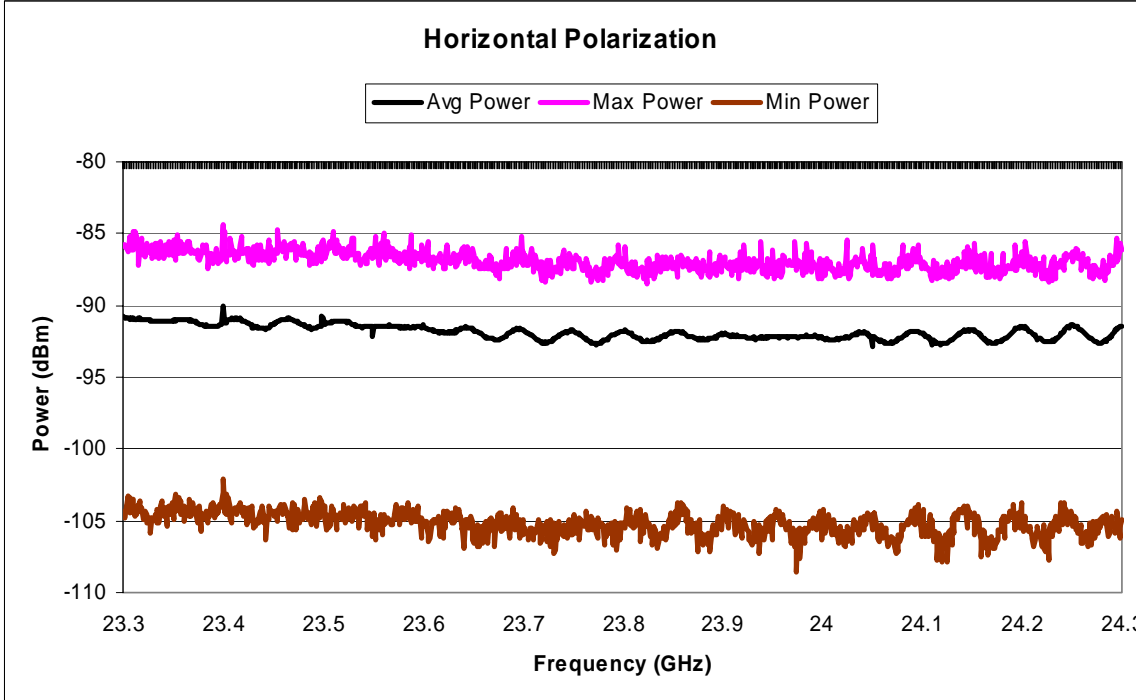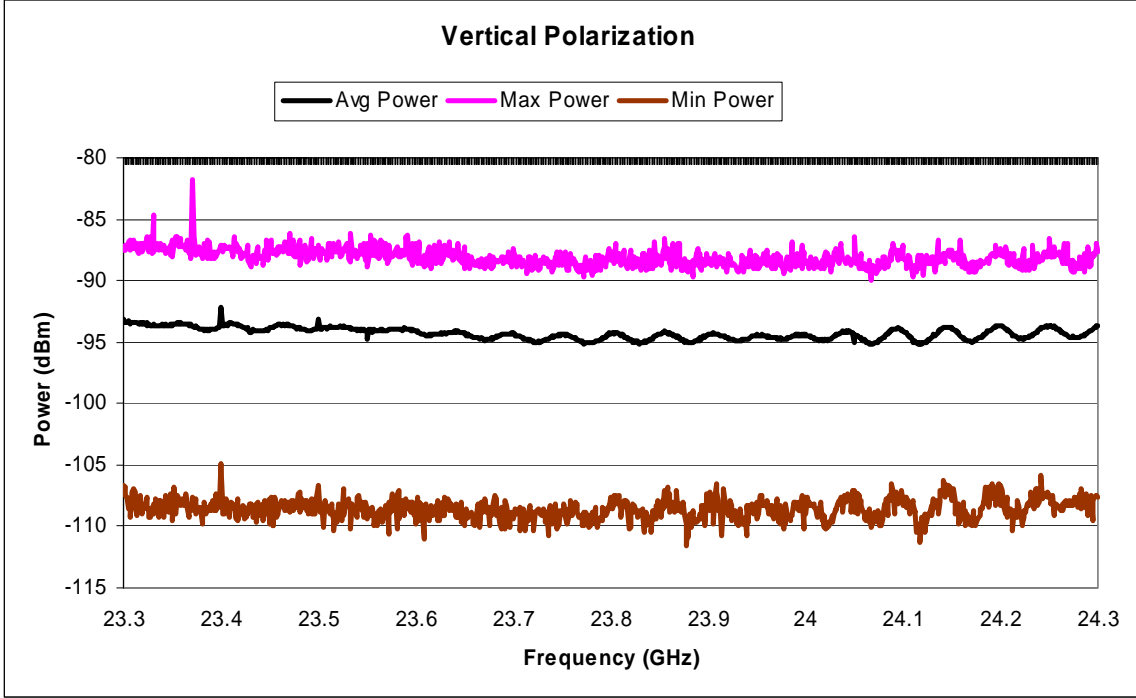
Figure B.89. I-85 Anderson: Sixty Degree Elevation, Spectral Analysis

216
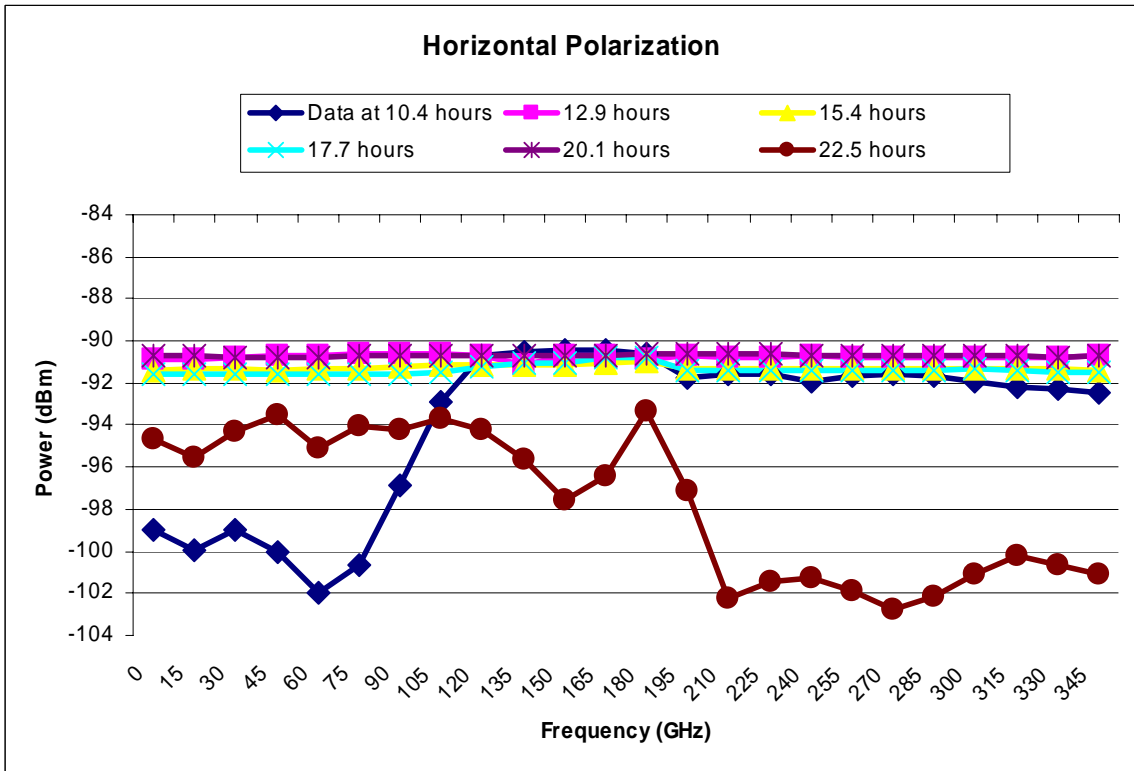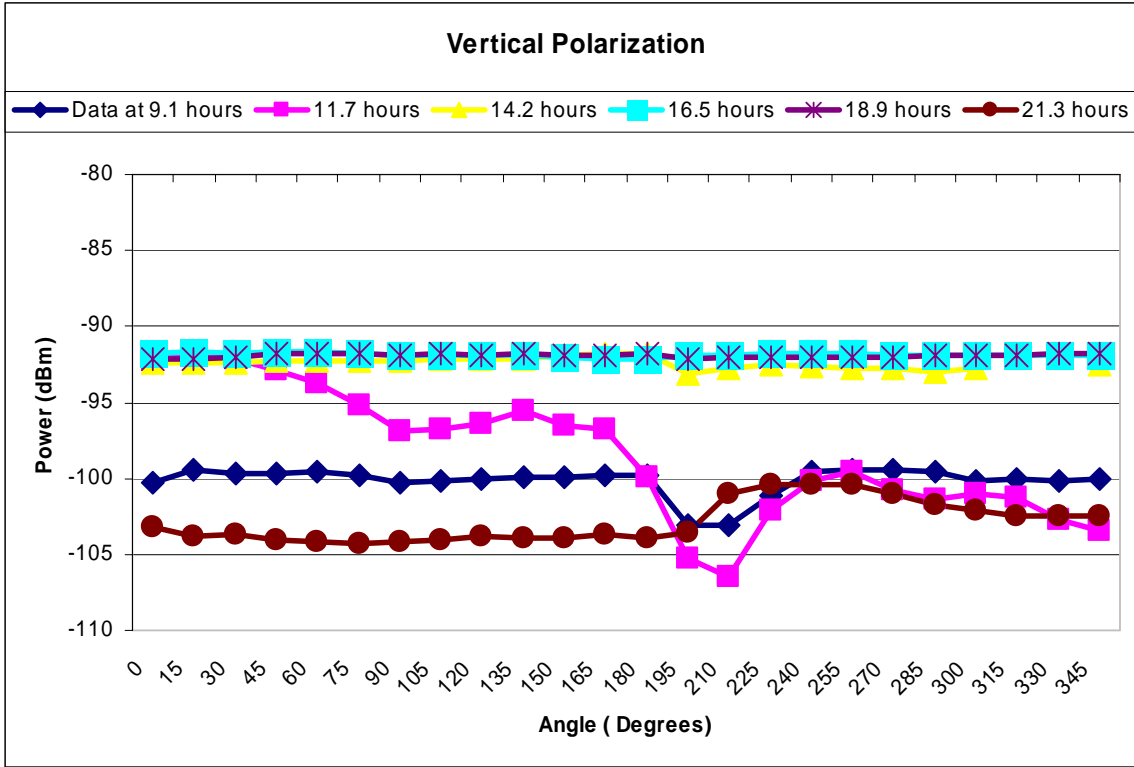
Figure B.90. I-85 Anderson: Sixty Degree Elevation, Angular Analysis

217
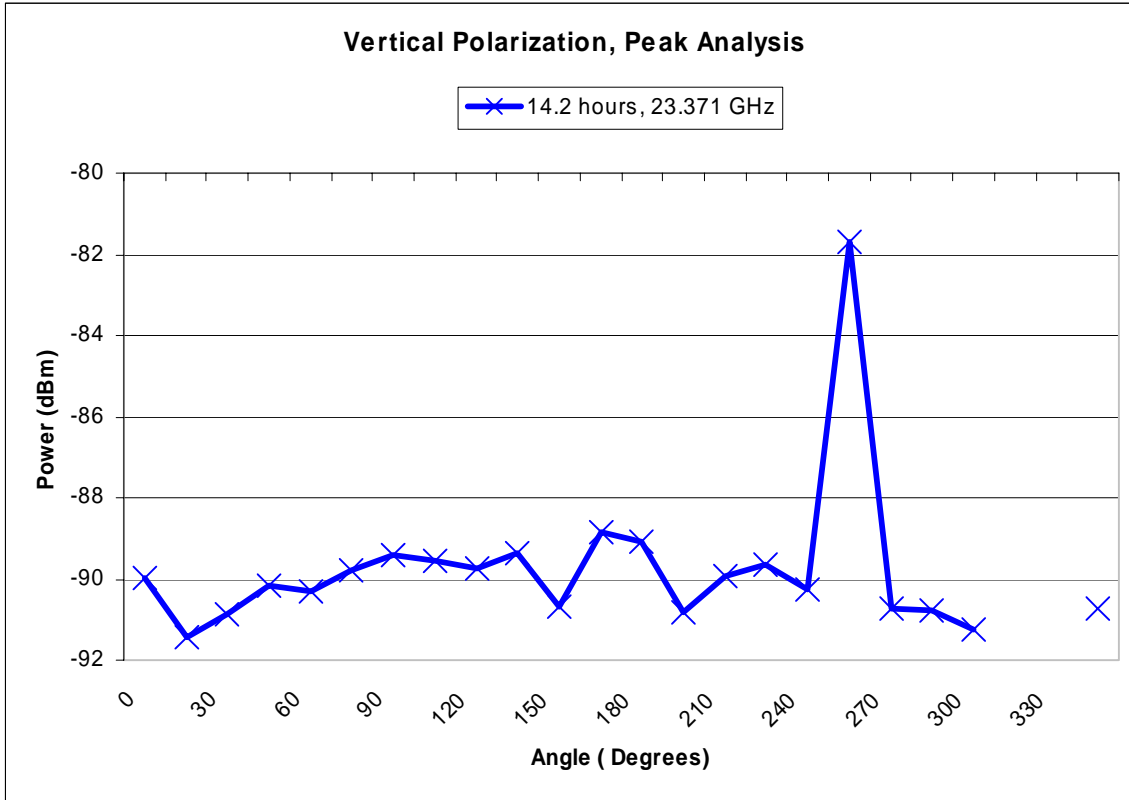
Figure B.91. I-85 Anderson: Sixty Degree Elevation, Angular Analysis of Spectral Peak
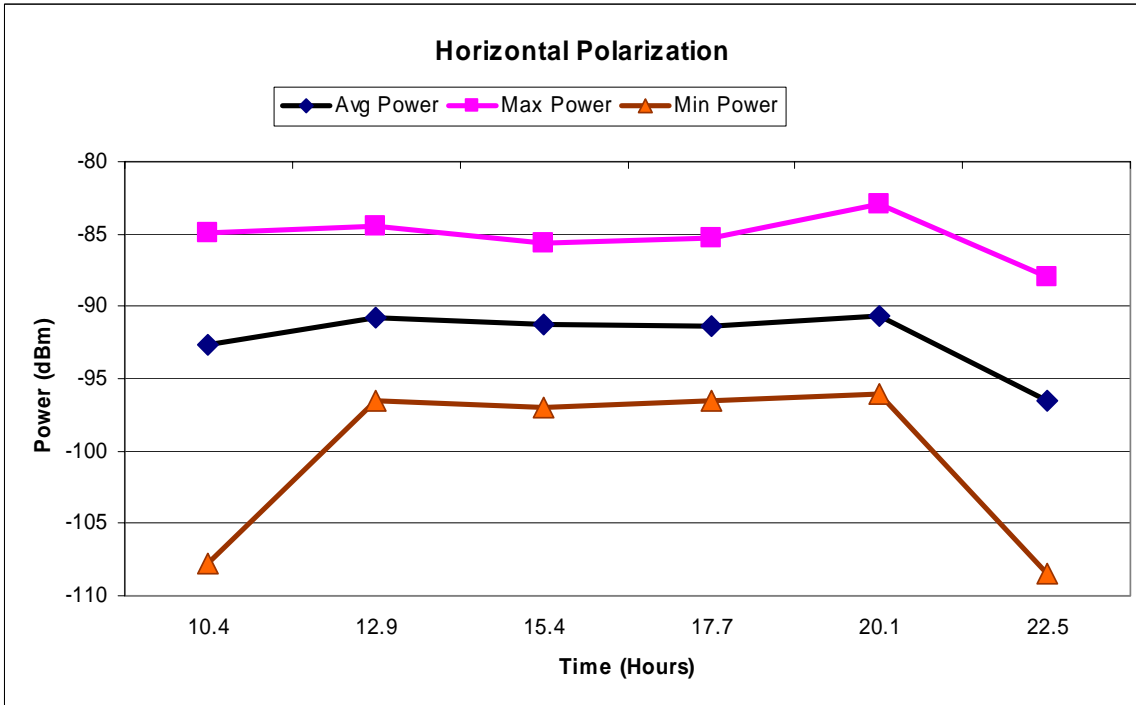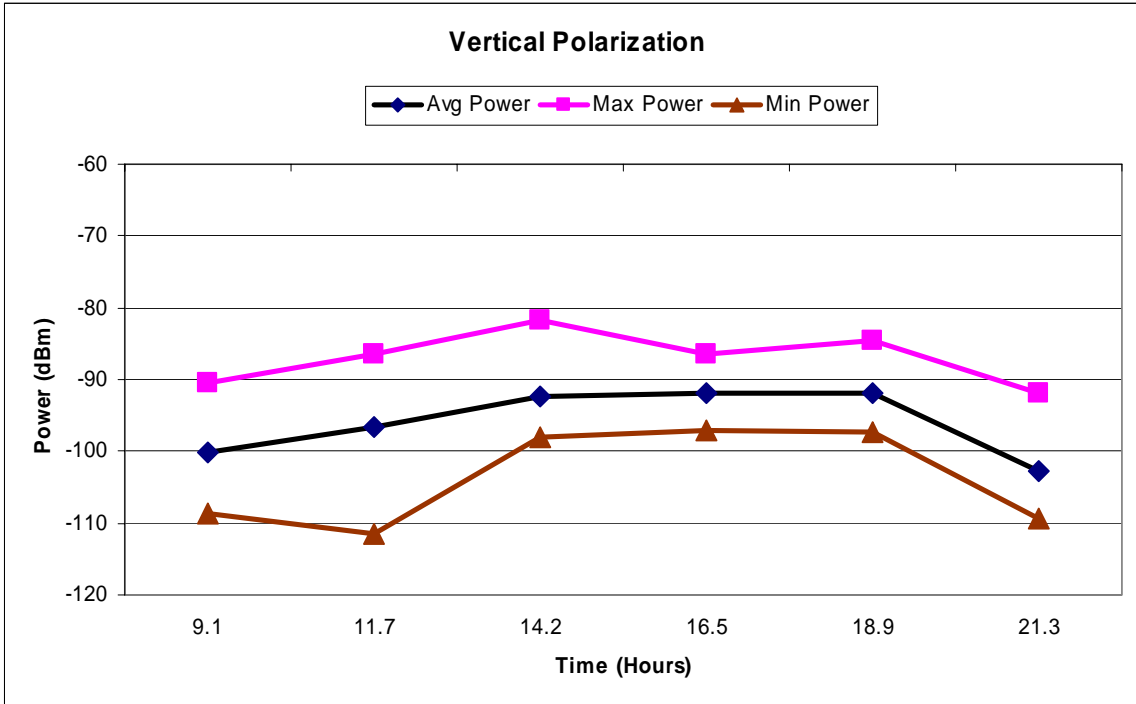
Figure B.92. I-85 Anderson: Sixty Degree Elevation, Temporal Analysis

219
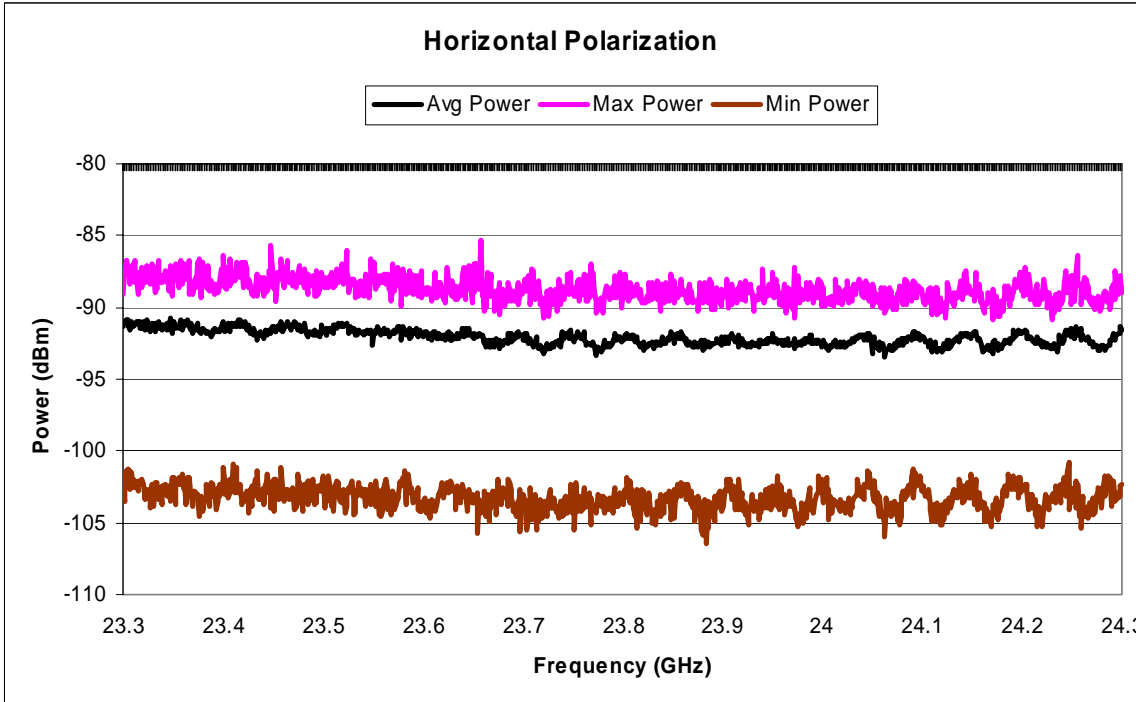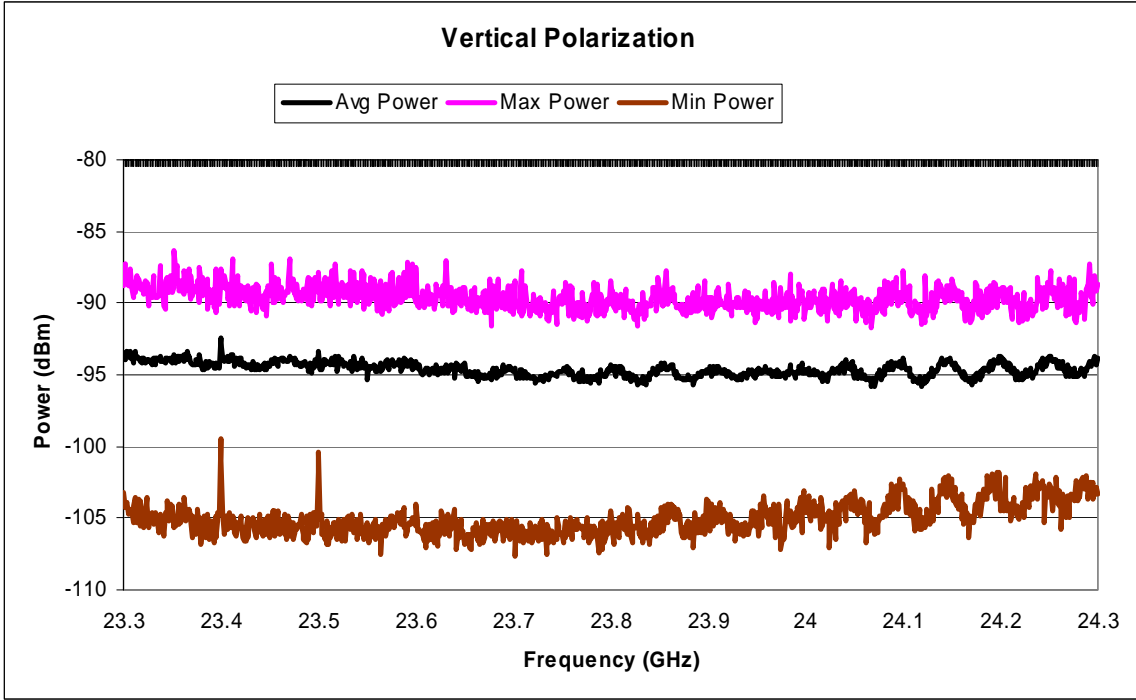
Figure B.93. I-85 Anderson: Ninety Degree Elevation, Spectral Analysis

220
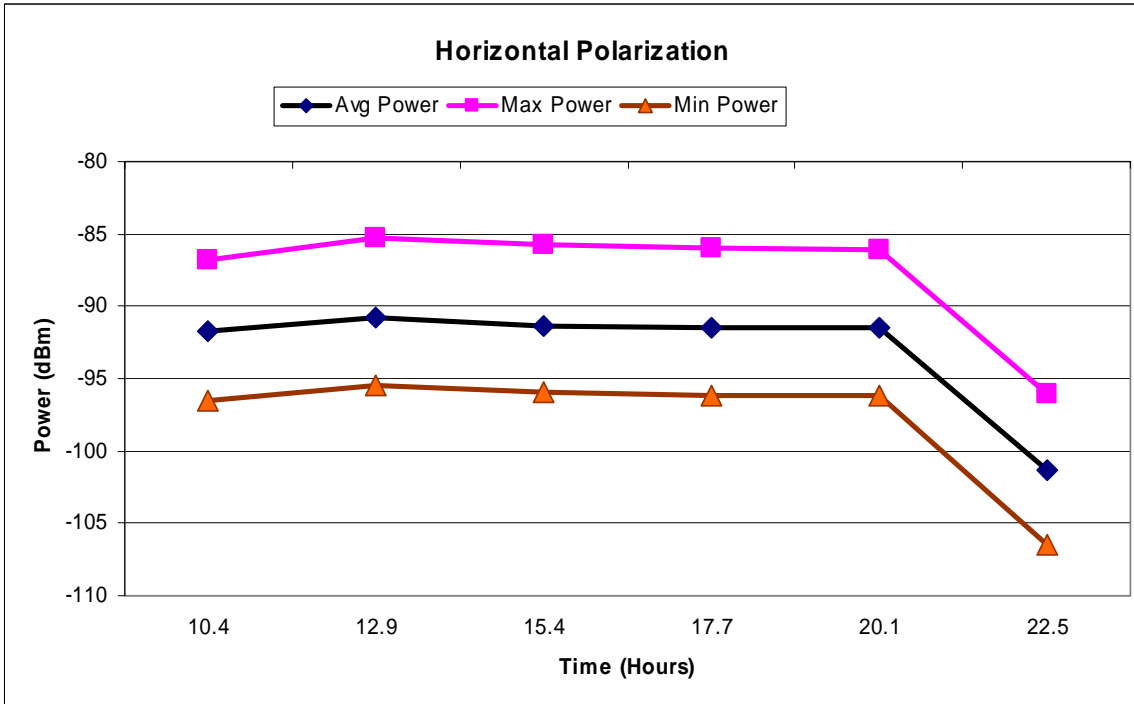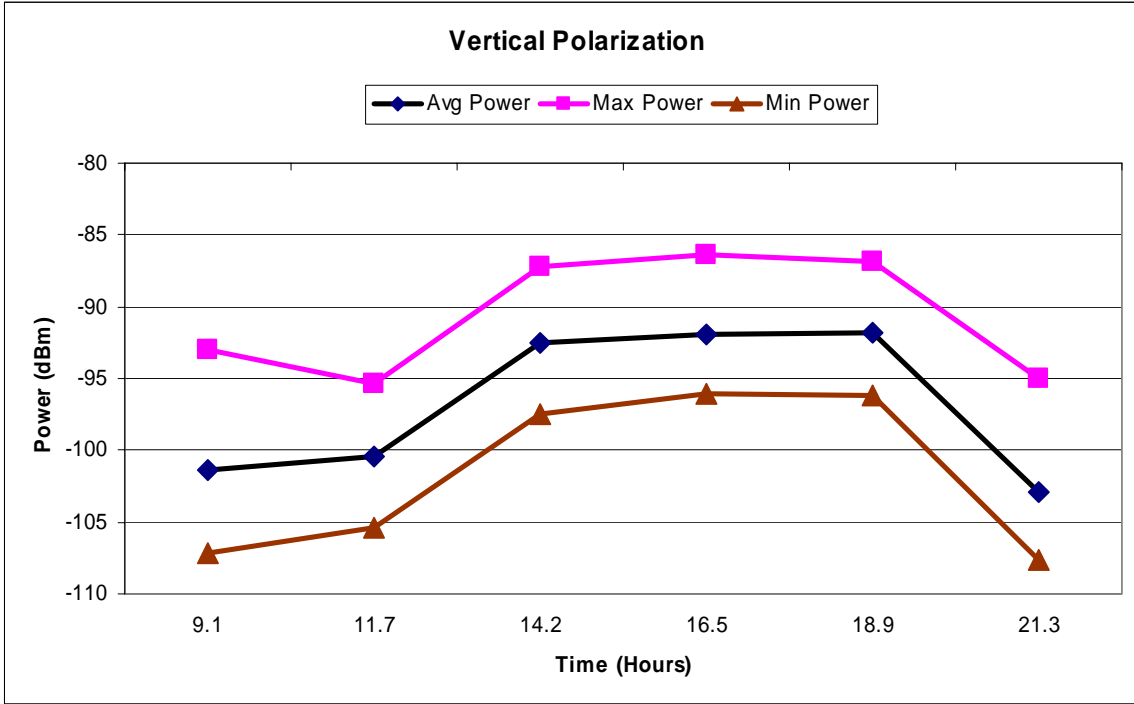
Figure B.94. I-85 Anderson: Ninety Degree Elevation, Temporal Analysis

(This page was left intentionally blank)

Appendix B.7: Georgia Institute of Technology Campus, Atlanta, GA (Site 6)

Date: 4/16/04
Map of Location: See Figure B.95
Noteworthy Results:

- Spectral trends: In general, uniform in frequency; spectral peak at 24.14 GHz at 12:15 pm. See Figures B. 96, B.98, B.100, B.103, and B.106.
- Angular trends: Seem to depend on humidity and moisture content, not on objects in path. See Figures B.97, B.99, B.101, and B.104.
- Temporal trends: Increased throughout the day, peak occurred in late evening. See Figures B.99, B.102, B.105, and B.107.
- Pre-measurement calibrated gain: 45.3 dB; Post-measurement calibrated gain: 45.8 dB.
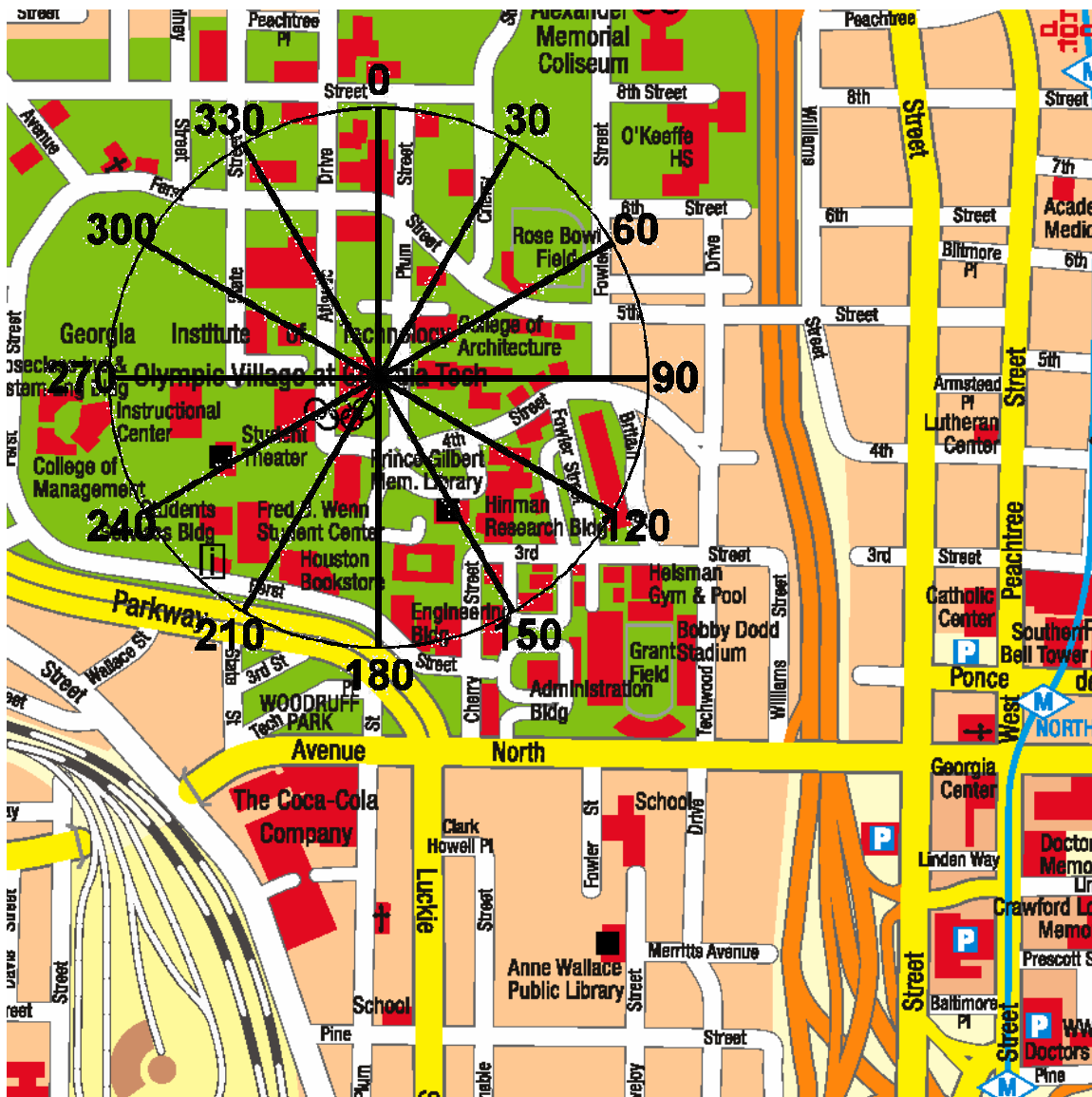
Figure B.95: Map Georgia Institute of Technology Measurement Site
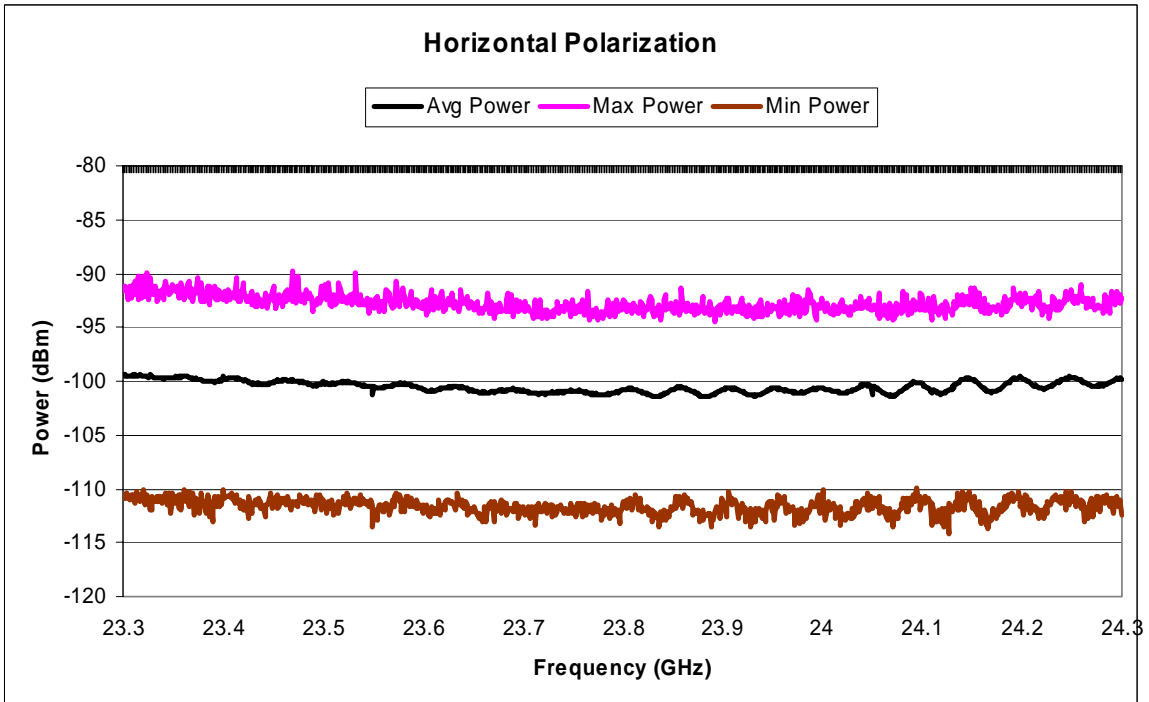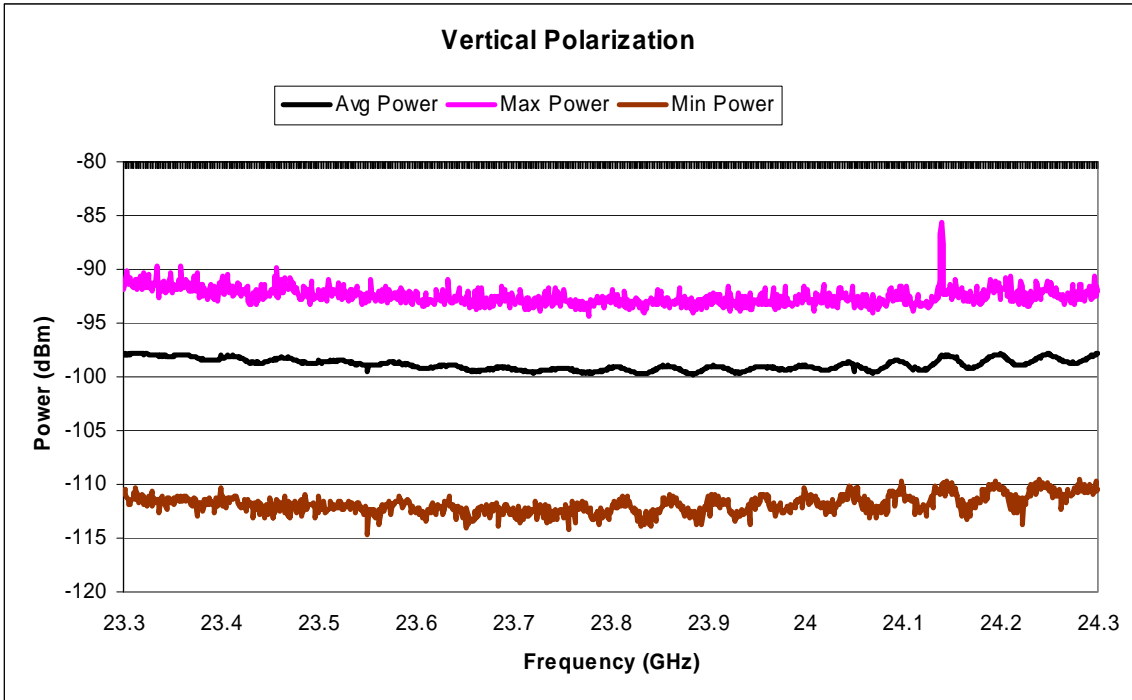
Figure B.96. Georgia Institute of Technology: Zero Degree Elevation, Spectral Analysis
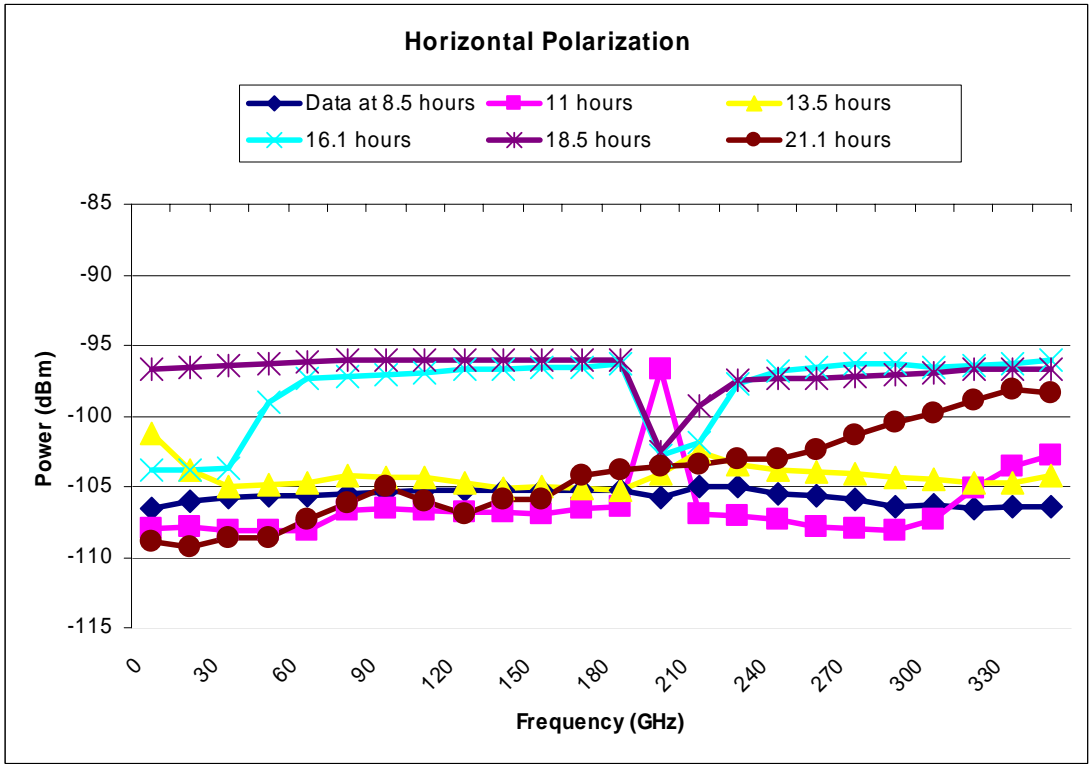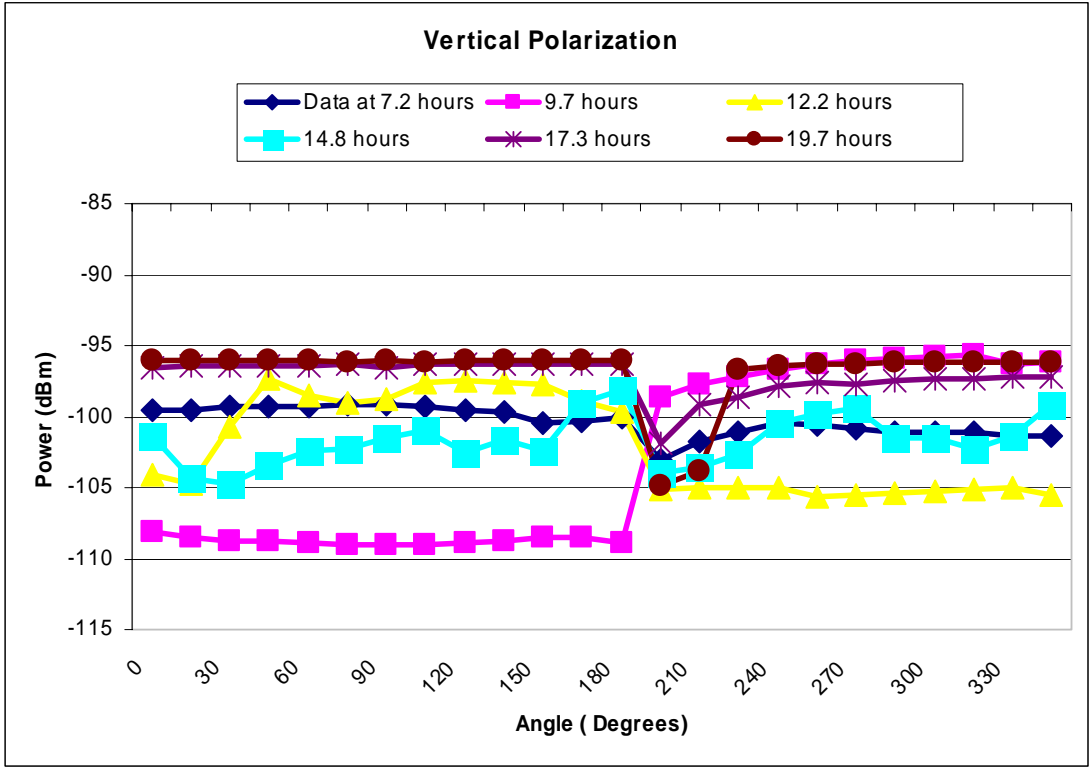
Figure B.97. Georgia Institute of Technology: Zero Degree Elevation, Angular Analysis
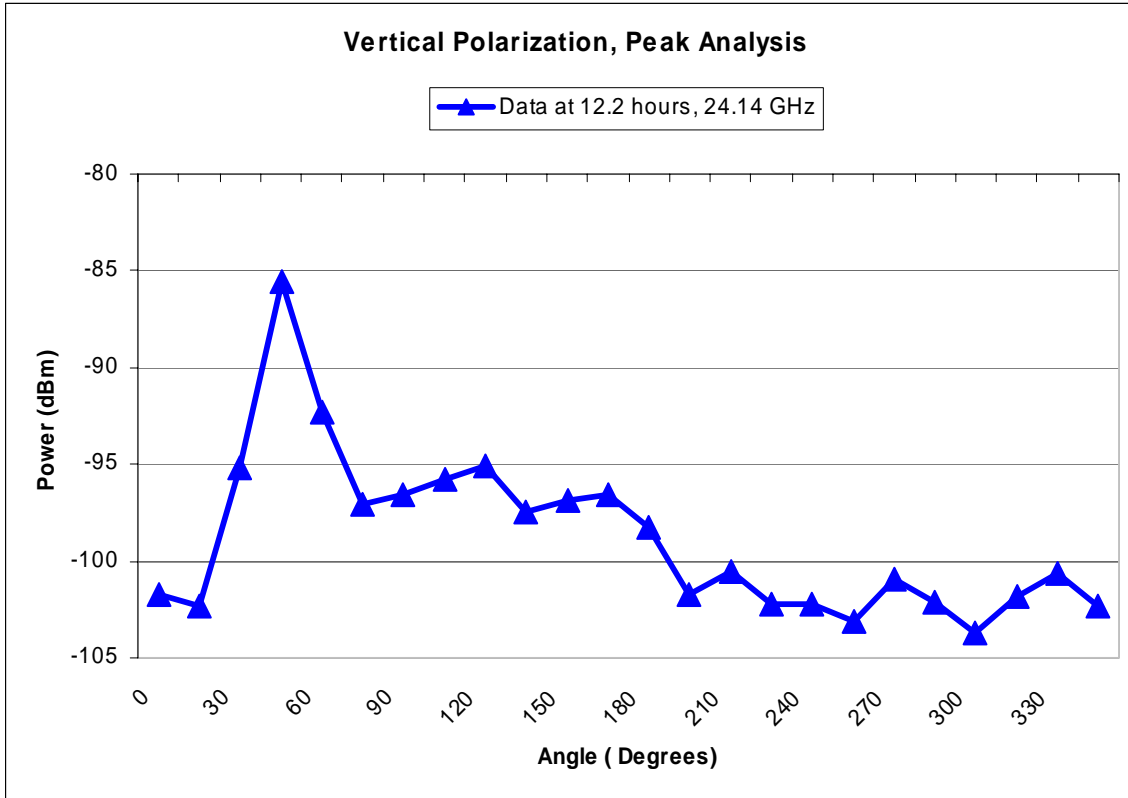
Figure B.98. Georgia Institute of Technology: Zero Degree Elevation, Angular Analysis of Spectral Peak
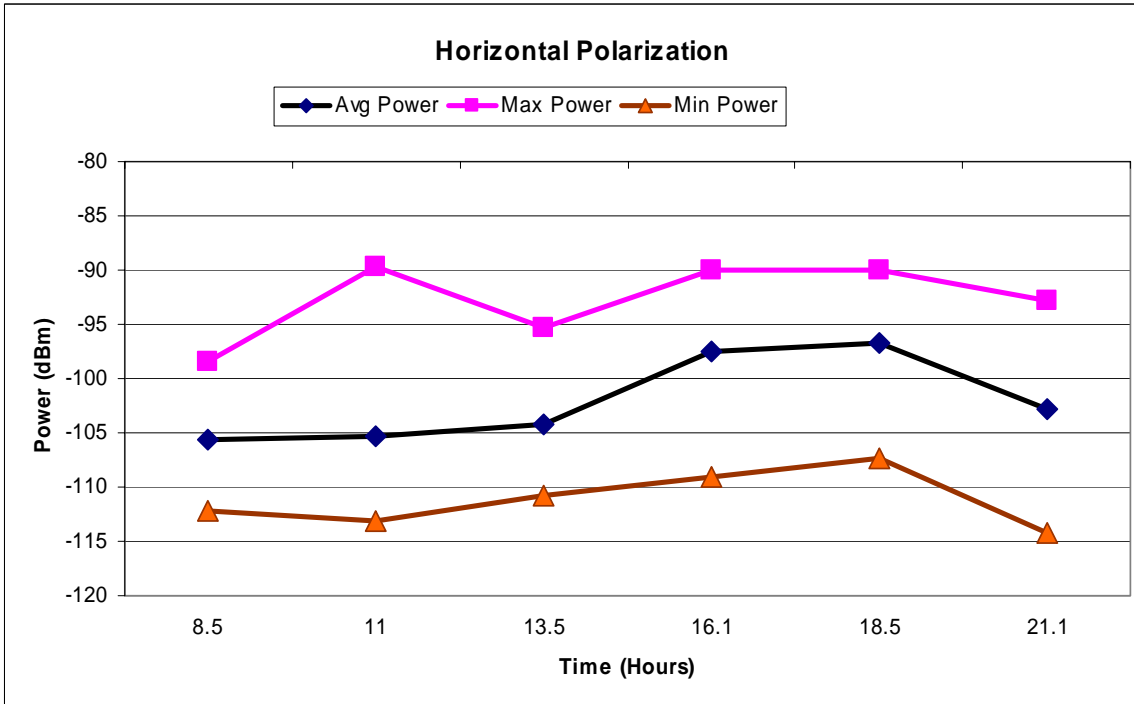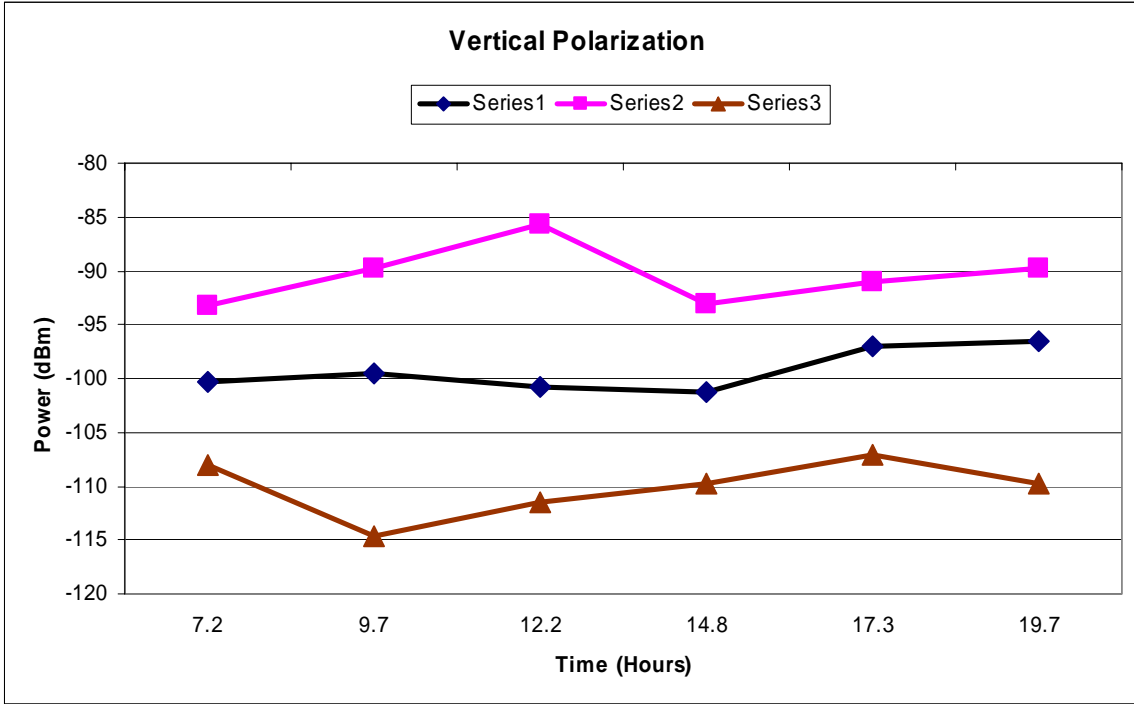
Figure B.99. Georgia Institute of Technology: Zero Degree Elevation, Temporal Analysis
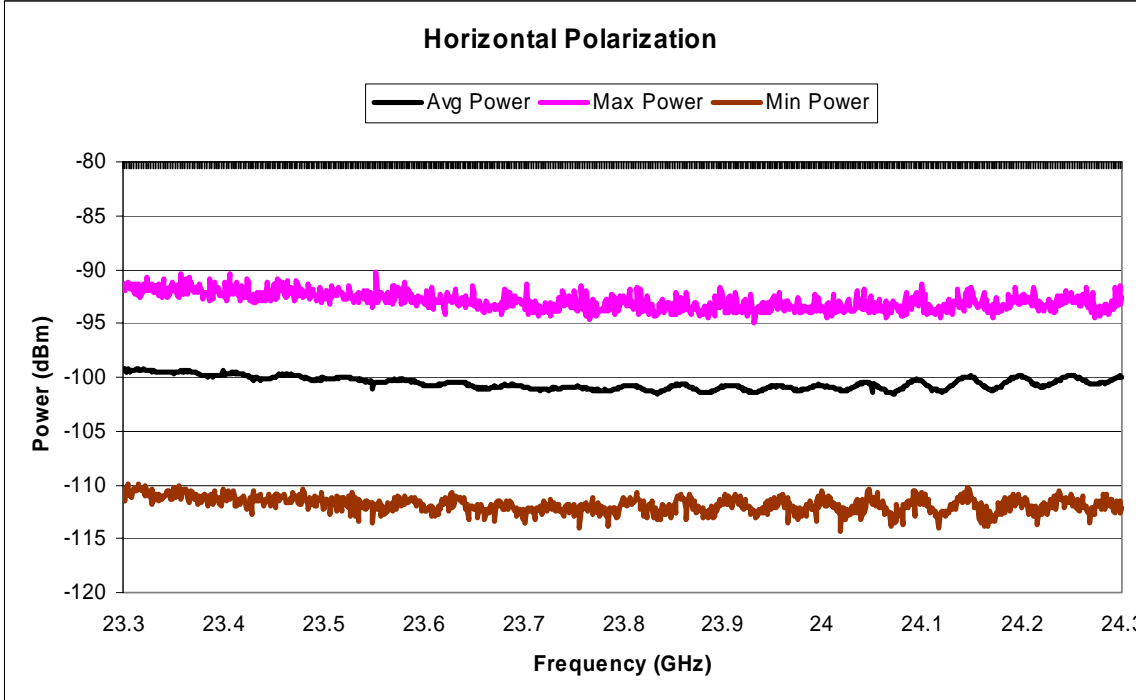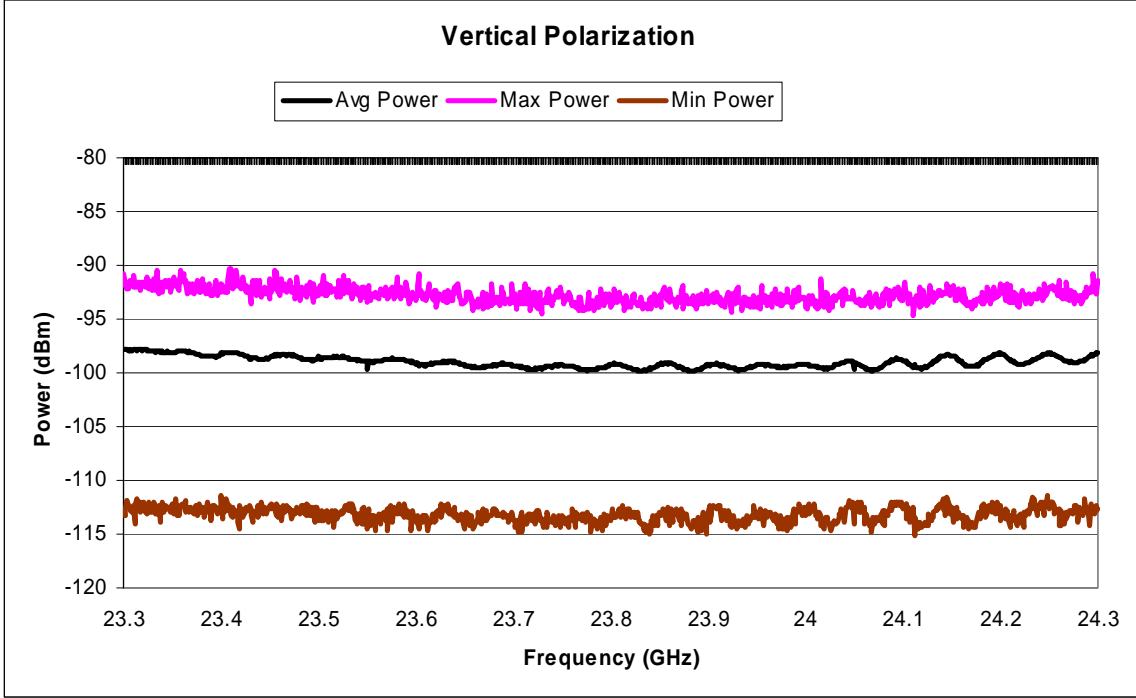
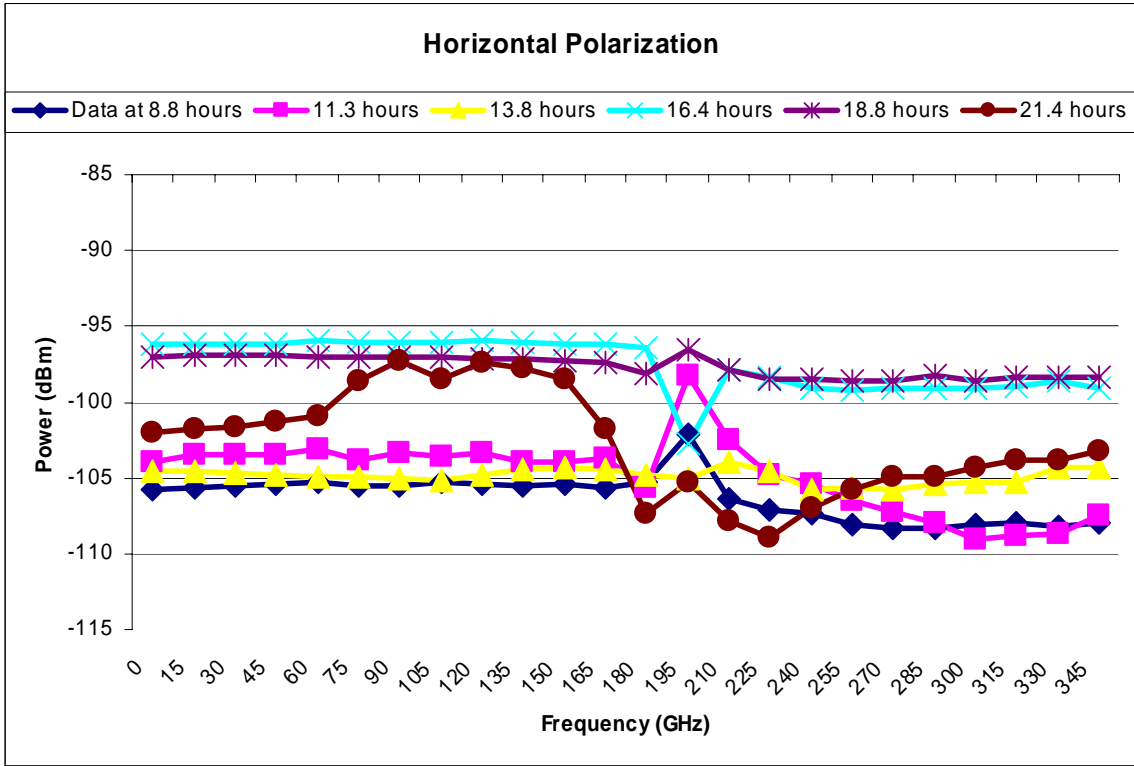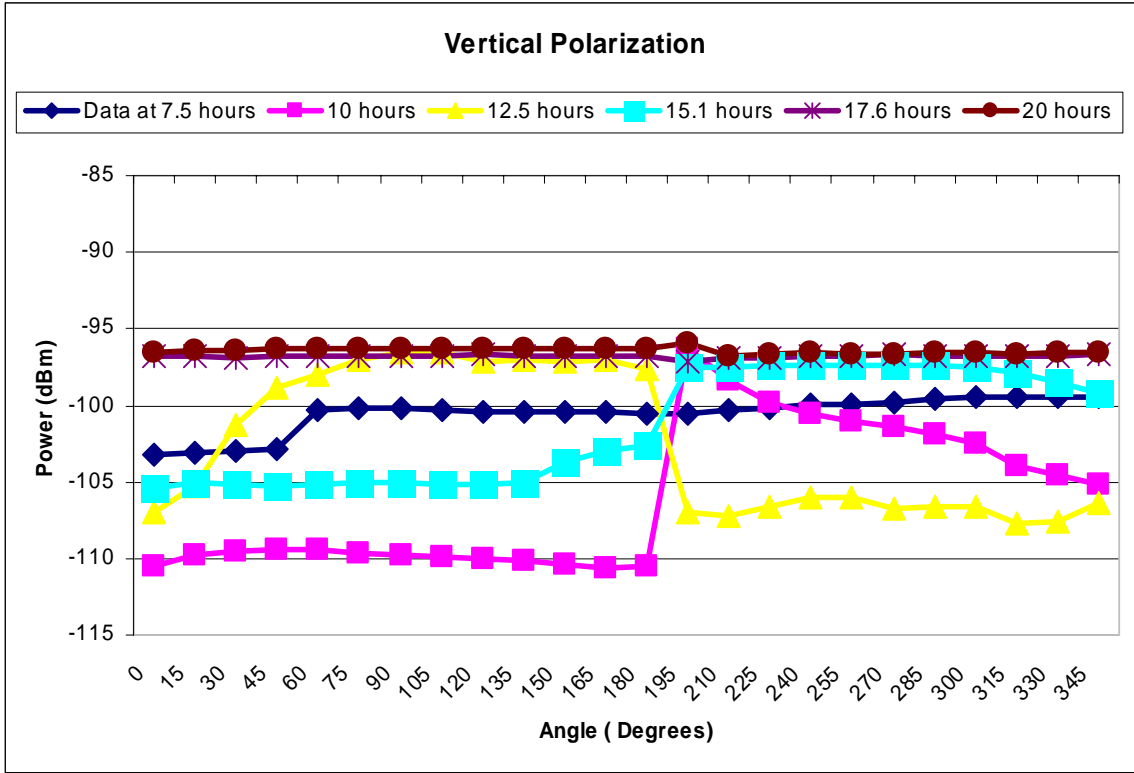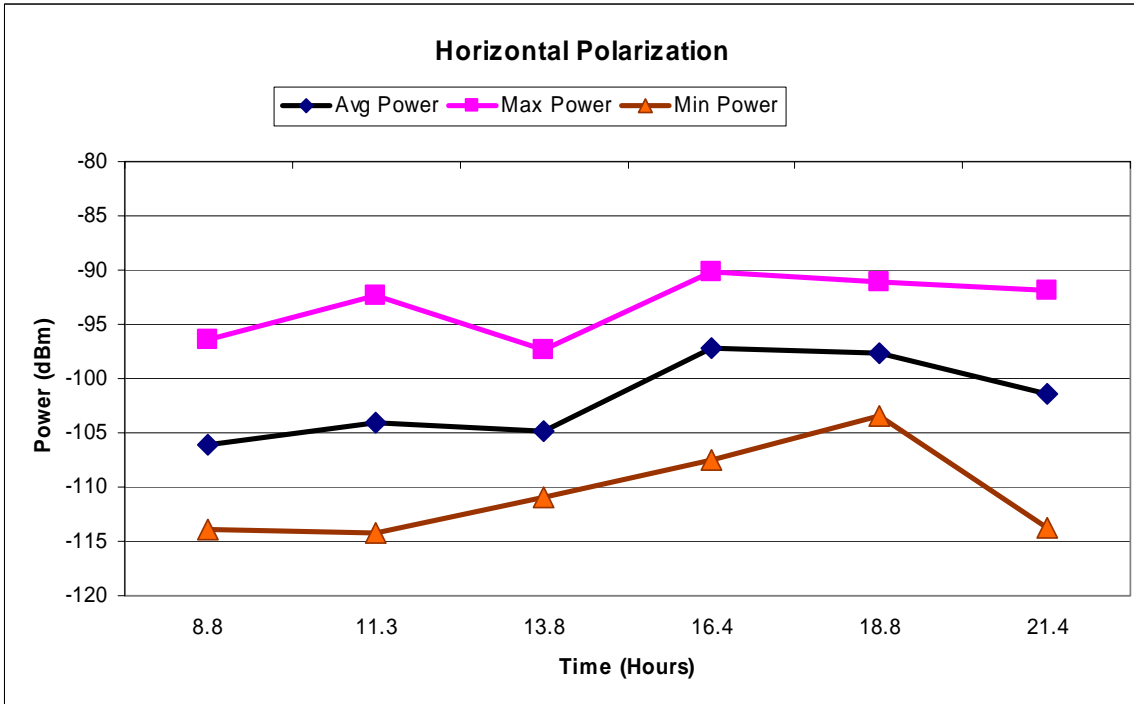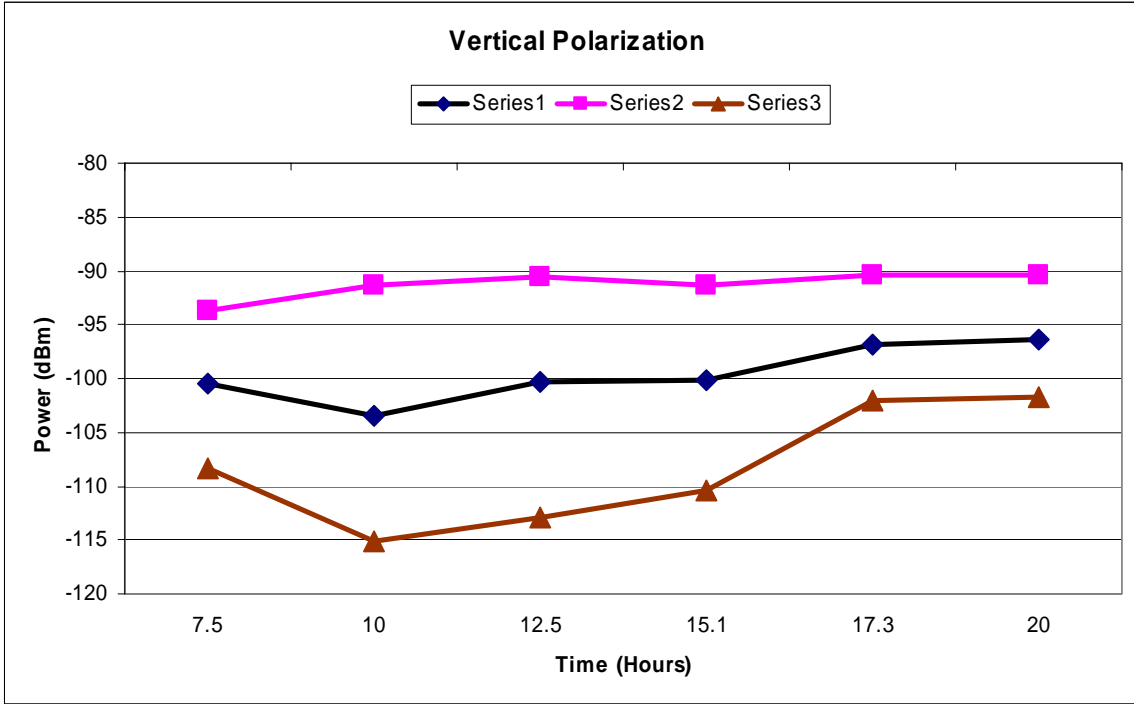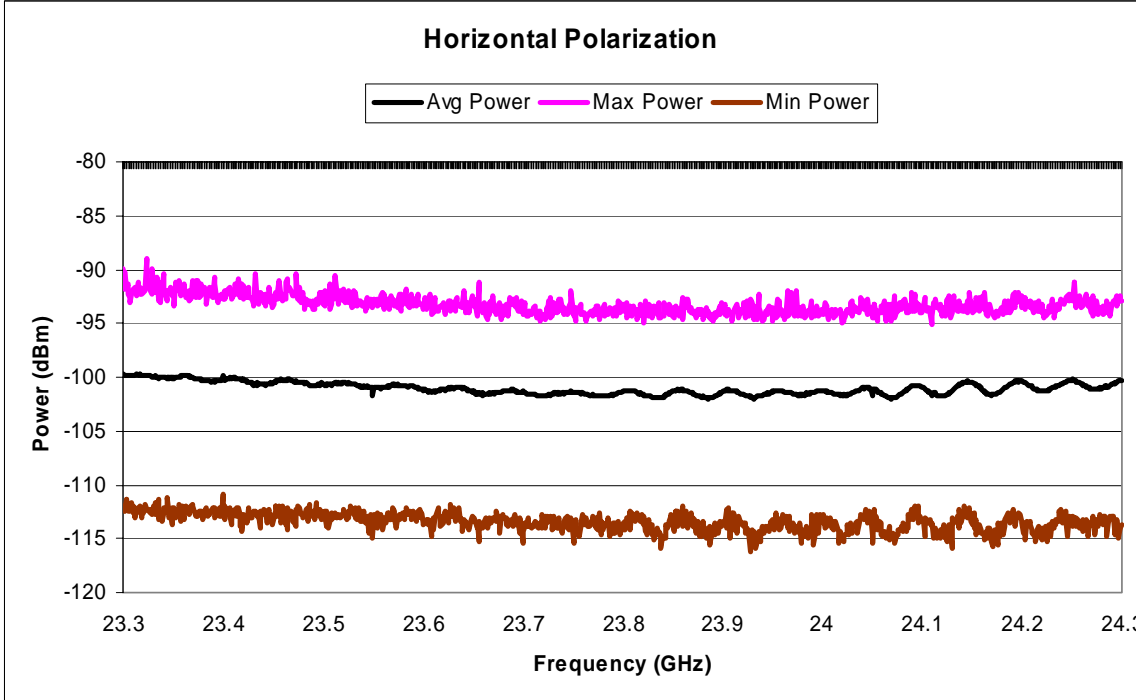Figure B.100. Georgia Institute of Technology: Thirty Degree Elevation, Spectral Analysis

Figure B.101. Georgia Institute of Technology: Thirty Degree Elevation, Angular Analysis

229

Figure B.102. Georgia Institute of Technology: Thirty Degree Elevation, Temporal Analysis
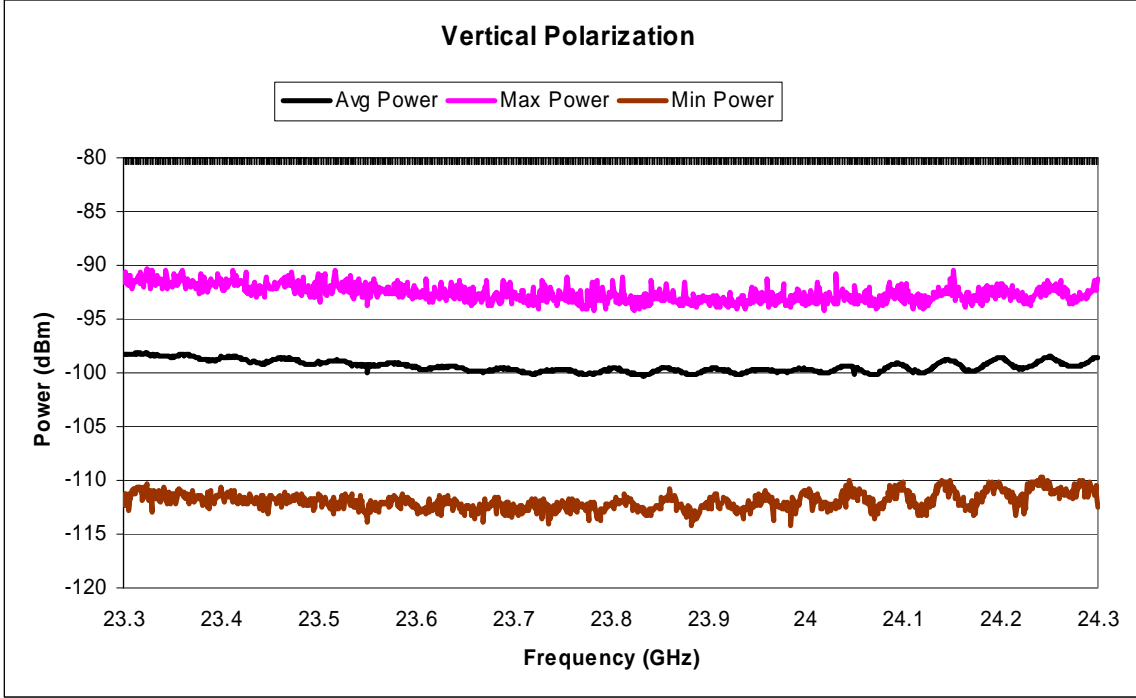
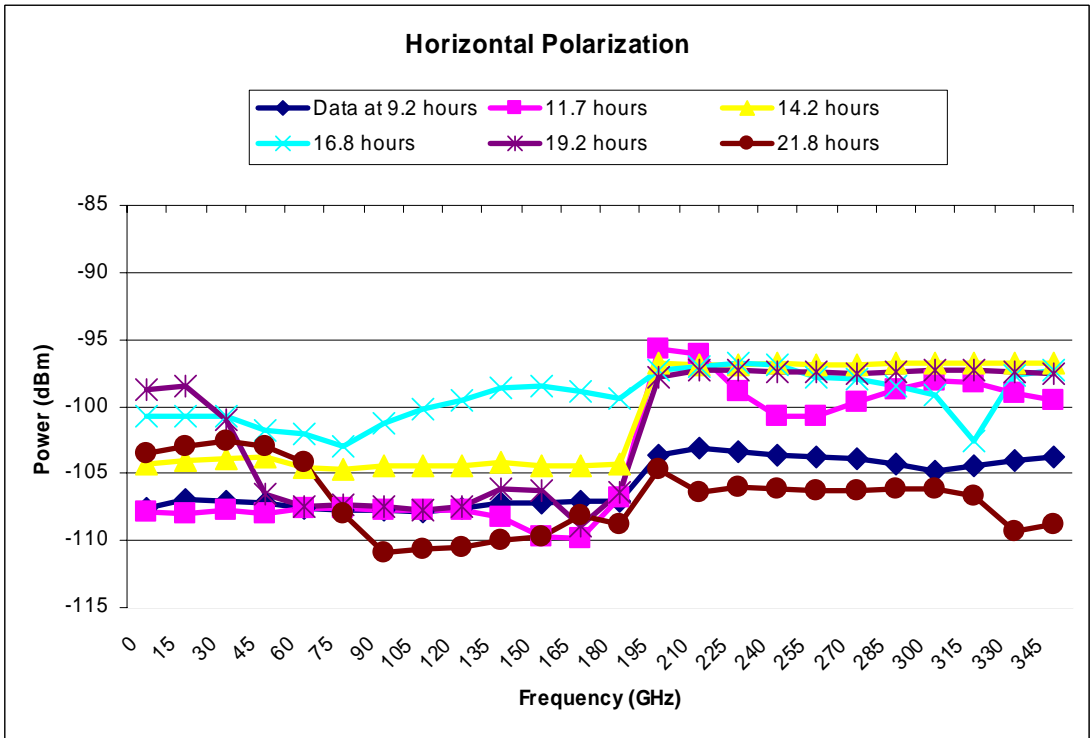Figure B.103. Georgia Institute of Technology: Sixty Degree Elevation, Spectral Analysis
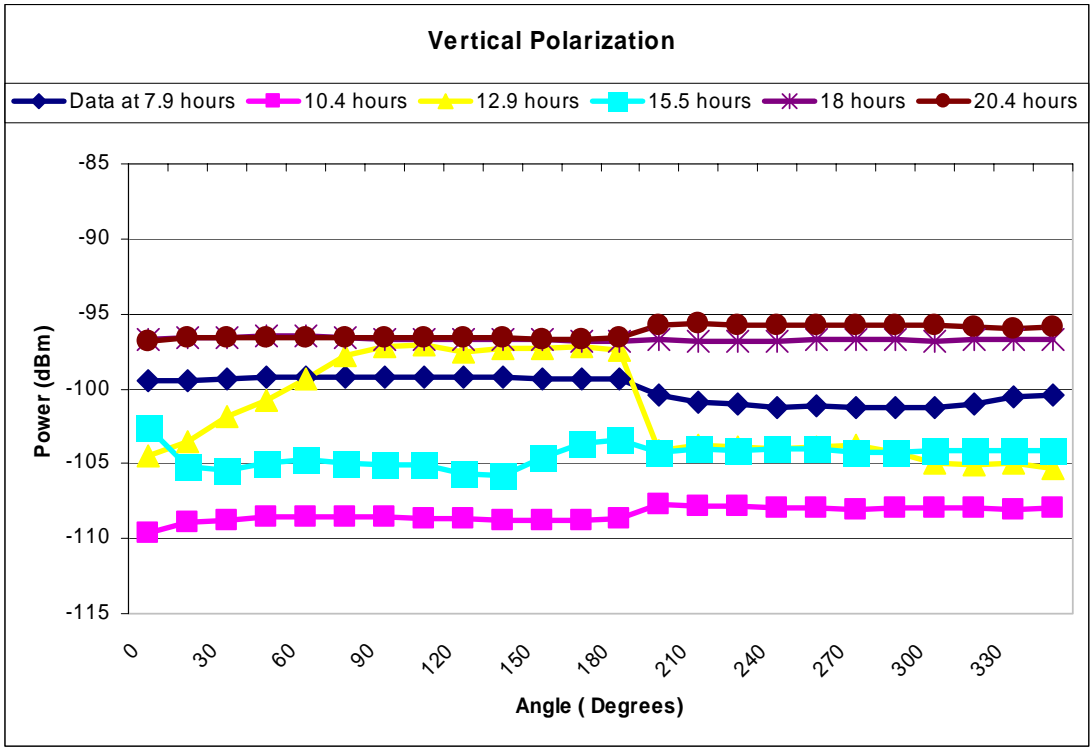
Figure B.104. Georgia Institute of Technology: Sixty Degree Elevation, Angular Analysis

Vertical Polarization
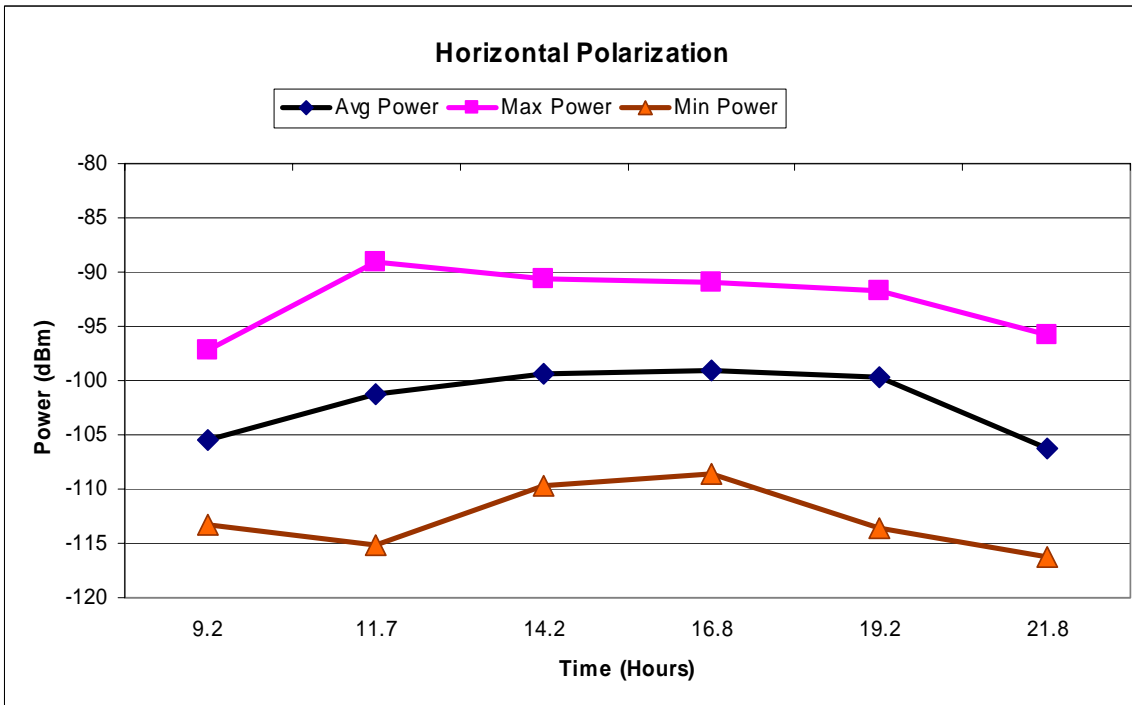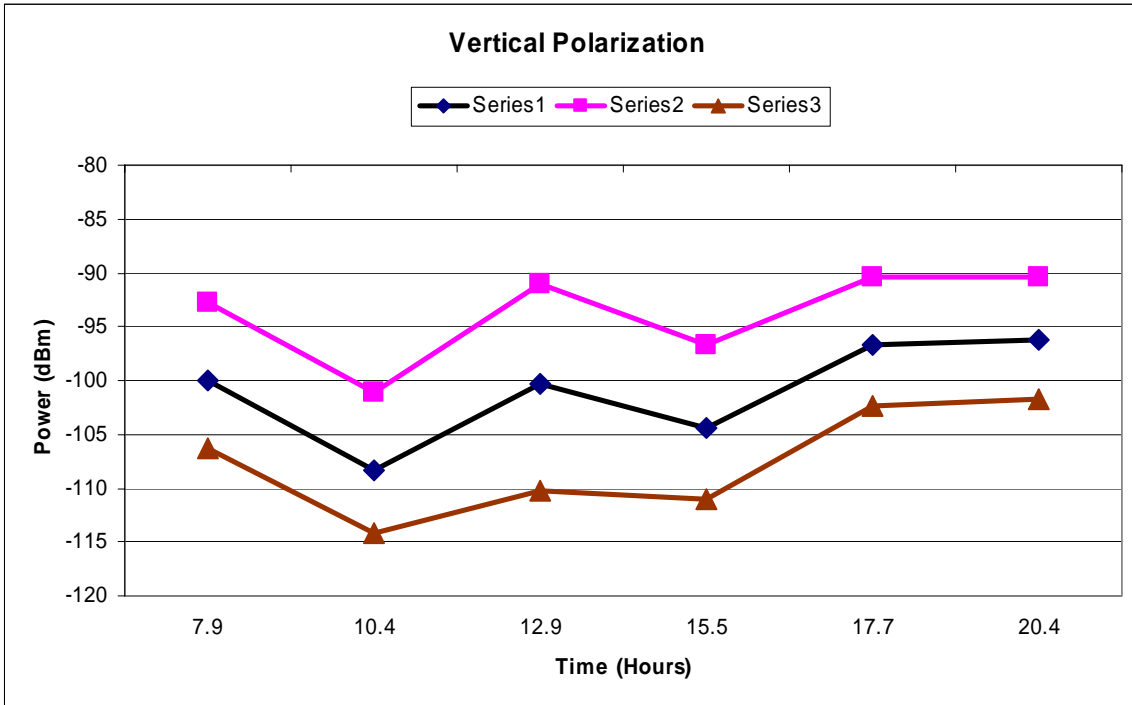

Horizontal Polarization

Figure B.105. Georgia Institute of Technology: Sixty Degree Elevation, Temporal Analysis
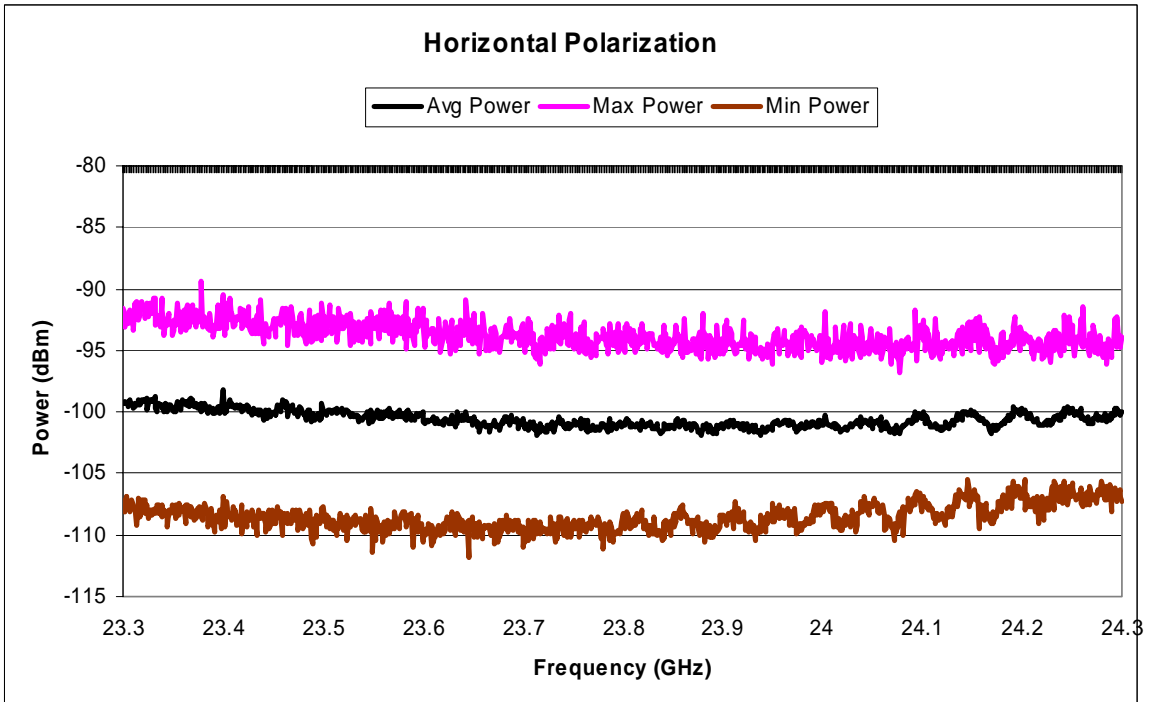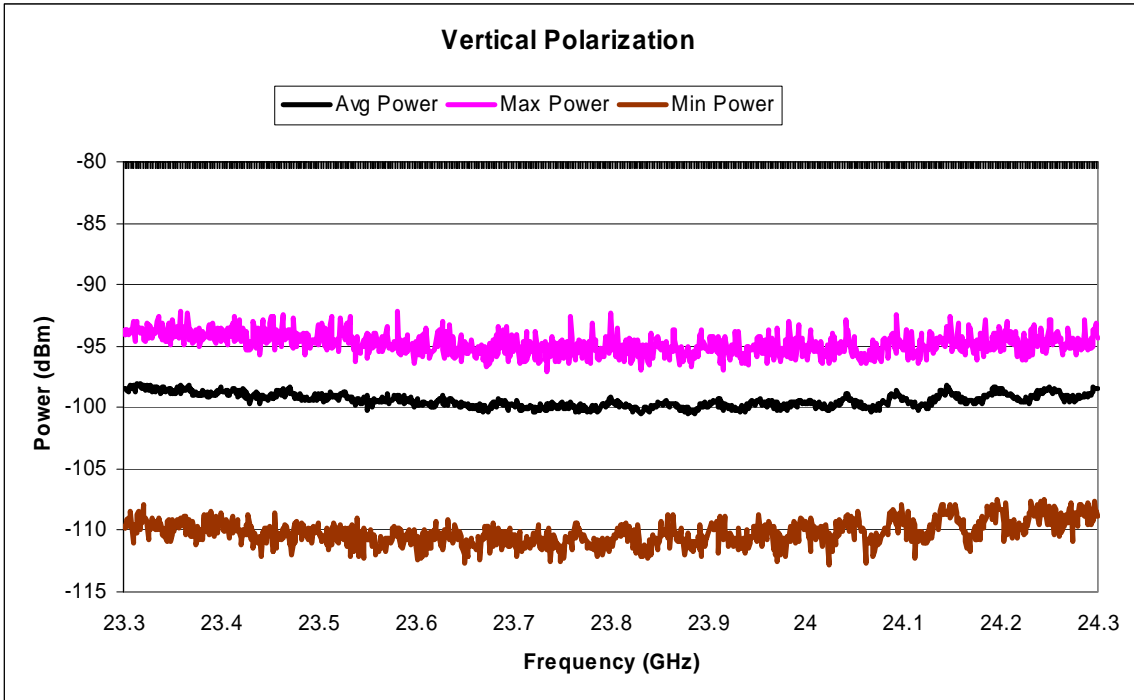
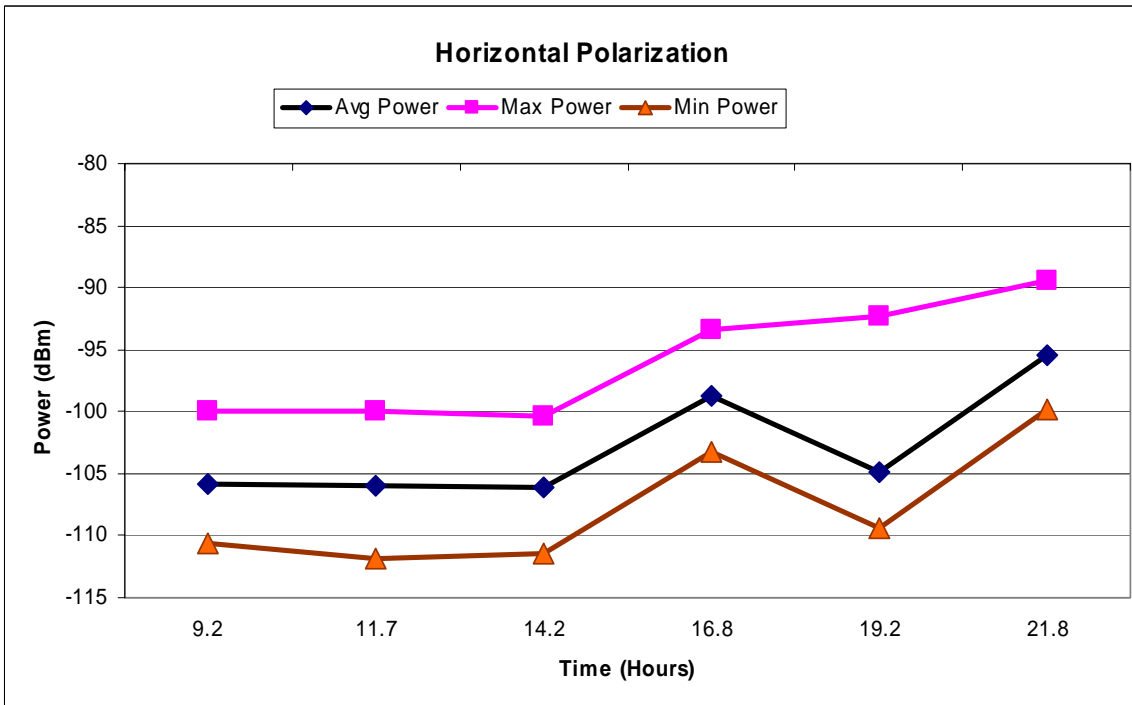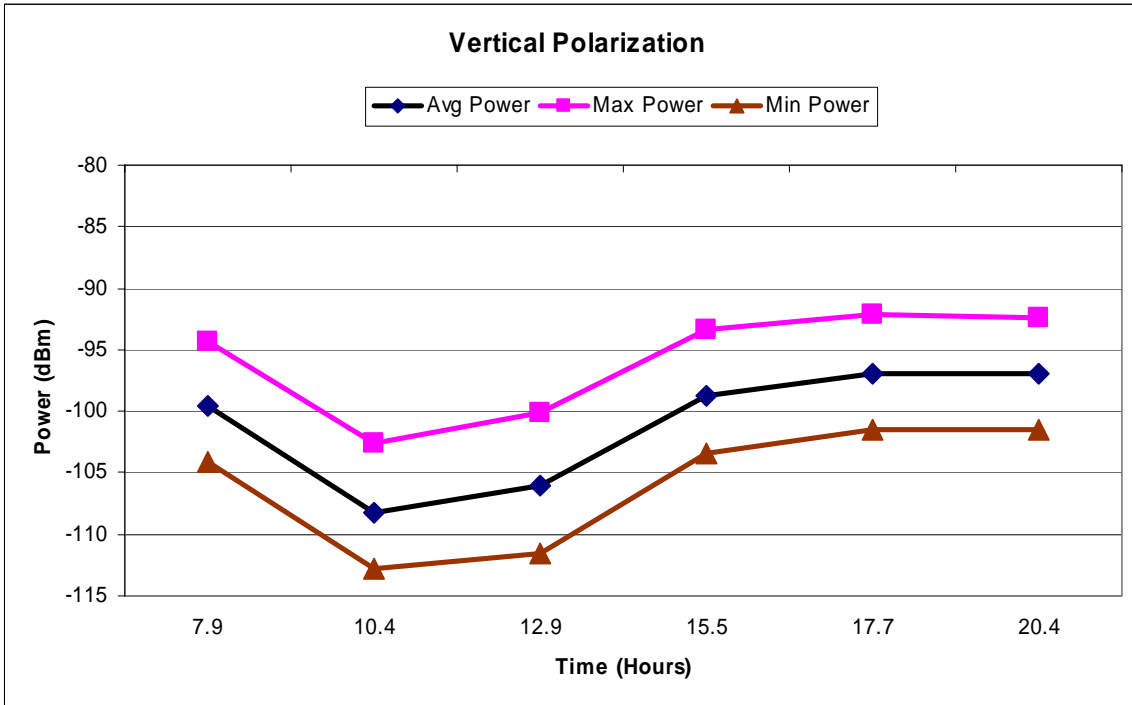Figure B.106. Georgia Institute of Technology: Ninety Degree Elevation, Spectral Analysis

234

Figure B.107. Georgia Institute of Technology: Ninety Degree Elevation, Temporal Analysis

(This page was left intentionally blank)

References

1. FCC Technical Advisory Committee (TAC) Report: Third Meeting of the FCC Technological Advisory Council, at 1 and 8. December 1999.

2. Letter from Dr. Robert W. Lucky, TAC Chairman, to the Hon William E. Kennard, FCC Chairman, at 3. January 7, 2000.

3. "Noise Floor Measurements in the Passive Sensor Band (23.6 to 24 GHz) Final Report". Clemson University, March 2004.

4. "L and S Bands Spectrum Survey in the San Francisco Bay Area", GPS Laboratory, Stanford University, March 2004.

5. National Telecommunications and Information Administration (NTIA) Report 02-390, "Man-made interference Power Measurements at VHF and UHF Frequencies", Dec. 2001

6. NTIA Report 99-367, "Broadband Spectrum Survey at San Francisco, California", July 1999

7. NTIA Report 97-336, "Broadband Spectrum Survey at Los Angeles, California", May 1997

8. NTIA Report 95-321, "Broadband Spectrum Survey at Denver, Colorado", Sept. 1995

9. RTCA Special Committee-159, "Assessment of Radio Frequency Interference Relevant to the GNSS, RTCA DO-235A", Dec. 2002

10. Titus B., Dafesh P. , Wong W. , Maine K. , Stansell T. , "Assessing Ultra Wide Band (UWB) Interference to GPS Receivers", GPS-ION 2002, 15th International Technical Meeting of the Satellite Division of the Institute of Navigation, Portland, OR, Sept. 2002

11. American National Standard Institute (ANSI) C63. 4-2001, "American National Standard for Methods of Measurement of Radio-Noise Emissions from Low-Voltage Electrical and Electronic Equipment in the Range of 9 kHz to 40 GHz", June 2001

12. ANSI T1.523-2001, American National Standard for Telecommunications - Telecom Glossary 2000.

13. First Report and Order Revision of Part 15 of the Commission's Rules Regarding Ultra-Wideband Transmission Systems, Federal Communications Commission, Washington, February 14, 2002.

14. "Noise Floor Measurements in the L Band, S Band and Passive Sensor Band (23.6 to 24 GHz) Objectives, Test Plan, Calibration and Test Procedure," Stanford University, Clemson University, August 22, 2003.

15. "Noise Figure Analyzers, NFA Series," Agilent Technologies, Palo Alto, CA, May 2001.

(This page was left intentionally blank)

REPORT DOCUMENTATION PAGE

The public reporting burden for this collection of information is estimated to average 1 hour per response, including the time for reviewing instructions, searching existing data sources, gathering and maintaining the data needed, and completing and reviewing the collection of information. Send comments regarding this burden estimate or any other aspect of this collection of information, including suggestions for reducing this burden, to Department of Defense, Washington Headquarters Services, Directorate for Information Operations and Reports (0704-0188), 1215 Jefferson Davis Highway, Suite 1204, Arlington, VA 22202-4302. Respondents should be aware that notwithstanding any other provision of law, no person shall be subject to any penalty for failing to comply with a collection of information if it does not display a currently valid OMB control number.
PLEASE DO NOT RETURN YOUR FORM TO THE ABOVE ADDRESS.

1. REPORT DATE *(DD-MM-YYYY)*

2. REPORT TYPE

3. DATES COVERED *(From - To)*

4. TITLE AND SUBTITLE

5a. CONTRACT NUMBER

5b. GRANT NUMBER

5c. PROGRAM ELEMENT NUMBER

6. AUTHOR(S)

5d. PROJECT NUMBER

5e. TASK NUMBER

5f. WORK UNIT NUMBER

7. PERFORMING ORGANIZATION NAME(S) AND ADDRESS(ES)

8. PERFORMING ORGANIZATION REPORT NUMBER

9. SPONSORING/MONITORING AGENCY NAME(S) AND ADDRESS(ES)

10. SPONSORING/MONITOR'S ACRONYM(S)

11. SPONSORING/MONITORING REPORT NUMBER

12. DISTRIBUTION/AVAILABILITY STATEMENT

13. SUPPLEMENTARY NOTES

14. ABSTRACT

15. SUBJECT TERMS

16. SECURITY CLASSIFICATION OF:			**17. LIMITATION OF ABSTRACT**	**18. NUMBER OF PAGES**	**19a. NAME OF RESPONSIBLE PERSON**
a. REPORT	**b. ABSTRACT**	**c. THIS PAGE**			**19b. TELEPHONE NUMBER** *(Include area code)*